THE UNIVERSITY OF QUEENSLAND

AUSTRALIA

Understanding the biodegradation products and pathways of selected pharmaceuticals atenolol and acyclovir by an enriched nitrifying sludge through experiments and modeling

Yifeng Xu

Master of Science

A thesis submitted for the degree of Doctor of Philosophy at

The University of Queensland in 2017

School of Chemical Engineering

Advanced Water Management Centre

Abstract

Pharmaceuticals could potentially pose detrimental effects on aquatic ecosystems and human health, with wastewater treatment being one of the major pathways for pharmaceuticals to enter into the environment. Enhanced removal of pharmaceuticals has been widely observed by ammonia oxidizing bacteria (AOB). However, the degradation mechanisms involved in pharmaceutical biotransformation were still ambiguous. In addition, pharmaceutical biotransformation models have not yet considered transformation products associated with the metabolic type of microorganisms. The overall objective of this thesis is to understand the contribution of different metabolisms by relevant microorganisms to the biotransformation of selected pharmaceuticals (i.e., atenolol and acyclovir) accompanied with the formation of their transformation products in an enriched nitrifying sludge, in terms of product identification, influencing factor assessment and mathematical modeling.

Biodegradation of atenolol in an enriched nitrifying sludge was studied under different metabolic conditions. The positive link was observed between atenolol biodegradation and the cometabolic activity of AOB in the presence of ammonium, likely due to a broad substrate spectrum of ammonia monooxygenase (AMO). In the presence of ammonium, atenolol was transformed into P267 (atenolol acid) and three new products including P117 (1-isopropylamino-2-propanol), P167 (1-amino-3-phenoxy-2-propanol), and an unknown product P227. However, atenolol was only transformed to P267 and P227 in the absence of ammonium. The formation of P117, P167 and P227 was further confirmed from follow-up atenolol acid biodegradation experiments in the presence of ammonium. Therefore, a tentative biodegradation pathway of atenolol is proposed in the enriched nitrifying sludge, consisting of two steps regardless of the presence of ammonium: i) microbial amide-bond hydrolysis to carboxyl group, producing P267 and ii) a possible formation of P227 and other two cometabolically induced reactions: iii) breakage of ether bond in the alkyl side chain to produce P117 and iv) a minor pathway through N-dealkylation and loss of acetamide moiety from the aromatic ring, yielding P167. An important insight was herein provided regarding the biotransformation pathways of pharmaceuticals under different metabolic conditions.

To further assess the influence of the growth substrate on atenolol biotransformation in enriched nitrifying culture, different ammonium concentrations were applied constantly to study atenolol degradation kinetics and the biotransformation product formation dynamics. Higher ammonium concentrations led to the lower atenolol removal efficiencies probably

due to the substrate competition between ammonium and atenolol. The formation of biotransformation product atenolol acid was positively related to the ammonium oxidation activity, resulting in a higher amount of atenolol acid at the end of experiments at higher ammonium concentrations. Positive correlations between ammonia oxidation rate and atenolol degradation rate at ammonium levels of both 25 and 50 mg-N L^{-1}, suggested the cometabolism of atenolol by AOB in the presence of ammonium. The revealed biotransformation reaction, i.e., hydroxylation on amide group to carboxylic group, could be catalyzed by the non-specific enzyme AMO. It was also demonstrated the formation of atenolol acid was independent on the ammonium availability.

Biotransformation of acyclovir by the enriched nitrifying culture was evaluated under different metabolic conditions at different initial levels of acyclovir (15 mg L^{-1} and 15 μg L^{-1}). Higher degradation rates of acyclovir were observed under higher ammonia oxidation rates in the presence of ammonium than those constant degradation rates in the absence of ammonium. The positive correlation between acyclovir degradation rate and ammonia oxidation rate further confirmed the cometabolic biodegradation of acyclovir by AOB in the presence of ammonium. Carboxy-acyclovir (P239) was produced from acyclovir biodegradation. The main biotransformation pathway was aerobic oxidation of the terminal hydroxyl group, which was independent on the metabolic type (i.e. cometabolism or metabolism). This enzyme-linked reaction might be catalyzed by monooxygenase from AOB or heterotrophs (HET). The formation of carboxy-acyclovir was irrelevant to the acyclovir concentrations applied, indicating the revealed biotransformation pathway might be dominant in acyclovir removal during wastewater treatment processes.

A comprehensive mathematical model was developed therein to describe and evaluate the biodegradation of pharmaceuticals accompanied with the formation of biotransformation products by enriched nitrifying culture. Microbial processes including cometabolism induced by AOB growth, metabolism by AOB, cometabolism by HET growth and metabolism by HET were involved. Model calibration and validation were accomplished using pharmaceutical biodegradation experimental data at environmentally-relevant initial concentrations, demonstrating a good prediction performance of the developed model under different metabolic conditions and the reliability of the established model in predicting different pharmaceuticals biotransformation. The linear positive relationship between ammonia oxidation rate and pharmaceutical degradation rate confirmed the potential role of cometabolism induced by AOB in pharmaceutical removal. Dissolved oxygen (DO) was able

to regulate the pharmaceutical biotransformation cometabolically and the substrate competition between ammonium and pharmaceuticals existed especially at higher ammonium concentrations.

The outcomes of this thesis improve our understanding of the microbially induced metabolic types involved in the pharmaceutical biotransformation in enriched nitrifying sludge. Potential application of these insights into the fate of pharmaceuticals in engineered systems could help optimize their removal during wastewater treatment processes.

Declaration by author

This thesis is composed of my original work, and contains no material previously published or written by another person except where due reference has been made in the text. I have clearly stated the contribution by others to jointly-authored works that I have included in my thesis.

I have clearly stated the contribution of others to my thesis as a whole, including statistical assistance, survey design, data analysis, significant technical procedures, professional editorial advice, and any other original research work used or reported in my thesis. The content of my thesis is the result of work I have carried out since the commencement of my research higher degree candidature and does not include a substantial part of work that has been submitted to qualify for the award of any other degree or diploma in any university or other tertiary institution. I have clearly stated which parts of my thesis, if any, have been submitted to qualify for another award.

I acknowledge that an electronic copy of my thesis must be lodged with the University Library and, subject to the policy and procedures of The University of Queensland, the thesis be made available for research and study in accordance with the Copyright Act 1968 unless a period of embargo has been approved by the Dean of the Graduate School.

I acknowledge that copyright of all material contained in my thesis resides with the copyright holder(s) of that material. Where appropriate I have obtained copyright permission from the copyright holder to reproduce material in this thesis.

Publications during candidature

Peer-reviewed papers

- **Xu, Y.,** Yuan, Z. Ni, B.J. (2017). Impact of ammonium availability on atenolol biotransformation during nitrification. *ACS Sustainable Chemistry & Engineering*, 5 (8): 7137-7144.
- **Xu, Y.,** Yuan, Z., Ni, B.J. (2017). Biotransformation of acyclovir by an enriched nitrifying culture. *Chemosphere*, 170: 25-32.
- **Xu, Y.,** Radjenovic, J., Yuan, Z., Ni, B.J. (2017). Biodegradation of atenolol by an enriched nitrifying sludge: products and pathways. *Chemical Engineering Journal*, 312: 351-359.
- **Xu, Y.,** Yuan, Z., Ni, B.J. (2016). Biotransformation of pharmaceuticals by ammonia oxidizing bacteria in wastewater treatment processes. *Science of The Total Environment*, 566–567: 796-805.
- Wang, D., Wang, Q., Laloo, A., **Xu, Y.,** Bond, P.L., Yuan, Z. (2016). Achieving Stable Nitritation for Mainstream Deammonification by Combining Free Nitrous Acid-Based Sludge Treatment and Oxygen Limitation. *Scientific Reports*, 6: 25547.
- Peng, L., Chen, X., **Xu, Y.,** Liu, Y., Gao, S.H., Ni, B.J. (2015). Biodegradation of pharmaceuticals in membrane aerated biofilm reactor for autotrophic nitrogen removal: A model-based evaluation. *Journal of Membrane Science*, 494: 39-47.

Conference abstracts

- **Xu, Y.,** Radjenovic, J., Yuan, Z., Ni, B.J. (2016). Enhanced biodegradation of atenolol by an enriched nitrifying culture and fate of transformation products. IWA World Water Congress & Exhibition 2016, Brisbane, Australia. Oral presentation.
- **Xu, Y.,** Radjenovic, J., Yuan, Z., Ni, B.J. (2016). Enhanced atenolol biodegradation by enriched nitrifying sludge. International conference on Emerging Contaminants (EmCon 2016) and Micropollutants (WiOW2016) in the Environment, Sydney, Australia. Poster presentation.
- **Xu, Y.,** Yuan, Z., Ni, B.J. (2016). Biodegradation of acyclovir by an enriched nitrifying sludge. The 9th European Conference on Pesticides and Related Organic Micropollutants in the Environment and the 15th Symposium on Chemistry and Fate of Modern Pesticides, Santiago de Compostela, Spain. Oral Presentation.
- **Xu, Y.,** Radjenovic, J., Yuan, Z., Ni, B.J. (2015). Biodegradation of selected pharmaceuticals by an enriched nitrifying sludge. The University of Queensland-

Technical University of Munich-Research Symposium on Water, Environment and Sustainability, Munich, Germany. Oral Presentation.

Publications included in this thesis

Xu, Y., Radjenovic, J., Yuan, Z., Ni, B.J. (2017) Biodegradation of atenolol by an enriched nitrifying sludge: products and pathways. *Chemical Engineering Journal*, 312: 351-359. – incorporated as Appendix A.

Contributor	Statement of contribution
Author Xu, Y. (Candidate)	Designed research methodology and experiments (75%) Conducted experiments (100%) Data analysis (90%) Wrote and edited paper (80%)
Author Radjenovic, J.	Designed research methodology and experiments (10%) Data analysis (5%) Wrote and edited paper (5%)
Author Yuan, Z.	Designed research methodology and experiments (5%) Wrote and edited paper (5%)
Author Ni, B.J.	Designed research methodology and experiments (10%) Data analysis (5%) Wrote and edited paper (10%)

Xu, Y., Yuan, Z. Ni, B.J. (2017). Impact of ammonium availability on atenolol biotransformation during nitrification. *ACS Sustainable Chemistry & Engineering*, 5 (8): 7137-7144. – incorporated as Appendix B.

Contributor	Statement of contribution
Author Xu, Y. (Candidate)	Designed research methodology and experiments (85%) Conducted experiments (100%) Data analysis (95%) Wrote and edited paper (85%)
Author Yuan, Z.	Designed research methodology and experiments (5%) Wrote and edited paper (5%)
Author Ni, B.J.	Designed research methodology and experiments (10%) Data analysis (5%) Wrote and edited paper (10%)

Xu, Y., Yuan, Z., Ni, B.J. (2017). Biotransformation of acyclovir by an enriched nitrifying culture. *Chemosphere*, 170: 25-32. – incorporated as Appendix C.

Contributor	Statement of contribution
Author Xu, Y. (Candidate)	Designed research methodology and experiments (85%) Conducted experiments (100%) Data analysis (95%) Wrote and edited paper (85%)
Author Yuan, Z.	Designed research methodology and experiments (5%) Wrote and edited paper (5%)
Author Ni, B.J.	Designed research methodology and experiments (10%) Data analysis (5%) Wrote and edited paper (10%)

Contributions by others to the thesis

This thesis includes contributions made by others, particularly in the chemical analysis of wastewater and reactor samples. These contributions are acknowledged as follows:

Dr. Beatrice Keller-Lehmann, Jianguang Li and Nathan Clayton operated the high performance liquid chromatography coupled with mass spectrometry (HPLC-MS/MS) and flow injection analyzer (FIA) to analyse pharmaceuticals and the biotransformation products and dissolved nitrogen species.

Statement of parts of the thesis submitted to qualify for the award of another degree

None.

Acknowledgements

First and foremost, I owe my heartfelt gratitude and respect to my principal supervisor, Dr. Bing-Jie Ni, for his excellent guidance and help during my PhD study. Without his support, I might not get the scholarship and chance to pursue my PhD here. Without his continuous guidance, encouragement and support, I might not fulfil all the research objectives and finish this thesis successfully. His endeavour on teaching me how to set about a new study really helps me to get through the tough first year. He always provides insightful advice when I am working on my journal papers. Not only his professional skills but also his personality has impressed me and will benefit my future work and life.

I would like to extend my sincere gratitude to my co-supervisor, Prof. Zhiguo Yuan, for his valued advice and significant support especially in terms of scientific thinking and critical assessment on my own research. I am very grateful for his kind help during my application for PhD research in this great team. I am also impressed with his passion and rigorous attitude towards research every time we had a meeting together. His clear and deep thinking on the experiment results will definitely benefit my future career. I would like to deeply thank my co-supervisor, Dr. Jelena Radjenovic, who taught me lab skills and how to develop a comprehensive experimental plan. I learnt the most important analytical method and structural identification knowledge from her. I was also educated with some tiny but significant things, which are beneficial for my research habit. Although she didn't have much time after leaving Advanced Water Management Centre, I could still get help once I had problems.

My sincere thanks also goes to Ampon Chumpia and Markus Fluggen for their help in PLC strategy development and maintenance, to ASL team especially Beatrice Keller-Lehmann for their rigorous attitude and to Dr. Lai Peng and Dr. Qilin Wang for their tutoring and mentoring during my first year of PhD.

I am grateful to the AWMC academics, researchers, laboratory staff, administrative staff, students who offered so generous support and help. Thanks to them for making the centre an enjoyable and fun place to work. Thank you all my friends in Australia and China. Their continuous friendship and love have made my life full of happiness.

I am grateful to the generous financial support from Advanced Water Management Centre and University of Queensland International scholarship. This study was funded by the Australian Research Council and The University of Queensland.

Last but not least, I would give my biggest thanks to my family for your unconditional love and wise education and to my beloved girlfriend for your strong support and encouragement.

Keywords

Pharmaceutical, atenolol, acyclovir, nitrification, ammonia oxidizing bacteria, cometabolism, biotransformation product, biotransformation pathway, modeling

Australian and New Zealand Standard Research Classifications (ANZSRC)

ANZSRC code: 090703, Environmental Technologies, 60%
ANZSRC code: 090702, Environmental Engineering Modelling, 20%
ANZSRC code: 030101, Analytical Spectrometry, 20%

Fields of Research (FoR) Classification

FoR code: 0907, Environmental Engineering, 80%
FoR code: 0301, Analytical Chemistry, 20%

Table of Contents

List of Figures & Tables

List of Abbreviations used in the thesis

AOA	Ammonia oxidizing archaea
AOB	Ammonia oxidizing bacteria
AMO	Ammonia monooxygenase
ATU	Allylthiourea
ASM	Activated Sludge Model
BP	Biotransformation product
COD	Chemical oxygen demand
DO	Dissolved oxygen
EE2	17α-ethinylestradiol
FIA	Flow injection analyzer
FISH	Fluorescence *in-situ* hybridization
HAO	Hydroxylamine oxidoreductase
HET	Heterotrophs
HRT	Hydraulic retention time
LC/MS-MS	Liquid chromatography coupled to tandem mass spectrometry
MBR	Membrane bioreactor
MLSS	Mixed liquid suspended solids
MLVSS	Mixed liquid volatile suspended solids
MRM	Multiple reaction monitoring
NOB	Nitrite oxidizing bacteria
OP	Other biotransformation products
PC	Parent compound
PLC	Programmable logic controllers
PNEC	Predicted no effect concentrations
QqQLIT-MS	Hybrid triple quadruple-linear ion trap mass spectrometer
SBR	Sequencing batch reactor
SPE	Solid phase extraction
SRT	Solid retention time
TKN	Total Kjedahl nitrogen
UFLC	Ultra-fast liquid chromatography
WWTP	Wastewater treatment plant

Chapter 1 Introduction

1.1 Background

During last decades, the ubiquitous occurrence of micropollutants such as pharmaceutical residues in the environment has attracted concerns due to their potential hazardous effects on ecosystems and public health (Daughton and Ternes, 1999; Luo et al., 2014; Petrie et al., 2015). Wastewater treatment plants (WWTPs) were deemed as the major pathway for these emerging contaminants entering into the environment, as the incomplete removal efficiencies were reported in extensive studies (Pomiès et al., 2013; Rivera-Utrilla et al., 2013; Ternes, 1998). Regarding the contribution from different sources to the occurrence of pharmaceuticals in the environment, human excretion and hospital discharge accounted for over 90% of pharmaceuticals entering the domestic wastewater while improper disposal and manufacturer discharge constituted less than 5-10 % (Caldwell, 2016). Other minor sources include animal feeding operations, land-applied bio-solids, row-crop production, on-site wastewater disposal systems, recreational activities, transportations or wash-off from roadways and atmospheric deposition (Tijani et al., 2013). Although the wastewater treatment processes were not designed originally for pharmaceutical removal, it is still of great importance to understand the fate and transformation of pharmaceuticals in the biological treatment stage.

Removal efficiencies of pharmaceuticals were reported to be dependent on the physico-chemical properties of the compounds and on the operating parameters of the WWTPs (Rivera-Utrilla et al., 2013). A significant association between pharmaceutical biotransformation rates and nitrification activities of nitrifying activated sludge during biological treatment processes was extensively reported in previous literature (Batt et al., 2006; Clara et al., 2005a; Helbling et al., 2012). Ammonia oxidizing bacteria (AOB) in the nitrifyign activated sludge might be responsible to cometabolically degrade pharmcauticals, due to its non-specific enzyme ammonia monooxygenase (AMO) with a broad substrate spectrum ranging from alimatic to aliphatic compounds (Skotnicka-Pitak et al., 2009; Tran et al., 2009; Yi and Harper Jr, 2007). The presence of growth substrate ammonium was necessary for AOB to induce cometabolic biodegradation (Tran et al., 2013). Heterotrophs (HET) were also recognized to be able to degrade pharmaceuticals alone or together with AOB (Gaulke et al., 2008; Khunjar et al., 2011), mainly via metabolism (Tran et al., 2013). However, little information is available in understanding the relative contributions of metabolism and cometabolism from responsible microorganisms in the nitrifying activated sludge to pharmaceutical biotransformation. Furthermore, the biotransformation products yielded from pharmaceuticals during biological treatment might be more toxic and persistent than the parent compounds (Miao and Metcalfe, 2003;

Quintana et al., 2005). Therefore, a better understanding of the fate of pharmaceuticals in the treatment processes should consider their biotransformation products.

Mathematical modeling offers a useful tool and is adopted widely to analyse complicated metabolic pathways. Cometabolic biotransformation was previously modeled through first-order kinetics and mixed order kinetics such as Monod expression (Fernandez-Fontaina et al., 2014; Liu et al., 2015; Oldenhuis et al., 1989), which have evolved from only considering the cometabolic substrates to incorporating the relationships between cometabolic substrates and growth substrates, such as competitive interaction and toxicity inhibition (Liu et al., 2015). However, the previous literature has rarely considered the formation of biotransformation products in the cometabolic biotransformation models for pharmaceuticals. An accurate and more comprehensive model was indeed required to provide regulators to fully understand the fate of pharmaceuticals, to evaluate the release of these compounds to the environment and thus to optimize or modify the existing wastewater treatment technologies for more efficient mitigation.

1.2 Thesis objectives

The aim of this PhD thesis is to investigate the biotransformation of typical pharmaceuticals by an enriched nitrifying culture under different metabolic conditions, in terms of the biotransformation products and pathways as well as process modeling. In particular, two compounds atenolol and acyclovir were selected as the model compound in this thesis, which were frequently found in the wastewater with the highest concentrations of 25 and 1.8 μg L^{-1}, respectively and reported to be increasingly removed under nitrification (Prasse et al., 2010; Sathyamoorthy et al., 2013; Verlicchi et al., 2012), to investigate the effect of metabolic type (i.e., metabolism or cometabolism) on the formation of biotransformation products. The impact of growth substrate ammonium was also studied on atenolol biodegradation and the formation of its transformation product. Furthermore, a comprehensive model was developed as part of the work to describe and predict the fate of the pharmaceutical and its biotransformation product in the enriched nitrifying sludge.

1.3 Thesis organization

This thesis is organised into four chapters and four appendices. Chapter 1 gives a general introduction to the background, objectives and organization of this thesis. Chapter 2 presents a comprehensive literature review. Firstly, the occurrence and removal of pharmaceuticals in the wastewater treatment processes were briefly introduced. Secondly, the effect of nitrification and the role of AOB on pharmaceutical removal was summarised. Thirdly, the possible biodegradation mechanisms of pharmaceutical by respective microorganisms were presented. This is then followed by the review on

the current proceedings on the formation of biotransformation products of pharmaceuticals. Lastly, the mathematical modeling of the fate of pharmaceuticals was reviewed. Chapter 3 consists of three sections, namely Research Objectives, Research Methods and Results and Discussion. Sections within this chapter are summaries and descriptions of the detailed investigations described in the papers/manuscripts presented as Appendix A to D. It provides an overview of the research undertaken as part of this thesis. Chapter 4 summarises the significant conclusions and promising prospects achieved from this work and the recommendations for further research.

The four appendices are papers and manuscripts containing the detailed experimental studies for the research objectives outlined and summarised in Chapter 3. Appendix A describes the enhanced biodegradation of atenolol by the enriched nitrifying sludge focusing on its biotransformation products and pathways under different metabolic conditions. Appendix B presents the investigation on the effect of ammonium concentrations on the biodegradation of atenolol at relatively realistic concentration and the formation of its biotransformation product, atenolol acid. Appendix C reports the effect of initial concentration and the role of microorganisms on the biotransformation of acyclovir by the enriched nitrifying culture. Appendix D shows the development of a comprehensive model to predict the fate of selected pharmaceuticals (i.e., atenolol and acyclovir) and their transformation products during nitrification processes.

Chapter 2 Literature review

For recent decades, one of the key issues in the aquatic environment is the emerging problem of micropollutants such as pharmaceuticals, personal care products, hormones, detergents and disinfectants due to their potential risk on the ecosystem (Daughton and Ternes, 1999; Heberer and Feldmann, 2005). Pharmaceutically active compounds are complex chemicals with different physicochemical and biological properties designed for different purposes. According to their therapeutical class, pharmaceuticals could be classified into several groups including antibiotics, anti-inflammatories, lipid regulators, psychiatric drugs, X-ray contrast media, β-blockers and etc. As the ubiquitous, persistent and biologically active substances, pharmaceuticals have provoked increasing concerns among other micropollutants although the directives and legal frameworks are not set-up yet. The occurrence of pharmaceuticals could affect water quality and potentially harm ecosystem and human health (Rivera-Utrilla et al., 2013; Sirés and Brillas, 2012; Yuan et al., 2009), especially for those pharmaceutical compounds with concentrations higher than predicted no effect concentrations (PNECs) (Verlicchi et al., 2012). Pharmaceuticals had the highest risk quotient compared to other micropollutants based on Lake Geneva investigations (Hoerger et al., 2014).

Reports indicated that the consumption of pharmaceuticals could vary considerably from country to country and over time (Goossens et al., 2007). The excretion by humans and animals are main sources for pharmaceuticals in the environment. After administration into the human body, the pharmaceuticals could be metabolized in the liver to different degrees and excreted as changed or unchanged forms in urine and faeces (Jones et al., 2005). Veterinary medicine and their metabolites are excreted with manure used to fertilize fields. Other sources of pharmaceuticals may come from the manufacturers, hospitals and illicit uses (Heberer and Feldmann, 2005; Li et al., 2008; Mackuľak et al., 2014).

Pharmaceuticals were ubiquitously present in wastewater, surface water and groundwater with concentrations ranging from a few nano-gram per litre to several hundred micro-gram per litre (Alder et al., 2010; Phillips et al., 2015; Verlicchi et al., 2012). As pharmaceuticals are persistent and biologically active compounds, they could pose a potential threat to wildlife. In the recent years, the effects on aquatic organisms have been studied extensively. Some pharmaceuticals were found at higher concentrations in river biota than their PNECs (Santos et al., 2009). Endocrine disrupting effects of pharmaceuticals and estrogens have been reported in the effluent and surface water at concentrations as low as nano-gram per litre (Desbrow et al., 1998).

2.1 Occurrence and removal of pharmaceuticals in wastewater treatment

WWTPs were one of the main routes for pharmaceuticals to enter into the environment due to the incomplete removal in treatment processes (Ternes, 1998). Pharmaceuticals were detected in the raw wastewater at concentrations from ng L^{-1} to μg L^{-1} according to their usage and properties. Table 1 lists the reported concentrations of selected pharmaceuticals in the WWTP influents in the literature.

Table 1. Occurrence of pharmaceuticals in the influents of WWTPs

Pharmaceuticals	Reported concentration range and mean value (μg L^{-1})
Analgesics and anti-inflammatories	
Acetaminophen	0.13-26.09, 10.19[a]; 29-246, 134[b]
Diclofenac	0.05-0.54, 0.25[a]; 3.02[c]; 0.204[d]
Ibuprofen	53.48-373.11, 150.73[e]; 34-168, 84[b]; 8.45[d]; 23.4[f]
Ketoprofen	0.108-0.369, 0.208[g]; 0.146[d]; 2.9[f]; 0.16-0.97, 0.451[a]
Naproxen	0.038-0.23, 0.1[g]; 1.8-4.6[h]; 8.6[f]; 5.58[d]
Antibiotics	
Sulfamethoxazole	ND-0.87, 0.59[a]; 0.58[h]
Trimethoprim	ND-4.22, 1.17[a]
β-blockers	
Atenolol	ND-0.74, 0.395[a]; 0.971[i]; 0.03[j]
Metoprolol	0.411[i]; 0.16[j]
Propranolol	0.08-0.29, 0.168[a]; 0.01[i]; 0.05[j]
Sotalol	0.12-0.2, 0.167[a]; 0.529[i]
Lipid regulators	
Bezafibrate	1.55-7.60[k]; 2.2[f]; 1.2[l]
Clofiric acid	ND-0.11, 0.072[a]; 1.0[l]; 10-170[m]
Gemfibrozil	0.453[d]; ND-0.36, 0.155[a], 0.71[j]
Psychiatric drugs	
Caffeine	52-192, 118[b]
Carbamazepine	0.015-0.27, 0.054[g]; ND-0.95, 0.42[a]; 0.12-0.31, 0.15[b]; 1.68[j]
X-ray contrast media	
Iopromide	6.0-7.0, 6.6[h]; 0.026-3.84[k]; 7.5[n]
Antiviral drugs	
Acyclovir	1.78[o]; 0.10-1.81[p]

[a](Gros et al., 2006), [b](Gómez et al., 2007), [c](Pham and Proulx, 1997), [d](Lishman et al., 2006), [e](Santos et al., 2007), [f](Vieno et al., 2005), [g](Nakada et al., 2006), [h](Carballa et al., 2004), [i](MacLeod et al., 2007), [j](Bendz et al., 2005), [k](Clara et al., 2005b), [l](Stumpf et al., 1999), [m](Soulet et al., 2002), [n](Ternes and Hirsch, 2000), [o](Prasse et al., 2010), [p](Yu et al., 2012). ND, not detected.

The occurrence of pharmaceuticals in the influent is related to the specific areas in each country. The highest influent loads from seven WWTPs in Spain were found for non-steroidal anti-inflammatory drugs (NSAIDs), lipid regulators, β-blockers and histamine H1- and H2- receptor antagonists (Gros et al., 2007). The results of a study in Italy indicated high inputs of antibiotics, atenolol, ranitidine, diuretics and ibuprofen (Castiglioni et al., 2006). A review by Verlicchi et al (Verlicchi et al., 2012) was conducted on the occurrence of 118 pharmaceuticals belonging to 17 different classes in 78 peer-reviewed papers worldwide. The most abundant pharmaceuticals were NSAIDs including the most commonly investigated compounds ibuprofen (37 μg L^{-1}), acetaminophen (38 μg L^{-1}), naproxen (6 μg L^{-1}), carbamazepine (1.2 μg L^{-1}), sulfamethoxazole (0.96 μg L^{-1}) and diclofenac (0.8 μg L^{-1}) in the WWTP influent.

While WWTPs are not designed for the removal of pharmaceuticals, these compounds could be mainly removed by biological treatment processes at an insufficient rate ranging from insignificant (e.g., <10%, carbamazepine) to >90% (e.g., ibuprofen) (Joss et al., 2005). Figure 1 shows the removal efficiencies of the most studied pharmaceuticals in 14 countries/regions (Luo et al., 2014). The varied removal efficiencies were likely due to the different physical-chemical properties and the variable operating parameters of wastewater treatment processes. A simple classification scheme for pharmaceuticals was proposed according to the degradation constant k_{bio} (Joss et al., 2006): (i) compounds with k_{bio} <0.1 L g VSS^{-1} d^{-1} are not removed to a significant extent (20%); (ii) compounds with k_{bio} >10 L g VSS^{-1} d^{-1} can be transformed by >90%; and (iii) compounds with a moderate biodegradability (0.1< k_{bio} <10) showed a partial removal. The degradation rate was assumed to follow pseudo-first order kinetics based on a series of batch experiments using activated sludge from nutrient eliminating municipal wastewater treatment plants. These intervals may be variable amongst different sludge types and reactor configurators.

According to therapeutic classes and usage of pharmaceuticals, the average removal efficiencies of anti-inflammatories were between 23% (e.g., tramadol) and 99% (e.g., acetaminophen) and the antibiotics could be removed between 0% (e.g., spiramycin) and 98% (e.g., cefachlor) during the typical wastewater treatment processes (Verlicchi et al., 2012). Bezafibrate, gemfibrozil and clofibric acid were most frequently reported lipid regulators with the removal efficiencies of 11-100%, 57-79% and 0-80%, respectively (Castiglioni et al., 2006; Jelić et al., 2012; Kasprzyk-Hordern et al., 2009;

Kosma et al., 2014; Miège et al., 2008). The psychiatric drug carbamazepine exhibited lower average removal efficiencies during wastewater treatment processes (Petrie et al., 2015). The negative values were also found due to enzymatic cleavage of its conjugated forms (Radjenovic et al., 2007; Vieno et al., 2007). For β-blockers, it was found that the removal efficiencies were ranging from 45 to 92% for atenolol, 59 to 75% for sotalol and 0 to 26% for metoprolol (Vieno et al., 2006).

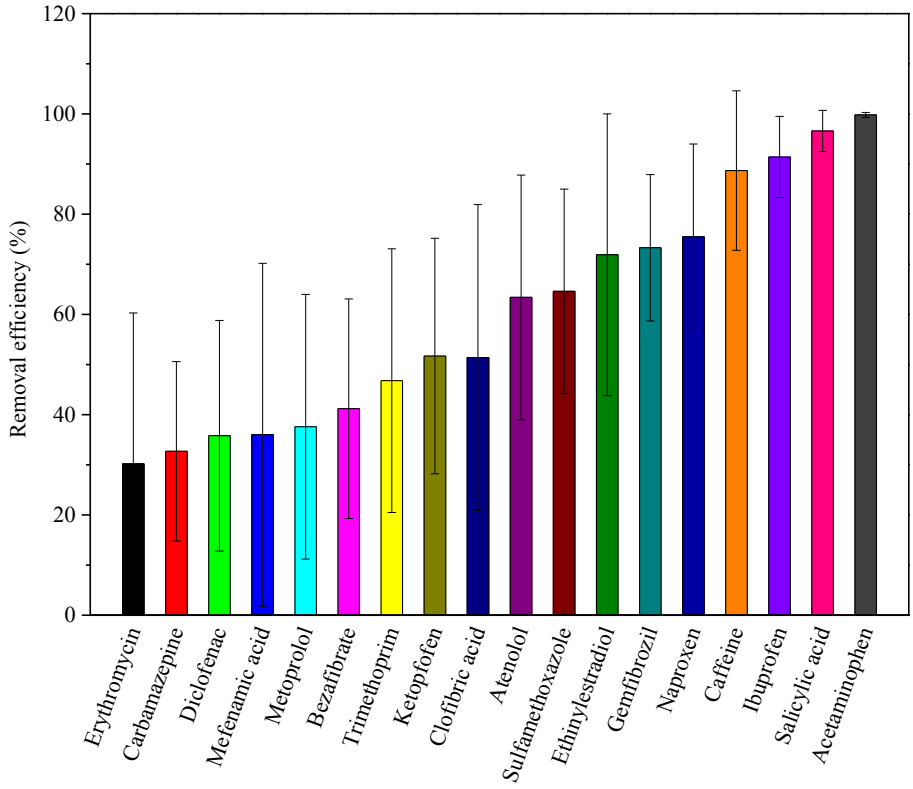

Figure 1. Removal efficiencies of the typical pharmaceuticals in wastewater treatment processes (based on (Luo et al., 2014)).

2.2 Pharmaceutical removal by AOB during nitrification

Nitrification is an important process in the wastewater treatment designed for nitrogen removal. Wastewater treatment plant influents always contain nitrogen in the forms of organic nitrogen and ammonia (Total Kjedahl Nitrogen, TKN). TKN can be converted into inorganic nitrogen (nitrite and nitrate) and nitrogen gas through a combination of aerobic and anaerobic treatment processes. In WWTPs, the processes commonly used for nitrogen removal include nitrification and denitrification. Nitrification is the biological oxidation of ammonium to nitrite and nitrate occurring in two steps, which initiate the removal of nitrogen compounds in the nitrogen cycle. In the first step, AOB and ammonia oxidizing archaea (AOA) take up the role of converting NH_4^+ to NO_2^-. The ammonia oxidizing microorganisms are generally dominated by AOB in municipal WWTPs while AOA have been found in some municipal and industrial WWTPs (Gao et al., 2013; Limpiyakorn et al., 2013;

Men et al., 2017). It was reported that some HET, fungi and autotrophic anammox bacteria could also oxidize ammonia (Suneethi and Joseph, 2011; Zhang et al., 2012). In the second step, nitrite oxidizing bacteria (NOB) is the key microorganism to oxidize NO_2^- to NO_3^- (Gao et al., 2013). In the conversion of ammonia to nitrite, two key enzymes are involved. AMO catalyzes the oxidation of ammonia to hydroxylamine (NH_2OH) and hydroxylamine oxidoreductase (HAO) is for the oxidation of hydroxylamine to nitrite. Complete conversion of ammonia into nitrate in one organism was recently found within two *Nitrospira* species, containing different AMO enzymes from the currently identified ones (van Kessel et al., 2015). Nitrosomonas and Nitrosospira were mostly considered as the dominant species of the AOB β-proteobacteria in different activated sludge (Baek et al., 2010) whereas the abundance of AOA was much lower than AOB based on analysis of amoA gene copy number (Zhang et al., 2011). Limited studies of AOA species in activated sludge indicated a composition difference from those in soil, water column and sediment (Park et al., 2006).

Nitrification could enhance pharmaceutical removal during treatment processes. Table 2 showed that the wastewater treatment processes with significant nitrification tend to have higher removal rates of pharmaceuticals than those without nitrification (Miège et al., 2008; Servos et al., 2005), especially for 17α-ethinylestradiol (EE2) (Layton et al., 2000; Vader et al., 2000). A positive linear relationship was found between the nitrifying activity and the removal of ibuprofen, erythromycin and roxithromycin, while no correlation was found with the heterotrophic rate (Alvarino et al., 2014). It was also demonstrated that the effluent concentration and removal of ammonium showed significant associations with overall target pharmaceuticals removal (Helbling et al., 2012).

With regard to the microorganism level, the relationship between AOB and pharmaceutical removal has been studied in both pure cultures and mixed communities such as activated sludge. The role of AOB could be suggested by the higher removal rates with nitrification as well as the significant decrease with the addition of allylthiourea (ATU) to inhibit AOB activity (Figure 2). The removal of EE2 corresponded well with ammonia oxidizing activity when AMO was enriched in the pure AOB culture (*Nitrosomonas europaea*) (Khunjar et al., 2008). Higher rates obtained in the enriched nitrifying cultures compared with those in the presence of ATU also proved the contribution of AOB on removal of fenoprofen, indomethacin, diclofenac, carbamazepine and propyphenazone (Tran et al., 2009). Similarly, null removal was observed for sulfamethoxazole, ibuprofen in the presence of ATU (Kassotaki et al., 2016; Roh et al., 2009).

Table 2. The removal efficiencies of pharmaceuticals with and without nitrification during wastewater treatment processes

Pharmaceuticals	With nitrification (%)	Without nitrification (%)	Reference
Iopromide	61	-	(Batt et al., 2006)
Trimethoprim	50	1	(Batt et al., 2006)
Naproxen	60	35	(Margot et al., 2016)
Gemfibrozil	41	9	(Maeng et al., 2013)
Diclofenac	21	1	(Maeng et al., 2013)
Bezafibrate	92	56	(Maeng et al., 2013)
Ketoprofen	63	10	(Maeng et al., 2013)
Clofibric acid	6	2	(Maeng et al., 2013)
Carbamazepine	6	-	(Maeng et al., 2013)
Pentoxifylline	88	69	(Maeng et al., 2013)
Ibuprofen	100	75	(Tran et al., 2009)
Fenoprofen	93.7	36	(Tran et al., 2009)
Indomethacin	89	14	(Tran et al., 2009)
Ketoprofen	90	38	(Tran et al., 2009)
Gemfibrozil	87	37	(Tran et al., 2009)
Naproxen	73	30	(Tran et al., 2009)
Diclofenac	76	25	(Tran et al., 2009)
Carbamazepine	38	12	(Tran et al., 2009)
Propyphenazone	39	5	(Tran et al., 2009)
Clofibric acid	15	6.2	(Tran et al., 2009)
Sulfamethoxazole	86	0	(Kassotaki et al., 2016)

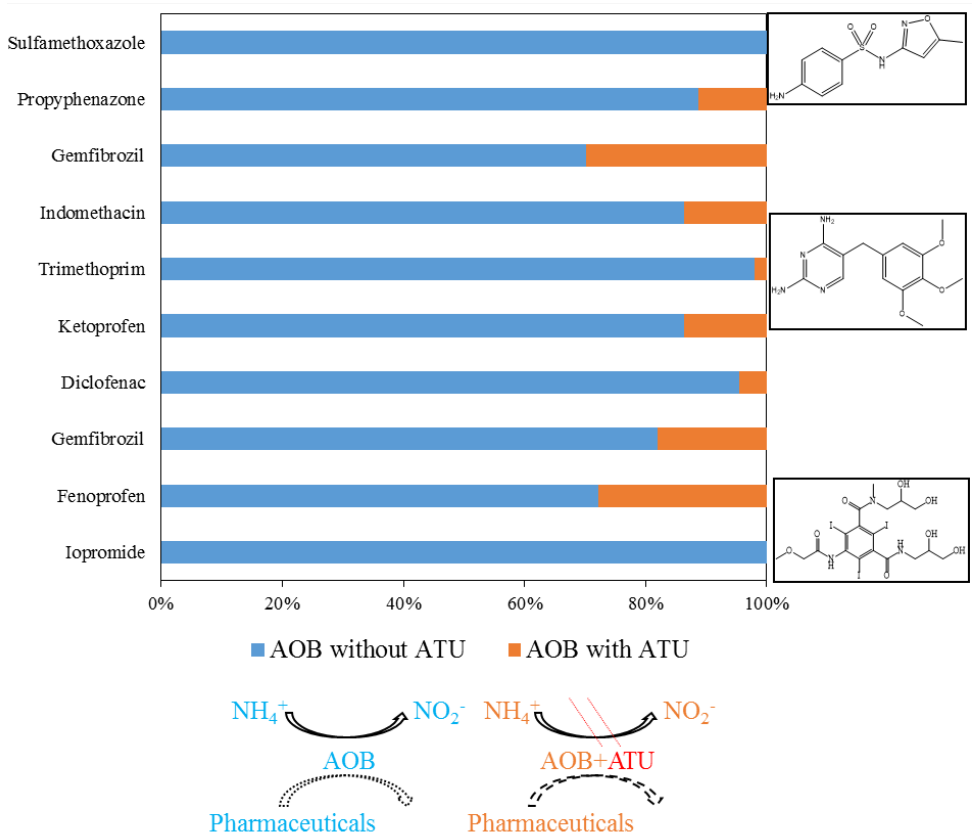

Figure 2. The comparison of pharmaceutical biodegradation by AOB (ammonia oxidizing bacteria) with and without ATU (allylthiourea) addition.

2.3 Biodegradation mechanisms of pharmaceuticals

Microorganisms in the treatment processes could utilize pharmaceuticals either in metabolic way (metabolism) or in cometabolic way (cometabolism) as shown in Figure 3. The mechanism that pharmaceuticals are used as primary substrates to support cell growth and energy consumption is called metabolism. HET are the main responsible microorganisms involved in metabolism pathway. Ketoprofen, acetaminophen, 17β-estradiol and ibuprofen were previously reported to be degraded by the corresponding microorganisms such as *Delftia tsuruhatensis*, *Pseudomonas aeruginosa*, and *Sphingomonas* Ibu-2 (De Gusseme et al., 2011; Iasur-Kruh et al., 2011; Murdoch and Hay, 2005; Quintana et al., 2005; Zeng et al., 2009). On the other hand, pharmaceuticals are usually present in the level of μg L^{-1} or ng L^{-1} in wastewater systems, with some of them being toxic to the microorganisms. Thus these pharmaceutically active compounds could rarely be utilized as the sole carbon source through metabolic biodegradation by microorganisms. The key pathway for their removal is via cometabolic biodegradation. Pharmaceuticals could be biodegraded by the corresponding microorganisms in the presence of growth substrate like easily degradable compounds or nutrients. Bezafibrate, naproxen and ibuprofen showed different degrees of transformation and

mineralization at the presence of external carbon source while they were not degraded metabolically (Quintana et al., 2005).

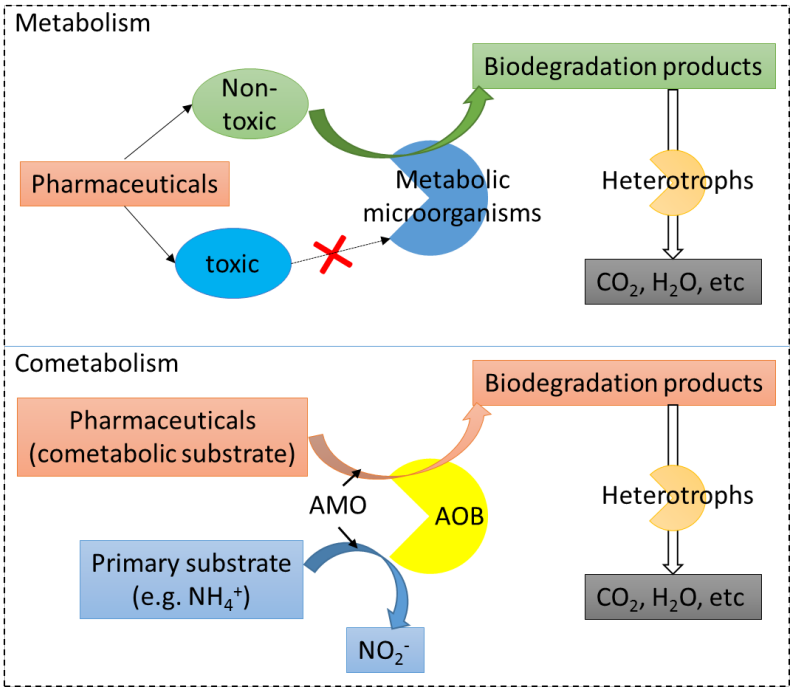

Figure 3. Metabolic and cometabolic pathways of pharmaceuticals biodegradation. AOB, ammonia oxidizing bacteria; and AMO, ammonia monooxygenase.

The biodegradation of pharmaceuticals by AOB was reported to follow the cometabolic pathway with ammonium being used as the primary substrate and energy source for microbial growth and enzyme induction (Figure 3). During the nitrification process, AOB take the role of converting NH_4^+ to NO_2^-, which is able to degrade a broad range of aromatic compounds through cometabolic biodegradation likely due to its non-specific enzyme AMO (Keener and Arp, 1994; Skotnicka-Pitak et al., 2009), such as hydrocarbons, phenol and aromatic compounds (Keener and Arp, 1993; Keener and Arp, 1994; Lauchnor and Semprini, 2013; Rasche et al., 1990). A significant association was found among archaeal *amoA* and ammonia oxidation rate as well as oxidative micropollutant biotransformation reaction rates (Helbling et al., 2012). AOB were also reported to transform pharmaceuticals under ammonium starvation conditions (Dawas-Massalha et al., 2014; Forrez et al., 2009). This seems to be a general catabolic repression mechanism for cometabolism when the high concentration of ammonium competitively inhibited cometabolic biotransformation until ammonia was depleted (Dawas-Massalha et al., 2014). Therefore, in order to obtain maximum cometabolic degradation rate of pharmaceuticals, the concentration ratio between pharmaceuticals and ammonia should be maintained within a certain range.

The important role of AOB in pharmaceutical biodegradation has been revealed by several pure cultures studies. The biotransformation of some micropollutants has been observed to be positively associated with ammonia oxidation activities and the transcript abundance of the archaeal ammonia monooxygenase gene (amoA) in nitrifying culture (Men et al., 2016). *Nitrosomonas europaea* has been used as the pure AOB culture to study its ability to degrade typical micropollutants including triclosan, bisphenol, ibuprofen, EE2, and trimethoprim (Khunjar et al., 2011; Roh et al., 2009). Although the responsible enzyme AMO was not substrate-specific, the pure AOB culture showed different degradation performance on different compounds. More recently, the capabilities of AOA pure cultures (*Nitrososphaera gargensis*) to biotransform micropollutants has also been assessed. *Nitrososphaera gargensis* was showed to be able to biotransform mianserin and ranitidine, exhibiting similar compound specificity as two AOB strains that were tested for comparison. The same biotransformation reactions were carried out by both the AOA and AOB strains (Men et al., 2016) and the biotransformation only occurred when ammonia oxidation was active, strongly indicated the key role of AMO in cometabolic transformations of pharmaceuticals. In addition, the mixed culture nitrifying sludge also showed the strong abilities to transform these compounds (Khunjar et al., 2011; Tran et al., 2009; Yu et al., 2007).

Biodegradation of pharmaceuticals generally follows the first-order kinetics (Helbling et al., 2012) or pseudo first-order kinetics (Joss et al., 2006; Suarez et al., 2010). Figure 4 shows the biodegradation of pharmaceuticals by the activated sludge from ten different wastewater treatment plants, with five of them applying nitrification. According to the parameter estimations based on the first-order kinetics, the calculated biodegradation rates of most pharmaceuticals with nitrification were clearly higher than those without nitrification (100 times at most for trinexepac over the rate without nitrification) (Helbling et al., 2012). The higher kinetic rates observed in enriched nitrifying cultures for atenolol, trimethoprim and sulfamazoxale compared to the kinetics in the presence of ATU further confirmed the important role of AOB in pharmaceuticals biotransformation mainly due to the cometabolic biodegradation (Batt et al., 2006; Kassotaki et al., 2016; Sathyamoorthy et al., 2013).

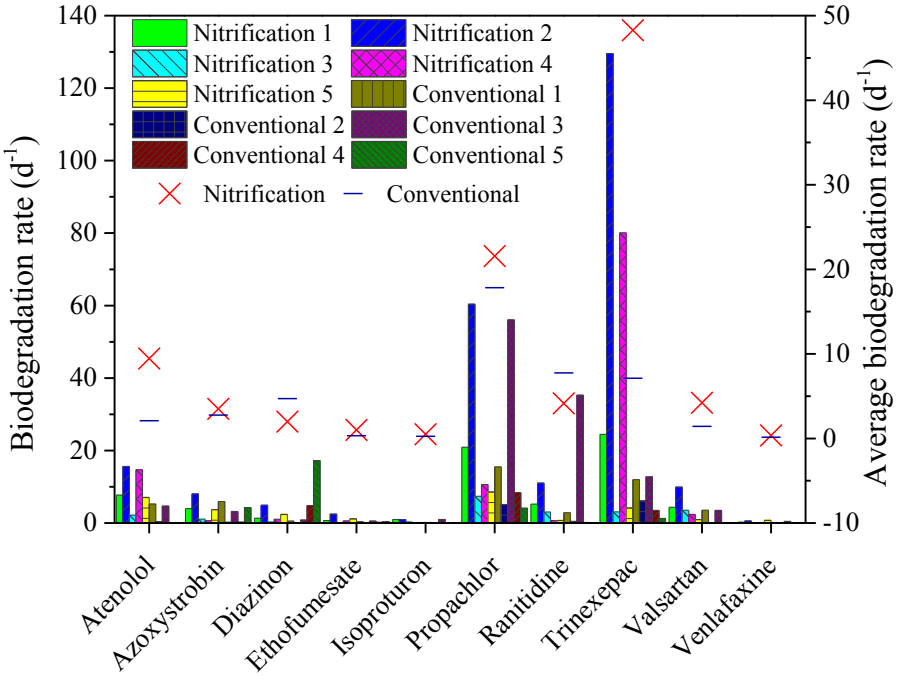

Figure 4. The biodegradation rates of selected pharmaceuticals in the investigated wastewater treatment processes. The red cross and the blue line indicate the average value of the biodegradation rate during nitrification and conventional treatment processes, respectively (based on (Helbling et al., 2012)).

Table 3 lists the biodegradation rate constants obtained and/or calculated from the literature to highlight the effect of cometabolism by AOB. Although the inoculum/activated sludge and the experimental conditions were various among these literature, it could be roughly concluded that the cometabolic biodegradation rate constants were significantly higher than the metabolic biodegradation rate constants for majority of the pharmaceuticals studied. The cometabolic biodegradation rates of ibuprofen, naproxen and trimethoprim were increased with the increasing nitrogen loading rate, which increased the biological activity of AOB producing more AMO (Fernandez-Fontaina et al., 2012). The cometabolic biodegradation rate constants were also dependent on the consumption rate of growing substrate (e.g. ammonium), which is the energy source for AOB.

Table 3. The cometabolic and metabolic biodegradation rate constants of typical pharmaceuticals in literature

Pharmaceuticals	Cometabolism	Metabolism
Ibuprofen	36 L g VSS^{-1} d^{-1} (10 d^{-1}) (Fernandez-Fontaina et al., 2012)	1.22 d^{-1} (Murdoch and Hay, 2005)

	2.43-3.01 L g VSS^{-1} d^{-1} (1.82-2.26 d^{-1}) (Tran et al., 2009)	0.53 d^{-1} (Urase and Kikuta, 2005)
Naproxen	19 L g VSS^{-1} d^{-1} (5.32 d^{-1}) (Fernandez-Fontaina et al., 2012)	0.084 L g VSS^{-1} d^{-1} (0.063 d^{-1}) (Tran et al., 2009) 0.012 d^{-1} (Urase and Kikuta, 2005)
Trimethoprim	6.5 L g VSS^{-1} d^{-1} (1.82 d^{-1}) (Fernandez-Fontaina et al., 2012)	0.073 d^{-1} (Khunjar et al., 2011)
Acetaminophen	1.3 L g VSS^{-1} d^{-1} (1 d^{-1}) (De Gusseme et al., 2011)	0.81 L g VSS^{-1} d^{-1} (0.61 d^{-1}) (De Gusseme et al., 2011)
Clofibric acid	0.04-0.09 L g VSS^{-1} d^{-1} (0.03-0.07 d^{-1}) (Tran et al., 2009)	0.009 L g VSS^{-1} d^{-1} (0.036 d^{-1}) (Urase and Kikuta, 2005)
Indomethacin	1.52-2.16 L g VSS^{-1} d^{-1} (1.14-1.62 d^{-1}) (Tran et al., 2009)	0.022 L g VSS^{-1} d^{-1} (0.017 d^{-1}) (Tran et al., 2009)
Gemfibrozil	1.35-2.45 L g VSS^{-1} d^{-1} (1.01-1.84 d^{-1}) (Tran et al., 2009)	0.099 L g VSS^{-1} d^{-1} (0.074 d^{-1}) (Tran et al., 2009)
Fenoprofen	1.57-2.23 L g VSS^{-1} d^{-1} (1.18-1.67 d^{-1}) (Tran et al., 2009)	0.083 L g VSS^{-1} d^{-1} (0.062 d^{-1}) (Tran et al., 2009)
Ketoprofen	0.91-2.12 L g VSS^{-1} d^{-1} (0.68-1.59 d^{-1}) (Tran et al., 2009)	0.10 L g VSS^{-1} d^{-1} (0.078 d^{-1}) (Tran et al., 2009)
Diclofenac	0.41-0.69 L g VSS^{-1} d^{-1} (0.31-0.52 d^{-1}) (Tran et al., 2009)	0.064 L g VSS^{-1} d^{-1} (0.048 d^{-1}) (Tran et al., 2009)
Propyphenazone	0.11-0.23 L g VSS^{-1} d^{-1} (0.08-0.17 d^{-1}) (Tran et al., 2009)	0.014 L g VSS^{-1} d^{-1} (0.010 d^{-1}) (Tran et al., 2009)
Carbamazepine	0.09-0.19 L g VSS^{-1} d^{-1} (0.07-0.14 d^{-1}) (Tran et al., 2009)	0.028 L g VSS^{-1} d^{-1} (0.021 d^{-1}) (Tran et al., 2009)

Experimental conditions:

- Nitrifier enrichment culture inoculated in an membrane bioreactor (MBR) with 100 μg L^{-1} acetaminophen in the influent. Batch experimens were conducted using the MBR biomass to study the degradation of acetaminophen under nitrification or without nitrification (De Gusseme et al., 2011).
- Biomass from nitrification/denitrification tanks of a sewage treatment plant as inoculum. Synthetic feeding in order to develop autotrophic nitrifying biomass with pharmaceuticals (80-320 μg L^{-1}) introduced (Fernandez-Fontaina et al., 2012).
- Biodegradation of trimethoprim was evaluated with pure AOB culture, enriched heterotrophic cultures without nitrifier activity and nitrifying activated sludge (Khunjar et al., 2011).
- Ibuprofen was used as a sole carbon and energy source by one isolated environmental bacteria from a wastewater

treatment plant (Murdoch and Hay, 2005).

- Batch degradation experiments were conducted with enriched nitrifying cultures under various initial conditions such as in the presence of different growth substrates and the inhibitors (Tran et al., 2009).
- A laboratory scale activated sludge reactor with initial pharmaceuticals of 100 μg L^{-1} (Urase and Kikuta, 2005).

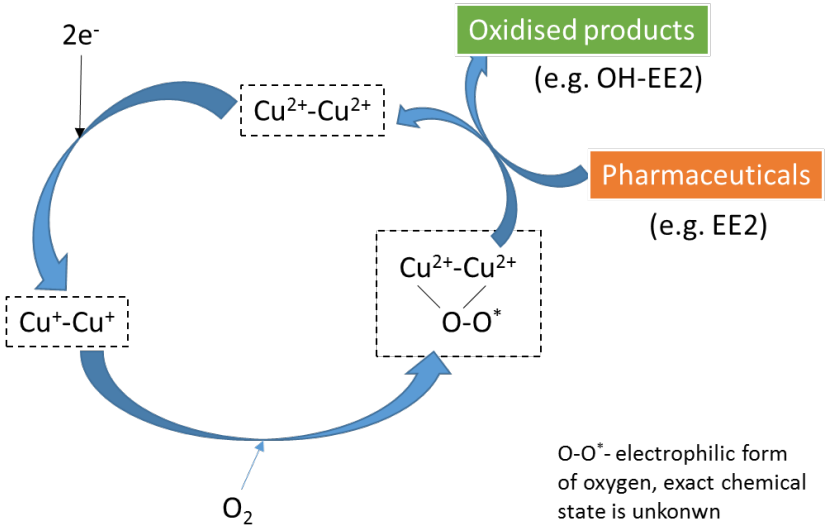

Figure 5. A mechanistic model for AMO role in cometabolic transformation of pharmaceuticals (based on (Yi and Harper Jr, 2007)): the active site of AMO contains copper ions. Oxygen will react to convert Cu^{+}-Cu^{+} into Cu^{2+}-Cu^{2+} under aerobic condition while the oxygen remains bound as O_2^{-}. The oxygenated form of AMO will react with pharmaceuticals to produce Cu^{2+}-Cu^{2+} and the biotransformation products.

A mechanistic model was proposed for AMO role in cometabolic transformation of EE2 as shown in Figure 5 (Yi and Harper Jr, 2007). The active site of AMO contains metal ions such as copper ions. Oxygen will react to convert Cu^{+}-Cu^{+} into Cu^{2+}-Cu^{2+} under aerobic condition while the oxygen remains bound as an electrophilic radical. The oxygenated form of AMO will react with EE2 to produce Cu^{2+}-Cu^{2+} and the biotransformation products. However, this conceptual model was proposed solely based on monooxygenase. The dioxygenase may also need to be considered in pharmaceuticals biodegradation mechanism as this enzyme is also functional in the cometabolic or metabolic biodegradation, particularly in mixed cultures consisting of different bacterial species and/or archaeal. In fact, the involvement of monooxygenase and dioxygenase can be distinguished by determining the ratio of NADH/EE2. For example, the obtained ratio of 2.2 demonstrated that monooxygenase-mediated biotransformation would be the dominant mechanism as this ratio is in accordance with that of monooxygenase (i.e., 2.0).

Nevertheless, the information on the underlying biodegradation mechanisms of pharmaceuticals in

the enriched nitrifying sludge is still ambiguous and the relative contribution of AOB and HET to pharmaceutical biotransformation needs to be elucidated further.

2.4 Biotransformation products and pathways of pharmaceuticals by AOB

Incomplete biotransformation of pharmaceuticals in wastewater treatment processes could result in more toxic products into the receiving water (Agüera et al., 2013; Kosjek et al., 2009). The formation of metabolites or biotransformation products of pharmaceuticals is related to the specific operating conditions. The cometabolism by AOB might induce different biodegradation pathways of pharmaceuticals. For example, iopromide could be transformed into different products with and without nitrification (Batt et al., 2006). As shown in Figure 6, oxidation of the primary alcohols (forming carboxylates) on the side chains of iopromide were identified in the conventional activated sludge while dehydroxylation at the two side chains occurred in the nitrifying activated sludge, which was likely a result of cometabolism (Pérez et al., 2006).

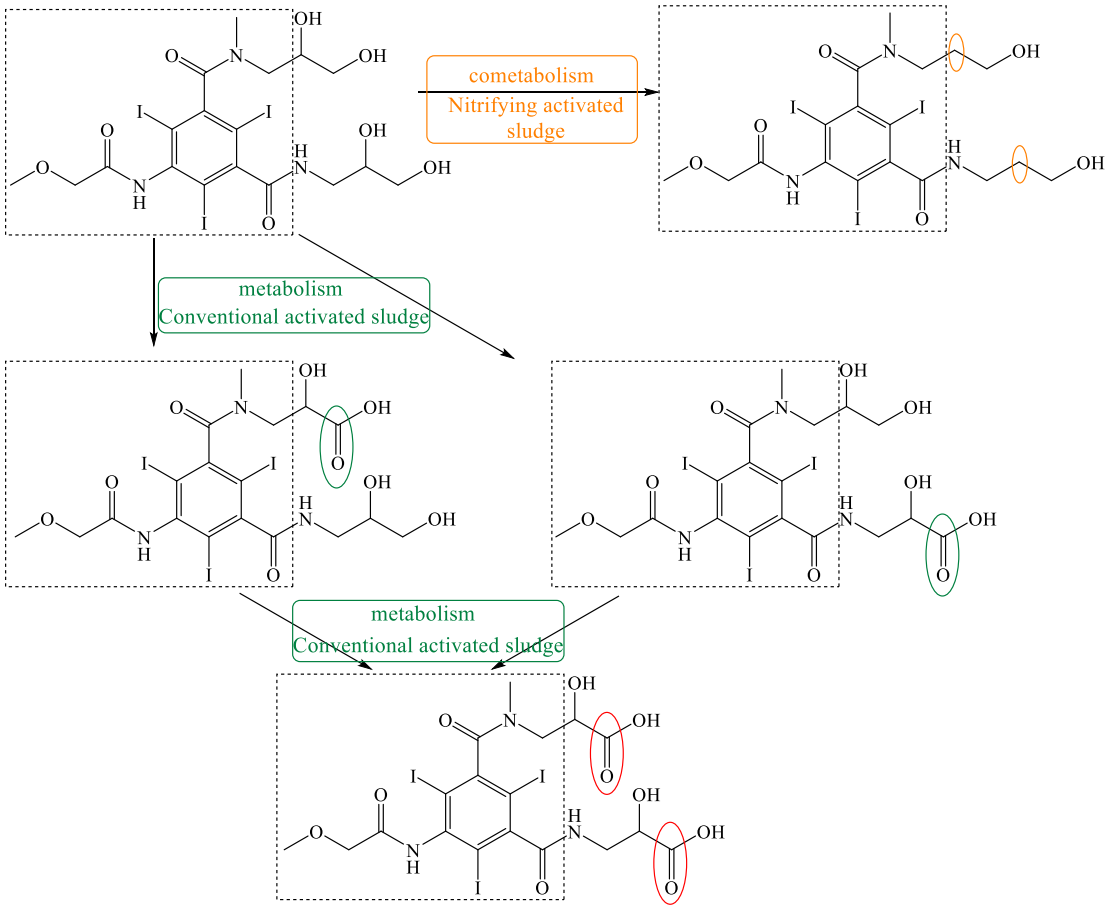

Figure 6. Biodegradation products and pathways of iopromide by conventional activated sludge and nitrifying activate sludge. The structural groups in the dash squares were not changed (based on (Pérez et al., 2006)).

During the biotransformation of trimethoprim by nitrifying activated sludge, it was oxidized to α-hydroxytrimethoprim (Eichhorn et al., 2005), whereas trimethoprim was reported to be persistent during the activated sludge treatment (Pérez et al., 2005). Oxidation of the primary hydroxyl group in acyclovir by nitrifying activated sludge led to the formation of carboxy-acyclovir with the guanine group unchanged. The biodegradation products of penciclovir were confirmed as the result of enzyme reactions such as the oxidation of terminal hydroxyl groups and β-oxidation followed by acetate cleavage (Prasse et al., 2011).

Hydroxylation is another biodegradation pathway of AOB for pharmaceuticals including ibuprofen (Dawas-Massalha et al., 2014; Zwiener et al., 2002), trimethoprim (Eichhorn et al., 2005), atenolol (Radjenović et al., 2008) and bezafibrate (Quintana et al., 2005). The enzyme AMO might be able to hydroxylate the pharmaceuticals just as it does with ammonia in AOB (Fernandez-Fontaina et al., 2012). In addition, abiotic nitration could be one minor transformation mechanism for EE2 (Gaulke et al., 2008), diclofenac and acetaminophen (Chiron et al., 2009). Acetaminophen was confirmed to be removed through nitration in real wastewater treatment plant with nitrogen removal as well as batch experiments with nitrifying activated sludge (Chiron et al., 2009). It was also confirmed that EE2 could be degraded via cometabolism and nitration by AOB (Gaulke et al., 2008; Skotnicka-Pitak et al., 2009). However, the involved carboxylation of EE2 was still unclear (Skotnicka-Pitak et al., 2009).

The biodegradation products and pathways for several pharmaceuticals are also affected by their respective structures. A rule-based biotransformation pathway prediction system was developed for amide-containing compounds (Helbling et al., 2010a). Observed biotransformation reactions of amide-containing compounds include amide hydrolysis and N-dealkylation, hydroxylation, oxidation, ester hydrolysis, dehalogenation, nitro reduction and glutathione conjugation. Primary amides like atenolol hydrolyzed rapidly while secondary amides hydrolyzed at rates influenced by steric effects. For tertiary amides, they were mostly N-dealkylated.

Overall, AOB-induced cometabolism could lead to different biotransformation products and pathways compared to those in the presence of inhibitor (ATU) for some pharmaceuticals (Kassotaki et al., 2016), probably due to the specific reactions via AMO or the involvement of formed intermediates from growth substrates. Nevertheless, the biotransformation products and pathways under metabolic and cometabolic conditions have not been fully identified for many pharmaceuticals so far due to the limited analytical techniques. Further efforts should be dedicated to understanding the underlying pathways in future work.

2.5 Mathematical modeling of pharmaceuticals biotransformation

Mathematical models for predicting the fate of pharmaceuticals in wastewater treatment have been developed for better understanding and optimization of their removal in recent years. The models described the involving physical-chemical processes, sorption, photolysis, volatilization and biotransformation processes (Pomiès et al., 2013). This section mainly focused on the models related to biotransformation or biodegradation processes of AOB.

The cometabolic models have been evolved from only considering the cometabolic substrate (Oldenhuis et al., 1989) to incorporating both cometabolic substrate and primary substrate (Boonchayaanant et al., 2008; Chang and Criddle, 1997; Criddle, 1993; Delgadillo-Mirquez et al., 2011; Liu et al., 2015; Verce et al., 2002). More reaction mechanisms have been integrated in the models, including competition between the cometabolic substrates (Kim et al., 2002; Verce et al., 2002) or from the primary substrates (Chang and Alvarez-Cohen, 1995; Maestre et al., 2013; Wahman et al., 2007), and the toxicity inhibition from biotransformation products (Alvarez-Cohen and McCarty, 1991; Semprini et al., 2007; Yu et al., 2005). The typical existing cometabolic models considering the competitive inhibition, reductant depletion, product toxicity, and/or primary substrates were summarized in Table 4 with the respective model components listed in Table 5.

The reductant model (M1) was developed assuming that there was no competition between ammonia (primary substrate) and cometabolic substrates (Maestre et al., 2013; Wahman et al., 2007). Oxygen was kept at non-limiting levels and there was no toxicity from products. The predicted concentration of cometabolic substrates would be significantly affected by both the primary and cometabolic rate constants. This model showed advantages in kinetic studies with *Nitrosomonas europaea* and good fits for some mixed culture nitrifiers.

The competition model (M2) included the primary substrate as the competitive substrate, which could inhibit the biodegradation of cometabolic substrates. There was only one limiting reactant (cometabolic substrates) in the model expression. As the affinity to the active sites in enzyme for the cometabolic substrate concentration was typically lower than for the growth substrate concentration, competition of cometabolic substrates on the primary substrate was not considered in this model.

The combined model (M3) integrated the reductant model with the competition model. They differed based on the assumptions about the presence of the competition between the primary substrate and the cometabolic substrates and whether the primary substrate should be regarded as the second

limiting reactant. Taking trihalomethanes biotransformation as example, in this model, ammonia (primary substrate) could compete with trihalomethanes (cometabolic substrate) while no competition was performed from trihalomethanes on ammonia and on each other. Both ammonia and trihalomethanes were the limiting reactants.

The fourth cometabolic model (M4) was proposed based on the biomass growth rate and yield and the uptake of primary substrate, which was applied to study the biotransformation of pharmaceuticals in nitrifying reactors (Fernandez-Fontaina et al., 2014). Two key parameters were introduced in the model development including the micropollutant transformation capacity (T_C) and the half-saturation constant (K_{SC}), which should be fairly stable for the same biomass under same conditions. The primary substrate (ammonium) biodegradation rate was expressed by applying the mass balance under steady state conditions.

The fifth cometabolic process based model (M5) was developed to describe biotransformation of three β-blockers during and after ammonia oxidation for specific enriched nitrifying cultures (Sathyamoorthy et al., 2013). This model linked the pharmaceutical biodegradation rate to the specific AOB growth as a cometabolic process. The atenolol may competitively inhibit the ammonia oxidation process, confirming the cometabolic biodegradation by AMO. The performance of this cometabolic process model was shown to be much better than the pseudo-first-order kinetic approach.

Finally, the parent compound concept was proposed aiming at producing micropollutants in the activated sludge treatment system (Plósz et al., 2012). For example, the dissolved micropollutants could come from the conjugated forms or sorbed contents on the suspended solids. Besides, the formation of biodegradation products was also important in predicting pharmaceuticals biotransformation. Hence the further development of cometabolic models should take into account the parent compound and biotransformation products or metabolites toward a comprehensive modeling of pharmaceuticals biotransformation by AOB.

Table 4. The existing cometabolic models with kinetic expressions for primary substrate, cometabolic substrate and biomass

Models	Primary substrate (S_p)	Cometabolic substrate (S_c)	Biomass (X)	Ref
M1: Reductant model	$\frac{dS_p}{dt} = -\frac{k_p X S_p}{K_{sp} + S_p}$	$\frac{dS_c}{dt} = -\left(\frac{k_c X S_c}{K_{sc} + S_c}\right)\left(\frac{S_p}{K_{sp} + S_p}\right)$	$\frac{dX}{dt} = -\frac{1}{T}\left(\frac{k_c X S_c}{K_{sc} + S_c}\right)\left(\frac{S_p}{K_{sp} + S_p}\right) + Y\frac{k_p X S_p}{K_{sp} + S_p} - bX$	(Maestre et al., 2013; Wahman et al., 2007)
M2: Competition model	$\frac{dS_p}{dt} = -\frac{k_p X S_p}{K_{sp} + S_p}$	$\frac{dS_c}{dt} = -\frac{k_c X S_c}{K_{S_c} + S_c + S_p\frac{K_{sc}}{K_{sp}}}$	$\frac{dX}{dt} = -\frac{1}{T}\left(\frac{k_c X S_c}{K_{sc} + S_c + S_p\frac{K_{sc}}{K_{sp}}}\right) + Y\frac{k_p X S_p}{K_{sp} + S_p} - bX$	(Verce et al., 2002; Wahman et al., 2005)
M3: Combined model	$\frac{dS_p}{dt} = -\frac{k_p X S_p}{K_{sp} + S_p}$	$\frac{dS_c}{dt} = -\frac{k_c X S_c}{K_{sc}\left(1 + \frac{S_p}{K_{sp}}\right) + S_c}\left(\frac{S_p}{K_{sp} + S_p}\right)$	$\frac{dX}{dt} = -\frac{1}{T}\frac{k_c X S_c}{K_{sc}\left(1 + \frac{S_p}{K_{sp}}\right) + S_c}\left(\frac{S_p}{K_{sp} + S_p}\right) + Y\frac{k_p X S_p}{K_{sp} + S_p} - bX$	(Wahman et al., 2005)
M4: Cometabolic-Monod model	$\frac{dS_{NH}}{dt} = \frac{S_{NH,in} - S_{NH,out}}{HRT} - \frac{\mu}{Y}\cdot X = 0$	$\frac{dS_C}{dt} = T_C \cdot \frac{\mu}{Y}\cdot\frac{S_C}{K_{SC} + S_C}\cdot X$	$\frac{dX}{dt} = \mu_{\max}\cdot\left(\frac{S_{NH}}{K_{S,NH} + S_{NH}}\right)\cdot\left(\frac{S_{O_2}}{K_{S,O_2} + S_{O_2}}\right)\cdot X$	(Fernandez-Fontaina et al., 2014)
M5: Cometabolic Process-Based model	$\frac{dS_{NH}}{dt} = -\left(i_{NBM} + \frac{1}{Y_{AOB}}\right)\left[\mu_{\max,AOB}\left(\frac{S_{NH}}{K_{NH} + S_{NH}}\right)\right]X_{AOB} - i_{NBM}\left[\mu_{\max,NOB}\left(\frac{S_{NO_2}}{K_{NO_2} + S_{NO_2}}\right)\right]X_{NOB}$	$\frac{dS_{PhAC}}{dt} = -(T_{PhAC-AOB}\mu_{AOB} + k_{PhAC-AOB})X_{AOB}S_{PhAC}$	$\frac{dX_{AOB}}{dt} = \left[\mu_{\max,AOB}\left(\frac{S_{NH}}{K_{NH} + S_{NH}}\right)\right]X_{AOB} - b_{AOB}X_{AOB}$	(Sathyamoorthy et al., 2013)

Table 5. The definition of all model components in Table 4 as well as the model parameter values

Model	Variable	Description	Unit	Typical values	Source
M1 M2 M3	S_p	Primary substrate concentration	mg L^{-1}	-	(Ely et al., 1997; Maestre et al., 2013; Verce et al., 2002; Wahman et al., 2005; Wahman et al., 2007)
	k_p	Maximum specific utilization rate of primary substrate	mg growth substrate (mg cell)$^{-1}$ d^{-1}	2.9[a]	
	K_{sp}	Primary substrate half-saturation coefficient	mg L^{-1}	0.13-0.16[a]	
	X	Microbial biomass concentration	g VSS L^{-1}	-	
	S_c	Cometabolic substrate concentration	mg L^{-1}	-	
	k_c	Maximum specific utilization rate of cometabolic substrate	mg nongrowth substrate (mg cell)$^{-1}$ d^{-1}	20.3[b]	
	K_{sc}	Cometabolic substrate half-saturation coefficient	mg L^{-1}	31.87[b]	
	T	Transformation capacity for biomass for the cometabolic substrate	mg cometabolic substrate (mg primary substrate)$^{-1}$	0.0092[c]	
	Y	Biomass yield on primary substrate	mg VSS (mg primary substrate)$^{-1}$	0.34[d]	
	b	First order decay coefficient	d^{-1}	0.02[d]	
M4	$S_{NH,in}$	Ammonium nitrogen concentration in the inlet	g NH_4^+-N L^{-1}	-	(Fernandez-Fontaina et al., 2014; Henze et al., 1987)
	$S_{NH,out}$	Ammonium nitrogen concentration in the outlet	g NH_4^+-N L^{-1}	-	
	HRT	Hydraulic retention time	d	-	
	μ	Specific biomass growth rate	d^{-1}	-	
	Y	Biomass yield	g VSS g NH_4^+-N^{-1}	0.07-0.28	
	X	Biomass concentration	g VSS L^{-1}	-	

	T_C	Micropollutant transformation capacity	μg g NH_4^+-N^{-1}	480[e]	
	K_{SC}	Micropollutant half-saturation constant	μg L^{-1}	3.2[e]	
	S_C	Micropollutant soluble concentration in the mixed liquor	μg L^{-1}	-	
	μ_{max}	Maximum growth rate	d^{-1}	0.34-0.65	
	S_{NH}	Ammonium nitrogen concentration	g NH_4^+-N L^{-1}	-	
	S_{O_2}	Dissolved oxygen concentration	mg L^{-1}	-	
	$K_{S,NH}$	Ammonium nitrogen half-saturation constant	g NH_4^+-N L^{-1}	0.0006-0.0036	
	K_{S,O_2}	Dissolved oxygen half-saturation constant	mg L^{-1}	0.5-2.0	
M5	i_{NBM}	Nitrogen fraction of biomass	mg N mg COD^{-1}	0.07	(Sathyamoorthy et al., 2013)
	Y_{AOB}	Ammonia-N yield	mg COD mg N^{-1}	0.11-0.21	
	$\mu_{max,AOB}$	Maximum AOB growth rate	d^{-1}	0.2-1.6	
	X_{AOB}	AOB concentration	mg COD L^{-1}	-	
	$\mu_{max,NOB}$	Maximum NOB growth rate	d^{-1}	0.2-2.6	
	S_{NO_2}	Nitrite concentration	mg N L^{-1}	-	
	K_{NO_2}	Nitrite half-saturation constant	mg L^{-1}	0.05-3	
	X_{NOB}	NOB concentration	mg COD L^{-1}	-	
	S_{PhAC}	Pharmaceutical concentration	μg L^{-1}	-	
	$T_{PhAC-AOB}$	AOB transformation coefficient of pharmaceuticals	L g COD^{-1}	71.5	
	μ_{AOB}	AOB growth rate	d^{-1}		

$k_{PhAC-AOB}$	AOB endogenous transformation coefficient of pharmaceuticals	L g COD^{-1} d^{-1}	16.1
b_{AOB}	AOB decay rate	d^{-1}	0.06-0.4

[a] (Maestre et al., 2013)

[b] these parameters were related to chloroform (Ely et al., 1997)

[c] this value was related to trichloromethane (Wahman et al., 2005)

[d] (Wahman et al., 2007)

[e] the parameters were assigned to ibuprofen (Fernandez-Fontaina et al., 2014)

2.6 Summary

Based on the previous findings in the literature review above, it is obvious that pharmaceutical removal efficiencies could be enhanced during nitrification, mainly due to the cometabolism by AOB. However, limited information was available on biotransformation products and pathways of pharmaceuticals under different metabolisms (i.e., cometabolism or metabolism) and it was ambiguous as to the contribution of the involved microorganisms (e.g., AOB or heterotrophs) to pharmaceutical biotransformation. In addition, as the growth substrate for AOB, the ammonium concentration is an important factor influencing pharmaceutical biodegradation and transformation products formation that requires further clarification. Furthermore, an integrated mathematical model is needed incorporating the biodegradation of parent compounds and the formation of transformation products simultaneously.

Chapter 3 Thesis overview

This chapter provides an overview of the research work undertaken in this thesis. First, the research objectives are presented. Then the key research methods and analytical techniques are described. Finally, the major outcomes and key results are outlined and discussed.

3.1 Research objectives

3.1.1 Enhanced biodegradation of atenolol by an enriched nitrifying sludge: products and pathways

Atenolol is one of the most commonly prescribed β-blockers, used in antihypertensive, antianginal and antiarrhythmic treatment. After human consumption, it is excreted mainly as an unchanged form. Atenolol was detected in the influent of WWTPs at the highest concentration of microgram per litre level (Radjenovic et al., 2007). Although the toxicity of atenolol as the individual compound is negligible, it shows a synergistic effect when atenolol is mixed with other β-blockers in the environment (Cleuvers, 2005). The removal efficiencies of pharmaceuticals are enhanced in nitrifying activated sludge. The responsible bacteria AOB are reported to be able to cometabolically degrade a range of aromatic compounds due to its non-specific enzyme, AMO. On the other hand, the formation of biodegradation products needs to be considered when studying the fate of the pharmaceuticals. The metabolites of atenolol have been investigated in the activated sludge and membrane bioreactor sludge (Radjenović et al., 2008), notwithstanding that it was not indicated clearly whether nitrification was involved. It was also confirmed that different metabolites could be formed under different environment conditions, i.e., with nitrification and with nitrification inhibited (Batt et al., 2006). However, the biodegradation products of atenolol are not yet studied during nitrification. Elucidating the underlying mechanisms and determining the relative roles of cometabolism and metabolism are important for better understanding biodegradation of pharmaceuticals during nitrification.

The main objectives of this study are to investigate the biodegradation mechanisms of atenolol by nitrifying sludge, to identify its biodegradation products and to propose possible biodegradation pathways under different metabolic conditions. Batch experiments were conducted at controlled ammonium concentration and without ammonium addition to investigate cometabolic and metabolic biodegradation of atenolol. Structural identification of the biodegradation products was performed to help elucidate the biodegradation pathways of atenolol.

3.1.2 Effect of ammonium availability on atenolol biodegradation in an enriched nitrifying sludge

Pharmaceuticals could be transformed cometabolically by AOB in the enriched nitrifying sludge in the presence of growth substrate ammonium (Arp et al., 2001). It is necessary to investigate the relationship between growth substrate and cometabolic substrate. The influence of initial ammonium concentration on biotransformation of ibuprofen and artificial sweetening agents has been investigated in previous reports (Dawas-Massalha et al., 2014; Tran et al., 2014), indicating that pulse feeding of growth substrate could enhance pharmaceutical removal efficiencies. The real wastewater contains the ammonium constantly, which would provide the condition for cometabolism for AOB involved and might induce the competition with the pharmaceuticals for AMO active sites as well. However, the effect of constant presence of ammonium on pharmaceutical biodegradation and on transformation product formation has not been studied yet for AOB induced cometabolism in enriched nitrifying cultures.

The objective of this study was to investigate the impact of the ammonium availability on atenolol biodegradation at relatively realistic level of 15 μg L^{-1} by an enriched nitrifying sludge. Batch experiments were conducted with different concentrations of growth substrate ammonium being constantly applied during the time course (0, 25, and 50 mg-N L^{-1}) to evaluate the atenolol degradation kinetics and the biotransformation product formation.

3.1.3 Biotransformation of acyclovir by the enriched nitrifying sludge

As an important antiviral drug, acyclovir has been consumed largely especially for influenza epidemics. Due to their potential ecosystem alterations and the development of viral resistances, antiviral drugs have recently attracted the interest of research. For example, a substantial removal (98%) of acyclovir was found in the wastewater treatment with the concentration decreasing from 1780 ng L^{-1} to 27 ng L^{-1} (Prasse et al., 2010). Although lab-scale biodegradation of acyclovir was previously studied by the activated sludge from the nitrification zone of a real wastewater treatment plant (Prasse et al., 2011), the effect of metabolic conditions on the formation of biotransformation products and the specific contributions of AOB and heterotrophs to acyclovir removal has not been clearly defined so far.

This study aims to investigate the biodegradation kinetics, products and pathways of acyclovir by an enriched nitrifying culture through batch biodegradation experiments under different metabolic conditions, i.e., with and without the addition of growth substrate, ammonium. The kinetic analysis was accompanied with the structural elucidation of biotransformation products. The initial acyclovir

concentration at 15 mg L^{-1} and 15 μg L^{-1} were applied to verify if the biotransformation products and pathways formed under high concentration would occur at relatively realistic levels.

3.1.4 Modeling of pharmaceutical biotransformation by enriched nitrifying culture under different metabolic conditions

Mathematical models of pharmaceutical biotransformation by the enriched nitrifying sludge can improve our understanding of the relevant microbially induced processes, help to assess the influence of operating conditions on removal efficiencies and allow us to design or optimize the bioremediation processes. In previously reported models, first-order kinetics and mixed order kinetics such as Monod expression were employed to describe the involved cometabolic biotransformation (Fernandez-Fontaina et al., 2014; Liu et al., 2015; Oldenhuis et al., 1989). More recent mathematical models considered the growth substrate and the cometabolic substrate, focusing on the relationships between substrates such as direct competitive interaction, indirect interaction by growth substrate and toxicity inhibition exerted by transformation products (Liu et al., 2015). On the other hand, the formation of transformation products should be considered in the fate of pharmaceuticals as transformation products might be more toxic and persistent than the parent compound. However, the previous literature has rarely considered the formation of biotransformation products into the cometabolic biotransformation models for pharmaceuticals.

The objective of this study is to develop a comprehensive biotransformation model to describe the fate of pharmaceuticals and transformation products at initial environmentally levels by the enriched nitrifying sludge. Different metabolic conditions were modeled through different sets of batch experiments. Model calibration and validation were carried out using atenolol biodegradation experimental data with key parameters estimated at best-fit values. Model evaluation with acyclovir biodegradation experiments in different experiments was also carried out. Simulation studies were performed to investigate the effects of dissolved oxygen (DO) and growth substrate ammonium on pharmaceutical biotransformation.

3.2 Research methods

3.2.1 Chemicals

Atenolol (≥98%) and atenolol acid were purchased from Sigma-Aldrich, Australia. Acyclovir (>98%) was obtained from Thermo Fisher, Australia. Carboxy-acyclovir was provided by Toronto Research Chemicals. Isotope labelled internal standard atenolol-d7 (≥97%) was obtained from Sigma-Aldrich, Australia and acyclovir-d4 from Santa Cruz Biotechnology. ATU (98%) and all the other HPLC grade

organic solvents (methanol, acetonitrile, hexane and acetone) were supplied by Sigma-Aldrich, Australia. Reference standards 1-isopropylamino-2-propanol (95%) and 1-amino-3-phenoxy-2-propanol (94%) were obtained from Enamine Ltd.

The individual standard stock solution for each compound (i.e., atenolol or acyclovir) was prepared in methanol at 1 g L^{-1} and stored at -20 °C. The individual calibration curve including the internal standard was obtained using a series working standards (1-200 μg L^{-1}), diluted from the stock solution appropriately in methanol/water (25:75, v/v). In order to provide initial 15 mg L^{-1} of pharmaceuticals in the batch experiments, the individual feed solution was prepared at 1 g L^{-1} in Milli-Q water (Millipore, Inc.) for atenolol or acyclovir. With the aim of providing initial 15 μg L^{-1} of pharmaceuticals for the batch biodegradation experiments, the individual feed solution for each compound was prepared at concentration of 1 mg L^{-1} in Milli-Q water.

3.2.2 Culture enrichment and reactor operation

Given the major aim of fundamental investigations on the biotransformation products and pathways of pharmaceuticals during nitrification, a highly enriched nitrifying sludge is needed instead of the real activated sludge in order to fully understand pharmaceutical biotransformation.

The sequencing batch reactor (SBR) inoculated with the seed biomass from a domestic wastewater treatment plant in Brisbane, Australia was set up at a total volume of 8 L at the room temperature in the laboratory in order to obtain an enriched nitrifying culture, containing AOB and NOB. A 6-h cycle strategy was employed for SBR running consisting of aerobic feeding (260 min), aeration (30 min), waste (1 min), settling (60 min) and decanting (9 min). 2 L synthetic wastewater consisting of 1 g L^{-1} NH_4^+-N was fed into the reactor during each cycle, resulting in the volumetric and sludge specific loading rates of 1 g NH_4^+-N L^{-1} d^{-1} and 700 mg NH_4^+-N g^{-1}VSS d^{-1}, respectively. The hydraulic retention time (HRT) and the solid retention time (SRT) were controlled at 24 h and approximately 15 d, respectively. The compressed air was supplied to the reactor during the feeding and aeration periods. DO and pH were continuously monitored through miniCHEM meters and controlled between 2.5-3.0 mg L^{-1} and in the range of 7.5-8.0, respectively using programmed logic controllers (PLC).

The feeding synthetic wastewater for the enriched nitrifying culture consisted of per liter (Kuai and Verstraete, 1998): 5.63 g of NH_4HCO_3 (1 g NH_4^+-N), 5.99 g of $NaHCO_3$, 0.064 g of each of KH_2PO_4 and K_2HPO_4 and 2 mL of a trace element solution. The trace element stock solution comprised: 1.25 g L^{-1} EDTA, 0.55 g L^{-1} $ZnSO_4 \cdot 7H_2O$, 0.40 g L^{-1} $CoCl_2 \cdot 6H_2O$, 1.275 g L^{-1} $MnCl_2 \cdot 4H_2O$, 0.40 g L^{-1}

$CuSO_4 \cdot 5H_2O$, 0.05 g L^{-1} $Na_2MoO_4 \cdot 2H_2O$, 1.375 g L^{-1} $CaCl_2 \cdot 2H_2O$, 1.25 g L^{-1} $FeCl_3 \cdot 6H_2O$ and 44.4 g L^{-1} $MgSO_4 \cdot 7H_2O$.

The SBR has been operated in the steady state with almost 100% conversion of NH_4^+ to NO_3^- for more than 1 year when the enriched nitrifying sludge was used as the inoculum for the batch experiments described in the following sections. The mixed liquor volatile suspended solids (MLVSS) concentration was stable at 1437.6 ± 112.9 mg L^{-1} (mean and standard errors, respectively, n=10). According to the microbial community analysis with fluorescence *in-situ* hybridization (FISH) (Law et al., 2011), AOB and NOB population accounted for over 80% of the microbial community. Specifically, ammonia-oxidizing *beta-proteobacteria* accounted for 46 ± 6% (n=20) of the bacterial populations and the *Nitrospira* genera (nitrite oxidizers) constituted 38 ± 5% (n=20) of the bacterial populations.

3.2.3 Batch experiments to assess the biodegradation of atenolol in terms of biotransformation products and pathways

In order to identify any possible transformation products, a high concentration (15 mg L^{-1}) was employed as the initial concentration of atenolol to conduct the biodegradation experiments due to the fact that the products may not be fully identified under low concentration condition (Radjenović et al., 2008). The 4-L beakers were used as the batch reactors wrapped in aluminium foil, in which 2.5 L freshly enriched nitrifying culture taken from the lab-scale SBR was used to achieve a MLVSS concentration of 1000 mg L^{-1}. Different experimental conditions were conducted in duplicates and the detailed experimental designs are provided in Table 6. Experimental protocol A1 was to assess atenolol biodegradation in the constant presence of ammonium at 50 mg-N L^{-1} through automatic dosing of a mixture of ammonium bicarbonate and sodium bicarbonate, which was also used to adjust the pH. The ammonium level was chosen to ensure the nitrifying conditions during batch experiments given the high ammonia oxidizing activities of enriched nitrifying sludge (Batt et al., 2006; Li et al., 2015) and high ammonium concentration (1000 mg N/L) for the parent SBR. Experimental protocol A2 was to assess atenolol biodegradation in the absence of ammonium. In this case, no initial ammonium pulse was fed at the beginning and no ammonium bicarbonate was supplied during the whole experimental period. Other operational conditions were same as those in the Experimental protocol A1. In Experimental protocol A3, the contribution of heterotrophs to atenolol biodegradation was studied with an initial addition of ATU at 30 mg L^{-1}. ATU probably chelated the copper of AMO active site as a strong and selective inhibitor of ammonia oxidation (Ali et al., 2013; Ginestet et al., 1998). Therefore, it was widely applied as a common method to inhibit AOB activity although whether ATU would affect all copper-containing enzymes was still ambiguous (Sathyamoorthy et al.,

2013). Batch controls to assess the contribution of abiotic and hydrolytic degradation were carried out in Experimental protocols A4 and A5, respectively. For protocol A4, the biomass was autoclaved at 121 °C and 103 kPa for 30 minutes to ensure entire inactivation of the microbial activity (Kassotaki et al., 2016). For protocol A5, hydrolysis of atenolol was studied in Milli-Q water without biomass. DO and pH were maintained at the same levels as in the parent SBR, i,e, 2.5-3.0 mg L^{-1} and 7.5-8.0, respectively, which would not affect the dynamics of the microbial community structure in the batch experiment. Aeration was provided during the experiments and the mixed liquor was mixed using a magnetic stirrer at 250 rpm. Samples were collected periodically for atenolol and the transformation products analysis.

Table 6. The protocols applied for atenolol biodegradation experiments

Experimental protocol	A1	A2	A3	A4	A5
Initial ammonium (mg L^{-1})	50	0	50	-	50
Ammonium control	Constant	0	Constant	-	Constant
Approximate VSS (g VSS L^{-1})	1	1	1	1	0
Volume (L)	4	4	4	4	4
ATU (mg L^{-1})	0	0	30	0	0
Autoclave	-	-	-	yes	-

3.2.4 Batch experiments to investigate the effect of ammonium availability on atenolol biodegradation

To achieve this objective, the target pharmaceutical atenolol was provided at an initial relatively realistic concentration (15 μg L^{-1}) to conduct the batch biodegradation experiments in 4-L beakers, covered by the aluminium foil. The enriched nitrifying culture from the SBR were provided at MLVSS concentration of approximately 1000 mg L^{-1} at the beginning of the experiments. Different ammonium concentrations (0, 25 and 50 mg L^{-1}) were controlled constantly for each biodegradation experiment with different ammonia oxidation levels in duplicates, namely as Experimental protocols A6, A7 and A8, respectively. Ammonium bicarbonate was supplied as the growth substrate at the beginning of the experiments with ammonium addition and was further frequently dosed into the beakers with sodium bicarbonate as a pH adjustment method as well as maintaining a constant level of ammonium. The experiments without ammonia oxidation were conducted in duplicates where ammonium concentration was zero during the whole time period. Experimental protocol A9 was

carried out to assess the contribution of heterotrophs on atenolol biodegradation by adding ATU at the beginning of the experiments. The control experiments were carried out to study the abiotic and hydrolytic degradation of atenolol with autoclaved biomass (121 °C and 103 kPa for 30 min) (Kassotaki et al., 2016) and without any biomass, respectively. For all batch experiments, pH was controlled between 7.5 and 8.0 and DO was supplied by aeration in the range of 2.5 and 3.0. After mixing well, the samples were taken periodically each day until 240 h for chemical analysis of atenolol and its products.

3.2.5 Batch experiments to study the biotransformation of acyclovir under different initial concentration

With the aim to study acyclovir biotransformation under different initial concentrations, a high concentration (15 mg L^{-1}) was selected to identify any possible biotransformation products and elucidate the biotransformation pathways whereas a low concentration (15 μg L^{-1}) was applied to study its degradation profile and verify the biotransformation products under relatively realistic concentration. All the batch experiments were divided into two series according to the initial acyclovir concentration. For each concentration level, different sets of experiments were performed (in duplicates for each experiment) (Table 7).

Table 7. Conditions of conducted batch experiments with acyclovir (same design of key experimental conditions for experiments at initial acyclovir of 15 mg L^{-1} and 15 μg L^{-1})

Experiment protocol	B1	B2	B3	B4	B5
Initial ammonium (mg L^{-1})	50	0	50	50	50
Ammonium control	Constant	0	Constant	Constant	Constant
Approximate VSS (mg L^{-1})	1000	1000	1000	1000	0
Volume (L)	4	4	4	4	4
ATU (mg L^{-1})	0	0	30	0	0
NaN_3 (mg L^{-1})	0	0	0	500	0

4-L beakers coupled with PLC controllers were used as the batch reactors seeded with enriched nitrifying biomass from the SBR. The MLVSS concentration was achieved at approximately 1000 mg L^{-1} at the beginning of the batch tests. Briefly, Experimental protocol B1 was conducted to assess biodegradation of acyclovir in the presence of ammonium. The constant ammonium concentration (50 mg L^{-1}) was provided by automatically adding a mixture of ammonium bicarbonate and sodium

bicarbonate, which was controlled by PLC as a pH adjustment process. The adding volume was controlled to be minor, which would not change the total volume significantly. Experimental protocol B2 was performed in the absence of ammonium during the overall time course when no initial and external ammonium were provided. Experimental protocol B3 was carried out with the initial addition of ATU, which could inhibit ammonia oxidation probably by chelating the copper of AMO active site (Ginestet et al., 1998). The control experimental protocols B4 and B5, were used to assess the contribution of abiotic degradation and hydrolytic degradation to acyclovir losses using NaN_3 and pure water (without biomass), respectively. NaN_3 was a chemical inhibitor used for the inactivation of microbial activities (Rattier et al., 2014). DO concentration was maintained between 2.5 and 3.0 mg L^{-1} through controlled air supply by PLC system. At the same time pH was maintained in the range of 7.5-8.0 during the time course. Mixed liquor samples were taken periodically and immediately frozen until analysis.

3.2.6 Sample preparation

The sample preparation procedures are divided into two groups according to the initial concentration of the pharmaceuticals. For batch experiments conducted at the higher initial concentration of the pharmaceutical (i.e., 15 mg L^{-1} in sections 3.2.3 and 3.2.5), the samples need to be diluted 100 times to ensure that the concentrations of the target compounds could fall within the range of the calibration curve (1-200 μg L^{-1}). Briefly, the samples were centrifuged at 12,000 g for 5 min without previous filtration in order to retain any possible biotransformation products. After centrifugation, 1 mL supernatant was obtained for further direct structural elucidation of the biotransformation products. Furthermore, a mixture of methanol/Milli-Q water (25:75, v/v) was used to dilute the supernatant 100 times for quantification.

For batch experiments carried out at the lower initial concentration for the pharmaceutical (i.e., 15 μg L^{-1} in sections 3.2.4 and 3.2.5), samples were concentrated through solid phase extraction (SPE) with the vacuum manifold (J. T. Baker, The Netherlands) prior to further quantification and structural identification of the target pharmaceuticals and the possible biotransformation products. The detailed SPE procedures were as follows. 50 mL non-filtrated samples were first centrifuged at 14,000 rpm for 5 min to avoid the unnecessary loss of the transformation products on the filter membrane. Conditioned with 10 mL methanol and 10 mL Milli-Q water, the Oasis HLB cartridges (6 mL, 200 mg, Waters, USA) was applied as the sorbent to conduct the SPE of the previous supernatant at a controlled flow rate of approximately 5 mL min^{-1}. The cartridges were rinsed with 5 mL Milli-Q water (for atenolol only) and then dried under vacuum for 30 min following by the elution with 10 mL methanol and 10 mL hexane/acetone (50/50, v/v) at a slow flow rate. The extracted elutes were

evaporated to dryness under a gentle stream of nitrogen. The residues were reconstituted in 250 µL methanol and 750 µL Milli-Q water. 20 µL internal standard (atenolol-d7 or acyclovir-d4) was added into each sample residue to achieve a concentration of 50 µg L^{-1} prior to further analysis.

The recovery test was carried out as a quality control to assess the efficiency of the SPE procedure. The samples were spiked with individual standards (i.e., atenolol or acyclovir) at different levels of 1, 5 and 20 µg L^{-1} in triplicates for each. Relative recoveries were calculated in the range between 99-110% for atenolol and acyclovir, indicating the high efficiency of sample preparation procedures.

3.2.7 Chemical analyses

Mixed liquor suspended solids (MLSS) and the volatile fraction (MLVSS) were measured at the beginning, middle and end of the batch biodegradation experiments according to the standard methods (APHA, 1998). NH_4^+-N concentrations were measured using a Lachat QuikChem8000 Flow Injection Analyzer (Lachat Instrument, Milwaukee). It was demonstrated in Figure 7 that the ammonium concentrations were controlled nearly constant during the entire experimental period for batch biodegradation experiments in the presence of ammonium. In addition, nitrite did not accumulate for all the batch experiments (less than 1 mg NH_4^+-N L^{-1}) and the nitrate concentration was similar to that in the SBR effluent (up to 1000 mg NH_4^+-N L^{-1}).

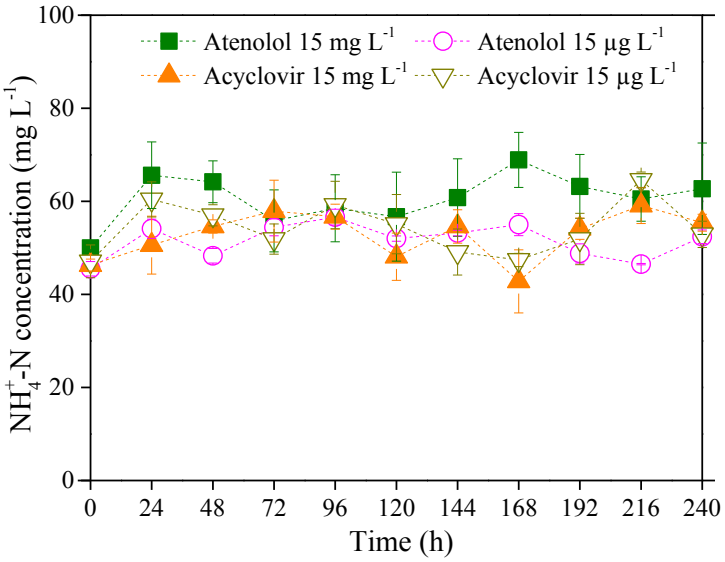

Figure 7. Ammonium concentrations in the biodegradation experiments of atenolol and acyclovir at initial concentration of 15 mg L^{-1} and 15 µg L^{-1} in the presence of ammonium.

Quantitative and qualitative analysis of the samples from batch experiments were realized by the ultra-fast liquid chromatography (UFLC) (Shimadzu, Japan) coupled with a 4000 QTRAP hybrid

triple quadruple-linear ion trap mass spectrometer (QqLIT-MS) equipped with a Turbo Ion Spray source (Applied Biosystems-Sciex, USA). Chromatographic separation was carried out using an Alltima C18 column (Alltech Associates Inc., USA) at 40 °C. The injection volume was 20 μL. The mobile phase contained (A) H_2O and (B) CH_3CN at a flow rate of 1 mL min^{-1}. The gradient of (B) was conducted as follows: it was linearly increased to 5% B after 0.5 min, further increased to 20% B for 12.5 min, increased to 50% B within 5 min, increased to 100% B for 2 min, kept constant for 4 min and finally was decreased to 5% B for 1 min. The total running time including the conditioning of the column to the initial conditions was 27 min. Positive electrospray ionization (ESI+) mode was applied with the corresponding parameters: drying gas temperature of 500 °C, drying gas 50 psi, curtain gas 30 psi, spraying gas 50 psi. The possible biodegradation products were identified through careful screening in the full scan chromatogram at a declustering potential of 80 V and mass range of 50-500 amu followed by spectrum analysis based on nitrogen rule and the existence of the peak [m+Na], etc. Tentative structures of biotransformation products were elucidated using product ion scan mode (MS^2) and sequential fragmentation using the ion trap. Concentrations of the target pharmaceuticals and their biotransformation products were analyzed in the multiple reaction monitoring (MRM) mode with two transition ions for confirmation and quantification, respectively. More detailed information related to parameters settings could be obtained in Table 8.

Table 8. Mass parameters applied for LC-MS/MS analysis

Compounds	Precursor ion (*m/z*)	DP (V)	Q1, *m/z* (quantification)	CE (eV) /CXP (V)	Q2, *m/z* (confirmation)	CE (eV) /CXP (V)
Atenolol	267	71	145	37/12	190	29/16
Atenolol acid	268	71	145	37/12	191	29/16
Atenolol-d7	274	71	145	37/12	79	33/6
Acyclovir	226	71	152	17/12	135	43/14
Carboxy-acyclovir	240	46	152	19/12	135	43/12
Acyclovir-d4	230	46	152	19/12	135	41/10

3.2.8 Model development

A comprehensive mathematical model involving multi-species and multi-substrates was developed herein to describe the pharmaceutical biotransformation processes by the enriched nitrifying sludge. In the proposed model system, the consumption of the pharmaceuticals and production of

biotransformation products were considered simultaneously accompanied with the ammonia oxidation in the enriched nitrifying sludge. As defined in Table 9, the model framework includes six soluble substrates, i.e., ammonium (S_{NH_4}), readily biodegradable substrates (S_S), oxygen (S_{O_2}), pharmaceutical (parent compound, PC, S_{PC}), primary biotransformation product (BP, S_{BP}) and other biotransformation products (OP, S_{OP}), and four particulate species, i.e., AOB (X_{AOB}), HET (X_{HET}), slowly biodegradable substrates (X_S) and inert biomass (X_I). For AOB and HET, both growth and endogenous respiration processes are included in the model. Seven microbially induced biochemical processes are considered in the developed model and the corresponding kinetic expressions are listed in Table 10: (1) AOB induced metabolic transformation of PC; (2) AOB growth linked cometabolic transformation of PC; (3) endogenous decay of AOB; (4) hydrolysis; (5) HET metabolic transformation of PC; (6) HET growth linked cometabolic transformation of PC; (7) endogenous decay of HET. The stoichiometric matrix of the proposed biotransformation model is summarized in Table 11. The definitions, values, units and sources of all parameters used in the biotransformation model are listed in Table 12.

Table 9. The definition of all model components

Variable	Description	Unit
S_{NH_4}	Ammonium concentration	g N m^{-3}
S_S	Readily biodegradable COD concentration	g COD m^{-3}
S_{O_2}	Dissolved oxygen concentration	g O_2 m^{-3}
X_{AOB}	Ammonia oxidizing bacteria (AOB) biomass concentration	g COD m^{-3}
X_{HET}	Heterotrophs (HET) biomass concentration	g COD m^{-3}
X_S	Slowly biodegradable COD concentration	g COD m^{-3}
X_I	Inert biomass concentration	g COD m^{-3}
S_{PC}	Parent compound (PC) concentration	mol m^{-3}
S_{BP}	Primary biotransformation product (BP) concentration	mol m^{-3}
S_{OP}	Other biotransformation product (OP) concentration	mol m^{-3}

In the model framework, Processes 2 and 6 (see Table 10) describe the microbial growth-linked kinetic expressions associated with cometabolic biotransformation of pharmaceuticals (Sathyamoorthy et al., 2013). These processes are described by the Monod equations, in which the concentrations of growth substrates S_{NH_4} and S_S are involved. For the cometabolic biotransformation expressions, key parameters are transformation coefficients such as AOB growth-linked $T^c_{PC\text{-}AOB}$ and HET growth-linked $T^c_{PC\text{-}HET}$. Processes 1 and 5 (see Table 10) indicate the pharmaceutical

biotransformation reactions directly conducted via metabolism by AOB and HET. These processes are described by pseudo-first order kinetic expressions, i.e., an explicit function of the concentrations of relevant pharmaceuticals. For microbial metabolic biodegradation of PC, the key parameters are biomass normalized PC degradation rate coefficients in the absence of AOB and HET growth, i.e. $k_{PC\text{-}AOB}$ and $k_{PC\text{-}HET}$. Processes 1, 2, 5 and 6 together contribute to pharmaceutical biotransformation in the enriched nitrifying sludge.

In addition, the proposed model framework considers the formation of biotransformation products employing the specific stoichiometry coefficients in relevant processes 1, 2, 5 and 6. The coefficients α_{BP}^{m} and α_{BP}^{c} indicate the transformation of PC to BP under metabolism and cometabolism by AOB, respectively. Similarly, the coefficients β_{BP}^{m} and β_{BP}^{c} mean the transformation of PC to BP under metabolism and cometabolism by HET, respectively.

Table 10. Process kinetic rate equations for the biotransformation model

	Process	Rate expression
1	Biotransformation of parent compound (PC) by ammonia oxidizing bacteria (AOB) under metabolism	$k_{PC\text{-}AOB} X_{AOB} S_{PC}$
2	Biotransformation of PC by AOB under cometabolism	$\mu_{max,AOB} \frac{S_{NH_4}}{S_{NH_4}+K_{NH_4}} \frac{S_{O_2}}{S_{O_2}+K_{O_2,AOB}} X_{AOB}$
3	Decay of AOB	$b_{AOB} X_{AOB}$
4	Hydrolysis	$k_{hyd} \frac{X_S/X_{HET}}{X_S/X_{HET}+K_X} X_{HET}$
5	Biotransformation of PC by heterotrophs (HET) under metabolism	$k_{PC\text{-}HET} X_{HET} S_{PC}$
6	Biotransformation of PC by HET under cometabolism	$\mu_{max,HET} \frac{S_S}{S_S+K_S} \frac{S_{O_2}}{S_{O_2}+K_{O_2,HET}} X_{HET}$
7	Decay of HET	$b_{HET} X_{HET}$

Table 11. The stoichiometric matrix for the biotransformation model (AOB, ammonia oxidizing bacteria; HET, heterotrophs)

Component (i)		Substance			Biomass				Substrate		
		1	2	3	4	5	6	7	8	9	10
Process (j)		S_{NH_4}	S_s	S_{O_2}	X_{AOB}	X_{HET}	X_S	X_I	S_{PC}	S_{BP}	S_{OP}
AOB	1								-1	α_{BP}^m	$1-\alpha_{BP}^m$
	2	$-i_{NBM}-\frac{1}{Y_{AOB}}$		$-\frac{3.43-Y_{AOB}}{Y_{AOB}}$	1				$-T_{PC-AOB}^c S_{PC}$	$\alpha_{BP}^c T_{PC-AOB}^c S_{PC}$	$(1-\alpha_{BP}^c)T_{PC-AOB}^c S_{PC}$
	3				-1		$1-f_I$	f_I			
HET	4		1				-1				
	5								-1	β_{BP}^m	$1-\beta_{BP}^m$
	6	$-i_{NBM}$	$-\frac{1}{Y_{HET}}$	$-\frac{1-Y_{HET}}{Y_{HET}}$		1			$-T_{PC-HET}^c S_{PC}$	$\beta_{BP}^c T_{PC-HET}^c S_{PC}$	$(1-\beta_{BP}^c)T_{PC-HET}^c S_{PC}$
	7					-1	$1-f_I$	$1-f_I$			

Table 12. Stoichiometric and kinetic parameters of the developed model

Parameter	Definition	Unit	Value	Source
Stoichiometric parameters				
Y_{AOB}	Yield coefficient for AOB	g COD g N^{-1}	0.15	(Sathyamoorthy et al., 2013)
Y_{HET}	Yield coefficient for HET	g COD g COD^{-1}	0.67	(Henze et al., 2000)
i_{NBM}	Nitrogen fraction of biomass	g N g COD^{-1}	0.086	(Henze et al., 2000)
f_I	Fraction of X_I in biomass decay	g COD g COD^{-1}	0.1	(Henze et al., 2000)
α_{BP}^{m}	Stoichiometry coefficient for primary biotransformation product (BP) by AOB under metabolism	-	0.29 (atenolol) 0.43 (acyclovir)	Calculated from experimental data
α_{BP}^{c}	Stoichiometry coefficient for BP by AOB under cometabolism	-	0.87 (atenolol) 0.29 (acyclovir)	Calculated from experimental data
β_{BP}^{m}	Stoichiometry coefficient for BP by HET under metabolism	-	0.63 (atenolol) 0.84 (acyclovir)	Calculated from experimental data
β_{BP}^{c}	Stoichiometry coefficient for BP by HET under cometabolism	-	0.63 (atenolol) 0.84 (acyclovir)	Calculated from experimental data
Ammonia oxidizing bacteria (AOB)				
$\mu_{max,AOB}$	Maximum specific growth rate of AOB	h^{-1}	Estimated in this study	-
b_{AOB}	AOB decay rate	h^{-1}	0.00625	(Sathyamoorthy et al., 2013)
$K_{O_2,AOB}$	Half saturation value for S_{O_2} of AOB	g O_2 m^{-3}	1.1	(Ghimire, 2012)
K_{NH_4}	Half saturation value for S_{NH_4}	g N m^{-3}	1.31 (25°C)	(Wiesmann, 1994)

$k_{PC\text{-}AOB}$	AOB transformation coefficient	m^3 g COD^{-1} h^{-1}	Estimated in this study	-
$T^c_{PC\text{-}AOB}$	Parent compound (PC) biotransformation coefficient rate linked to AOB growth (cometabolism)	m^3 g COD^{-1}	Estimated in this study	-
Heterotrophs (HET)				
k_{hyd}	Maximum hydrolysis rate of HET	h^{-1}	0.125	(Henze et al., 2000)
$\mu_{max,HET}$	Maximum specific growth rate of HET	h^{-1}	0.25	(Henze et al., 2000)
b_{HET}	HET decay rate	h^{-1}	0.026	(Henze et al., 2000)
$K_{O_2,HET}$	Half saturation value for S_{O_2} of HET	g O_2 m^{-3}	0.2	(Henze et al., 2000)
K_S	Half saturation value for S_{COD}	g COD m^{-3}	20	(Henze et al., 2000)
K_X	Half saturation value for hydrolysis	g COD g COD^{-1}	1.0	(Henze et al., 2000)
$k_{PC\text{-}HET}$	HET transformation coefficient	m^3 g COD^{-1} h^{-1}	Estimated in this study	-
$T^c_{PC\text{-}HET}$	PC biotransformation coefficient rate linked to HET growth (cometabolism)	m^3 g COD^{-1}	0	(Sathyamoorthy et al., 2013)

3.2.9 Model calibration and validation

Experimental data from biodegradation of atenolol (Case *I* as described in section 3.2.4) and acyclovir (Case *II* as described in section 3.2.5) at an initial concentration of 15 μg L^{-1} by an enriched nitrifying sludge were used for model evaluation. A brief summary of the experimental conditions applied under different metabolic types is provided in Table 13 and detailed experimental procedures could be found in previous sections. For example, EXP 1 in Case *I* for model evaluation is linked to experimental protocol A9 in section 3.2.4. All the batch experiments were conducted in duplicates. The designs for EXP1, EXP2 and EXP3 were same for atenolol (Case *I*) and acyclovir (Case *II*). EXP4 was exclusively designed for atenolol biotransformation, where constant ammonium concentrations of 25 mg-N L^{-1} were provided using the dosing method in EXP3 during the experimental period.

Table 13. Experimental conditions and designs for model calibration and validation

Purpose	Model calibration			Model validation	Model evaluation		
	Atenolol (Case *I*)				Acyclovir (Case *II*)		
	EXP1	EXP2	EXP3	EXP4	EXP1	EXP2	EXP3
Linked to experimental protocols in previous sections	A9	A6	A8	A7	B3	B2	B1
Parameters calibrated	$k_{PC\text{-}HET}$	$k_{PC\text{-}AOB}$	$T_{PC\text{-}AOB}$, $\mu_{max,\ AOB}$	N/A	$k_{PC\text{-}HET}$	$k_{PC\text{-}AOB}$	$T_{PC\text{-}AOB}$, $\mu_{max,\ AOB}$
Initial parent compound concentration	15 μg L^{-1}						
Experimental conditions	NH_4^+-N: 50 mg L^{-1} (initial) ATU: 30 mg L^{-1} MLVSS: 1 g VSS L^{-1} Volume: 4 L DO: 2.5-3.0 pH: 7.55-7.60	NH_4^+-N: 0 mg L^{-1} MLVSS: 1 g VSS L^{-1} Volume: 4 L DO: 2.5-3.0 pH: 7.55-7.60	NH_4^+-N: 50 mg L^{-1} (constant) MLVSS: 1 g VSS L^{-1} Volume: 4 L DO: 2.5-3.0 pH: 7.55-7.60	NH_4^+-N: 25 mg L^{-1} (constant) MLVSS: 1 g VSS L^{-1} Volume: 4 L DO: 2.5-3.0 pH: 7.55-7.60	NH_4^+-N: 50 mg L^{-1} (initial) ATU: 30 mg L^{-1} MLVSS: 1 g VSS L^{-1} Volume: 4 L DO: 2.5-3.0 pH: 7.55-7.60	NH_4^+-N: 0 mg L^{-1} MLVSS: 1 g VSS L^{-1} Volume: 4 L DO: 2.5-3.0 pH: 7.55-7.60	NH_4^+-N: 50 mg L^{-1} (constant) MLVSS: 1 g VSS L^{-1} Volume: 4 L DO: 2.5-3.0 pH: 7.55-7.60
Experimental period	240 h						
Chemical analysis	NH_4^+, NO_2^-, NO_3^-, atenolol, atenolol acid, MLVSS				NH_4^+, NO_2^-, NO_3^-, acyclovir, carboxy-acyclovir, MLVSS		

The contribution of sorption to removal of atenolol and acyclovir was insignificant based on our previous studies (Xu et al., 2017a; Xu et al., 2017b). This is in consistency with low sorption coefficient K_D (0.04) and low octanol-water partition coefficient Log K_{OW} (0.16) of atenolol and Log K_{OW} (-1.59) of acyclovir (Kasim et al., 2004; Maurer et al., 2007; Mohsen-Nia et al., 2012). Volatilization was considered negligible given the low values of Henry's law constants for atenolol (1.37×10^{-18} atm m^3 mol^{-1}) and acyclovir (3.2×10^{-22} atm m^3 mol^{-1}) (Küster et al., 2010). Photodegradation was also insignificant considering the turbidity of the sludge and the aluminium foil covering the reactor. Therefore, microbially induced biodegradation should be the main mechanism for pharmaceutical removal.

The developed model system consists of 7 biochemical processes and 22 stoichiometric and kinetic parameters (Table 10 and Table 12). For most of these parameters, the reported values were well established in previous literature and therefore directly used in this proposed model. However, the information on biomass growth-linked PC transformation coefficients $T^c_{PC\text{-}AOB}$ and $T^c_{PC\text{-}HET}$ and microbial endogenous transformation coefficients $k_{PC\text{-}AOB}$ and $k_{PC\text{-}HET}$ was limited (Sathyamoorthy et al., 2013). Considering the key role of cometabolism induced by AOB growth, the maximum specific growth rate of AOB $\mu_{max,\ AOB}$ was of significance to the developed model. Model calibration was therefore conducted to estimate the values for $k_{PC\text{-}AOB}$, $k_{PC\text{-}HET}$, $T^c_{PC\text{-}AOB}$ and $\mu_{max,\ AOB}$ based on experimental measurements through minimizing the sum of squares of the deviations between the measured and modeled values for the concentrations of parent compounds and biotransformation products under different metabolic conditions. In addition, the four stoichiometric coefficients, i.e., α^m_{BP}, α^c_{BP}, β^m_{BP} and β^c_{BP}, indicating the transformation of PC to BP under metabolism and cometabolism conditions could be determined based on the concentrations of BP and PC measured in the experiments.

Model calibration was firstly conducted using experimental data from atenolol biotransformation (Case *I*) of EXP 1-3. The predicted results were fitted with measured concentrations of atenolol and atenolol acid from EXP1 and EXP2 to estimate $k_{PC\text{-}HET}$ and $k_{PC\text{-}AOB}$, respectively, whilst the corresponding experimental data from EXP3 were fitted to estimate $\mu_{max,\ AOB}$ and $T^c_{PC\text{-}AOB}$, using the $k_{PC\text{-}HET}$ and $k_{PC\text{-}AOB}$ values obtained in previous experiments (EXP1 and EXP2). Model validation was then carried out with the calibrated parameters using the independent experimental data sets from EXP4, which was not used for model calibration. To further verify the validity and applicability of the model, the model was also applied to evaluating the acyclovir biotransformation from Case *II* of

EXP 1-3. The key model parameters were recalibrated for acyclovir biotransformation using the three sets of batch experimental data (Table 13).

3.3 Results and Discussion

3.3.1 Different metabolic conditions on atenolol biodegradation could lead to the formation of different biotransformation products

This section summarises the findings of the work described in Appendix A which is published in Chemical Engineering Journal.

Atenolol biodegradation by the enriched nitrifying sludge was assessed under different metabolic conditions, i.e., in the presence of constant ammonium, in the absence of ammonium and with addition of ATU. Abiotic and hydrolytic control experimental results demonstrated the stability of atenolol without any biotransformation products during the 240 h experimental period as shown in Figure 8d and Supplement information in Appendix A. The degradation efficiencies for atenolol were observed to be 50%, 40% and 39% in the experiments in the presence of ammonium, in the absence of ammonium and with addition of ATU, respectively (Figure 8).

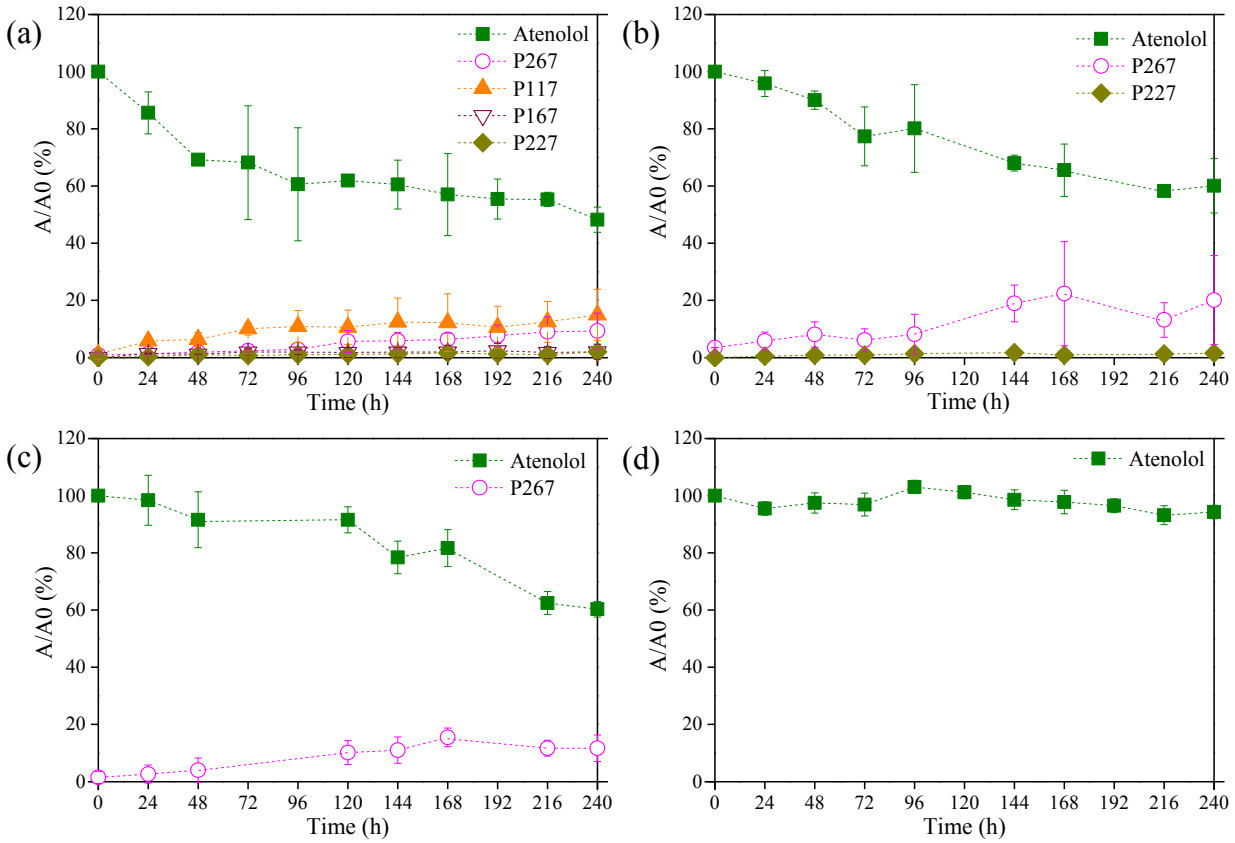

Figure 8. Qualitative profiles of atenolol and its biodegradation products in biodegradation

experiments: (a) in the presence of ammonium, (b) without ammonium addition, (c) with the addition of ATU and (d) with autoclaved biomass. Y-axis indicates the peak areas of the extracted ion chromatograms of atenolol or its biodegradation products (A) normalized to the initial peak area of atenolol (A0).

Non-linear regression analysis was performed on atenolol degradation in the presence of ammonium with a highest degradation rate of 0.088 mg atenolol g VSS^{-1} h^{-1}, whereas atenolol degradation rates were 0.023 and 0.028 mg atenolol g VSS^{-1} h^{-1} in the absence of ammonium and with addition of ATU, respectively, confirming the potential role of cometabolism by the enriched nitrifying culture on atenolol biodegradation.

In the presence of growth substrate ammonium, atenolol biodegradation was associated with the nitrifying activity, which was confirmed from a linear positive relationship between ammonia oxidation rate and atenolol degradation rate as shown in Figure 9b. Ammonia oxidation rate was calculated based on the amounts of ammonium added and the measured NH_4^+-N concentration at each sampling time. As demonstrated in Figure 9a, ammonia oxidation rate experienced a decrease trend during the experimental period accompanied with a decrease in atenolol degradation rate, which could be due to substrate competition between growth substrate and cometabolic substrate or inhibition from atenolol or its biotransformation products (Arp et al., 2001; Radniecki et al., 2008; Sathyamoorthy et al., 2013).

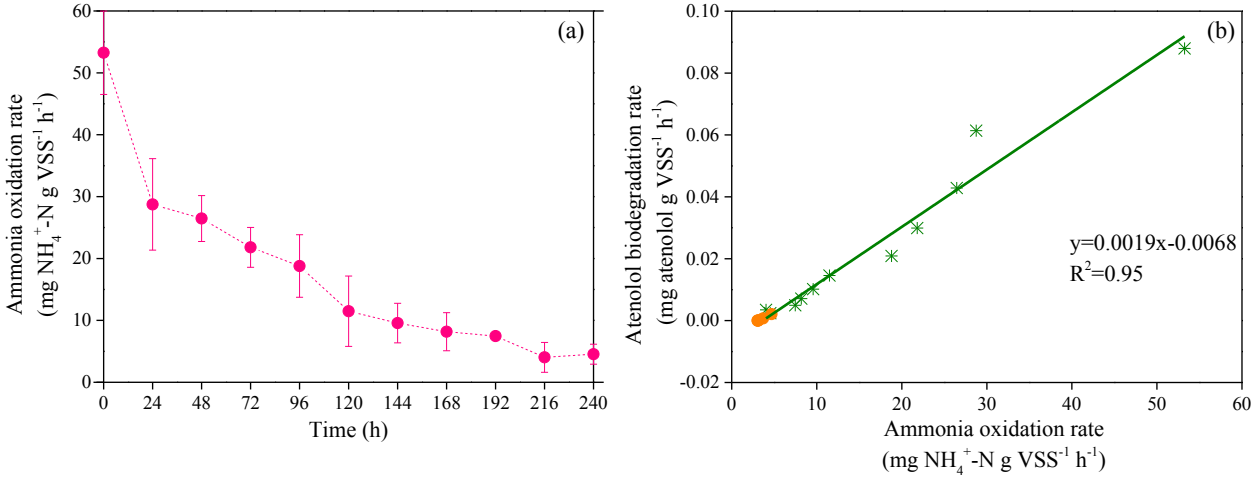

Figure 9. (a) The calculated ammonia oxidation rate during biodegradation experiments in the presence of ammonium and (b) Relationship between ammonia oxidation rate and atenolol biodegradation rate (orange dots indicated the modeled values).

The experimental results revealed that four biotransformation products (namely with their nominal mass, P117, P167, P227 and P267) were identified in the presence of ammonium whereas only P267 and P227 were formed in the absence of ammonium (see Figure 8a and b). Atenolol was transformed into the sole product P267 with addition of ATU (Figure 8c). The structures of these products were identified through full-scan mode analysis, product ion mode analysis, structural proposal based on the mass spectrum and mass spectrum comparison with the available reference standards. Briefly, their structures were proposed based on these fragment ions and the structural information of atenolol followed by confirmation with the standards. The detailed structural identification procedures could be found in Appendix A. P267, P117 and P167 were confirmed as atenolol acid, 1-isopropylamino-2-propanol and 1-amino-3-phenoxy-2-propanol, respectively. The structure of P227 could not be accurately identified due to the very low signal intensity notwithstanding the evidence that it might contain one nitrogen atom and have been formed through amide-bond hydrolysis to carboxylic acid, similar to the product P267. Atenolol acid was previously identified as the main product during atenolol biodegradation by conventional activated sludge, membrane bioreactor sludge or activated sludge from a full-scale aerobic nitrification reactor (Radjenović et al., 2008; Rubirola et al., 2014). Nevertheless, other three products P117, P167 and P227 were first reported in this study, probably due to the cometabolism given the constant ammonium feeding condition. This was in accordance with the observation that bezafibrate, naproxen, ibuprofen and diclofenac were transformed only by cometabolism (Quintana et al., 2005).

Different metabolic conditions could lead to different biotransformation pathways of atenolol by the enriched nitrifying sludge. As presented in Figure 10, the first step of atenolol biotransformation pathways was same regardless of the presence of ammonium: hydrolysis of the amide group to its carboxylic moiety, producing atenolol acid (P267). The transformation pathway to P227 was not sure due to its unidentified structure. In the presence of ammonium, AOB induced cometabolim might lead to a further transformation of P267, resulting in the formation of P117 and P167 through the cleavage of ether bond in the alkyl side chain and N-dealkylation and loss of acetamide moiety from the aromatic ring, respectively. These pathways were further confirmed in the experiments with atenolol acid as the parent compound. Results indicated that P117, P167 and P227 were produced from the beginning of the experiments with increasing trends. Microbial-induced hydrolysis was a typical reaction for most amide-containing compounds (Helbling et al., 2010b; Quintana et al., 2005), catalysed by amidases and proteolytic enzymes and two genes found in *Nitrosomonas eutropha* including N-acetylmuramoyl-L-alanine amidase (Neut_1623) and amidohydrolase-2 (Neut_1622) (Fournand and Arnaud, 2001; Sharma et al., 2009; Stein et al., 2007). Although information was limited on cleavage of ether bond in the alkyl side (Hyman et al., 1994; Pieper et al., 1988), it could

be speculated that there might exist some intermediates formed from the typical ether bond cleavage or that the reported bond cleavage in this study was due to cometabolism by AOB. N-dealkylation was a common reported biochemical reaction for most amine-containing compounds in either the nitrifying sludge system or the mammalian system (Gulde et al., 2016). Notwithstanding the absence of previous direct evidence of AMO on dealkylation, it was suspected that the monooxygenase from AOB likely catalyze this biochemical reaction. As for the loss of acetamide group from aromatic ring, it also requires more efforts on identifying this reaction in the future.

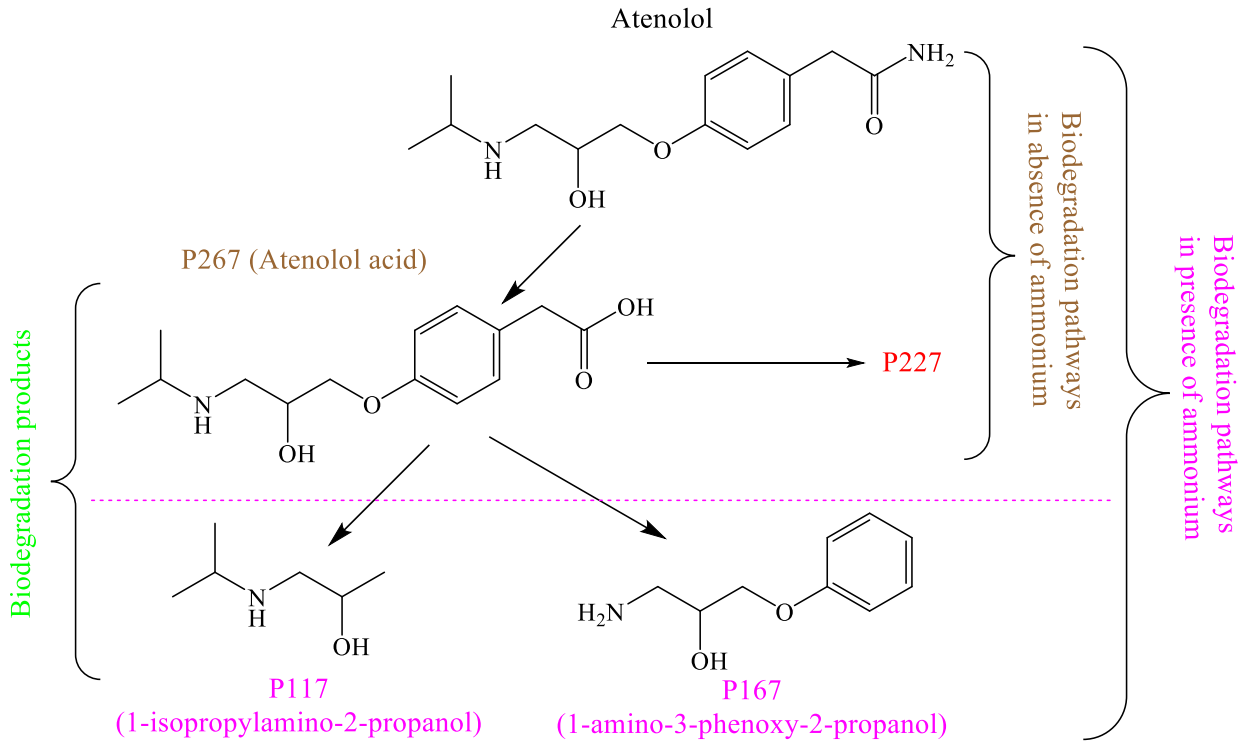

Figure 10. Proposed biodegradation pathways of atenolol by the enriched nitrifying culture in the presence of ammonium as well as in the absence of ammonium.

3.3.2 Impact of ammonium availability on atenolol biodegradation and atenolol acid formation by an enriched nitrifying sludge

This section summarises the findings of the work described in Appendix B which is published in ACS Sustainable Chemistry & Engineering.

As the presence of growth substrate was necessary for cometabolic biodegradation, the impact of ammonium availability was investigated on atenolol biodegradation at relatively realistic level (15 μg L^{-1}) together with the formation of its transformation product by the enriched nitrifying sludge in this work. As shown in Figure 11, three levels of ammonium concentrations were applied at 0, 25 and

50 mg-N L^{-1} with atenolol degradation and atenolol acid formation profiles plotted respectively. It was obvious that atenolol removal efficiencies were decreased with increasing ammonium concentration while atenolol acid formation was increased with the increase of ammonium availability. Contrast to previous reports where the pharmaceutical degradation was enhanced at higher initial ammonium concentration (Tran et al., 2009), the different trending in this work could be due to the growth substrate providing strategy. Constant ammonium concentrations were supplied during the entire experimental period whereas only initial pulse feeding of ammonium was provided at the beginning of batch experiments in the previous study. On the other hand, the formation of biotransformation products was positively related to ammonia oxidizing rate (details presented in Appendix B), further confirming the importance of cometabolism. Although AOB could degrade pharmaceuticals under starvation conditions (Forrez et al., 2009; Khunjar et al., 2011), its contribution to the transformation was less than AOB with the adequate growth substrates, indicating the formation of transformation products could be positively linked to the nitrifying activity.

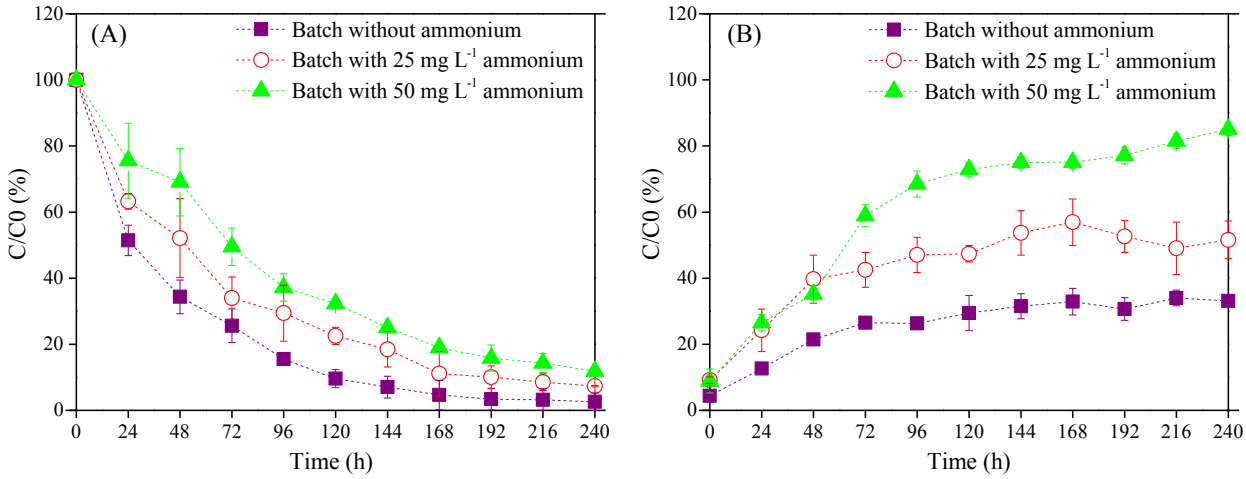

Figure 11. The effect of ammonium (NH_4^+-N) concentration on the degradation of atenolol at an initial concentration of 15 µg L^{-1} (A) and on the formation of its biotransformation product atenolol acid (B). C is the concentration of atenolol or atenolol acid and C0 is the initial concentration of atenolol.

The fact that atenolol biodegradation was adversely linked to the ammonium concentration (see Figure 11A) might attribute to the competition between the growth substrate (ammonium) and the cometabolic substrate (atenolol), especially in case where the concentration of growth substrate was several magnitudes higher than the cometabolic substrate (Fernandez-Fontaina et al., 2012). This substrate competition was previously reported for biodegradation of cis-1,2-dichloroethene and tetrachloroethylene (Schäfer and Bouwer, 2000; Tsien et al., 1989). As shown in Figure 11B, the formation of atenolol acid experienced a slow increase after 96 h for experiments in the presence of

25 and 50 mg-N L^{-1} ammonium, probably due to a decreasing ammonia oxidation rate influenced by the competitive inhibition by atenolol (Sathyamoorthy et al., 2013).

Positive relationships were observed between atenolol biodegradation rate and ammonia oxidation rate as well as atenolol acid formation rate and ammonia oxidation rate as shown in Figure 12, further confirmed the cometabolism in the presence of ammonium. The valid molar ratios of atenolol to ammonia for this positive relationship were calculated as 2.4×10^{-6}-2.1×10^{-5} and 2.8×10^{-6}-3.6×10^{-5} with ammonium concentrations of 50 and 25 mg-N L^{-1}, respectively. Different fitted slopes were obtained with a higher value at constant 25 mg-N L^{-1} than that at constant 50 mg-N L^{-1}. Higher atenolol biodegradation rate would be achieved at the lower ammonium concentration given the same ammonia oxidation rate, further supporting the proposed substrate competition for AMO active sites between growth substrate and cometabolic substrate (Arp et al., 2001; Tran et al., 2013). With regard to the relationship between ammonia oxidation rate and atenolol acid formation rate, a critical value of ammonia oxidation rate was observed. When ammonia oxidation rate was lower than 14.5 mg NH_4^+-N g VSS^{-1} h^{-1}, the higher formation rate of atenolol acid would be achieved at the higher ammonium concentrations provided that the same ammonia oxidation rate was obtained for both constant ammonium concentrations conditions (25 or 50 mg-N L^{-1}) (Figure 12B). However, the higher formation rate of atenolol acid was found for 25 mg-N L^{-1} conditions at the assumed same ammonia oxidation rate when it was higher than 14.5 mg NH_4^+-N g VSS^{-1} h^{-1}. Both cometabolism and substrate competition might involve in the mechanisms contributing to atenolol biodegradation in this study with the competition being the limiting step in formation of atenolol acid when ammonia oxidizing rate was higher than the critical value (Fischer and Majewsky, 2014), which requires further confirmation.

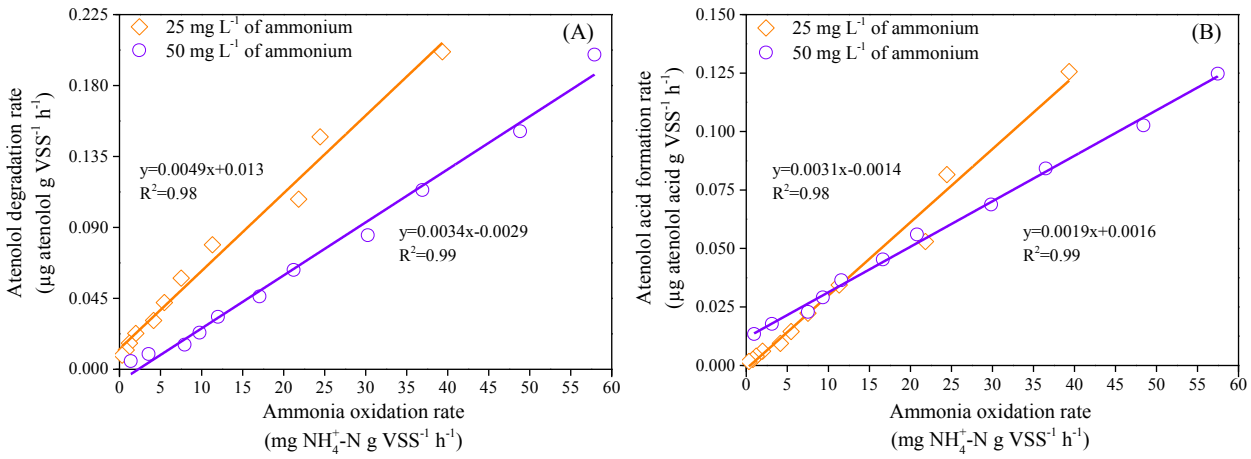

Figure 12. The relationships between ammonia oxidation rate and atenolol degradation rate (A);

between ammonia oxidation rate and atenolol acid formation rate (B).

Biodegradation pathway of atenolol at relatively realistic level was proved to be irrelevant to the presence/availability of the growth substrate ammonium. Either metabolic biodegradation or cometabolic biodegradation could lead to the hydroxylation on the amide group of atenolol to its carboxylic form. In contrast, four products including atenolol acid, P117, P167 and P227 were formed as the result of cometabolic biodegradation in our previous work probably due to the applied high initial concentration of atenolol (Xu et al., 2017b), which requires further efforts. Microbially induced hydroxylation was also reported for mianserin, catalyzed by monooxygenase (Lauchnor and Semprini, 2013; Men et al., 2016). The responsible enzyme in the enriched nitrifying culture for cometabolic biodegradation, AMO, could degrade a broad range of substrates due to its non-specific property (Keener and Arp, 1993; Lauchnor and Semprini, 2013). As it does with ammonia, AMO could also catalyze the hydroxylation reaction of atenolol to yield atenolol acid in this work.

3.3.3 Effect of initial concentration and role of microorganisms in biotransformation of acyclovir

This section summarises the findings of the work described in Appendix C which is published in Chemosphere.

Acyclovir biodegradation by the enriched nitrifying sludge was assessed in this study with the aim to investigate the effect of the metabolic type, the initial concentration and the role of microorganisms in biotransformation pathways. Control experiments indicated the negative contributions from sorption, abiotic degradation and hydrolytic degradation on acyclovir transformation as detailed in Appendix C.

It was noted that the biotransformation pathway of acyclovir by the enriched nitrifying culture was independent on the metabolic type. The availability of growth substrate ammonium became a critical condition for enriched nitrifying biomass to carry out the cometabolic or metabolic biodegradation on acyclovir. As shown in Figure 13 and Figure 14, only one product P239, namely as its nominal mass, was identified during the experiments in the presence of ammonium and in the absence of ammonium. P239 was identified as carboxy-acyclovir according to the structural identification procedures detailed in Appendix C. Carboxy-acyclovir was a reported transformation product of acyclovir in previous literature (Prasse et al., 2011). Regardless of the presence of ammonium, alcohol oxidation occurred on the terminal hydroxyl group of acyclovir to its carboxy moiety, carboxy-

acyclovir. This observation was contradictory to the previous report that the production of 4-chlorobenzoic acid was only related to the cometabolic transformation on bezafibrate (Quintana et al., 2005). This might be due to structural discrepancies among studied pharmaceuticals, leading to different responses to the metabolic type. On the other hand, alcohol oxidation was not observed in biodegradation of ibuprofen and no carboxy-ibuprofen was formed (Quintana et al., 2005). In comparison, the primary hydroxyl group of acyclovir was probably vulnerable to endure alcohol oxidation as the guanine group showed no significant changes during biodegradation.

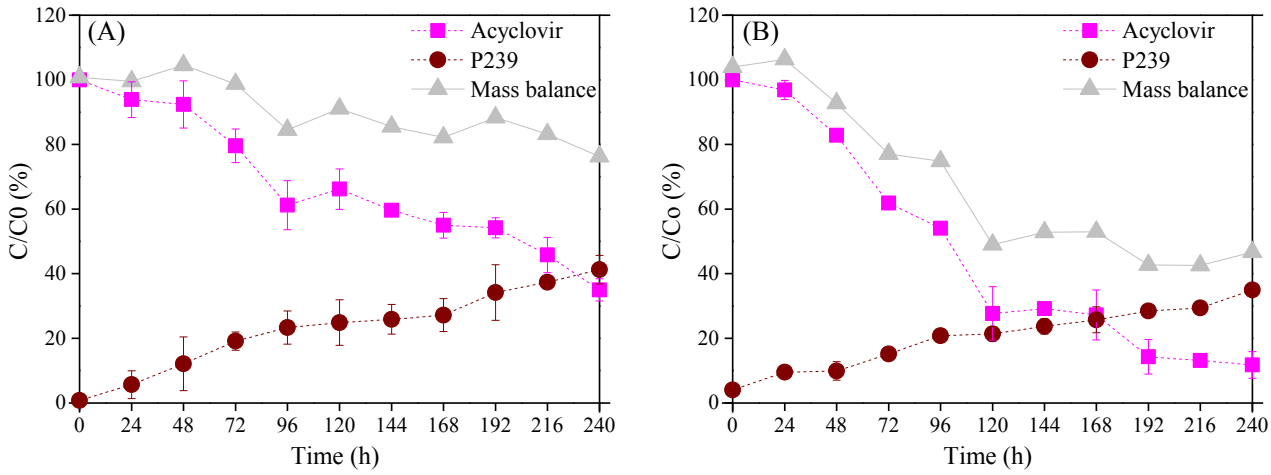

Figure 13. Concentration profiles of acyclovir and its product normalized to the initial acyclovir of (A) 15 mg L^{-1} and (B) 15 μg L^{-1} in the experiments with ammonia oxidation.

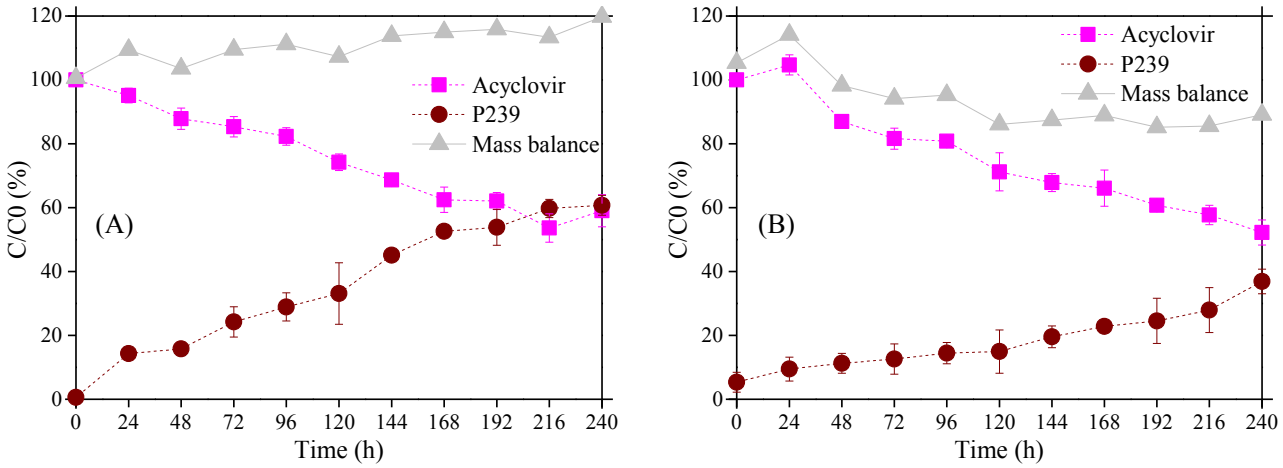

Figure 14. Concentration profiles of acyclovir and its product normalized to the initial (A) 15 mg L^{-1} and (B) 15 μg L^{-1} in the experiments without ammonia addition.

Acyclovir could be transformed into carboxy-acyclovir through catalysis by AOB or HET. By comparison of the experimental results in the presence of ammonium and with addition of ATU, only

carboxy-acyclovir was identified as the transformation product in both cases as shown in Figure 13 and Figure 15. This biochemical reaction was typically catalyzed by AMO from AOB or ammonia oxidizing archaea (AOA) for most pharmaceuticals including other antiviral drugs (abacavir, emtricitabine, ganciclovir, lamivudine and zidovudine), amide-containing compounds (e.g. propachlor) and tertiary amines such as mianserin (Funke et al., 2016; Helbling et al., 2010a; Men et al., 2016). On the other hand, the experimental evidence on the role of heterotrophs on enzyme-induced alcohol oxidation is limited in previous literature. The formation of carboxy-acyclovir with ATU addition in this work indicated that the monooxygenase from heterotrophs could also catalyze the alcohol oxidation, which was also proposed in previous research (Men et al., 2016). The fact that the same biotransformation products for 17β-ethinylestradiol were formed by AOB or heterotrophs (Khunjar et al., 2011) was in consistency with our observations in this study. Furthermore, the nearly closed mass balance results demonstrated that no other products were formed during acyclovir biodegradation with ATU addition (see Figure 15).

In this work, different initial acyclovir levels in terms of 15 mg L^{-1} and 15 μg L^{-1} were applied to study acyclovir biodegradation by the enriched nitrifying culture. Observed from the concentration profiles of acyclovir and its transformation products as shown in Figure 13, Figure 14 and Figure 15, carboxy-acyclovir was formed with the alcohol oxidation reaction being irrelevant to the initial concentration. However, previous reports on the effect of initial concentrations on biotransformation pathways of pharmaceuticals were contradictory. The same degradation route was reported on trimethoprim by nitrifying activated sludge with two metabolites produced at initial concentrations of 20 mg L^{-1} and 20 μg L^{-1} whereas different biotransformation products were found under different spiked concentration (500 μg L^{-1} and 5 μg L^{-1}) in another study (Eichhorn et al., 2005; Jewell et al., 2016). This discrepancy might be due to the properties of the activated sludge and the dominant microorganisms in different studies, which deserve further research.

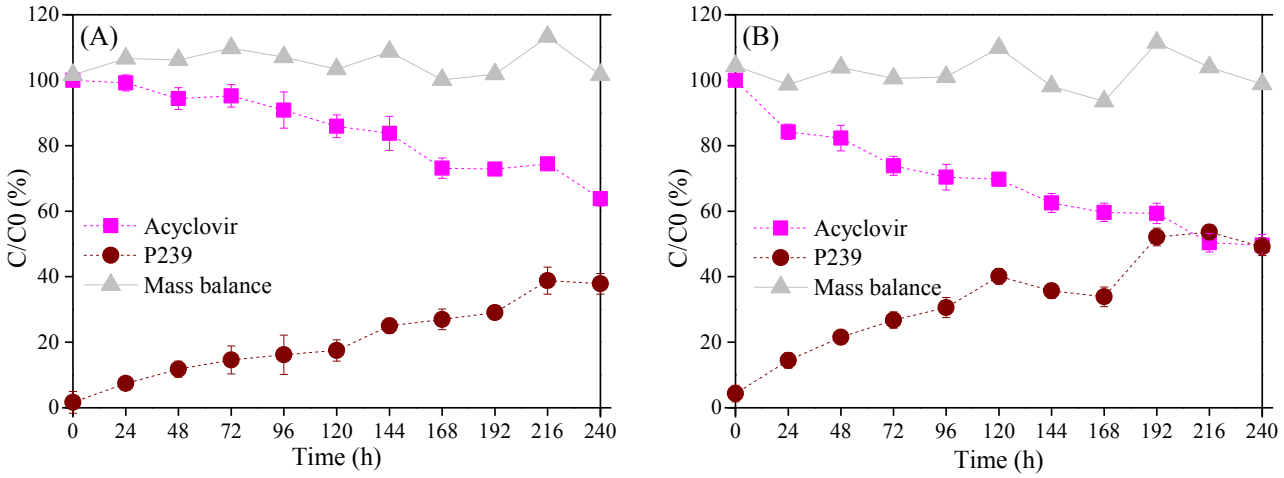

Figure 15. Concentration profiles of acyclovir and its product normalized to the initial (A) 15 mg L^{-1} and (B) 15 μg L^{-1} in the experiments with inhibition of ammonia oxidation of AOB by allythiourea (ATU) addition.

It should be noted that there might be other transformation products which were not identified in this study as the mass balance results indicated a decreasing trend in the presence of ammonium as shown in Figure 13. Compared with the closed mass balance with the addition of ATU (see Figure 15), biodegradation catalyzed by heterotrophs led to the unique transformation of acyclovir while cometabolic biodegradation by the enriched nitrifying culture might result in other pathways, requiring more effort in the future.

3.3.4 Modeling of biotransformation of atenolol and acyclovir by enriched nitrifying culture under different metabolic conditions

This section summarises the findings of the work described in Appendix D which is submitted.

In this work, the formation of biotransformation products was incorporated into the modeling framework to describe the fate of selected pharmaceuticals in the enriched nitrifying culture. Microbially induced metabolic types contributing to pharmaceutical biodegradation were considered as follows: cometabolism linked to AOB growth, metabolism by AOB, cometabolism linked to HET growth and metabolism by HET.

The proposed model framework was calibrated to estimate four key parameters including $k_{PC\text{-}HET}$, $k_{PC\text{-}AOB}$, $T^{c}_{PC\text{-}AOB}$ and $\mu_{max,\,AOB}$ using atenolol biodegradation experimental data under different metabolic conditions. As shown in Figure 16, the developed biotransformation model could

satisfactorily capture all dynamics associated with atenolol and atenolol acid in all batch biodegradation experiments under different metabolic conditions. The best-fit parameters were listed in the Appendix D. Briefly, the parameter $k_{PC\text{-}HET}$ associated with HET-induced metabolism was estimated as 0.000180 ± 0.000017 m^3 g COD^{-1} h^{-1} in EXP1 when atenolol biotransformation was exclusively attributed to metabolism by HET. The parameter $k_{PC\text{-}AOB}$ was estimated as 0.000140 ± 0.000012 m^3 g COD^{-1} h^{-1} in EXP2 when only the metabolic biotransformation by AOB and HET were involved in the biotransformation of atenolol. Parameters $T^c_{PC\text{-}AOB}$ and $\mu_{max,\ AOB}$ were estimated at 0.012 ± 0.000036 m^3 g COD^{-1} and 0.012 ± 0.0023 h^{-1} in EXP3, incorporating with the cometabolic biodegradation by AOB. Furthermore, the good agreement observed between model predictions and independent experimental data (EXP4) which were not used for model calibration could confirm the validity and reliability of the developed model as demonstrated in Figure 17. Compared to the previously limited reported values ($k_{PC\text{-}HET}$, $k_{PC\text{-}AOB}$ and $T^c_{PC\text{-}AOB}$ of 0.00093 ± 0.00018 m^3 g COD^{-1} h^{-1}, 0.00067 ± 0.00023 m^3 g COD^{-1} h^{-1} and 0.0715 ± 0.0227 m^3 g COD^{-1}) (Sathyamoorthy et al., 2013), the discrepancy in these parameters could be probably due to the difference in the community structure in the adopted nitrifying cultures or different operating conditions. The model could be potentially applied to a widespread extent despite that the parameter values would vary according to the experimental conditions. Observed higher value of $T^c_{PC\text{-}AOB}$ than $k_{PC\text{-}HET}$ and $k_{PC\text{-}AOB}$ could support the major role of cometabolism by AOB in atenolol biodegradation (Xu et al., 2017b). It was also reported that atenolol degradation was linked to AOB growth instead of HET and NOB (Sathyamoorthy et al., 2013).

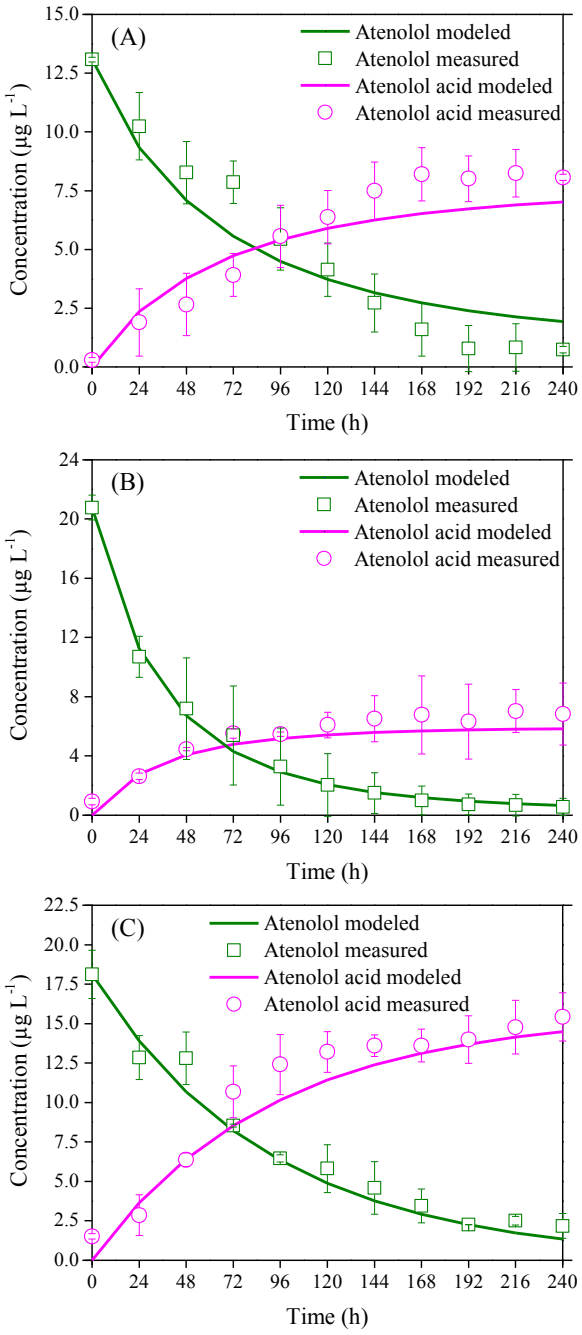

Figure 16. Model calibration with experimental data from atenolol biodegradation: (A) EXP1, with addition of allylthiourea (ATU); (B) EXP2, in the absence of ammonium; and (C) EXP3, in the presence of ammonium (50 mg NH_4^+-N L^{-1}).

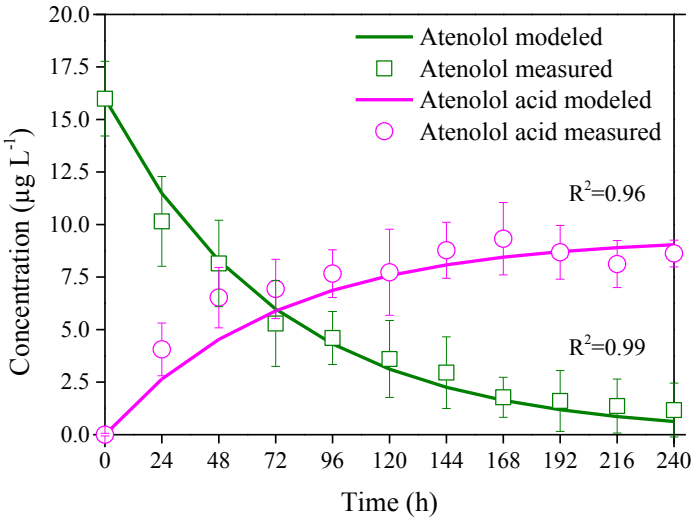

Figure 17. Model validation results of atenolol biotransformation by the enriched nitrifying culture in the presence of ammonium of 25 mg-N L^{-1} (EXP4).

Model evaluation using acyclovir biotransformation data under different conditions further demonstrated the validity of the developed model. As shown in Figure 18, model simulations and experimental data matched very well after recalibrating the parameters related to the target parent compound ($k_{PC\text{-}HET}$, $k_{PC\text{-}AOB}$ and $T^c_{PC\text{-}AOB}$). The parameter $\mu_{max,\ AOB}$ was set to be the same as in case of atenolol due to the same nitrifying culture. These values were also listed in the Appendix D with $k_{PC\text{-}HET}$, $k_{PC\text{-}AOB}$ and $T^c_{PC\text{-}AOB}$ of 0.00035 ± 0.00002 m^3 g COD^{-1} h^{-1}, 0.00005 ± 0.00003 m^3 g COD^{-1} h^{-1} and 0.00093 ± 0.00049 m^3 g COD^{-1}, respectively. The highest biotransformation conversion efficiency of acyclovir in EXP1 (with addition of ATU) compared to those values in EXP2 and WXP3 indicated the importance of metabolism by HET on acyclovir biotransformation. Oxidation of acyclovir to carboxy-acyclovir might be dominated by unspecific monooxygenase from HET (Men et al., 2016), which needs to be confirmed in the further work. Considering the molecular differences between atenolol and acyclovir, obvious differences in $k_{PC\text{-}AOB}$ and $T^c_{PC\text{-}AOB}$ values may imply an affinity property of AOB for different compounds probably due to a preferential substrate selection to AMO active sites (Fernandez-Fontaina et al., 2012).

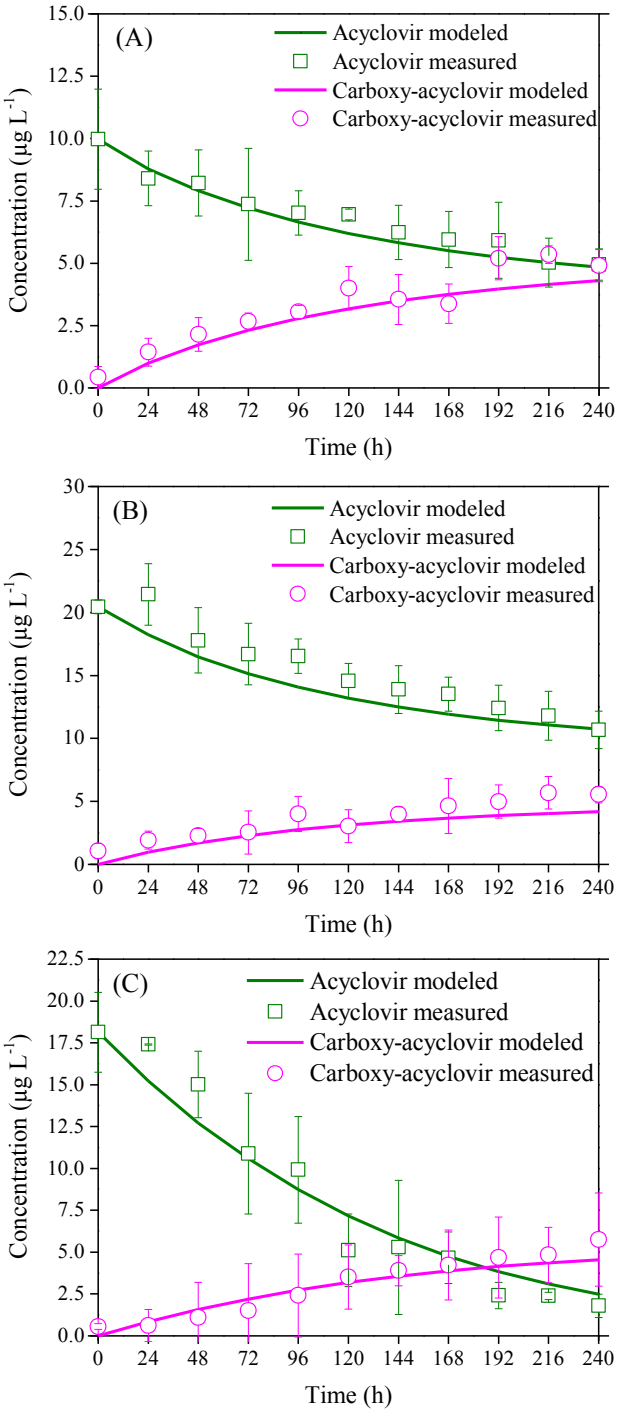

Figure 18. Model evaluation with experimental data from acyclovir biodegradation: (A) EXP1, with addition of allylthiourea (ATU), (B) EXP2, in the absence of ammonium and (C) EXP3, in the presence of ammonium (50 mg NH_4^+-N L^{-1}).

Positive relationships were observed between ammonia oxidation rate and pharmaceutical biodegradation rates in terms of atenolol and acyclovir based on the established model (see Figure 19), supporting the notion of cometabolic biodegradation by the enriched nitrifying culture (Yi and Harper Jr, 2007). By simulating the concentration profiles of pharmaceuticals after 240 h, the valid

molar ratio of the pharmaceutical to ammonia was assessed at 8.42×10^{-7} to 1.91×10^{-5} and 1.62×10^{-11} to 2.26×10^{-5} for atenolol and acyclovir, respectively. The same slope was found for atenolol biodegradation within 240 h and after 240 h (Figure 19A) while a different slope was found for the relationship between ammonia oxidation rate and the acyclovir degradation rate after 240 h (Figure 19B). In case of higher ammonia oxidation rate than the critical value (2.3 mg NH_4^+-N g VSS^{-1} h^{-1} in this study), the lower slope might indicate a slower increasing trend in acyclovir degradation rate with an increasing ammonia oxidation rate. On the other hand, a higher increasing trend in acyclovir degradation rate would arise at higher slope when ammonia oxidation rate was lower than 2.3 mg NH_4^+-N g VSS^{-1} h^{-1}. The observation that pharmaceutical would not be degraded until the ammonia was depleted (Dawas-Massalha et al., 2014) revealed a higher pharmaceutical degradation rate at lower ammonia oxidation rate, which could also support the finding in this study.

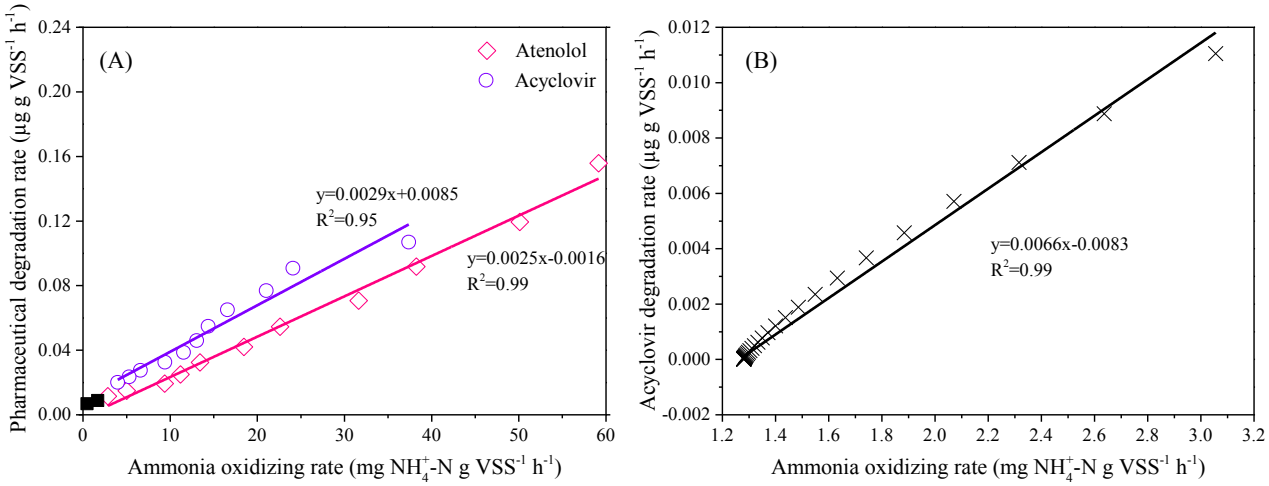

Figure 19. (A) The relationship between ammonia oxidizing rate and the pharmaceutical degradation rates in terms of atenolol and acyclovir (black solid squares indicate the atenolol degradation rates after 240 h); and (B) The relationship between ammonia oxidizing rate and the acyclovir degradation rate after 240 h at a different linear fit slope.

The effects of DO and ammonium concentrations on pharmaceutical biotransformation were investigated by performing model simulations under varying conditions. Different DO concentrations were applied ranging from 0 to 4 mg L^{-1} with ammonium concentration of 50 mg-N L^{-1}. The final concentrations of atenolol and acyclovir decreased rapidly with a prompt increase of atenolol acid and carboxy-acyclovir as DO increased to 1 mg L^{-1}. When DO further increased to 4 mg L^{-1}, a gradual decrease of pharmaceutical concentrations was observed accompanied with a slight increase of their biotransformation products. Therefore, DO concentration would play an important role in

pharmaceutical biotransformation. Contrarily, DO in the WWTP had no influence on oxidative biotransformation of selected micropollutants in the previous report (Helbling et al., 2012). Such contradiction might ascribe to the enriched nitrifying culture utilised in this study instead of the regular activated sludge in WWTP, suggesting that DO might regulate the pharmaceutical biotransformation cometabolically. With regards to growth substrate ammonium, substrate competition might be the limiting mechanism when assessing its influence on pharmaceutical biotransformation under different ammonium concentrations from 0 to 100 mg-N L^{-1}. Rapid increase in pharmaceutical biotransformation was observed with increasing ammonium concentration from 0 to 20 mg-N L^{-1} whereas no significant enhancement was exhibited with the increase of ammonium concentration from 20 to 100 mg-N L^{-1}. Previously, initial pulse of ammonium was applied resulting in the contrary conclusion that pharmaceutical removal efficiencies were enhanced at higher initial ammonium concentrations (Tran et al., 2009). Therefore, it was proposed that substrate competition might exist between ammonium and atenolol or acyclovir, leading to a decreasing degradation rates at higher ammonium concentrations (Dawas-Massalha et al., 2014; Fernandez-Fontaina et al., 2012).

Chapter 4 Conclusions and Future Work

4.1 Main conclusions of the thesis

This thesis describes the biodegradation of selected pharmaceuticals (i.e., atenolol and acyclovir) by the enriched nitrifying culture in terms of identification of their biotransformation products, elucidation of transformation pathways under different metabolisms, understanding the role of involved microorganisms, investigating the effect of key factors on pharmaceutical biotransformation and mathematical modeling of the biotransformation processes. The key conclusions are:

- Positive relationships were observed between ammonia oxidation rate and pharmaceutical biodegradation rate with the valid range of the ratio of ammonia to pharmaceutical (i.e., atenolol or acyclovir) identified, indicating the cometabolism in the presence of growth substrate ammonium.

- Different biotransformation products were found for atenolol at high initial concentrations under different metabolic conditions while the same metabolite was obtained when low initial concentration was applied. AOB induced cometabolism contributed to the formation of P117 and P167, confirmed from biodegradation experiments of atenolol acid. Lower initial concentration of atenolol might lead to formation of transformation products unable to be identified under current conditions, which require further efforts.

- Only one biotransformation product, carboxy-acyclovir was formed during acyclovir biodegradation experiments regardless of the initial concentrations.

- Metabolic condition had different influences on the formation of transformation products from pharmaceuticals (i.e., atenolol or acyclovir), probably due to the specific chemical structures of the investigated parent compounds.

- Both AOB and heterotrophs could contribute to the hydroxylation of the amide group of atenolol to carboxylic moiety, producing atenolol acid or contribute to alcohol oxidation of acyclovir to carboxy-acyclovir.

- Substrate competition between ammonia and atenolol for AMO sites might lead to decreasing rates of atenolol biodegradation and ammonia oxidation. An adverse effect on atenolol

biodegradation was also observed with the increasing ammonium concentration. However, atenolol acid formation was positively related to the increasing ammonia oxidation rate.

- A mathematical model that describes pharmaceutical biotransformation by enriched nitrifying biomass was developed considering parent compound degradation and transformation products formation simultaneously. The developed model was validated and further evaluated with independent experimental data. Good prediction performance was obtained with the proposed model. It was found that DO might play an important role in pharmaceutical biotransformation whereas a further increase in ammonium concentration would not enhance biotransformation, probably due to substrate competition especially under higher ammonium concentration.

- The further biodegradation of atenolol acid into small molecular compounds with simpler structures gives insights that enriched nitrifying biomass could be applied in the wastewater treatment process to break down micropollutants or even achieve complete mineralization. With the aid of the proposed model, DO in the wastewater treatment plays an important role in regulating the removal of studied atenolol and acyclovir. An optimum DO concentration was obtained at 1 mg L^{-1} in this thesis, which may require further validation in the real environment.

4.2 Recommendations for future research

During the whole period of my PhD, many research challenges, in addition to the research objectives investigated so far, have been identified that entail further research. Some of these are summarized below:

- In this thesis, atenolol and acyclovir were selected as the model compounds to study their biodegradation by the enriched nitrifying culture. Our study demonstrated that different products and pathways were found for atenolol biodegradation under different metabolic types. The further work should be conducted on the structurally similar compound to validate the metabolism-dependent pathways and undermine the transformation reaction induced by corresponding microorganisms.

- Although the chemical structures of biotransformation products of atenolol were mostly identified such as P267, P117 and P167, structural information of P227 was not available in

this thesis. Further work should be done in order to understand the basic information of P227 and quantify its concentration profiles if possible.

- As the enriched nitrifying sludge used in this thesis was not adapted to the pharmaceuticals during enrichment processes, the biodegradation potential on pharmaceuticals might exhibit different performance in the long-term operation. This could be achieved by designing a continuous feed strategy with the selected pharmaceuticals at relatively realistic level to study their biotransformation under different scenarios.

- Two structure-identified transformation products P117 (1-isopropylamino-2-propanol), P167 (1-amino-3-phenoxy-2-propanol) from atenolol biodegradation were firstly reported in this thesis. However, their presence has not been confirmed in the real wastewater, which provided an insight for further research. As the references standards for P117 and P167 are available, their concentration could be determined and therefore an understanding of the mass balance of atenolol and its transformation products during the treatment processes could be achieved.

- The biotransformation of pharmaceuticals at realistic concentrations reported in the environment should be further verified in order to investigate the presence of similar transformation products and pathways.

- The proposed model framework only considers the biotransformation of one single pharmaceutical by the enriched nitrifying sludge. However, a variety of pharmaceuticals were present in the environment concurrently. The competition might exist among the pharmaceuticals with similar structures or those with different structures, which require further work to develop a more comprehensive model to describe the fate of pharmaceuticals in the real environment or treatment processes.

- Substrate competition was proposed as the mechanism that might explain the decreasing pharmaceutical degradation rates at higher ammonium concentrations. However, the underlying mechanism was unclear. Pure AOB cultures might be applied to elucidate the competition for AMO active sites between cometabolic substrates and growth substrates through a series of batch experiments using different ammonium concentrations.

- In terms of the effect of pharmaceuticals on microorganisms, the long-term response in microbial communities and the gene expression to the continuous exposure to the relatively realistic concentrations of pharmaceuticals should be investigated in the further work.

References

Agüera, A., Martínez Bueno, M.J. Fernández-Alba, A.R., 2013. New trends in the analytical determination of emerging contaminants and their transformation products in environmental waters. Environ. Sci. Pollut. Res. 20 (6), 3496-3515.

Alder, A.C., Schaffner, C., Majewsky, M., Klasmeier, J. Fenner, K., 2010. Fate of β-blocker human pharmaceuticals in surface water: Comparison of measured and simulated concentrations in the Glatt Valley Watershed, Switzerland. Water Res. 44 (3), 936-948.

Ali, T.U., Kim, M. Kim, D.J., 2013. Selective inhibition of ammonia oxidation and nitrite oxidation linked to n2o emission with activated sludge and enriched nitrifiers. J. Microbio. Biotechnol. 23 (5), 719-723.

Alvarez-Cohen, L. McCarty, P.L., 1991. Product toxicity and cometabolic competitive inhibition modeling of chloroform and trichloroethylene transformation by methanotrophic resting cells. Appl. Environ. Microbiol. 57 (4), 1031-1037.

Alvarino, T., Suarez, S., Lema, J.M. Omil, F., 2014. Understanding the removal mechanisms of PPCPs and the influence of main technological parameters in anaerobic UASB and aerobic CAS reactors. J. Hazard. Mater. 278, 506-513.

APHA, 1998. Standard methods for the examination of water and wastewater, American Public Health Association, Washington, DC.

Arp, D., Yeager, C. Hyman, M., 2001. Molecular and cellular fundamentals of aerobic cometabolism of trichloroethylene. Biodegradation 12 (2), 81-103.

Baek, K., Park, C., Oh, H.M., Yoon, B.D. Kim, H.S., 2010. Diversity and abundance of ammonia-oxidizing bacteria in activated sludge treating different types of wastewater. J. Microbiol. Biotechnol. 20 (7), 1128-1133.

Batt, A.L., Kim, S. Aga, D.S., 2006. Enhanced biodegradation of iopromide and trimethoprim in nitrifying activated sludge. Environ. Sci. Technol. 40 (23), 7367-7373.

Bendz, D., Paxéus, N.A., Ginn, T.R. Loge, F.J., 2005. Occurrence and fate of pharmaceutically active compounds in the environment, a case study: Höje River in Sweden. J. Hazard. Mater. 122 (3), 195-204.

Boonchayaanant, B., Kitanidis, P.K. Criddle, C.S., 2008. Growth and cometabolic reduction kinetics of a uranium- and sulfate-reducing *Desulfovibrio*/clostridia mixed culture: Temperature effects. Biotechnol. Bioeng. 99 (5), 1107-1119.

Caldwell, D.J. 2016. Sources of pharmaceutical residues in the environment and their control. In: Hester, R.E. and Harrison, R.M. eds. Pharmaceuticals in the Environment. The Royal Society of Chemistry, pp. 92-119.

Carballa, M., Omil, F., Lema, J.M., Llompart, M.a., García-Jares, C., Rodríguez, I., Gómez, M. Ternes, T., 2004. Behavior of pharmaceuticals, cosmetics and hormones in a sewage treatment plant. Water Res. 38 (12), 2918-2926.

Castiglioni, S., Bagnati, R., Fanelli, R., Pomati, F., Calamari, D. Zuccato, E., 2006. Removal of pharmaceuticals in sewage treatment plants in Italy. Environ. Sci. Technol. 40 (1), 357-363.

Chang, H.L. Alvarez-Cohen, L., 1995. Model for the cometabolic biodegradation of chlorinated organics. Environ. Sci. Technol. 29 (9), 2357-2367.

Chang, W.K. Criddle, C.S., 1997. Experimental evaluation of a model for cometabolism: Prediction of simultaneous degradation of trichloroethylene and methane by a methanotrophic mixed culture. Biotechnol. Bioeng. 56 (5), 492-501.

Chiron, S., Gomez, E. Fenet, H., 2009. Nitration processes of acetaminophen in nitrifying activated sludge. Environ. Sci. Technol. 44 (1), 284-289.

Clara, M., Kreuzinger, N., Strenn, B., Gans, O. Kroiss, H., 2005a. The solids retention time—a suitable design parameter to evaluate the capacity of wastewater treatment plants to remove micropollutants. Water Res. 39 (1), 97-106.

Clara, M., Strenn, B., Gans, O., Martinez, E., Kreuzinger, N. Kroiss, H., 2005b. Removal of selected pharmaceuticals, fragrances and endocrine disrupting compounds in a membrane bioreactor and conventional wastewater treatment plants. Water Res. 39 (19), 4797-4807.

Cleuvers, M., 2005. Initial risk assessment for three β-blockers found in the aquatic environment. Chemosphere 59 (2), 199-205.

Criddle, C.S., 1993. The kinetics of cometabolism. Biotechnol. Bioeng. 41 (11), 1048-1056.

Daughton, C.G. Ternes, T.A., 1999. Pharmaceuticals and personal care products in the environment: Agents of subtle change? Environ. Health Perspect. 107 (SUPPL. 6), 907-938.

Dawas-Massalha, A., Gur-Reznik, S., Lerman, S., Sabbah, I. Dosoretz, C.G., 2014. Co-metabolic oxidation of pharmaceutical compounds by a nitrifying bacterial enrichment. Bioresour. Technol. 167, 336-342.

De Gusseme, B., Vanhaecke, L., Verstraete, W. Boon, N., 2011. Degradation of acetaminophen by *Delftia tsuruhatensis* and *Pseudomonas aeruginosa* in a membrane bioreactor. Water Res. 45 (4), 1829-1837.

Delgadillo-Mirquez, L., Lardon, L., Steyer, J.-P. Patureau, D., 2011. A new dynamic model for bioavailability and cometabolism of micropollutants during anaerobic digestion. Water Res. 45 (15), 4511-4521.

Desbrow, C., Routledge, E.J., Brighty, G.C., Sumpter, J.P. Waldock, M., 1998. Identification of estrogenic chemicals in STW effluent. 1. Chemical fractionation and in vitro biological screening. Environ. Sci. Technol. 32 (11), 1549-1558.

Eichhorn, P., Ferguson, P.L., Pérez, S. Aga, D.S., 2005. Application of ion trap-MS with H/D exchange and QqTOF-MS in the identification of microbial degradates of trimethoprim in nitrifying activated sludge. Anal. Chem. 77 (13), 4176-4184.

Ely, R.L., Williamson, K.J., Hyman, M.R. Arp, D.J., 1997. Cometabolism of chlorinated solvents by nitrifying bacteria: Kinetics, substrate interactions, toxicity effects, and bacterial response. Biotechnol. Bioeng. 54 (6), 520-534.

Fernandez-Fontaina, E., Omil, F., Lema, J.M. Carballa, M., 2012. Influence of nitrifying conditions on the biodegradation and sorption of emerging micropollutants. Water Res. 46 (16), 5434-5444.

Fernandez-Fontaina, E., Carballa, M., Omil, F. Lema, J.M., 2014. Modelling cometabolic biotransformation of organic micropollutants in nitrifying reactors. Water Res. 65, 371-383.

Fischer, K. Majewsky, M., 2014. Cometabolic degradation of organic wastewater micropollutants by activated sludge and sludge-inherent microorganisms. Appl. Microbiol. Biotechnol. 98 (15), 6583-6597.

Forrez, I., Carballa, M., Boon, N. Verstraete, W., 2009. Biological removal of 17α-ethinylestradiol (EE2) in an aerated nitrifying fixed bed reactor during ammonium starvation. J. Chem. Technol. Biotechnol. 84 (1), 119-125.

Fournand, D. Arnaud, A., 2001. Aliphatic and enantioselective amidases: from hydrolysis to acyl transfer activity. J. Appl. Microbiol. 91 (3), 381-393.

Funke, J., Prasse, C. Ternes, T.A., 2016. Identification of transformation products of antiviral drugs formed during biological wastewater treatment and their occurrence in the urban water cycle. Water Res. 98, 75-83.

Gao, J.-F., Luo, X., Wu, G.-X., Li, T. Peng, Y.-Z., 2013. Quantitative analyses of the composition and abundance of ammonia-oxidizing archaea and ammonia-oxidizing bacteria in eight full-scale biological wastewater treatment plants. Bioresour. Technol. 138, 285-296.

Gaulke, L.S., Strand, S.E., Kalhorn, T.F. Stensel, H.D., 2008. 17α-ethinylestradiol transformation via abiotic nitration in the presence of ammonia oxidizing bacteria. Environ. Sci. Technol. 42 (20), 7622-7627.

Ghimire, B.K., 2012. Investigation of Oxygen Half Saturation Coefficients for Nitrification. M.S., The George Washington University, Ann Arbor.

Ginestet, P., Audic, J.M., Urbain, V. Block, J.C., 1998. Estimation of nitrifying bacterial activities by measuring oxygen uptake in the presence of the metabolic inhibitors allylthiourea and azide. Appl. Environ. Microbiol. 64 (6), 2266-2268.

Gómez, M.J., Martínez Bueno, M.J., Lacorte, S., Fernández-Alba, A.R. Agüera, A., 2007. Pilot survey monitoring pharmaceuticals and related compounds in a sewage treatment plant located on the Mediterranean coast. Chemosphere 66 (6), 993-1002.

Goossens, H., Ferech, M., Coenen, S., Stephens, P. The European Surveillance of Antimicrobial Consumption Project, G., 2007. Comparison of Outpatient Systemic Antibacterial Use in 2004 in the United States and 27 European Countries. Clin. Infect. Dis. 44 (8), 1091-1095.

Gros, M., Petrović, M. Barceló, D., 2006. Development of a multi-residue analytical methodology based on liquid chromatography–tandem mass spectrometry (LC–MS/MS) for screening and trace level determination of pharmaceuticals in surface and wastewaters. Talanta 70 (4), 678-690.

Gros, M., Petrović, M. Barceló, D., 2007. Wastewater treatment plants as a pathway for aquatic contamination by pharmaceuticals in the Ebro river basin (Northeast Spain). Environ. Toxicol. Chem. 26 (8), 1553-1562.

Gulde, R., Meier, U., Schymanski, E.L., Kohler, H.-P.E., Helbling, D.E., Derrer, S., Rentsch, D. Fenner, K., 2016. Systematic Exploration of Biotransformation Reactions of Amine-Containing Micropollutants in Activated Sludge. Environ. Sci. Technol. 50 (6), 2908-2920.

Heberer, T. Feldmann, D., 2005. Contribution of effluents from hospitals and private households to the total loads of diclofenac and carbamazepine in municipal sewage effluents—modeling versus measurements. J. Hazard. Mater. 122 (3), 211-218.

Helbling, D.E., Hollender, J., Kohler, H.-P.E. Fenner, K., 2010a. Structure-based interpretation of biotransformation pathways of amide-containing compounds in sludge-seeded bioreactors. Environ. Sci. Technol. 44 (17), 6628-6635.

Helbling, D.E., Johnson, D.R., Honti, M. Fenner, K., 2012. Micropollutant biotransformation kinetics associate with WWTP process parameters and microbial community characteristics. Environ. Sci. Technol. 46 (19), 10579-10588.

Helbling, D.E., Hollender, J., Kohler, H.P.E., Singer, H. Fenner, K., 2010b. High-throughput identification of microbial transformation products of organic micropollutants. Environ. Sci. Technol. 44 (17), 6621-6627.

Henze, M., Gujer, W., Mino, T. van Loosdrecht, M.C.M., 2000. Activated sludge models ASM1, ASM2, ASM2d and ASM3, IWA Publishing, London.

Henze, M., Grady Jr, C.P.L., Gujer, W., Marais, G.V.R. Matsuo, T., 1987. A general model for single-sludge wastewater treatment systems. Water Res. 21 (5), 505-515.

Hoerger, C.C., Akhtman, Y., Martelletti, L., Rutler, R., Bonvin, F., Grange, A., Arey, J.S. Kohn, T., 2014. Spatial extent and ecotoxicological risk assessment of a micropollutant-contaminated wastewater plume in Lake Geneva. Aquat. Sci. 76 (1), 7-19.

Hyman, M.R., Page, C.L. Arp, D.J., 1994. Oxidation of methyl fluoride and dimethyl ether by ammonia monooxygenase in *Nitrosomonas europaea*. Appl. Environ. Microbiol. 60 (8), 3033-3035.

Iasur-Kruh, L., Hadar, Y. Minz, D., 2011. Isolation and bioaugmentation of an estradiol-degrading bacterium and its integration into a mature biofilm. Appl. Environ. Microbiol. 77 (11), 3734-3740.

Jelić, A., Gros, M., Petrović, M., Ginebreda, A. Barceló, D., 2012. Occurrence and Elimination of Pharmaceuticals During Conventional Wastewater Treatment. In: Guasch, H., Ginebreda, A. and Geiszinger, A. eds. Emerging and Priority Pollutants in Rivers. Springer Berlin Heidelberg, pp. 1-23.

Jewell, K.S., Castronovo, S., Wick, A., Falås, P., Joss, A. Ternes, T.A., 2016. New insights into the transformation of trimethoprim during biological wastewater treatment. Water Res. 88, 550-557.

Jones, O.A., Lester, J.N. Voulvoulis, N., 2005. Pharmaceuticals: A threat to drinking water? Trends Biotechnol. 23 (4), 163-167.

Joss, A., Keller, E., Alder, A.C., Göbel, A., McArdell, C.S., Ternes, T. Siegrist, H., 2005. Removal of pharmaceuticals and fragrances in biological wastewater treatment. Water Res. 39 (14), 3139-3152.

Joss, A., Zabczynski, S., Göbel, A., Hoffmann, B., Löffler, D., McArdell, C.S., Ternes, T.A., Thomsen, A. Siegrist, H., 2006. Biological degradation of pharmaceuticals in municipal wastewater treatment: Proposing a classification scheme. Water Res. 40 (8), 1686-1696.

Kasim, N.A., Whitehouse, M., Ramachandran, C., Bermejo, M., Lennernäs, H., Hussain, A.S., Junginger, H.E., Stavchansky, S.A., Midha, K.K., Shah, V.P. Amidon, G.L., 2004. Molecular properties of WHO essential drugs and provisional biopharmaceutical classification. Mol. Pharmaceutics 1 (1), 85-96.

Kasprzyk-Hordern, B., Dinsdale, R.M. Guwy, A.J., 2009. The removal of pharmaceuticals, personal care products, endocrine disruptors and illicit drugs during wastewater treatment and its impact on the quality of receiving waters. Water Res. 43 (2), 363-380.

Kassotaki, E., Buttiglieri, G., Ferrando-Climent, L., Rodriguez-Roda, I. Pijuan, M., 2016. Enhanced sulfamethoxazole degradation through ammonia oxidizing bacteria co-metabolism and fate of transformation products. Water Res. 94, 111-119.

Keener, W.K. Arp, D.J., 1993. Kinetic studies of ammonia monooxygenase inhibition in *Nitrosomonas europaea* by hydrocarbons and halogenated hydrocarbons in an optimized whole-cell assay. Appl. Environ. Microbiol. 59 (8), 2501-2510.

Keener, W.K. Arp, D.J., 1994. Transformations of aromatic compounds by *Nitrosomonas europaea*. Appl. Environ. Microbiol. 60 (6), 1914-1920.

Khunjar, W.O., Skotnicka-Pitak, J., Love, N.G., Aga, D. Harper Jr, W.F. 2008. Biotransformation of pharmaceuticals and personal care products (PPCPs) during nitrification: the role of ammonia oxidizing bacteria versus heterotrophic bacteria. World Environmental and Water Resources Congress 2008, Honolulu, Hawaii, United States.

Khunjar, W.O., Mackintosh, S.A., Skotnicka-Pitak, J., Baik, S., Aga, D.S. Love, N.G., 2011. Elucidating the relative roles of ammonia oxidizing and heterotrophic bacteria during the biotransformation of 17α-ethinylestradiol and trimethoprim. Environ. Sci. Technol. 45 (8), 3605-3612.

Kim, Y., Arp, D.J. Semprini, L., 2002. A combined method for determining inhibition type, kinetic parameters, and inhibition coefficients for aerobic cometabolism of 1,1,1-trichloroethane by a butane-grown mixed culture. Biotechnol. Bioeng. 77 (5), 564-576.

Kosjek, T., Heath, E., Pérez, S., Petrović, M. Barceló, D., 2009. Metabolism studies of diclofenac and clofibric acid in activated sludge bioreactors using liquid chromatography with quadrupole - time-of-flight mass spectrometry. J. Hydrol. 372 (1-4), 109-117.

Kosma, C.I., Lambropoulou, D.A. Albanis, T.A., 2014. Investigation of PPCPs in wastewater treatment plants in Greece: Occurrence, removal and environmental risk assessment. Sci. Total Environ. 466–467, 421-438.

Kuai, L. Verstraete, W., 1998. Ammonium removal by the oxygen-limited autotrophic nitrification-denitrification system. Appl. Environ. Microbiol. 64 (11), 4500-4506.

Küster, A., Alder, A.C., Escher, B.I., Duis, K., Fenner, K., Garric, J., Hutchinson, T.H., Lapen, D.R., Péry, A., Römbke, J., Snape, J., Ternes, T., Topp, E., Wehrhan, A. Knackerk, T., 2010. Environmental risk assessment of human pharmaceuticals in the European union: A case study with the β-blocker atenolol. Integr. Environ. Assess. Manage. 6 (SUPPL. 1), 514-523.

Lauchnor, E.G. Semprini, L., 2013. Inhibition of phenol on the rates of ammonia oxidation by *Nitrosomonas europaea* grown under batch, continuous fed, and biofilm conditions. Water Res. 47 (13), 4692-4700.

Law, Y., Lant, P. Yuan, Z., 2011. The effect of pH on N2O production under aerobic conditions in a partial nitritation system. Water Res. 45 (18), 5934-5944.

Layton, A.C., Gregory, B.W., Seward, J.R., Schultz, T.W. Sayler, G.S., 2000. Mineralization of steroidal hormones by biosolids in wastewater treatment systems in Tennessee U.S.A. Environ. Sci. Technol. 34 (18), 3925-3931.

Li, D., Yang, M., Hu, J., Ren, L., Zhang, Y. Li, K., 2008. Determination and fate of oxytetracycline and related compounds in oxytetracycline production wastewater and the receiving river. Environ. Toxicol. Chem. 27 (1), 80-86.

Li, F., Jiang, B., Nastold, P., Kolvenbach, B.A., Chen, J., Wang, L., Guo, H., Corvini, P.F.X. Ji, R., 2015. Enhanced transformation of tetrabromobisphenol a by nitrifiers in nitrifying activated sludge. Environ. Sci. Technol. 49 (7), 4283-4292.

Limpiyakorn, T., Fürhacker, M., Haberl, R., Chodanon, T., Srithep, P. Sonthiphand, P., 2013. amoA-encoding archaea in wastewater treatment plants: a review. Appl. Microbiol. Biotechnol. 97 (4), 1425-1439.

Lishman, L., Smyth, S.A., Sarafin, K., Kleywegt, S., Toito, J., Peart, T., Lee, B., Servos, M., Beland, M. Seto, P., 2006. Occurrence and reductions of pharmaceuticals and personal care products and estrogens by municipal wastewater treatment plants in Ontario, Canada. Sci. Total Environ. 367 (2–3), 544-558.

Liu, L., Binning, P.J. Smets, B.F., 2015. Evaluating alternate biokinetic models for trace pollutant cometabolism. Environ. Sci. Technol. 49 (4), 2230-2236.

Luo, Y., Guo, W., Ngo, H.H., Nghiem, L.D., Hai, F.I., Zhang, J., Liang, S. Wang, X.C., 2014. A review on the occurrence of micropollutants in the aquatic environment and their fate and removal during wastewater treatment. Sci. Total Environ. 473-474, 619-641.

Mackuľak, T., Škubák, J., Grabic, R., Ryba, J., Birošová, L., Fedorova, G., Špalková, V. Bodík, I., 2014. National study of illicit drug use in Slovakia based on wastewater analysis. Sci. Total Environ. 494–495, 158-165.

MacLeod, S.L., Sudhir, P. Wong, C.S., 2007. Stereoisomer analysis of wastewater-derived β-blockers, selective serotonin re-uptake inhibitors, and salbutamol by high-performance liquid chromatography–tandem mass spectrometry. J. Chromatogr. A 1170 (1–2), 23-33.

Maeng, S.K., Choi, B.G., Lee, K.T. Song, K.G., 2013. Influences of solid retention time, nitrification and microbial activity on the attenuation of pharmaceuticals and estrogens in membrane bioreactors. Water Res. 47 (9), 3151-3162.

Maestre, J.P., Wahman, D.G. Speitel Jr, G.E., 2013. Monochloramine cometabolism by *Nitrosomonas europaea* under drinking water conditions. Water Res. 47 (13), 4701-4709.

Margot, J., Lochmatter, S., Barry, D.A. Holliger, C., 2016. Role of ammonia-oxidizing bacteria in micropollutant removal from wastewater with aerobic granular sludge. Water Sci. Technol. 73 (3), 564-575.

Maurer, M., Escher, B.I., Richle, P., Schaffner, C. Alder, A.C., 2007. Elimination of β-blockers in sewage treatment plants. Water Res. 41 (7), 1614-1622.

Men, Y., Achermann, S., Helbling, D.E., Johnson, D.R. Fenner, K., 2017. Relative contribution of ammonia oxidizing bacteria and other members of nitrifying activated sludge communities to micropollutant biotransformation. Water Res. 109, 217-226.

Men, Y., Han, P., Helbling, D.E., Jehmlich, N., Herbold, C., Gulde, R., Onnis-Hayden, A., Gu, A.Z., Johnson, D.R., Wagner, M. Fenner, K., 2016. Biotransformation of Two Pharmaceuticals by the Ammonia-Oxidizing Archaeon *Nitrososphaera gargensis*. Environ. Sci. Technol. 50 (9), 4682-4692.

Miao, X.S. Metcalfe, C.D., 2003. Determination of carbamazepine and its metabolites in aqueous samples using liquid chromatography - Electrospray tandem mass spectrometry. Anal. Chem. 75 (15), 3731-3738.

Miège, C., Choubert, J.M., Ribeiro, L., Eusèbe, M. Coquery, M., 2008. Removal efficiency of pharmaceuticals and personal care products with varying wastewater treatment processes and operating conditions - Conception of a database and first results. Water Sci. Technol. 57 (1), 49-56.

Mohsen-Nia, M., Ebrahimabadi, A.H. Niknahad, B., 2012. Partition coefficient n-octanol/water of propranolol and atenolol at different temperatures: Experimental and theoretical studies. J. Chem. Thermodyn. 54, 393-397.

Murdoch, R.W. Hay, A.G., 2005. Formation of catechols via removal of acid side chains from ibuprofen and related aromatic acids. Appl. Environ. Microbiol. 71 (10), 6121-6125.

Nakada, N., Tanishima, T., Shinohara, H., Kiri, K. Takada, H., 2006. Pharmaceutical chemicals and endocrine disrupters in municipal wastewater in Tokyo and their removal during activated sludge treatment. Water Res. 40 (17), 3297-3303.

Oldenhuis, R., Vink, R.L.J.M., Janssen, D.B. Witholt, B., 1989. Degradation of chlorinated aliphatic hydrocarbons by *Methylosinus trichosporium* OB3b expressing soluble methane monooxygenase. Appl. Environ. Microbiol. 55 (11), 2819-2826.

Park, H.D., Wells, G.F., Bae, H., Griddle, C.S. Francis, C.A., 2006. Occurrence of ammonia-oxidizing archaea in wastewater treatment plant bioreactors. Appl. Environ. Microbiol. 72(8), 5643-5647.

Pérez, S., Eichhorn, P. Aga, D.S., 2005. Evaluating the biodegradability of sulfamethazine, sulfamethoxazole, sulfathiazole, and trimethoprim at different stages of sewage treatment. Environ. Toxicol. Chem. 24 (6), 1361-1367.

Pérez, S., Eichhorn, P., Celiz, M.D. Aga, D.S., 2006. Structural characterization of metabolites of the X-ray contrast agent iopromide in activated sludge using ion trap mass spectrometry. Anal. Chem.78 (6), 1866-1874.

Petrie, B., Barden, R. Kasprzyk-Hordern, B., 2015. A review on emerging contaminants in wastewaters and the environment: Current knowledge, understudied areas and recommendations for future monitoring. Water Res. 72, 3-27.

Pham, T.-T. Proulx, S., 1997. PCBs and PAHs in the Montreal Urban Community (Quebec, Canada) wastewater treatment plant and in the effluent plume in the St Lawrence River. Water Res. 31 (8), 1887-1896.

Phillips, P.J., Schubert, C., Argue, D., Fisher, I., Furlong, E.T., Foreman, W., Gray, J. Chalmers, A., 2015. Concentrations of hormones, pharmaceuticals and other micropollutants in groundwater affected by septic systems in New England and New York. Sci. Total Environ. 512-513, 43-54.

Pieper, D.H., Reineke, W., Engesser, K.H. Knackmuss, H.J., 1988. Metabolism of 2,4-dichlorophenoxyacetic acid, 4-chloro-2-methylphenoxyacetic acid and 2-methylphenoxyacetic acid by *Alcaligenes eutrophus* JMP 134. Arch. Microbiol. 150 (1), 95-102.

Plósz, B.G., Langford, K.H. Thomas, K.V., 2012. An activated sludge modeling framework for xenobiotic trace chemicals (ASM-X): Assessment of diclofenac and carbamazepine. Biotechnol. Bioeng. 109 (11), 2757-2769.

Pomiès, M., Choubert, J.M., Wisniewski, C. Coquery, M., 2013. Modelling of micropollutant removal in biological wastewater treatments: A review. Sci. Total Environ. 443, 733-748.

Prasse, C., Schlüsener, M.P., Schulz, R. Ternes, T.A., 2010. Antiviral drugs in wastewater and surface waters: a new pharmaceutical class of environmental relevance? Environ. Sci. Technol. 44 (5), 1728-1735.

Prasse, C., Wagner, M., Schulz, R. Ternes, T.A., 2011. Biotransformation of the antiviral drugs acyclovir and penciclovir in activated sludge treatment. Environ. Sci. Technol. 45 (7), 2761-2769.

Quintana, J.B., Weiss, S. Reemtsma, T., 2005. Pathways and metabolites of microbial degradation of selected acidic pharmaceutical and their occurrence in municipal wastewater treated by a membrane bioreactor. Water Res. 39 (12), 2654-2664.

Radjenovic, J., Petrovic, M. Barceló, D., 2007. Analysis of pharmaceuticals in wastewater and removal using a membrane bioreactor. Anal. Bioanal. Chem. 387 (4), 1365-1377.

Radjenović, J., Pérez, S., Petrović, M. Barceló, D., 2008. Identification and structural characterization of biodegradation products of atenolol and glibenclamide by liquid chromatography coupled to hybrid quadrupole time-of-flight and quadrupole ion trap mass spectrometry. J. Chromatogr. A 1210 (2), 142-153.

Radniecki, T.S., Dolan, M.E. Semprini, L., 2008. Physiological and transcriptional responses of *Nitrosomonas europaea* to toluene and benzene inhibition. Environ. Sci. Technol. 42 (11), 4093-4098.

Rasche, M.E., Hicks, R.E., Hyman, M.R. Arp, D.J., 1990. Oxidation of monohalogenated ethanes and n-chlorinated alkanes by whole cells of *Nitrosomonas europaea*. J. Bacteriol. 172 (9), 5368-5373.

Rattier, M., Reungoat, J., Keller, J. Gernjak, W., 2014. Removal of micropollutants during tertiary wastewater treatment by biofiltration: Role of nitrifiers and removal mechanisms. Water Res. 54, 89-99.

Rivera-Utrilla, J., Sánchez-Polo, M., Ferro-García, M.Á., Prados-Joya, G. Ocampo-Pérez, R., 2013. Pharmaceuticals as emerging contaminants and their removal from water. A review. Chemosphere 93 (7), 1268-1287.

Roh, H., Subramanya, N., Zhao, F., Yu, C.-P., Sandt, J. Chu, K.-H., 2009. Biodegradation potential of wastewater micropollutants by ammonia-oxidizing bacteria. Chemosphere 77 (8), 1084-1089.

Rubirola, A., Llorca, M., Rodriguez-Mozaz, S., Casas, N., Rodriguez-Roda, I., Barceló, D. Buttiglieri, G., 2014. Characterization of metoprolol biodegradation and its transformation products generated in activated sludge batch experiments and in full scale WWTPs. Water Res. 63, 21-32.

Santos, J.L., Aparicio, I. Alonso, E., 2007. Occurrence and risk assessment of pharmaceutically active compounds in wastewater treatment plants. A case study: Seville city (Spain). Environ. Int. 33 (4), 596-601.

Santos, J.L., Aparicio, I., Callejón, M. Alonso, E., 2009. Occurrence of pharmaceutically active compounds during 1-year period in wastewaters from four wastewater treatment plants in Seville (Spain). J. Hazard. Mater. 164 (2–3), 1509-1516.

Sathyamoorthy, S., Chandran, K. Ramsburg, C.A., 2013. Biodegradation and cometabolic modeling of selected beta blockers during ammonia oxidation. Environ. Sci. Technol. 47 (22), 12835-12843.

Schäfer, A. Bouwer, E.J., 2000. Toluene induced cometabolism of cis-1,2-dichloroethylene and vinyl chloride under conditions expected downgradient of a permeable Fe(0) barrier. Water Res. 34 (13), 3391-3399.

Semprini, L., Dolan, M.E., Mathias, M.A., Hopkins, G.D. McCarty, P.L., 2007. Laboratory, field, and modeling studies of bioaugmentation of butane-utilizing microorganisms for the in situ cometabolic treatment of 1,1-dichloroethene, 1,1-dichloroethane, and 1,1,1-trichloroethane. Adv. Water Resour. 30 (6-7), 1528-1546.

Servos, M.R., Bennie, D.T., Burnison, B.K., Jurkovic, A., McInnis, R., Neheli, T., Schnell, A., Seto, P., Smyth, S.A. Ternes, T.A., 2005. Distribution of estrogens, 17β-estradiol and estrone, in Canadian municipal wastewater treatment plants. Sci. Total Environ. 336 (1–3), 155-170.

Sharma, M., Sharma, N.N. Bhalla, T.C., 2009. Amidases: Versatile enzymes in nature. Rev. Environ. Sci. Biotechnol. 8 (4), 343-366.

Sirés, I. Brillas, E., 2012. Remediation of water pollution caused by pharmaceutical residues based on electrochemical separation and degradation technologies: A review. Environ. Int. 40 (1), 212-229.

Skotnicka-Pitak, J., Khunjar, W.O., Love, N.G. Aga, D.S., 2009. Characterization of metabolites formed during the biotransformation of 17α-ethinylestradiol by *Nitrosomonas europaea* in batch and continuous flow bioreactors. Environ. Sci. Technol. 43 (10), 3549-3555.

Soulet, B., Tauxe, A. Tarradellas, J., 2002. Analysis of acidic drugs in Swiss wastewaters. Int. J. Environ. Anal. Chem. 82 (10), 659-667.

Stein, L.Y., Arp, D.J., Berube, P.M., Chain, P.S.G., Hauser, L., Jetten, M.S.M., Klotz, M.G., Larimer, F.W., Norton, J.M., Op den Camp, H.J.M., Shin, M. Wei, X., 2007. Whole-genome analysis of the ammonia-oxidizing bacterium, *Nitrosomonas eutropha* C91: implications for niche adaptation. Environ. Microbiol. 9 (12), 2993-3007.

Stumpf, M., Ternes, T.A., Wilken, R.-D., Silvana Vianna, R. Baumann, W., 1999. Polar drug residues in sewage and natural waters in the state of Rio de Janeiro, Brazil. Sci. Total Environ. 225 (1–2), 135-141.

Suarez, S., Lema, J.M. Omil, F., 2010. Removal of Pharmaceutical and Personal Care Products (PPCPs) under nitrifying and denitrifying conditions. Water Res. 44 (10), 3214-3224.

Suneethi, S. Joseph, K., 2011. Batch culture enrichment of ANAMMOX populations from anaerobic and aerobic seed cultures. Bioresour. Technol. 102 (2), 585-591.

Ternes, T.A., 1998. Occurrence of drugs in German sewage treatment plants and rivers. Water Res. 32 (11), 3245-3260.

Ternes, T.A. Hirsch, R., 2000. Occurrence and behavior of X-ray contrast media in sewage facilities and the aquatic environment. Environ. Sci. Technol. 34 (13), 2741-2748.

Tijani, J.O., Fatoba, O.O. Petrik, L.F., 2013. A review of pharmaceuticals and endocrine-disrupting compounds: Sources, effects, removal, and detections. Water Air Soil Pollut. 224 (11), 1770-1798.

Tran, N.H., Urase, T. Kusakabe, O., 2009. The characteristics of enriched nitrifier culture in the degradation of selected pharmaceutically active compounds. J. Hazard. Mater. 171 (1–3), 1051-1057.

Tran, N.H., Nguyen, V.T., Urase, T. Ngo, H.H., 2014. Role of nitrification in the biodegradation of selected artificial sweetening agents in biological wastewater treatment process. Bioresour. Technol. 161, 40-46.

Tran, N.H., Urase, T., Ngo, H.H., Hu, J. Ong, S.L., 2013. Insight into metabolic and cometabolic activities of autotrophic and heterotrophic microorganisms in the biodegradation of emerging trace organic contaminants. Bioresour. Technol. 146, 721-731.

Tsien, H.C., Brusseau, G.A., Hanson, R.S. Wackett, L.P., 1989. Biodegradation of trichloroethylene by *Methylosinus trichosporium* OB3b. Appl. Enviton. Microbiol. 55 (12), 3155-3161.

Urase, T. Kikuta, T., 2005. Separate estimation of adsorption and degradation of pharmaceutical substances and estrogens in the activated sludge process. Water Res. 39 (7), 1289-1300.

Vader, J.S., van Ginkel, C.G., Sperling, F.M.G.M., de Jong, J., de Boer, W., de Graaf, J.S., van der Most, M. Stokman, P.G.W., 2000. Degradation of ethinyl estradiol by nitrifying activated sludge. Chemosphere 41 (8), 1239-1243.

van Kessel, M.A.H.J., Speth, D.R., Albertsen, M., Nielsen, P.H., Op den Camp, H.J.M., Kartal, B., Jetten, M.S.M. Lücker, S., 2015. Complete nitrification by a single microorganism. Nature 528 (7583), 555-559.

Verce, M.F., Gunsch, C.K., Danko, A.S. Freedman, D.L., 2002. Cometabolism of cis-1,2-dichloroethene by aerobic cultures grown on vinyl chloride as the primary substrate. Environ. Sci. Technol. 36 (10), 2171-2177.

Verlicchi, P., Al Aukidy, M. Zambello, E., 2012. Occurrence of pharmaceutical compounds in urban wastewater: Removal, mass load and environmental risk after a secondary treatment—A review. Sci. Total Environ. 429, 123-155.

Vieno, N., Tuhkanen, T. Kronberg, L., 2007. Elimination of pharmaceuticals in sewage treatment plants in Finland. Water Res. 41 (5), 1001-1012.

Vieno, N.M., Tuhkanen, T. Kronberg, L., 2005. Seasonal variation in the occurrence of pharmaceuticals in effluents from a sewage treatment plant and in the recipient water. Environ. Sci. Technol. 39 (21), 8220-8226.

Vieno, N.M., Tuhkanen, T. Kronberg, L., 2006. Analysis of neutral and basic pharmaceuticals in sewage treatment plants and in recipient rivers using solid phase extraction and liquid chromatography–tandem mass spectrometry detection. J. Chromatogr. A 1134 (1–2), 101-111.

Wahman, D.G., Katz, L.E. Speitel Jr, G.E., 2005. Cometabolism of trihalomethanes by *Nitrosomonas europaea*. Appl. Environ. Microbiol. 71 (12), 7980-7986.

Wahman, D.G., Katz, L.E. Speitel Jr, G.E., 2007. Modeling of trihalomethane cometabolism in nitrifying biofilters. Water Res. 41 (2), 449-457.

Wiesmann, U. 1994. Biological nitrogen removal from wastewater. In: Ghosh, P., Hasegawa, S., and Kuhad, R. Ch. eds. Biotechnics/Wastewater. Springer Berlin Heidelberg, Berlin, Heidelberg, pp. 113-154.

Xu, Y., Yuan, Z. Ni, B.-J., 2017a. Biotransformation of acyclovir by an enriched nitrifying culture. Chemosphere 170, 25-32.

Xu, Y., Radjenovic, J., Yuan, Z. Ni, B.J., 2017b. Biodegradation of atenolol by an enriched nitrifying sludge: Products and pathways. Chem. Eng. J. 312, 351-359.

Yi, T. Harper Jr, W.F., 2007. The link between nitrification and biotransformation of 17α-ethinylestradiol. Environ. Sci. Technol. 41 (12), 4311-4316.

Yu, C.P., Roh, H. Chu, K.H., 2007. 17β-estradiol-degrading bacteria isolated from activated sludge. Environ. Sci. Technol. 41 (2), 486-492.

Yu, K., Li, B. Zhang, T., 2012. Direct rapid analysis of multiple PPCPs in municipal wastewater using ultrahigh performance liquid chromatography–tandem mass spectrometry without SPE pre-concentration. Anal. Chim. Acta 738, 59-68.

Yu, S., Dolan, M.E. Semprini, L., 2005. Kinetics and inhibition of reductive dechlorination of chlorinated ethylenes by two different mixed cultures. Environ. Sci. Technol. 39 (1), 195-205.

Yuan, F., Hu, C., Hu, X., Qu, J. Yang, M., 2009. Degradation of selected pharmaceuticals in aqueous solution with UV and UV/H2O2. Water Res. 43 (6), 1766-1774.

Zeng, Q., Li, Y., Gu, G., Zhao, J., Zhang, C. Luan, J., 2009. Sorption and biodegradation of 17β-estradiol by acclimated aerobic activated sludge and isolation of the bacterial strain. Environ. Eng. Sci. 26 (4), 783-790.

Zhang, Q., Illing, R., Hui, C.K., Downey, K., Carr, D., Stearn, M., Alshafi, K., Menzies-Gow, A., Zhong, N. Fan Chung, K., 2012. Bacteria in sputum of stable severe asthma and increased airway wall thickness. Respir. Res. 13 (1), 35-42.

Zhang, T., Ye, L., Tong, A.H.Y., Shao, M.-F. Lok, S., 2011. Ammonia-oxidizing archaea and ammonia-oxidizing bacteria in six full-scale wastewater treatment bioreactors. Appl. Microbiol. Biotechnol. 91 (4), 1215-1225.

Zwiener, C., Seeger, S., Glauner, T. Frimmel, F., 2002. Metabolites from the biodegradation of pharmaceutical residues of ibuprofen in biofilm reactors and batch experiments. Anal. Bioanal. Chem. 372 (4), 569-575.

Appendix A

Biodegradation of Atenolol by an Enriched Nitrifying Sludge: Products and Pathways

Yifeng Xu [a], Jelena Radjenovic [a,b,*], Zhiguo Yuan [a], Bing-Jie Ni [a,*]

This paper is published in *Chemical Engineering Journal*.

[a] Advanced Water Management Centre, The University of Queensland, St. Lucia, Brisbane, QLD 4072, Australia

[b] Catalan Institute for Water Research (ICRA), Scientific and Technological Park of the University of Girona, 17003 Girona, Spain

***Corresponding authors:**

Dr. Bing-Jie Ni, Phone: + 61 7 3346 3230; Fax: +61 7 3365 4726; E-mail: b.ni@uq.edu.au

Dr. Jelena Radjenovic, Phone: +34 972 18 33 80; Fax: +34 972 18 32 48; E-mail: jradjenovic@icra.cat

Abstract

Biodegradation of β-blocker atenolol was investigated using an enriched nitrifying culture at controlled ammonium concentration and without ammonium addition. Analysis of the kinetics and structural elucidation of biodegradation products showed that atenolol biodegradation was found to be linked to the activity of nitrifying bacteria in the presence of ammonium. Atenolol was degraded cometabolically by ammonia-oxidizing bacteria (AOB), likely due to a broad substrate range of ammonia monooxyenase (AMO). Four products were formed during atenolol biodegradation with ammonia oxidation, including P267 (atenolol acid) and three new products P117 (1-isopropylamino-2-propanol), P167 (1-amino-3-phenoxy-2-propanol), and an unknown product P227 with a nominal molecular mass of 227. In comparison, only P267 and P227 were identified during atenolol biodegradation without ammonia oxidation. Follow-up experiments using atenolol acid as the parent compound indicated the formation of products P117, P167 and P227 in the presence of ammonium. Based on the products identified, a tentative biodegradation pathway of atenolol is suggested, which involves two steps independent of the presence of ammonium: i) microbial amide-bond hydrolysis to carboxyl group and formation of P267 (atenolol acid) and ii) a possible formation of P227 with its unidentified structure and other two cometabolically induced reactions: iii) breakage of ether bond in the alkyl side chain and formation of P117 and iv) a minor pathway through N-dealkylation and loss

of acetamide moiety from the aromatic ring, yielding P167. This study provided an important insight regarding the biotransformation pathways under different metabolic conditions.

Keywords: Biodegradation; Ammonia oxidizing bacteria (AOB); Atenolol; Cometabolism; Transformation products; Pathways

1. Introduction

The occurrence of pharmaceutical residues in wastewater treatment plant (WWTP) effluents has attracted growing scientific and regulatory concerns during the last decade due to their potential detrimental effects on the ecosystem (Daughton and Ternes, 1999; Kolpin et al., 2002; Ternes, 1998). Conventional WWTPs are primarily designed to remove easily and moderately biodegradable carbon, nitrogen and phosphorus compounds and microbiological organisms, while pharmaceuticals and other trace organic contaminants are only partially transformed (Carballa et al., 2004; Evgenidou et al., 2015; Rivera-Utrilla et al., 2013; Ternes, 1998).

Enhanced removal of pharmaceuticals was observed in nitrifying activated sludge system (Batt et al., 2006; Clara et al., 2005). Another study showed that the oxidative removal of trace organic contaminants correlated with the removal of ammonium (NH_4^+-N) (Helbling et al., 2012). Ammonia oxidizing bacteria (AOB) in the nitrifying activated sludge are able to degrade a range of aromatic compounds due to its non-specific enzyme ammonium monooxygenase (AMO) (Keener and Arp, 1994; Skotnicka-Pitak et al., 2009), following cometabolism in the presence of a growth substrate such as ammonium (Tran et al., 2014). AMO was capable of oxidizing a broad range of aromatic substrates (Keener and Arp, 1994; Hooper et al., 1997), probably due to the mechanism of reaction with oxygenated form of AMO (Yi and Harper, 2007). On the other hand, heterotrophs also showed the ability to degrade some pharmaceuticals (ketoprofen, acetaminophen) following metabolic biodegradation pathways (De Gusseme et al., 2011; Quintana et al., 2005). However, the underlying biodegradation mechanisms of pharmaceuticals in nitrifying sludge are still ambiguous and need to be elucidated. Given that biodegradation products formed could be more persistent and toxic than their parent compound and related to the operating conditions (Pérez et al., 2006; Zwiener et al., 2002), it is important to study the biotransformation pathways of pharmaceuticals under different metabolic conditions and identify the microbial communities involved.

Atenolol is one of the most commonly prescribed β-blockers, used in antihypertensive, antianginal and antiarrhythmic treatment (Delamoye et al., 2004). After human consumption it is excreted mainly unchanged, leading to its frequent detection in raw wastewater and effluents of the WWTPs

(Verlicchi et al., 2012). Although the toxicity of atenolol is negligible, it may have a synergistic effect in the presence of other β-blockers in the environment (Cleuvers, 2005). Previously, amide-bond hydrolysis and formation of atenolol acid was reported as the main biodegradation pathway of atenolol in conventional activated sludge and membrane bioreactor sludge (Radjenović et al., 2008). Biodegradation of atenolol by nitrifying sludge was linked to the presence of AOB and heterotrophs (Sathyamoorthy et al., 2013). However, biodegradation products and pathways of atenolol in the nitrifying activated sludge remain unclear.

The main objectives of this study are to investigate the biodegradation mechanisms of atenolol by nitrifying sludge, to identify its biodegradation products and to propose possible biodegradation pathways under different metabolic conditions. Batch experiments were conducted at controlled ammonium concentration and without ammonium addition to investigate cometabolic and metabolic biodegradation of atenolol. Structural identification of the biodegradation products was performed to help elucidate the biodegradation pathways of atenolol.

2. Materials and methods

2.1 Chemicals

Atenolol (≥98%), atenolol acid, allylthiourea (ATU, 98%) and all the other organic solvents (LC grade) were purchased from Sigma-Aldrich, Australia. 1-isopropylamino-2-propanol (95%) and 1-amino-3-phenoxy-2-propanol (94%) were obtained from Enamine Ltd. The individual standard stock solution of atenolol was prepared in methanol at 1 g L^{-1} and stored at -20 °C. Working standards were obtained through dilution of the standard stock solution with purified water, obtained from a Milli-Q system (Millipore, Inc.). Atenolol feed solution for batch biodegradation experiments was prepared at 1 g L^{-1} in Milli-Q water.

2.2 Culture enrichment

A lab-scale sequencing batch reactor (SBR) seeded with activated sludge from a domestic wastewater treatment plant in Brisbane was used to enrich the nitrifying cultures, consisting of AOB and nitrite oxidizing bacteria (NOB). It was operated on a 6-h cycle consisting of 260 min aerobic feeding, 30 min aerobic reacting, 1 min wasting, 60 min settling and 9 min decanting periods. During each cycle, 2 L synthetic wastewater was fed into the reactor resulting in a hydraulic retention time (HRT) of 24 h. The solid retention time (SRT) was kept at 15 days. Reactor pH and dissolved oxygen (DO) were monitored using miniCHEM meters and controlled in the range of 7.5-8.0 and 2.5-3.0 mg L^{-1}, respectively, with programmed logic controllers (PLC). The synthetic wastewater for the AOB+NOB culture contained per liter (Kuai and Verstraete, 1998): 5.63 g of NH_4HCO_3 (1 g NH_4^+-N), 5.99 g of

$NaHCO_3$, 0.064 g of each of KH_2PO_4 and K_2HPO_4 and 2 mL of a trace element solution. The trace element stock solution contained: 1.25 g L^{-1} EDTA, 0.55 g L^{-1} $ZnSO_4 \cdot 7H_2O$, 0.40 g L^{-1} $CoCl_2 \cdot 6H_2O$, 1.275 g L^{-1} $MnCl_2 \cdot 4H_2O$, 0.40 g L^{-1} $CuSO_4 \cdot 5H_2O$, 0.05 g L^{-1} $Na_2MoO_4 \cdot 2H_2O$, 1.375 g L^{-1} $CaCl_2 \cdot 2H_2O$, 1.25 g L^{-1} $FeCl_3 \cdot 6H_2O$ and 44.4 g L^{-1} $MgSO_4 \cdot 7H_2O$.

The reactor was operated in steady state for more than 10 months, with 98.6 ± 3.5% conversion of NH_4^+ to NO_3^-, at the time of the batch tests. The mixed liquor volatile suspended solids (MLVSS) concentration was stable at 1437.6 ± 112.9 mg L^{-1} (mean and standard errors, respectively, n=10). Characterization of the biomass composition using fluorescence *in-situ* hybridization (FISH) indicated that 46 ± 6% (n=20) of the bacterial populations were ammonia-oxidizing *beta-proteobacteria* and 38 ± 5% (n=20) of the bacterial populations belonged to the *Nitrospira* genera (nitrite oxidizers). We also conducted 16S rRNA gene sequencing to identify the predominant AOB species of the enriched nitrifying culture. The result revealed that the AOB in the sludge were dominated by *Nitrosomonadaceae* (~80%).

2.3 Atenolol biodegradation experiments

Biodegradation experiments were conducted in 4 L beakers, wrapped in aluminum foil. 2.5 L freshly enriched nitrifying culture taken from the lab-scale SBR was used as the inoculum. To provide fundamental understanding of atenolol biodegradation and identify possible biodegradation products, they were amended with a relatively high concentration of atenolol, i.e., 15 mg L^{-1}, due to the fact that the products may not be fully identified under low concentration condition (Radjenović et al., 2008). The detailed batch experimental designs are provided in Table S1 in Supporting information (SI), consisting of five types of experimental protocols in duplicates for each. Experimental protocol 1 was to assess biodegradation of atenolol in the presence of ammonium with the addition of ammonium at 50 mg-N L^{-1}. This concentration was kept constant during the experiment through automatic addition of a mixture of ammonium bicarbonate and sodium bicarbonate with the purposes to provide ammonium and to adjust the pH. Experimental protocol 2 was to assess biodegradation of atenolol in absence of ammonium. The operational conditions were same as those in the experimental protocol 1, except that the culture did not contain any ammonium initially and no ammonium bicarbonate was supplied. Experimental protocol 3 was to study the contribution of heterotrophs on atenolol biodegradation with the addition of AMO inhibitor. ATU was reported to be a strong and selective inhibitor of ammonia oxidation (Ali et al., 2013), probably by chelating the copper of AMO active site (Ginestet et al., 1998). It was widely applied as a common method to inhibit AOB activity although it was not confirmed whether ATU would affect all copper-containing enzymes (Sathyamoorthy et al., 2013). 30 mg L^{-1} ATU was added before starting the experiment. Experimental

protocols 4 and 5 were used as control to assess the contribution of abiotic and hydrolytic degradation, respectively. For protocol 4, the biomass was autoclaved at 121 °C and 103 kPa for 30 minutes to ensure entire inactivation of the microbial activity (Kassotaki et al., 2016). For protocol 5, hydrolysis of atenolol was studied in Milli-Q water. DO and pH were maintained at the same levels as in the parent SBR, i,e, 2.5-3.0 mg L^{-1} and 7.5-8.0, respectively, which would not affect the dynamics of the microbial community structure in the batch experiment. The MLVSS concentration was kept at approximately 1 g L^{-1} in all experiments except the hydrolytic control. The batch experimental reactors were mixed using a magnetic stirrer at 250 rpm, and aerated during the entire experimental period. Samples were collected periodically for atenolol and the biodegradation products analysis.

2.4 Analytical methods

Samples from the biodegradation experiments were centrifuged at 12000 g for 5 min and 1 mL supernatant was used for structural elucidation of the biodegradation products. All samples were diluted 100 times for accurate quantification due to the limitation of the sensitivity and the range of the calibration curve (1-200 μg L^{-1}). Samples were analyzed with an ultra-fast liquid chromatography (UFLC) (Shimadzu, Japan) coupled with a 4000 QTRAP hybrid triple quadruple-linear ion trap mass spectrometer (QqLIT-MS) equipped with a Turbo Ion Spray source (Applied Biosystems-Sciex, USA). LC separation was performed using an Alltima C18 column at 40 °C, supplied by Alltech Associates Inc (USA). The injection volume was 20 μL. Atenolol and its biodegradation products were analyzed in positive electrospray ionization (ESI+) mode with a mobile phase containing (A) H_2O and (B) CH_3CN at 1 mL min^{-1}. The gradient elution procedure was conducted as follows: it was linearly increased to 5% B after 0.5 min, further increased to 20% B for 12.5 min, increased to 50% B within 5 min, increased to 100% B for 2 min, kept constant for 4 min and finally was decreased to 5% B for 1 min. The total running time including the conditioning of the column to the initial conditions was 27 min. The turbo ion spray source was operated in ESI+ mode using the following settings for the ion source and mass spectrometer: curtain gas 30 psi, spraying gas 50 psi, drying gas 50 psi, drying gas temperature of 500 °C. The declustering potential was 80 V under full scan mode. Mass range was set as 50-300 amu. Atenolol was analyzed in the multiple reaction monitoring (MRM) mode at transition ions of *m/z* 267→190 for confirmation and *m/z* 267→145 for quantification. The possible biodegradation products were identified through careful screening in the full scan chromatogram followed by spectrum analysis based on nitrogen rule and the existence of the peak [m+Na], etc. Tentative structures of biodegradation products were elucidated using the product ion scan mode (MS^2) and sequential fragmentation using the ion trap.

The ammonium concentrations were analyzed using a Lachat QuikChem8000 Flow Injection Analyzer (Lachat Instrument, Milwaukee) with the concentration profiles provided in Figure S1 in SI. No significant nitrite accumulation was observed (less than 1 mg L^{-1}) during experiments, which suggests nitration reactions were not relevant (Gaulke et al., 2008). Nitrate concentration was at similar level with the SBR effluent (up to 1000 mg L^{-1}). The mixed liquid suspended solid (MLSS) concentration and its volatile fraction (MLVSS) were analyzed in triplicate according to the standard methods (APHA, 1998).

3. Results and Discussion

3.1 Control experiments

The abiotic control experiment demonstrated a nearly constant trend of atenolol without formation of any transformation products during the 240 h experimental period (Figure 1d). Although autoclave might alter the structure of the sludge and affect the sorption capacity of the biomass, it could completely inactivate the biomass compared with the method using NaN_3 (Helbling et al., 2010a). The contribution of sorption to removal of atenolol was negligible in accordance with the previously reported low sorption coefficient K_D (0.04) and low octanol-water partition coefficient Log K_{OW} (0.16) of atenolol (Maurer et al., 2007; Mohsen-Nia et al., 2012). Hydrolytic control showed that the atenolol concentration remained nearly constant, which was also supported by the fact that no products were detected (Figure S2 in SI). Given the low value of Henry's Law coefficient of atenolol (1.37×10^{-18} atm m^3 mol^{-1}) (Küster et al., 2010), pH control and the exclusion of light in batch experiments, microbial biodegradation of atenolol was the major removal pathway in batch experiments.

3.2 Atenolol biodegradation with ammonia oxidation

Figure 1a illustrates the decrease of atenolol from an initial concentration of 15 mg L^{-1} and formation of its biodegradation products in the presence of ammonium. The concentration of atenolol decreased continuously with approximately 50% transformed by the end of the 240 h experiments. The observed trend did not follow a typical first order process and there was no linear correlation relationship between ln(C/C0) (C, atenolol concentration; C0, initial atenolol concentration) and t (time) for 240 h, probably influenced by ammonia oxidizing activity and inhibition from atenolol or its products. Therefore, non-linear regression analysis of atenolol concentration profile was performed as shown in Figure S3a in SI. At time 0, 24, 48 and 72 h, the atenolol biodegradation rates were calculated as 0.088, 0.061, 0.043 and 0.03 mg atenolol g VSS^{-1} h^{-1}, respectively. The pseudo-first order kinetics analysis for first 96 h indicated a degradation constant of 0.07 L g_{SS}^{-1} d^{-1}. It is lower than the reported values (1.1-1.9 L g_{SS}^{-1} d^{-1}) in the literature (Pomiès et al., 2013), likely due to the unaccustomed sludge to atenolol in this study. It is expected that the long-term adaption of the nitrifying culture to

atenolol presence will significantly enhance its degradation capacity, as confirmed in previous study regarding pharmaceutical degradation using nitrifying sludge (Fernandez-Fontaina et al., 2012). Ammonia oxidation rate was calculated based on the amounts of ammonium added and the measured NH_4^+-N concentration at each sampling time. The fact that atenolol biodegradation rate decreased with the decreasing ammonia oxidation rate (data shown in Figure 2a) was likely due to the substrate competition with ammonium (Sathyamoorthy et al., 2013) or inhibition by the more toxic biodegradation products (Arp et al., 2001). The competition for active AMO sites could result in decreasing degradation rates of both substrates. Atenolol inhibition on nitrification rate was associated with a lower inhibition constant (~4-33 nM), suggesting a greater affinity of AMO for atenolol (Sathyamoorthy et al., 2013). The biotransformation products (for example phenol, transformed from benzene) might also inhibit AOB activity (Radniecki et al., 2008).

Figure 2b illustrates a positive linear relationship between ammonia oxidation rate and atenolol biodegradation rate. Such a positive correlation was also reported for 17α-ethinylestradiol (Yi and Harper, 2007). This supported the cometabolic biodegradation of atenolol in the presence of ammonium (Tran et al., 2014), likely mediated by the enriched nitrifying culture through the non-specific enzyme AMO (Keener and Arp, 1993; Keener and Arp, 1994; Lauchnor and Semprini, 2013; Rasche et al., 1990). As the ammonium concentration was controlled nearly constant in the experiments with ammonia oxidation, the ratio of atenolol to ammonia was decreasing due to the decreased atenolol concentration during the time course. The positive relationship between atenolol degradation rate and ammonia oxidation rate would thus be valid as the ratio of atenolol to ammonia was between 0.006 and 0.017 in our experiments. The positive correlation between modeled atenolol degradation rate and ammonia oxidation rate after 240 h (orange dots in Figure 2b, based on the calculation using the model in Figure S3a) further confirmed the possible wide range of application for such relationship at different atenolol to ammonia ratios. However, the ratio range for the positive relationship in Figure 2b was confirmed to reside in the studied experimental conditions, with the further verification being required for lower atenolol concentration or different atenolol to ammonia ratios. On the other hand, the correlation might be present at the different slope if applying the modest concentration of atenolol, given the inhibition from studied high concentration of atenolol on ammonia oxidation rate.

Simultaneously with the decrease in atenolol concentration (Figure 1a), four new peaks appeared, at retention times of 11.12 (P267), 2.92 (P117), 5.25 (P167) and 3.89 min (P227) (Figure S4 in SI). The structural elucidation process is described in the following section 3.5. The formation of biodegradation products of atenolol was firstly determined qualitatively, using the peak areas of the

extracted ion chromatograms (A), normalized to the initial peak area of atenolol (A0). As shown in Figure 1a, the product P267 was formed continuously until the end of the experiment (240 h). As the reference standard for this compound (atenolol acid) is available, its concentration was then quantified, which was determined to increase up to 1.3 mg L^{-1} (8.6% of conversion from initial atenolol concentration) at the end of the experiment. The products P117 (molecular ion at *m/z* 118) and P167 (molecular ion at *m/z* 168) were quantified to increase to 37.4 μg L^{-1} and 97.6 μg L^{-1} at the end of the experiment (based on the purchased standards after structural identification). In the presence of ammonium another product P227 was also observed. Its molecular ion *m/z* 228 had very low signal intensity, with a normalized peak area of only 2% relative to the initial peak area of atenolol.

3.3 Atenolol biodegradation without ammonia oxidation

Figure 1b represents a decrease in atenolol concentration with 40% removal at the end of the experiment (240 h) in the absence of ammonium, which was lower than the removal obtained in the batch experiments with ammonia oxidation (50%). The atenolol biodegradation rate (0.023 mg atenolol g VSS^{-1} h^{-1}, Figure S3b in SI) was also lower than the values in the presence of ammonium during higher ammonia oxidation rate, confirming the potential role of cometabolism in atenolol biodegradation by the enriched nitrifying culture.

Without the presence of ammonium, AOB lacked an important growth substrate to support their growth and energy consumption and enzyme synthesis, therefore leading to non-cometabolic biodegradation of atenolol. Under such conditions, some pharmaceuticals could be utilized as sole substrates for carbon and energy source following various metabolic biodegradation pathways, mostly conducted by heterotrophs (De Gusseme et al., 2011; Quintana et al., 2005).

During atenolol biodegradation in the absence of ammonium, two new peaks were detected at *m/z* 268 (P267, atenolol acid) and a low intensity peak at *m/z* 228 (P227). Atenolol acid seemed to be formed in higher amounts than during biodegradation in the presence of ammonium, which could be probably due to the formation of P117 and P167 in the latter case. The concentration of P267 reached 2.9 mg L^{-1} at the end of the experiment. On the other hand, the signal intensity of the molecular ion at *m/z* 228 was very low (<2%) (Figure 1b).

3.4 Role of heterotrophs in atenolol biodegradation

Figure 1c illustrates a decrease in atenolol concentration (at the degradation rate of -0.024 mg atenolol g VSS^{-1} h^{-1}, Figure S3c) and formation of product P267 (atenolol acid), which was the only product identified in the presence of ATU. The removal efficiency of atenolol over the 240 h experimental

period was 39%, similar to the removal obtained in the absence of ammonium. As the ammonium released from cell lysis process during bacterial decay was minor, cometabolic biodegradation by AOB without addition of ammonium would not contribute to atenolol biodegradation significantly. Therefore, non-cometabolism by AOB was negligible and biodegradation by heterotrophs mainly contributed to the removal of atenolol in the absence of ammonium, which can be confirmed from the similar atenolol removal efficiencies when AOB activity was inhibited by ATU (Figures 1b and 1c). In the presence of ATU, ammonia oxidation was inhibited and atenolol biodegradation rate was calculated as 0.028 mg atenolol g VSS^{-1} h^{-1}, which was constant during the time course. Therefore, the contribution of heterotrophs would not change significantly during atenolol biodegradation and thus would not affect the linear relationship between atenolol biodegradation rate and ammonia oxidation rate in the presence of ammonium (Figure 2b), which could also be confirmed from the approximately same slope in the corresponding relationship subtracting the contribution by heterotrophs (Figure S5).

However, the accumulation of P267 reached 1.7 mg L^{-1} at the end of the experiment in the presence of ATU, which was lower than the value of 2.9 mg L^{-1} in the absence of ammonium. Based on these observations (Figures 1b and 1c), P267 could be possibly formed through atenolol biodegradation by both AOB and heterotrophs.

The atenolol biodegradation with ammonia oxidation and with the addition of ATU further proved the role of AOB and heterotrophs in pharmaceutical biodegradation (Khunjar et al., 2011). Previously, same biotransformation products of EE2 were formed in the biodegradation experiments by either AOB or heterotrophs (Khunjar et al., 2011), whereas the metabolic type had a significant influence in the biotransformation products and pathways of atenolol in this study (detailed in the following sections).

3.5 Structural elucidation of biodegradation products

Based on the analysis of their full scan spectra, no biotransformation products were detected in the atenolol standard solution without biodegradation as well as in the enriched nitrifying biomass sample without the addition of atenolol, respectively (Figure S6). Furthermore, the qualitative profiles of P117, P167, P227 and P267 showed a gradual increase trend during the time course (Figure 1). Therefore, the formation of products P117, P167, P227 and P267 should be solely produced from atenolol biodegradation.

The chemical structures of these products were elucidated through analysis of their product ion scan mass spectrum and comparison with the available standard. Briefly, their structures were proposed based on these fragment ions and the structural information of atenolol followed by confirmation with the standards.

The most abundant fragment ions detected in the MS^2 spectrum of atenolol (molecular ion *m/z* 267) were *m/z* 190 and 145 (Figure S7a). Fragment ion *m/z* 190 was formed by the loss of 77 Da from the molecular ion, characteristic for β-blockers bearing the –NH-CH(CH_3)$_2$ side chain (Escher et al., 2006). Further loss of ammonia and CO followed by an intramolecular cyclization yielded fragment ion *m/z* 145. A similar fragmentation pattern was observed for the biodegradation product P267, with a molecular ion *m/z* 268 (Figure S7b). Comparing with the MS^2 spectrum of the standard solution of atenolol acid (Figure S8a), it could be confirmed based on the same fragment ions and fragmentation pattern that the product P267 was atenolol acid in this work. Product ion spectra of atenolol and atenolol acid have been described in previous studies as well as the structural identification process of the transformation products (Kern et al., 2010; Radjenović et al., 2008). However, to date only one biodegradation product, i.e., atenolol acid (P267), has been identified in the biodegradation of atenolol by conventional activated sludge, membrane bioreactor sludge or activated sludge from a full-scale aerobic nitrification reactor (Radjenović et al., 2008; Rubirola et al., 2014). In this study, P267 formation was likely due to the contribution by both AOB and heterotrophs. This joint contribution was also previously confirmed from the formation of the biodegradation products of 17α-ethinylestradiol in enriched nitrifying cultures (Khunjar et al., 2011). As heterotrophs in the enriched nitrifying sludge might live on more complex carbon source such as decaying cells, the products formed by heterotrophs in other cultures (e.g. WWTP sludge) may be different, which deserves further research.

MS^2 spectrum of molecular ion *m/z* 118 (product P117) is shown in Figure 3a. Two fragment ions were detected at *m/z* 58 and *m/z* 59, presumably formed by the loss of isopropylamine and isopropanol, respectively. Further fragmentation of fragment ions *m/z* 58 and *m/z* 59 did not show any new signals in the mass spectrum of P117. In comparison with the standard spectrum in Figure S8b, product P117 could be identified as 1-isopropylamino-2-propanol. Collision induced dissociation of the molecular ion at *m/z* 168 (P167) resulted in fragment ions *m/z* 151, *m/z* 133 and *m/z* 107 (Figure 3b). Formation of fragment ion *m/z* 151 was assigned to the loss of ammonia from the molecular ion *m/z* 168. Further fragmentation of *m/z* 151 led to a loss of water to form *m/z* 133, and further cleavage of acetylene (C_2H_2) to yield a signal at *m/z* 107. Based on the obtained information and the spectrum of the standard in Figure S8c, P167 was assigned to 1-amino-3-phenoxy-2-propanol. The structure of P227

could not be accurately identified using the MS^2 experiments due to the very low signal intensity of the molecular ion *m/z* 228. Based on its MS^2 spectrum presented in Figure 3c, molecular ion *m/z* 228 underwent two consecutive losses of 18 Da to form fragment ions *m/z* 210 and *m/z* 192. According to the nitrogen rule, P227 contained one nitrogen atom and may have been formed through amide-bond hydrolysis to carboxylic acid, similar to the product P267. Additional analytical methods including accurate mass measurements are required for accurate identification of P227.

The formation of additional products P117, P167 and P227 was firstly reported in this study, which could be explained by the constant ammonium feed favoring cometabolic biodegradation by nitrifying cultures. AOB-induced cometabolic biodegradation led to the production of P117 and P167 compared with the biodegradation in absence of ammonium, indicating the cometabolism could affect the formation of biodegradation products of pharmaceuticals. As previously reported, bezafibrate, naproxen, ibuprofen and diclofenac were biotransformed only by the cometabolic biodegradation (Quintana et al., 2005). Given that P227 was not found when ATU was added to inhibit AOB growth, this biodegradation product may be assigned to AOB instead of heterotrophs.

3.6 Biodegradation of atenolol acid in the presence of ammonium

In order to further confirm the formation of biotransformation products, the follow-up experiments were conducted on atenolol acid as the parent compound to study its biodegradation pathway in the presence of ammonium. The batch experimental designs were same as those for atenolol. Figure 4 shows the qualitative profiles of atenolol acid and its biotransformation products during 240 h. After a short period of lag phase, atenolol acid dissipated to the final concentration of 9.95 mg L^{-1} with the removal up to 28%. Three products P117, P167 and P227 were found from the beginning of the experiments with the increasing trends. As the reference standards for P117 and P167 were available, their final concentrations were quantified as 450.5 and 96.6 μg L^{-1}, respectively.

3.7 Biodegradation pathways by enriched nitrifying sludge

Based on the identified products, the possible biodegradation pathway by the enriched nitrifying sludge was proposed in Figure 5. It indicated that cometabolic biodegradation by AOB would lead to different biotransformation pathways of atenolol (forming P267, P227, P117 and P167) compared to its metabolic biodegradation (producing P267 and P227). The main biodegradation pathway of atenolol was the hydrolysis of the amide group to its carboxylic moiety (P267, atenolol acid) regardless of the presence of ammonium. Microbial-induced hydrolysis of atenolol has previously been observed in conventional activated sludge and membrane bioreactor as well as activated sludge receiving sanitary sewage (Helbling et al., 2010b, Radjenović et al., 2008). Hydrolysis was typical

for most amide-containing compounds such as bezafibrate and levetiracetam (Helbling et al., 2010b, Quintana et al., 2005). It can be catalyzed by amidases and proteolytic enzymes (Fournand and Arnaud, 2001; Sharma et al., 2009). While these enzymes were not found in *Nitrosomonas eutropaea* (Chain et al., 2003), two genes found in *Nitrosomonas eutropha* including N-acetylmuramoyl-L-alanine amidase (Neut_1623) and amidohydrolase-2 (Neut_1622) could favor the hydrolysis of the C-N bond of amide groups (Stein et al., 2007).

Formation of P227 likely involved the hydrolysis of amide bond. One human metabolite of atenolol is a hydroxylated compound (Escher et al., 2006; Reeves et al., 1978). Although it was not detected in this study, the similar hydroxylation at the carbon atom neighboring ether oxygen atom may be part of the reactions producing P227.

P267 likely underwent further transformation through the cleavage of ether bond in the alkyl side chain (i.e., formation of P117), and N-dealkylation (loss of isopropyl group) and loss of acetamide moiety from the aromatic ring, yielding the product P167 under cometabolic conditions. These pathways were related to AOB activity, which was also confirmed through the experiments using P267 (atenolol acid) as the parent compound. The cleavage of ether bond in 2,4-dichlorophenoxyacetic acid, 4-chloro-2-methylphenoxyacetic acid and 2-methylphenoxyacetic acid was reported by *Alcaligenes eutrophus* JMP 134 (Pieper et al., 1988). Dimethyl ether could be cooxidized to form methanol and formaldehyde by an ammonia monooxygenase of *Nitrosomonas europaea* (Hyman et al., 1994). Although there was not much direct work confirming the same bond cleavage as this study (P267 was transformed to P117), it could be speculated that there might exist some intermediates formed from the typical ether bond cleavage or that the reported bond cleavage in this study was due to cometabolism by AOB. Further research would be required to confirm this biochemical reaction. Another β-blocker propranolol also underwent dealkylation reaction to produce desisopropylpropranolol in rat, dog and man (Chen and Nelson, 1982; Nelson and Bartels, 1984). Few reports were documented for dealkylation on amine group of atenolol by nitrifying bacteria. Dealkylation reaction was reported as an important pathway for a variety of amine-containing compounds in either the biotransformation system by nitrifying sludge or the mammalian system (Gulde et al., 2016). Previously reported dealkylation of secondary amine occurs in catalysis by monooxygenase from *Pseudomonas aminovorans*, which had the same function as cytochrome P450 or by monoamine oxidase-w-Transaminase cascade (Alberta et al., 1989; O'Reilly et al., 2014). Notwithstanding the absence of previous direct evidence of AMO on dealkylation, it was suspected that the monooxygenase from AOB likely catalyze this biochemical reaction. As for the loss of acetamide group from aromatic ring, it also requires more efforts on identifying this reaction in the

future. On the other hand, atenolol biodegradation at relatively realistic concentrations also needs to be conducted in order to verify the formation of the biodegradation products and the proposed biodegradation pathways, which was confirmed in Appendix B.

4. Conclusions

In this work, the biodegradation of β-blocker atenolol was investigated using an enriched nitrifying culture at controlled ammonium concentration and without ammonium addition. The key conclusions are:

- Atenolol biodegradation was found to be related to ammonia oxidation rate, indicating the cometabolism by AOB in the enriched nitrifying sludge.
- Four compounds including P117, P167, P227 and P267 (atenolol acid) were produced under cometabolic condition in the presence of ammonium while only two products P267 and P227 were formed in the absence of ammonium.
- P117, P167 and P227 were not reported previously. The chemical structures of P117 and P167 were identified as 1-isopropylamino-2-propanol and 1-amino-3-phenoxy-2-propanol.
- Atenolol was hydroxylated to P267 (atenolol acid) and was converted to P227 regardless of the presence of ammonium. Under cometabolic conditions, the biodegradation product P117 and P167 could be further formed through the cleavage of ether bond in the alkyl side chain and N-dealkylation and loss of acetamide moiety, respectively.

Acknowledgment

This study was supported by the Australian Research Council (ARC) through Discovery Early Career Researcher Award DE130100451. Bing-Jie Ni acknowledges the support of ARC Discovery Project DP130103147.

References

Alberta, J.A., Andersson, L.A., Dawson, J.H., 1989. Spectroscopic characterization of secondary amine mono-oxygenase. Comparison to cytochrome P-450 and myoglobin. J. Biol. Chem. 264 (34), 20467-20473.

Ali, T.U., Kim, M. Kim, D.J., 2013. Selective inhibition of ammonia oxidation and nitrite oxidation linked to n2o emission with activated sludge and enriched nitrifiers. J. Microbiol. Biotechnol. 23 (5), 719-723.

APHA, 1998. Standard methods for the examination of water and wastewater. American Public Health Association, American Water Works Association and Water Environment Federation, Washington, DC, U.S.A.

Arp, D., Yeager, C., Hyman, M., 2001. Molecular and cellular fundamentals of aerobic cometabolism of trichloroethylene. Biodegradation 12 (2), 81-103.

Batt, A.L., Kim, S., Aga, D.S., 2006. Enhanced biodegradation of iopromide and trimethoprim in nitrifying activated sludge. Environ. Sci. Technol. 40 (23), 7367-7373.

Carballa, M., Omil, F., Lema, J.M., Llompart, M.a., García-Jares, C., Rodríguez, I., Gómez, M., Ternes, T., 2004. Behavior of pharmaceuticals, cosmetics and hormones in a sewage treatment plant. Water Res. 38 (12), 2918-2926.

Chain, P., Lamerdin, J., Larimer, F., Regala, W., Lao, V., Land, M., Hauser, L., Hooper, A., Klotz, M., Norton, J., Sayavedra-Soto, L., Arciero, D., Hommes, N., Whittaker, M., Arp, D., 2003. Complete genome sequence of the ammonia-oxidizing bacterium and obligate chemolithoautotroph *Nitrosomonas europaea*. J. Bacteriol. 185 (9), 2759-2773.

Chen, C.H., Nelson, W.L., 1982. N-dealkylation of propranolol: Trapping of the 3-(1-naphthoxy)-2-hydroxypropionaldehyde formed in rat liver microsomes. Drug Metab. Dispos. 10 (3), 277-278.

Clara, M., Kreuzinger, N., Strenn, B., Gans, O., Kroiss, H., 2005. The solids retention time—a suitable design parameter to evaluate the capacity of wastewater treatment plants to remove micropollutants. Water Res. 39 (1), 97-106.

Cleuvers, M., 2005. Initial risk assessment for three β-blockers found in the aquatic environment. Chemosphere 59 (2), 199-205.

Daughton, C.G., Ternes, T.A., 1999. Pharmaceuticals and personal care products in the environment: Agents of subtle change? Environmental Health Perspectives 107 (SUPPL. 6), 907-938.

De Gusseme, B., Vanhaecke, L., Verstraete, W., Boon, N., 2011. Degradation of acetaminophen by *Delftia tsuruhatensis* and *Pseudomonas aeruginosa* in a membrane bioreactor. Water Res. 45 (4), 1829-1837.

Delamoye, M., Duverneuil, C., Paraire, F., De Mazancourt, P., Alvarez, J.C., 2004. Simultaneous determination of thirteen β-blockers and one metabolite by gradient high-performance liquid chromatography with photodiode-array UV detection. Forensic Sci. Int. 141 (1), 23-31.

Escher, B.I., Bramaz, N., Richter, M., Lienert, J., 2006. Comparative ecotoxicological hazard assessment of beta-blockers and their human metabolites using a mode-of-action-based test battery and a QSAR approach. Environ. Sci. Technol. 40 (23), 7402-7408.

Evgenidou, E.N., Konstantinou, I.K., Lambropoulou, D.A., 2015. Occurrence and removal of transformation products of PPCPs and illicit drugs in wastewaters: A review. Sci. Total Environ. 505, 905-926.

Fernandez-Fontaina, E., Omil, F., Lema, J.M. Carballa, M., 2012. Influence of nitrifying conditions on the biodegradation and sorption of emerging micropollutants. Water Res. 46 (16), 5434-5444.

Fournand, D., Arnaud, A., 2001. Aliphatic and enantioselective amidases: from hydrolysis to acyl transfer activity. J. Appl. Microbiol. 91 (3), 381-393.

Gaulke, L.S., Strand, S.E., Kalhorn, T.F. Stensel, H.D., 2008. 17α-ethinylestradiol transformation via abiotic nitration in the presence of ammonia oxidizing bacteria. Environ. Sci. Technol. 42(20), 7622-7627.

Ginestet, P., Audic, J.M., Urbain, V., Block, J.C., 1998. Estimation of nitrifying bacterial activities by measuring oxygen uptake in the presence of the metabolic inhibitors allylthiourea and azide. Appl. Environ. Microbiol. 64 (6), 2266-2268.

Gulde, R., Meier, U., Schymanski, E.L., Kohler, H.-P.E., Helbling, D.E., Derrer, S., Rentsch, D. Fenner, K., 2016. Systematic Exploration of Biotransformation Reactions of Amine-Containing Micropollutants in Activated Sludge. Environ. Sci. Technol. 50 (6), 2908-2920.

Helbling, D.E., Hollender, J., Kohler, H.-P.E., Fenner, K., 2010a. Structure-based interpretation of biotransformation pathways of amide-containing compounds in sludge-seeded bioreactors. Environ. Sci. Technol. 44 (17), 6628-6635.

Helbling, D.E., Hollender, J., Kohler, H.P.E., Singer, H., Fenner, K., 2010b. High-throughput identification of microbial transformation products of organic micropollutants. Environ. Sci. Technol. 44 (17), 6621-6627.

Helbling, D.E., Johnson, D.R., Honti, M., Fenner, K., 2012. Micropollutant biotransformation kinetics associate with WWTP process parameters and microbial community characteristics. Environ. Sci. Technol. 46 (19), 10579-10588.

Hooper, A.B., Vannelli, T., Bergmann, D.J. Arciero, D.M., 1997. Enzymology of the oxidation of ammonia to nitrite by bacteria. Antonie van Leeuwenhoek, Int. J. Gen. Mol. Microbiol. 71 (1-2), 59-67.

Hyman, M.R., Page, C.L., Arp, D.J., 1994. Oxidation of methyl fluoride and dimethyl ether by ammonia monooxygenase in *Nitrosomonas europaea*. Appl. Environ. Microbiol. 60 (8), 3033-3035.

Kassotaki, E., Buttiglieri, G., Ferrando-Climent, L., Rodriguez-Roda, I. Pijuan, M., 2016. Enhanced sulfamethoxazole degradation through ammonia oxidizing bacteria co-metabolism and fate of transformation products. Water Res. 94, 111-119.

Keener, W.K., Arp, D.J., 1993. Kinetic studies of ammonia monooxygenase inhibition in *Nitrosomonas europaea* by hydrocarbons and halogenated hydrocarbons in an optimized whole-cell assay. Appl. Environ. Microbiol. 59 (8), 2501-2510.

Keener, W.K., Arp, D.J., 1994. Transformations of aromatic compounds by Nitrosomonas europaea. Appl. Environ. Microbiol. 60 (6), 1914-1920.

Kern, S., Baumgartner, R., Helbling, D.E., Hollender, J., Singer, H., Loos, M.J., Schwarzenbach, R.P., Fenner, K., 2010. A tiered procedure for assessing the formation of biotransformation products of pharmaceuticals and biocides during activated sludge treatment. J. Environ. Monit. 12 (11), 2100-2111.

Khunjar, W.O., Mackintosh, S.A., Skotnicka-Pitak, J., Baik, S., Aga, D.S., Love, N.G., 2011. Elucidating the relative roles of ammonia oxidizing and heterotrophic bacteria during the biotransformation of 17α-ethinylestradiol and trimethoprim. Environ. Sci. Technol. 45 (8), 3605-3612.

Kolpin, D.W., Furlong, E.T., Meyer, M.T., Thurman, E.M., Zaugg, S.D., Barber, L.B., Buxton, H.T., 2002. Pharmaceuticals, hormones, and other organic wastewater contaminants in U.S. streams, 1999-2000: A national reconnaissance. Environ. Sci. Technol. 36 (6), 1202-1211.

Kuai, L., Verstraete, W., 1998. Ammonium removal by the oxygen-limited autotrophic nitrification-denitrification system. Appl. Environ. Microbiol. 64 (11), 4500-4506.

Küster, A., Alder, A.C., Escher, B.I., Duis, K., Fenner, K., Garric, J., Hutchinson, T.H., Lapen, D.R., Péry, A., Römbke, J., Snape, J., Ternes, T., Topp, E., Wehrhan, A., Knackerk, T., 2010. Environmental risk assessment of human pharmaceuticals in the European union: A case study with the β-blocker atenolol. Integr. Environ. Assess. Manage. 6 (SUPPL. 1), 514-523.

Lauchnor, E.G., Semprini, L., 2013. Inhibition of phenol on the rates of ammonia oxidation by *Nitrosomonas europaea* grown under batch, continuous fed, and biofilm conditions. Water Res. 47 (13), 4692-4700.

Maurer, M., Escher, B.I., Richle, P., Schaffner, C., Alder, A.C., 2007. Elimination of β-blockers in sewage treatment plants. Water Res. 41 (7), 1614-1622.

Mohsen-Nia, M., Ebrahimabadi, A.H., Niknahad, B., 2012. Partition coefficient n-octanol/water of propranolol and atenolol at different temperatures: Experimental and theoretical studies. J. Chem. Thermodyn. 54, 393-397.

Nelson, W.L., Bartels, M.J., 1984. N-dealkpylation of propranolol in rat, dog, and man. Chemical and stereochemical aspects. Drug Metab. Dispos. 12 (3), 345-352.

O'Reilly, E., Iglesias, C., Turner, N.J., 2014. Monoamine oxidase-ω-transaminase cascade for the deracemisation and dealkylation of amines. ChemCatChem 6 (4), 992-995.

Pérez, S., Eichhorn, P., Celiz, M.D., Aga, D.S., 2006. Structural characterization of metabolites of the X-ray contrast agent iopromide in activated sludge using ion trap mass spectrometry. Anal. Chem. 78 (6), 1866-1874.

Pieper, D.H., Reineke, W., Engesser, K.H., Knackmuss, H.J., 1988. Metabolism of 2,4-dichlorophenoxyacetic acid, 4-chloro-2-methylphenoxyacetic acid and 2-methylphenoxyacetic acid by *Alcaligenes eutrophus* JMP 134. Arch. Microbiol. 150 (1), 95-102.

Pomiès, M., Choubert, J.M., Wisniewski, C. Coquery, M., 2013. Modelling of micropollutant removal in biological wastewater treatments: A review. Sci. Total Environ. 443, 733-748.

Quintana, J.B., Weiss, S., Reemtsma, T., 2005. Pathways and metabolites of microbial degradation of selected acidic pharmaceutical and their occurrence in municipal wastewater treated by a membrane bioreactor. Water Res. 39 (12), 2654-2664.

Radjenović, J., Pérez, S., Petrović, M., Barceló, D., 2008. Identification and structural characterization of biodegradation products of atenolol and glibenclamide by liquid chromatography coupled to hybrid quadrupole time-of-flight and quadrupole ion trap mass spectrometry. J. Chromatogr. A 1210 (2), 142-153.

Radniecki, T.S., Dolan, M.E. Semprini, L., 2008. Physiological and transcriptional responses of Nitrosomonas europaea to toluene and benzene inhibition. Environ. Sci. Technol. 42 (11), 4093-4098.

Rasche, M.E., Hicks, R.E., Hyman, M.R., Arp, D.J., 1990. Oxidation of monohalogenated ethanes and n-chlorinated alkanes by whole cells of *Nitrosomonas europaea*. J. Bacteriol. 172 (9), 5368-5373.

Reeves, P.R., McAinsh, J., McIntosh, D.A.D., Winrow, M.J., 1978. Metabolism of atenolol in man. Xenobiotica 8 (5), 313-320.

Rivera-Utrilla, J., Sánchez-Polo, M., Ferro-García, M.Á., Prados-Joya, G., Ocampo-Pérez, R., 2013. Pharmaceuticals as emerging contaminants and their removal from water. A review. Chemosphere 93 (7), 1268-1287.

Rubirola, A., Llorca, M., Rodriguez-Mozaz, S., Casas, N., Rodriguez-Roda, I., Barceló, D., Buttiglieri, G., 2014. Characterization of metoprolol biodegradation and its transformation products generated in activated sludge batch experiments and in full scale WWTPs. Water Res. 63, 21-32.

Sathyamoorthy, S., Chandran, K., Ramsburg, C.A., 2013. Biodegradation and cometabolic modeling of selected beta blockers during ammonia oxidation. Environ. Sci. Technol. 47 (22), 12835-12843.

Sharma, M., Sharma, N.N., Bhalla, T.C., 2009. Amidases: Versatile enzymes in nature. Rev. Environ. Sci. Biotechnol. 8 (4), 343-366.

Skotnicka-Pitak, J., Khunjar, W.O., Love, N.G., Aga, D.S., 2009. Characterization of metabolites formed during the biotransformation of 17α-ethinylestradiol by *Nitrosomonas europaea* in batch and continuous flow bioreactors. Environ. Sci. Technol. 43 (10), 3549-3555.

Stein, L.Y., Arp, D.J., Berube, P.M., Chain, P.S.G., Hauser, L., Jetten, M.S.M., Klotz, M.G., Larimer, F.W., Norton, J.M., Op den Camp, H.J.M., Shin, M., Wei, X., 2007. Whole-genome analysis of the ammonia-oxidizing bacterium, *Nitrosomonas eutropha* C91: implications for niche adaptation. Environ. Microbiol. 9 (12), 2993-3007.

Ternes, T.A., 1998. Occurrence of drugs in German sewage treatment plants and rivers. Water Res. 32 (11), 3245-3260.

Tran, N.H., Nguyen, V.T., Urase, T., Ngo, H.H., 2014. Role of nitrification in the biodegradation of selected artificial sweetening agents in biological wastewater treatment process. Bioresour. Technol. 161, 40-46.

Verlicchi, P., Al Aukidy, M., Zambello, E., 2012. Occurrence of pharmaceutical compounds in urban wastewater: Removal, mass load and environmental risk after a secondary treatment—A review. Sci. Total Environ. 429, 123-155.

Yi, T., Harper Jr, W.F., 2007. The link between nitrification and biotransformation of 17α-ethinylestradiol. Environ. Sci. Technol. 41, 4311-4316.

Zwiener, C., Seeger, S., Glauner, T., Frimmel, F., 2002. Metabolites from the biodegradation of pharmaceutical residues of ibuprofen in biofilm reactors and batch experiments. Anal. Bioanal. Chem. 372 (4), 569-575.

Figure Legends

Figure 1. Qualitative profiles of atenolol at an initial concentration of 15 mg L^{-1} and its biodegradation products in biodegradation experiments: (a) in the presence of ammonium, (b) without ammonium addition, (c) with the addition of ATU and (d) with autoclaved biomass. Y-axis indicates the peak areas of the extracted ion chromatograms of atenolol or its biodegradation products (A) normalized to the initial peak area of atenolol (A0).

Figure 2. (a) The calculated ammonia oxidation rate during biodegradation experiments in the presence of ammonium and (b) Relationship between ammonia oxidation rate and atenolol biodegradation rate (orange dots indicated the modeled values).

Figure 3. Proposed fragmentation pathways of biodegradation products under ESI+ conditions derived from MS^2 experiments in the QqLIT mass spectrometer: (a) P117, (b) P167 and (c) P227.

Figure 4. Qualitative profiles of atenolol acid (P267) at an initial concentration of 15 mg L^{-1} and its biotransformation products in biodegradation experiments in the presence of ammonium. Y-axis indicates the peak areas of the extracted ion chromatograms of atenolol acid or its biotransformation products (A) normalized to the initial peak area of atenolol acid (A0).

Figure 5. Proposed biodegradation pathways of atenolol by the enriched nitrifying culture in the presence of ammonium as well as in the absence of ammonium.

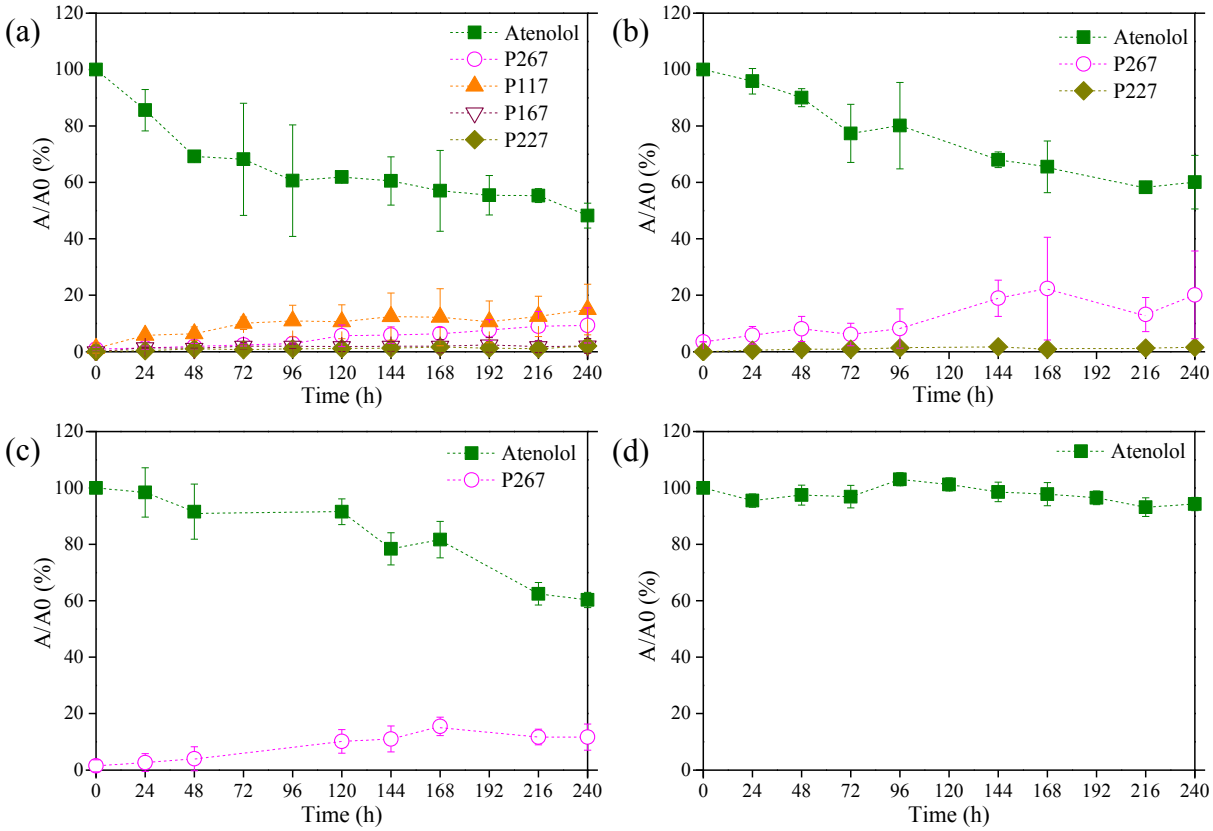

Figure 1. Qualitative profiles of atenolol at an initial concentration of 15 mg L^{-1} and its biodegradation products in biodegradation experiments: (a) in the presence of ammonium, (b) without ammonium addition, (c) with the addition of ATU and (d) with autoclaved biomass. Y-axis indicates the peak areas of the extracted ion chromatograms of atenolol or its biodegradation products (A) normalized to the initial peak area of atenolol (A0).

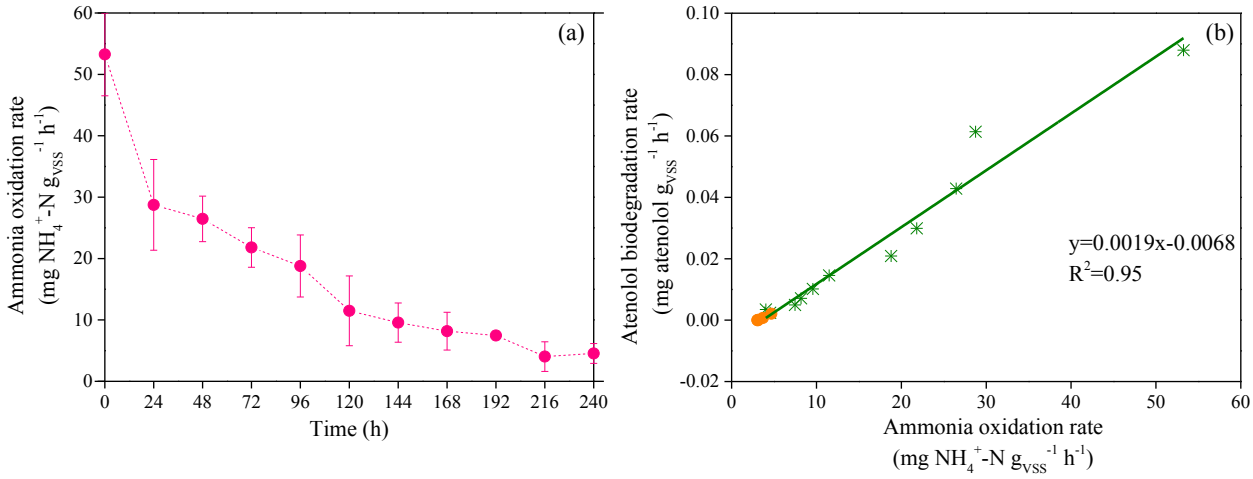

Figure 2. (a) The calculated ammonia oxidation rate during biodegradation experiments in the presence of ammonium and (b) Relationship between ammonia oxidation rate and atenolol biodegradation rate (orange dots indicated the modeled values).

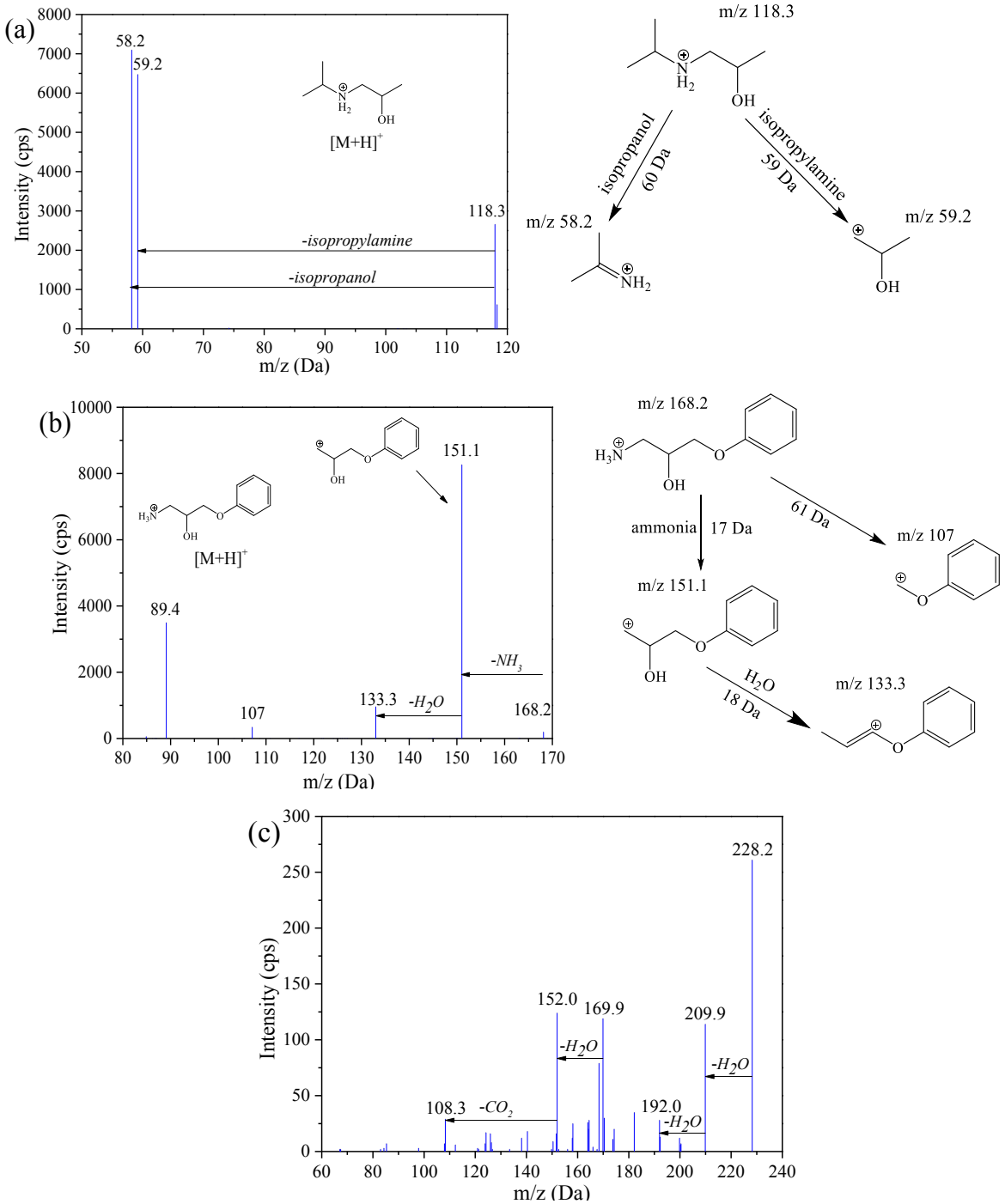

Figure 3. Proposed fragmentation pathways of biodegradation products under ESI+ conditions derived from MS2 experiments in the QqLIT mass spectrometer: (a) P117, (b) P167 and (c) P227.

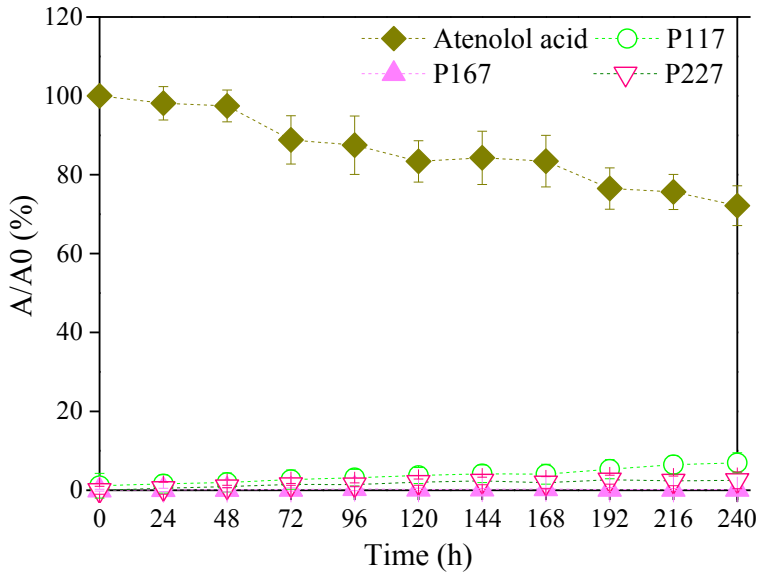

Figure 4. Qualitative profiles of atenolol acid (P267) at an initial concentration of 15 mg L^{-1} and its biotransformation products in biodegradation experiments in the presence of ammonium. Y-axis indicates the peak areas of the extracted ion chromatograms of atenolol acid or its biotransformation products (A) normalized to the initial peak area of atenolol acid (A0).

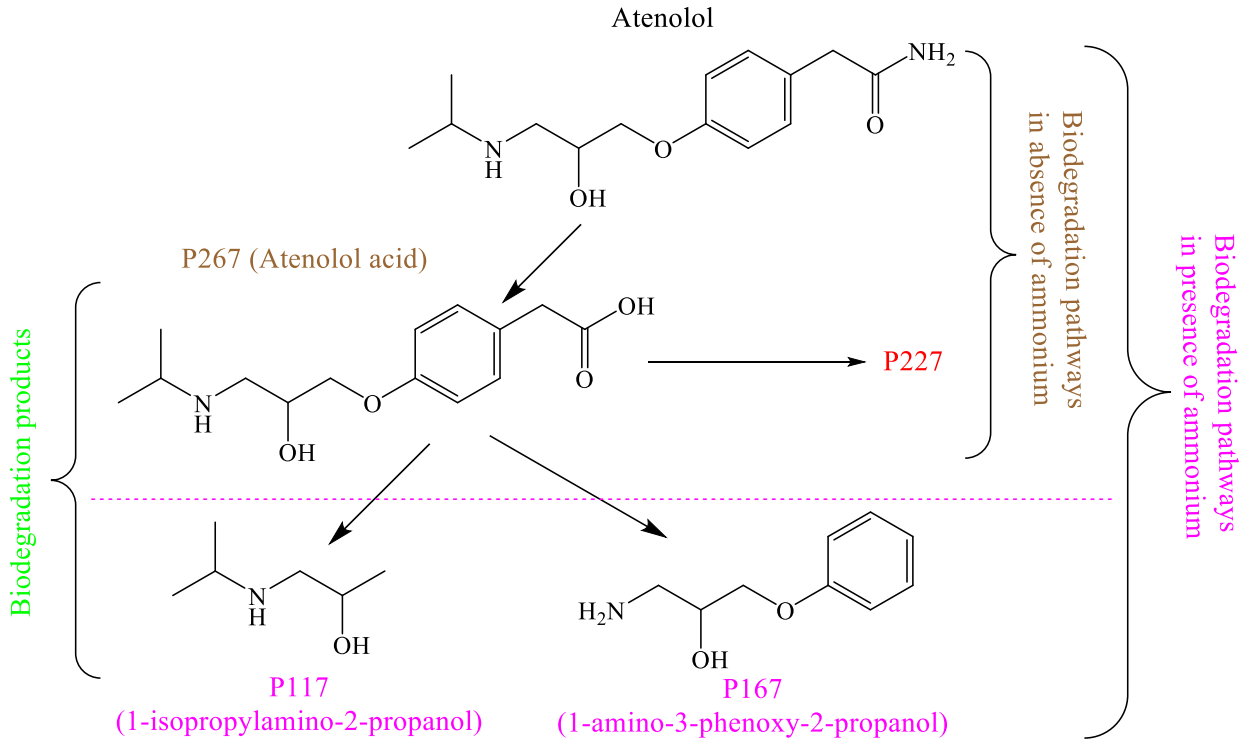

Figure 5. Proposed biodegradation pathways of atenolol by the enriched nitrifying culture in the presence of ammonium as well as in the absence of ammonium.

Supporting Information

Table S1. The protocols applied for atenolol biodegradation experiments

Protocol	**1**	**2**	**3**	**4**	**5**
Initial ammonium ($mg\ L^{-1}$)	50	0	50	-	50
Ammonium control	Constant	0	Constant	-	Constant
Approximate VSS ($g\ VSS\ L^{-1}$)	1	1	1	1	0
Volume (L)	4	4	4	4	4
ATU ($mg\ L^{-1}$)	0	0	30	0	0
Autoclave	-	-	-	yes	-

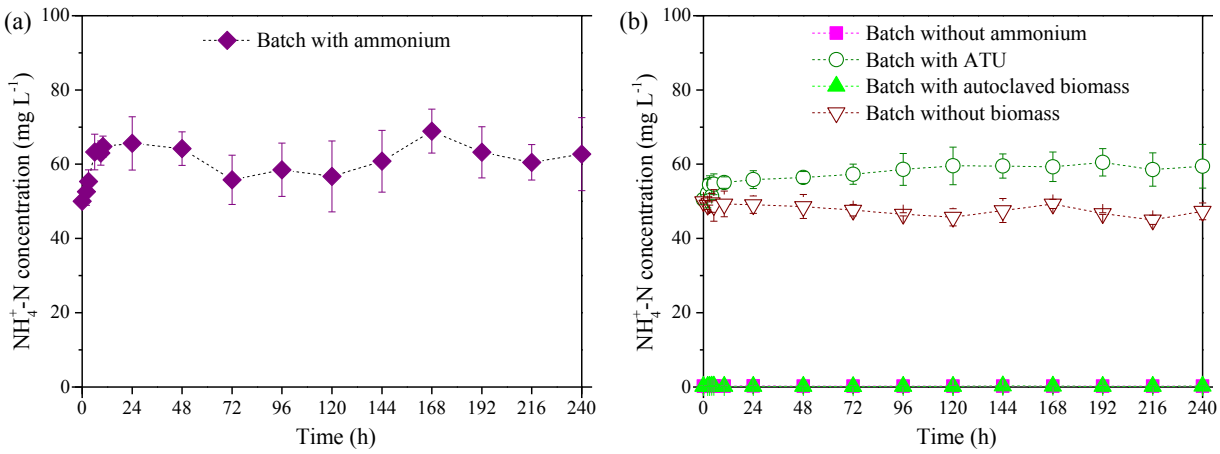

Figure S1. The NH_4^+-N concentration profiles in different batch experiments: (a) batch with ammonia oxidation (in the presence of ammonium) and (b) batch in the presence of ATU, with autoclaved biomass and without biomass or no ammonium addition (in the absence of ammonium).

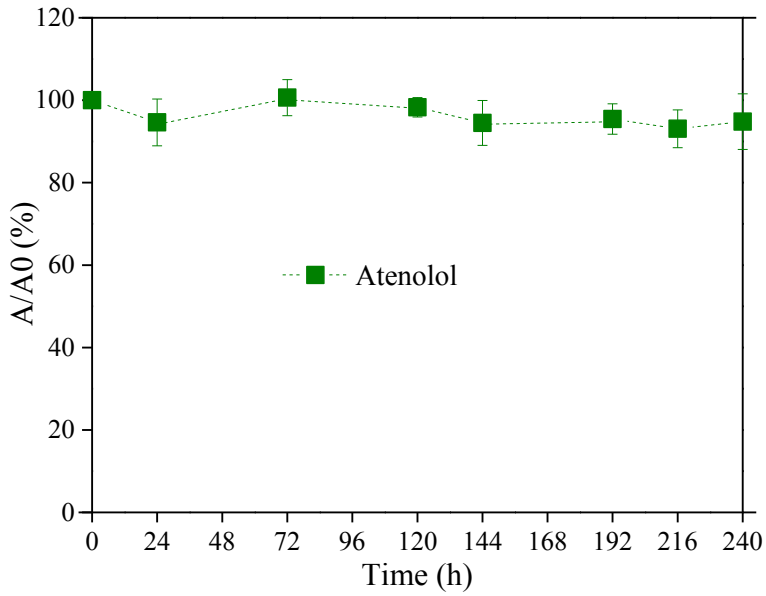

Figure S2. The qualitative profile of atenolol at an initial concentration of 15 mg L^{-1} in control experiments without biomass. Y-axis indicates the peak areas of the extracted ion chromatograms (A) normalized to the initial peak area of atenolol (A0).

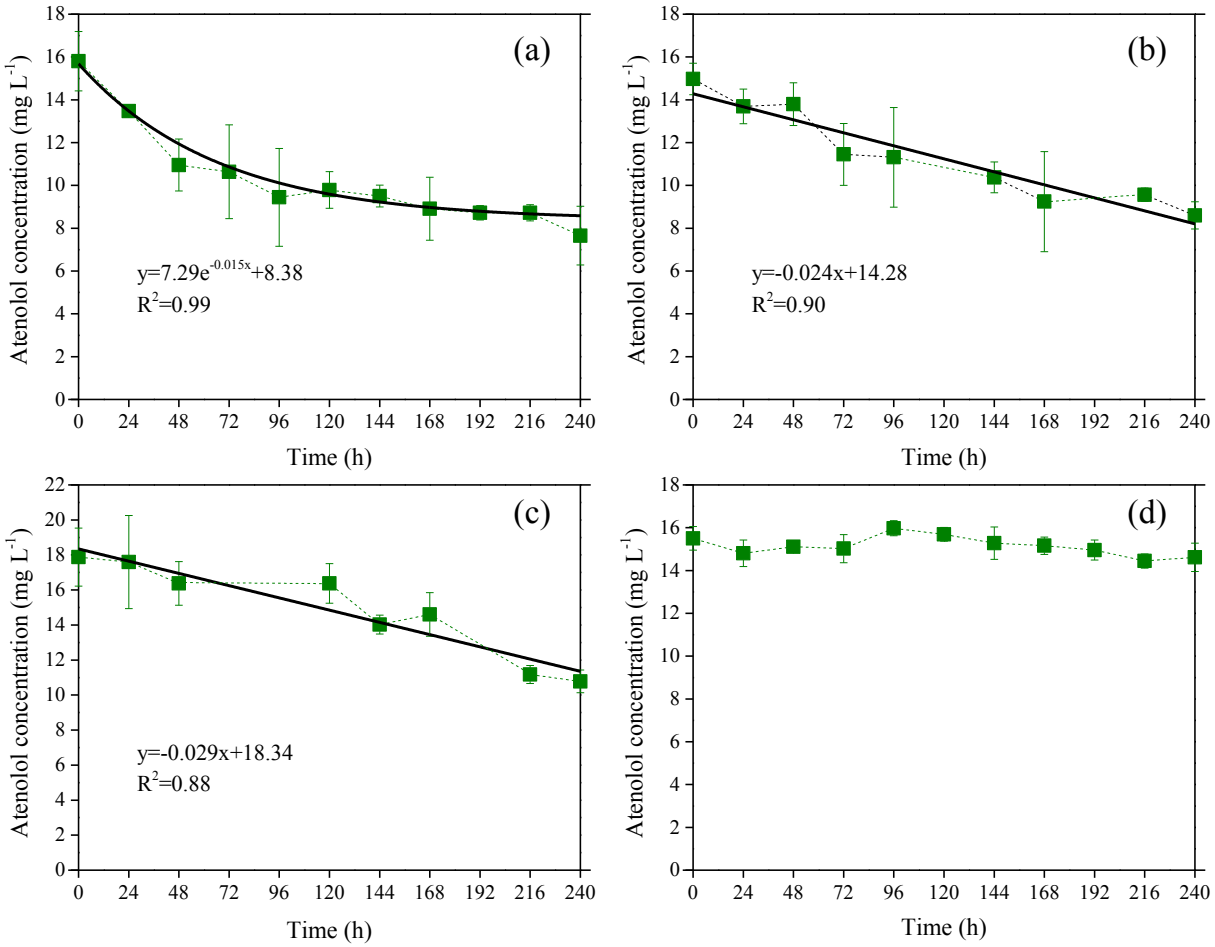

Figure S3. Concentration profiles of atenolol in biodegradation experiments: (a) in the presence of ammonium, (b) without ammonium addition, (c) with the addition of ATU and (d) with autoclaved biomass accompanied with the respective regression curves (black solid lines).

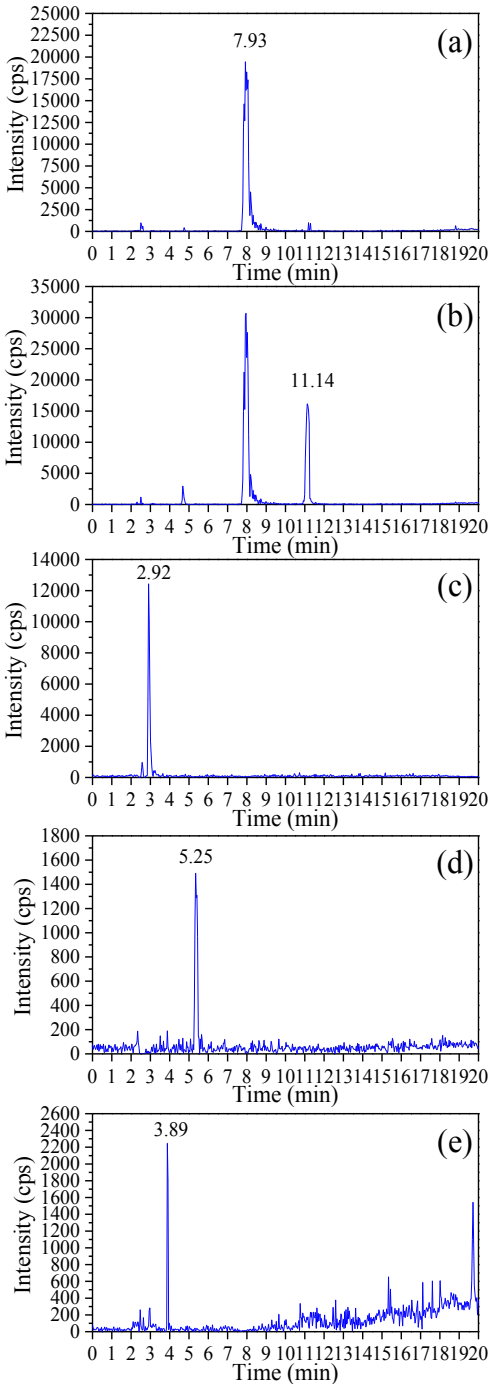

Figure S4. Extracted ion chromatograms (XIC) of (a) atenolol, (b) P267, (c) P117, (d) P167 and (e) P227, recorded in full scan mode analysis of the samples from the biodegradation experiments in the presence of ammonium and at initial atenolol concentration of 15 mg L^{-1}.

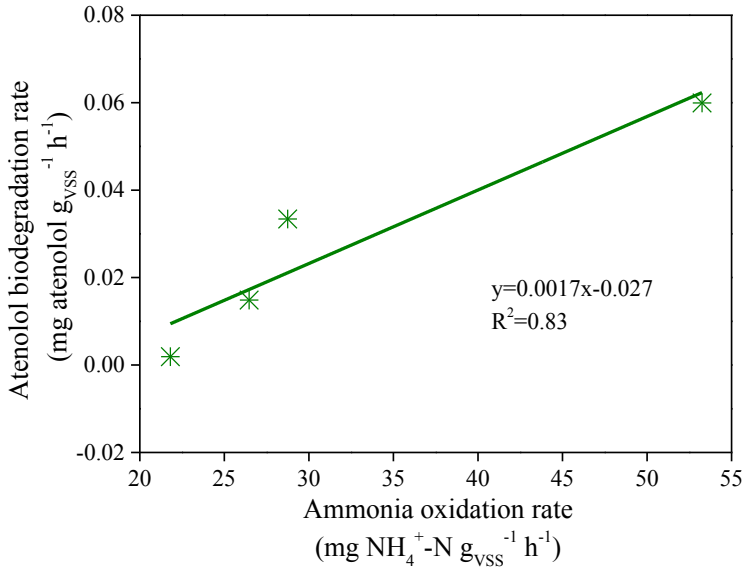

Figure S5. Relationship between ammonia oxidation rate and atenolol biodegradation rate (subtracting the contribution from heterotrophs).

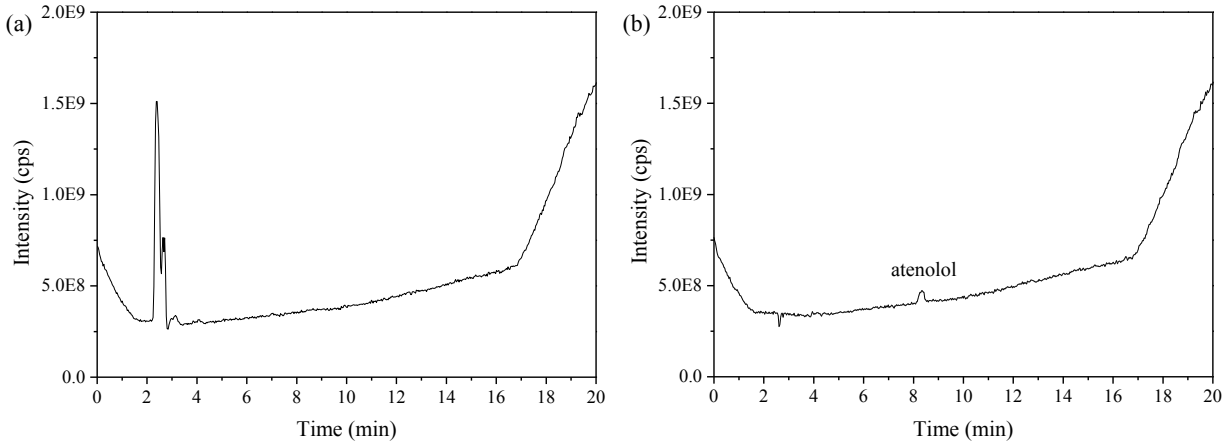

Figure S6. The full scan chromatograms (TIC) of the enriched nitrifying biomass sample without addition of atenolol (a) and atenolol standard solution without biodegradation (b).

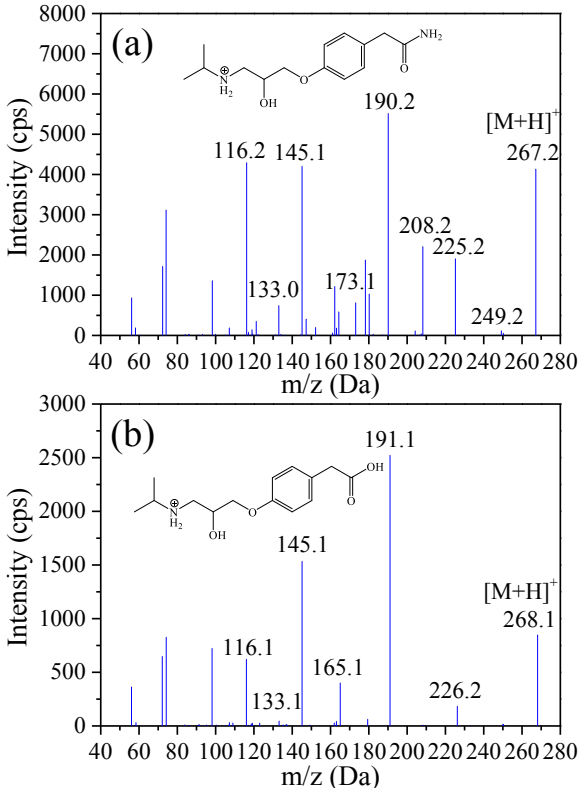

Figure S7. ESI+ MS^2 spectrum of: (a) atenolol and (b) P267, recorded for samples from the biodegradation experiments in the presence of ammonium and at initial atenolol concentration of 15 mg L^{-1}.

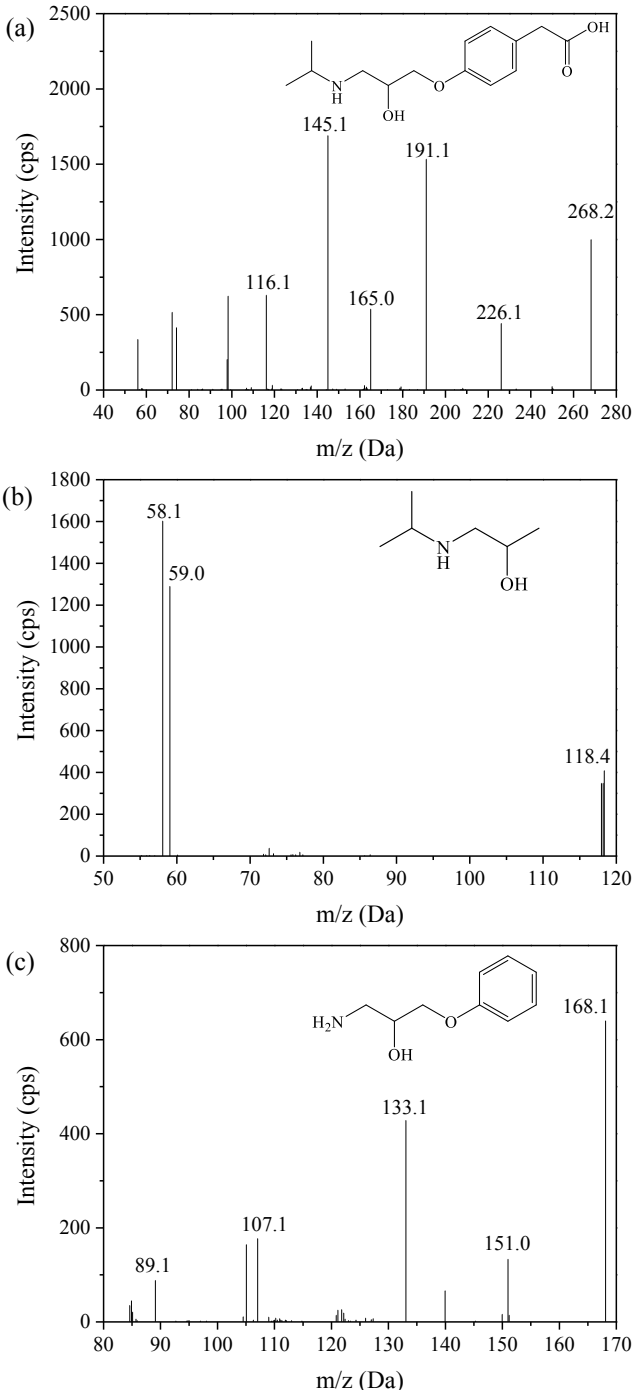

Figure S8. ESI+ MS^2 spectrum of the individual standards: (a) 4-(2-Hydroxy-3-isopropylaminopropoxy)phenylacetic acid (atenolol acid, MW 267), (b) 1-isopropylamino-2-propanol (MW 117) and (c) 1-amino-3-phenoxy-2-propanol (MW167) with their structures.

Appendix B

Impact of the Ammonium Availability on Atenolol Biodegradation by an Enriched Nitrifying Sludge

Yifeng Xu, Zhiguo Yuan, Bing-Jie Ni*

This manuscript is published in *ACS Sustainable Chemistry & Engineering*.

Advanced Water Management Centre, The University of Queensland, St. Lucia, Brisbane, QLD 4072, Australia

***Corresponding author:**
Dr. Bing-Jie Ni
Advanced Water Management Centre
The University of Queensland
Australia
Phone: + 61 7 3346 3219
Fax: +61 7 3365 4726
E-mail: b.ni@uq.edu.au

Abstract

In this work, the impact of the ammonium availability on atenolol biodegradation at relatively realistic level of 15 μg L^{-1} by an enriched nitrifying sludge was investigated in terms of the atenolol degradation kinetics and the biotransformation product formation. Batch experiments were conducted with different concentrations of growth substrate ammonium (0, 25, and 50 mg-N L^{-1}) being constantly applied during the time course. The results suggested the higher ammonium concentrations led to the lower atenolol removal efficiencies probably due to the substrate competition between ammonium and atenolol. The formation of biotransformation product atenolol acid was observed to be positively related to the ammonium oxidation activity, resulting in a higher amount of atenolol acid formed at the end of experiments at higher ammonium concentrations. The pseudo-first order kinetics analysis indicated linear correlations between ammonia oxidation rate and atenolol degradation rate at ammonium levels of both 25 and 50 mg-N L^{-1}, suggested the cometabolism of atenolol by ammonia oxidizing bacteria (AOB) in the presence of ammonium. The revealed biotransformation reaction, i.e., hydroxylation on amide group to carboxylic group, could be

catalyzed by the non-specific enzyme ammonia monooxygenase (AMO) of AOB. The comparison between the atenolol degradation at ammonium levels of 0 and 50 mg-N L^{-1} demonstrated the formation of product atenolol acid was independent on the ammonium availability.

Keywords: Ammonia oxidizing bacteria; ammonium; atenolol; biotransformation product; cometabolism; biodegradation

1. Introduction

For recent decades emerging organic micropollutants including pesticides, pharmaceuticals and personal care products have attracted increasing public and research concerns due to their potential adverse effects on human and ecosystems (Fenner et al., 2013; Luo et al., 2014; Ternes et al., 2015). Their ubiquitous occurrence has been reported ranging from a few nano-gram per litre to several hundred micro-gram per litre in wastewater, surface water and groundwater (Petrie et al., 2015). Wastewater treatment processes have been identified as the main point of discharge of pharmaceuticals into the environment as they were originally designed for bulk nutrients removal such as nitrogen and phosphorus (Joss et al., 2006; Sengupta et al., 2014). In addition, biodegradation of pharmaceuticals in wastewater treatment processes might form the transformation products that might be more toxic and persistent (Ternes et al., 2007). Thus, an in-depth understanding of the fate of pharmaceuticals in wastewater treatment is needed to assess the removal of these compounds and their biotransformation products.

The positive relationships between pharmaceutical biotransformation and nitrification rates have been reported in previous studies (Batt et al., 2006; Margot et al., 2016). Enhanced pharmaceutical removal were found to be attributed to the non-specific enzyme ammonia monooxygenase (AMO) from ammonia oxidizing bacteria (AOB), with a broad substrate range including aromatic and aliphatic compounds (Fernandez-Fontaina et al., 2012; Fischer and Majewsky, 2014; Tran et al., 2009). It was hypothesized that some pharmaceuticals could be biotransformed cometabolically by AOB in nitrifying cultures (Roh et al., 2009; Tran et al., 2013). In particular, higher biodegradation efficiencies of the emerging micropollutants were obtained at higher nitrogen loading rates that could promote the development of biomass with high nitrification activities (Tran et al., 2009). However, the impact of the ammonium availability as a constant growth substrate of AOB on pharmaceutical transformation has not been well documented at relatively realistic level for AOB induced cometabolism in enriched nitrifying cultures.

Atenolol was among the most frequently reported pharmaceuticals in the wastewater with the highest concentration being up to 25 μg L^{-1} (Verlicchi et al., 2012). Biodegradation of atenolol was linked to the activity of AOB and heterotrophs in the enriched nitrifying cultures (Sathyamoorthy et al., 2013). The objective of this study was to investigate the impact of the ammonium availability on atenolol biodegradation at relatively realistic level of 15 μg L^{-1} by an enriched nitrifying sludge. Batch experiments were conducted with different concentrations of growth substrate ammonium being constantly applied during the time course (0, 25, and 50 mg-N L^{-1}) to evaluate the atenolol degradation kinetics and the biotransformation product formation.

2. Materials and Methods

2.1 Chemicals

Atenolol (≥98%), atenolol acid, allylthiourea (ATU, 98%) and all the other organic solvents (LC grade) were purchased from Sigma-Aldrich, Australia. The internal standard atenolol-d7 (≥97%) was also provided by Sigma-Aldrich, Australia. The standard stock solution of atenolol was prepared in methanol at 1 g L^{-1} and stored at -20 °C. Working standards used for calibration curves were obtained through dilution of the standard stock solution with purified water, obtained from a Milli-Q system (Millipore, Inc.). Atenolol feed solution for all the batch biodegradation experiments was prepared at 1 mg L^{-1} in Milli-Q water.

2.2 Nitrifying culture enrichment

Seed biomass for nitrifying enrichment was collected from a domestic wastewater treatment plant in Brisbane, Australia. The enriched nitrifying sequencing batch reactor (SBR) was operated on a 6-h cycle (260 min fill, 30 min aerobic react, 1 min waste, 60 min settle, 9 min decant) during the time period when biomass was collected for batch experiments with atenolol. The feed solution consisted of 5.63 g of NH_4HCO_3 (1 g NH_4^+-N), 5.99 g of $NaHCO_3$, 0.064 g of each of KH_2PO_4 and K_2HPO_4 and 2 mL of a trace element solution per litre (Kuai and Verstraete, 1998). The trace element stock solution contained: 1.25 g L^{-1} EDTA, 0.55 g L^{-1} $ZnSO_4 \cdot 7H_2O$, 0.40 g L^{-1} $CoCl_2 \cdot 6H_2O$, 1.275 g L^{-1} $MnCl_2 \cdot 4H_2O$, 0.40 g L^{-1} $CuSO_4 \cdot 5H_2O$, 0.05 g L^{-1} $Na_2MoO_4 \cdot 2H_2O$, 1.375 g L^{-1} $CaCl_2 \cdot 2H_2O$, 1.25 g L^{-1} $FeCl_3 \cdot 6H_2O$ and 44.4 g L^{-1} $MgSO_4 \cdot 7H_2O$. Reactor pH and dissolved oxygen (DO) were continuously monitored using miniCHEM meters and controlled in the range of 7.5-8.0 and 2.5-3.0 mg L^{-1}, respectively, with programmed logic controllers (PLC). HRT and SRT were 24 h and 15 d, respectively.

After operation in the steady state for more than one year, the enriched nitrifying culture was utilized as the inoculum for batch biodegradation experiments. The bacterial community analysis was

conducted to obtain the fractions of enrolled bacteria using fluorescence *in-situ* hybridization (FISH) (Law et al., 2011). AOB and nitrite oxidizing bacteria (NOB) together would contribute more than 80% of the enriched nitrifying biomass with their corresponding percentages of 46 ± 6% (n=20) and 38 ± 5% (n=20), respectively.

2.3 Batch experiments with different ammonium availability

4 L beakers were filled with enriched nitrifying culture from the SBR. Covered by the aluminum foil, the beakers were used as the inoculum to carry out the biodegradation experiments. The Mixed liquor volatile suspended solids (MLVSS) was achieved at approximately 1000 mg L^{-1} at the beginning of the experiments. The target pharmaceutical, atenolol, was then added into the beakers to obtain an initial relatively realistic concentration (15 μg L^{-1}). Different ammonium concentrations (0, 25 and 50 mg L^{-1}) were controlled constantly for each biodegradation experiment with different ammonia oxidation levels in duplicates. Ammonium bicarbonate was supplied as the growth substrate at the beginning of the experiments with ammonium addition and was further frequently added into the beakers with sodium bicarbonate as a pH adjustment method as well as maintaining a constant level of ammonium. The experiments without ammonia oxidation were conducted in duplicates where ammonium concentration was zero during the whole time period. The control experiments were carried out to study the abiotic and hydrolytic degradation of atenolol with autoclaved biomass (121 °C and 103 kPa for 30 min) (Kassotaki et al., 2016) and without any biomass, respectively. For all batch experiments, pH was controlled between 7.5 and 8.0 and DO was supplied by aeration in the range of 2.5 and 3.0. After mixing well, the samples were taken periodically each day until 240 h for chemical analysis of atenolol and its products.

2.4 Chemical analysis

Mixed liquor suspended solids (MLSS) and the volatile fraction (MLVSS) were measured at the beginning, middle and end of the batch biodegradation experiments according to the standard methods (APHA, 1998). NH_4^+-N concentrations were measured using a Lachat QuikChem8000 Flow Injection Analyzer (Lachat Instrument, Milwaukee). Figure S1 in Supporting Information (SI) demonstrated that the ammonium concentrations were controlled nearly constant during the entire experimental period for batch biodegradation experiments in the presence of ammonium. In addition, nitrite was not accumulated for all the batch experiments (less than 1 mg L^{-1}) and the nitrate concentration was similar to that in the SBR effluent (up to 1000 mg L^{-1}).

For sample preparation, solid phase extraction (SPE) with vacuum manifold (J. T. Baker, The Netherlands) was carried out first in order to achieve the pre-concentration of atenolol and its products

at lower levels. Oasis HLB cartridges (6 mL, 200 mg, Waters, USA) were conditioned using 10 mL methanol and 10 mL Milli-Q water. After centrifugation of 50 mL samples at 14000 rpm for 5 min, the supernatants were passed through the conditioned cartridges with a flow rate of approximately 5 mL min^{-1}. Following sample pre-concentration, cartridges were rinsed with 5 mL Milli-Q water and were dried under vacuum for 30 min. The analytes were eluted with 10 mL methanol and 10 mL of hexane/acetone (50:50, v/v) at a slower flow rate. Sample extracts were evaporated to dryness using a gentle stream of nitrogen and were reconstituted to 250 µL methanol and 750 µL Milli-Q water. 20 µL atenolol-d7 was added into each sample as an internal standard to achieve a concentration of 50 µg L^{-1} before further analysis.

The liquid chromatograph used in this study was an ultra-fast liquid chromatography (UFLC) (Shimadzu, Japan). An Alltima C18 column (Alltech Associates Inc., USA) was used for chromatographic separation using Milli-Q (A) and acetonitrile (B) as mobile phases at a flow rate of 1 mL min^{-1}. The gradient elution program was set as follows: initial, 0% B; 0-0.5 min, 0-5% B; 0.5-13 min, 5-20% B; 13-18 min, 20-50% B; 18-20 min, 50-100% B; 20-24 min, 100% B; 24-25 min, 100-5% B. The total running time including the conditioning of the column to the initial conditions was 27 min. The column oven was set to 40 °C. The injection volume was 20 µL. The mass spectrometric analysis was performed on a 4000 QTRAP hybrid triple quadruple-linear ion trap mass spectrometer (QqLIT-MS) equipped with a Turbo Ion Spray source (Applied Biosystems-Sciex, USA) under positive ionization mode (ESI+) for all acquisitions. The drying gas (50 psi) was used at 500 °C with curtain gas 30 psi and spraying gas 50 psi applied. For qualitative purposes, full scan mode was performed on the samples at the declustering potential of 80 V and mass range of 50-500 amu followed by product ion scan mode and sequential fragmentation. For quantitative purposes, multiple reaction monitoring (MRM) mode was conducted with two MRM transition ions for each compound (Table 1), the first one for quantification and the second one for confirmation of the compound.

3. Results

3.1 Nitrification performance and control experiments

Prior to the beginning of the batch biodegradation experiments with atenolol, the MLVSS concentration of SBR was stable at 1437.6±112.9 mg L^{-1} (mean and standard errors, respectively, n=10) and the stable nitrification performance was achieved in the SBR, which was assessed through a series of cycle studies in duplicates. An initial pulse of 20 mg L^{-1} ammonium was added into the batch reactor with the enriched nitrifying sludge at the MLVSS concentration of 95 mg L^{-1}. The concentration profiles of different nitrogen species were shown in Figure 1A as NH_4^+-N, NO_2^--N and NO_3^--N, respectively. Ammonium was completely consumed by the enriched nitrifying sludge within

5 h, leading to a sharp increase of NO_3^--N to approximately same concentration of the initial NH_4^+-N level. The concentration of nitrite was increased at first 4 h and then decreased to zero until the end of experiments, which indicated its consumption by NOB. Overall, a good nitrification performance of the enriched nitrifying sludge was achieved with a highest ammonia oxidizing rate (approximately 52 mg NH_4^+-N g VSS^{-1} h^{-1}).

The abiotic control and hydrolytic control experiments demonstrated a rather stable atenolol concentration over 240 h without the formation of any transformation products (Figure S2). Given the lower adsorption ability and the aluminum cover avoiding photodegradation, biodegradation by the enriched nitrifying biomass was therefore the main removal mechanism in the investigated batch experiments.

3.2 Impact of ammonium availability on atenolol biodegradation

To determine the effect of the growth substrate (ammonium) availability on the cometabolic activity on atenolol by the enriched nitrifying culture, a series of ammonium concentrations among 0, 25 and 50 mg L^{-1} were applied in different batch biodegradation experiments with initial 15 µg L^{-1} atenolol. It can be concluded from Figure 2A that the removal efficiencies of atenolol decreased with the increase of the availability ammonium at constant levels during the experimental period. Such observation is different from the previous studies where the degradation of selected pharmaceuticals (e.g., clofibric acid, diclofenac, carbamazepine, propyphenazone) was enhanced at higher initial ammonium concentration (Tran et al., 2009). In comparison, the ammonium concentration was provided with pulse feeding at the beginning of the experiments in previous studies, leading to completely different ammonium availability (constant concentrations in this study) during the time course. Enriched nitrifying sludge responsible for the cometabolic biodegradation was reported to have a different affinity for each pharmaceutical compounds, probably due to a preferential substrate selection to AMO active sites (Fernandez-Fontaina et al., 2012). Ammonia oxidation rate was calculated based on the measured ammonium concentration and the adding volume of ammonium bicarbonate for each time. Based on Figure 1B, the ammonium availability at constant level had a positive effect on ammonia oxidation rate, whereas atenolol removal efficiency was adversely related to the constant ammonium concentration.

3.3 Impact of ammonium availability on formation of atenolol acid

In this study, the influence of ammonium availability on the formation of biotransformation products of atenolol was also investigated (Figure 2B). Accompanied with the decrease of atenolol (Figure 2A), only one biotransformation product was found in all the experiments and was confirmed as

atenolol acid. The structural elucidation of atenolol acid was detailed in previous studies (Radjenović et al., 2008). It can be clearly concluded that atenolol acid was produced more in the presence of ammonium than that in the absence of ammonium, and was formed increasingly with the increase of ammonium availability. Although AOB were able to degrade pharmaceuticals during ammonium starvation (Forrez et al., 2009; Khunjar et al., 2011), its contribution to the formation of atenolol acid was yet less than AOB with the adequate growth substrates. It was also confirmed that the formation of biotransformation products was due to cometabolic biodegradation by AOB, as ammonia oxidation rate showed a positive correlation with the formation of atenolol acid. The biotransformation of atenolol to atenolol acid was via hydrolysis on the primary amide group to the carboxylic acids catalyzed by AMO, which was dependent on the nitrifying activities (Helbling et al., 2012; Radjenović et al., 2008).

3.4 Comparison between atenolol biodegradation with and without ammonium

As shown in Figure 3A, a gradual decrease of atenolol at an initial concentration of 15 μg L^{-1} was found during the entire experimental period in the presence of ammonium (at 50 mg L^{-1}). The overall removal rate of atenolol could reach 88.0% with the final concentration of 2.2 μg L^{-1} in the batch reactor. The formation of atenolol acid was correlated to the decrease of atenolol. Atenolol acid experienced a sharp increase for first 120 h when ammonia oxidation rate was higher. With the available reference standard, atenolol acid was quantified to increase to 15.4 μg L^{-1}. Furthermore, atenolol acid was proved to be the only biotransformation product through the nearly closed mass balance analysis. Figure 3B plotted the concentration profiles of atenolol and atenolol acid in the absence of ammonium (at 0 mg L^{-1}). Dropping from the initial 15 μg L^{-1} concentration, atenolol experienced a sharp decrease to 51.5% in the first 24 h. The degradation of atenolol became slower with the decreasing ammonia oxidation rate until the atenolol concentration became 0.6 μg L^{-1}. The concentration of atenolol acid was increased to 6.8 μg L^{-1} at 240 h with an approximate conversion rate of 29.1% from atenolol biodegradation. The removal efficiency of atenolol was higher in the absence of ammonium (97.4%) than that in the presence of ammonium, which was contradictory to the results reported previously (Tran et al., 2013). The cometbolic biodegradation induced by AOB in the enriched nitrifying culture showed the lower contribution to atenolol removal at the relatively realistic concentration compared to the metabolic biodegradation by nitrifying culture, which could be caused by the substrate competition especially in the case when growth substrate concentration was higher (Dawas-Massalha et al., 2014).

3.5 Kinetic analysis of atenolol biodegradation

An exponential decrease of atenolol concentration was observed for each experiment without the presence of ammonium, and in the presence of 25 mg L^{-1} or 50 mg L^{-1} ammonium (NH_4^+-N) (Figure 2A), indicating a pseudo first order degradation kinetics for atenolol removal by the enriched nitrifying sludge (Figure S3). The biodegradation rate constants k_{bio} could be calculated using:

$$k_{biol}=-\frac{\ln\left(\frac{C_t}{C_0}\right)}{t\cdot X_{VSS}};\quad t_{1/2}=\frac{\ln(2)}{k_{biol}\cdot X_{VSS}} \tag{1}$$

where C is the total compound concentration (μg L^{-1}), t is time (h), k_{biol} is the biodegradation rate constant (L g VSS^{-1} h^{-1}), X_{VSS} is the VSS concentration in the batch beakers (g VSS L^{-1}) and $t_{1/2}$ is the biodegradation half-life (h).

For the batch experiments without the presence of ammonium, the biodegradation rate constant of atenolol was calculated as 0.018 L g VSS^{-1} h^{-1} with the degradation half-life of 40.2 h. For atenolol biodegradation in the presence of ammonium, the half-lives were 63.1 h and 77.3 h at the constant ammonium concentrations of 25 and 50 mg L^{-1}, respectively. The degradation constants of 0.0078 and 0.0072 L g VSS^{-1} h^{-1} indicated a slower degradation of atenolol in the presence of ammonium compared to the batch experiments without the presence of ammonium. This further supported that atenolol could be degraded during ammonium starvation like other pharmaceuticals (Dawas-Massalha et al., 2014) and the substrate competition existed between ammonium and atenolol (Fischer and Majewsky, 2014), leading to a decreasing degradation rate under high concentrations of ammonium. These degradation constants were lower than the reported values for atenolol (1.1-1.9 L g_{SS}^{-1} d^{-1}) (Pomiès et al., 2013), likely due to the unaccustomed sludge to atenolol in this work.

4. Discussion

4.1 Competitive inhibition of ammonium on atenolol biodegradation

As shown in Figure 2A, the removal efficiency of atenolol was adversely linked to the ammonium concentration. The higher removal of atenolol was observed under the lower ammonium concentration at constant level. Such observations suggested there might exist a competition between the growth substrate (ammonium) and cometabolic substrate (atenolol), in particular when the concentration of growth substrate was much higher than that of the non-growth substrate (Fernandez-Fontaina et al., 2012), which was previously confirmed in the biodegradation study on cis-1,2-dichloroethene and tetrachloroethylene (Schäfer and Bouwer, 2000; Tsien et al., 1989). As the ammonia oxidation and hydroxylation of atenolol were both catalyzed by AMO, it could be hypothesized that the competition for AMO active sites between two substrates would be the crucial mechanism in this study and ammonia oxidation might be the limiting step, leading to the lower

removal rate of atenolol under higher constant ammonium concentrations. When ammonium concentrations were maintained zero in the batch experiments, metabolism induced by enriched nitrifying sludge might be the main degradation mechanism. There were evidences that AOB can transform pharmaceuticals during ammonium starvation (Dawas-Massalha et al., 2014; Forrez et al., 2009). For example, ibuprofen would not be degraded unless ammonia was depleted completely, therefore showing a decreased biodegradation rate at high ammonium concentration (100 mg L^{-1}) (Dawas-Massalha et al., 2014).

However, the formation of atenolol acid was enhanced with increasing ammonium concentration (Figure 2B), specifically with increasing ammonium oxidizing rates shown in Figure 1B. AMO activities might be the dominant factor determining the formation of atenolol acid as AMO could catalyze hydroxylation and oxidation (Keener and Arp, 1993; Men et al., 2016). Therefore, the final concentrations of atenolol acid were increased from 8.6 to 15.4 μg L^{-1} with the increasing ammonium concentrations from 25 to 50 mg L^{-1}. Due to the competitive inhibition by atenolol (Sathyamoorthy et al., 2013), ammonia oxidation rates also showed a decreasing trend along with the time course thus leading to a slow increase of atenolol acid in both cases. The formation efficiency of atenolol acid was the lowest without the presence of ammonium amongst these experiments, probably due to the lowest AMO activities lacking of growth substrates.

4.2 Relationship between ammonia oxidation and atenolol degradation

The cometabolic biodegradation by AOB was also confirmed from the linear positive relationship between ammonia oxidation rate and atenolol biodegradation rate as shown in Figure 4A, which was also reported in previous literature (Yi and Harper Jr, 2007). This linear relationship was valid at the investigated mole ratio of atenolol to ammonium from 2.4×10^{-6} to 2.1×10^{-5} in the biodegradation experiment with 50 mg L^{-1} ammonium while the corresponding ratio was from 2.8×10^{-6} to 3.6×10^{-5} in the biodegradation experiments with 25 mg L^{-1} ammonium. The atenolol biodegradation rate decreased from 7.6×10^{-4} to 3.3×10^{-5} μmol g VSS^{-1} h^{-1} whereas the ammonia oxidation rate decreased from 2.8 to 0.02 mmol NH_4^+-N g VSS^{-1} h^{-1} along with the experimental time at the constant 25 mg L^{-1} ammonium. For batch experiments at the constant 50 mg L^{-1} ammonium, the atenolol degradation rate decreased from 7.8×10^{-4} to 5.6×10^{-5} μmol g VSS^{-1} h^{-1} with a decreasing ammonia oxidation rate from 4.2 to 0.2 mmol NH_4^+-N g VSS^{-1} h^{-1}. Comparing the fitted slopes between the experiments at constant 25 mg L^{-1} and 50 mg L^{-1} ammonium, it could be clearly concluded that a higher atenolol degradation rate would be achieved at the lower concentration of growth substrate with the same ammonia oxidation rate, further supporting the substrate competition for AMO active sites between ammonium and atenolol (Arp et al., 2001; Tran et al., 2013).

The observed relationship between ammonia oxidation rate and atenolol acid formation rate in Figure 4B indicated that the formation of biotransformation product of atenolol was consistent with the monooxygenase activity (Fernandez-Fontaina et al., 2016). This suggested the involvement of AMO in the biotransformation reaction (Men et al., 2016). When ammonia oxidation rate was lower than 14.5 mg NH_4^+-N g VSS^{-1} h^{-1}, the higher formation rate of atenolol acid would be achieved at the higher ammonium concentrations provided that the same ammonia oxidation rate was obtained for both constant ammonium concentrations conditions (25 or 50 mg L^{-1}) (Figure 4B). The relationship implied that the batch experiments at 25 mg L^{-1} ammonium would show a higher formation rate of atenolol acid at the assumed same ammonia oxidation rate when it was higher than 14.5 mg NH_4^+-N g VSS^{-1} h^{-1}. This might be due to the involvement of cometabolism and substrate competition together (Fischer and Majewsky, 2014; Tran et al., 2013). The competition might play an important role in formation of biotransformation products when ammonia oxidizing rate was higher than a critical value (e.g. 14.5 mg NH_4^+-N g VSS^{-1} h^{-1} in this study), which requires further confirmation.

With regards to the corresponding concentration profiles of atenolol acid in Figure 2B, it demonstrated a relatively rapid increasing trend under the lower ammonium concentration (25 mg L^{-1}) for the first 48 h. However, ammonia oxidation rates under the higher ammonium concentration (50 mg L^{-1}) were still higher than those under the lower ammonium concentration (25 mg L^{-1}) for each sampling time until 240 h, thus leading to a higher atenolol acid formation rate correspondingly and a higher final concentration of atenolol acid.

4.3 Atenolol biodegradation pathway with different ammonium availability

Different metabolic conditions with regards to the presence or the absence of ammonium were applied in this study to investigate the degradation of atenolol and the formation of its biotransformation product atenolol acid by the enriched nitrifying culture. It was shown that atenolol could be hydroxylated to its carboxylic form, i.e., atenolol acid, regardless of the presence/availability of the growth substrate ammonium. Atenolol acid was also a biotransformation product observed in the conventional activated sludge and membrane bioreactor as well as activated sludge receiving sanitary sewage (Helbling et al., 2010; Radjenović et al., 2008). This biotransformation reaction was previously reported to be catalyzed by amidohydrolase produced from bacteria (Golan-Rozen et al., 2015). The hydroxylation step of mianserin was also reported to be catalyzed by monooxygenase (Men et al., 2016; Silverman, 2002). AMO was a non-specific enzyme with a broad substrate range (Keener and Arp, 1993; Lauchnor and Semprini, 2013). This cometabolism-induced

biotransformation reaction was catalyzed by AMO, which was mostly produced by AOB in the presence of ammonium in this work.

5. Conclusion

The impact of ammonium availability on the biodegradation of atenolol and the formation of its biotransformation product by an enriched nitrifying culture was investigated using batch experiments with relatively realistic levels of atenolol. The key conclusions are:

- The ammonium availability had an adverse effect on atenolol removal efficiency in the enriched nitrifying sludge likely due to the substrate competition.
- Higher concentration of atenolol acid was formed at the end of experiments with higher ammonia oxidation rate of AOB.
- A linear relationship between ammonia oxidation rate and atenolol degradation rate as well as atenolol formation rate confirmed the cometabolic biodegradation by enriched nitrifying biomass.
- Atenolol could be transformed to atenolol acid through the hydroxylation reaction catalyzed by AMO as a cometabolism induced by AOB.

Acknowledgement

This study was supported by the Australian Research Council (ARC) through Discovery Early Career Researcher Award DE130100451. Bing-Jie Ni acknowledges the support of ARC Discovery Project DP130103147 and The University of Queensland Foundation Research Excellence Award.

References

APHA, 1998. Standard methods for the examination of water and wastewater. American Public Health Association, American Water Works Association and Water Environment Federation, Washington, DC, U.S.A.

Arp, D., Yeager, C. Hyman, M., 2001. Molecular and cellular fundamentals of aerobic cometabolism of trichloroethylene. Biodegradation 12 (2), 81-103.

Batt, A.L., Kim, S. Aga, D.S., 2006. Enhanced biodegradation of iopromide and trimethoprim in nitrifying activated sludge. Environ. Sci. Technol. 40 (23), 7367-7373.

Dawas-Massalha, A., Gur-Reznik, S., Lerman, S., Sabbah, I. Dosoretz, C.G., 2014. Co-metabolic oxidation of pharmaceutical compounds by a nitrifying bacterial enrichment. Bioresour. Technol. 167, 336-342.

Fenner, K., Canonica, S., Wackett, L.P. Elsner, M., 2013. Evaluating pesticide degradation in the environment: Blind spots and emerging opportunities. Science 341 (6147), 752-758.

Fernandez-Fontaina, E., Omil, F., Lema, J.M. Carballa, M., 2012. Influence of nitrifying conditions on the biodegradation and sorption of emerging micropollutants. Water Res. 46 (16), 5434-5444.

Fernandez-Fontaina, E., Gomes, I.B., Aga, D.S., Omil, F., Lema, J.M. Carballa, M., 2016. Biotransformation of pharmaceuticals under nitrification, nitratation and heterotrophic conditions. The Sci. Total Environ. 541, 1439-1447.

Fischer, K. Majewsky, M., 2014. Cometabolic degradation of organic wastewater micropollutants by activated sludge and sludge-inherent microorganisms. Appl. Microbiol. Biotechnol. 98 (15), 6583-6597.

Forrez, I., Carballa, M., Boon, N. Verstraete, W., 2009. Biological removal of 17α-ethinylestradiol (EE2) in an aerated nitrifying fixed bed reactor during ammonium starvation. J. Chem. Technol. Biotechnol. 84 (1), 119-125.

Golan-Rozen, N., Seiwert, B., Riemenschneider, C., Reemtsma, T., Chefetz, B. Hadar, Y., 2015. Transformation Pathways of the Recalcitrant Pharmaceutical Compound Carbamazepine by the White-Rot Fungus *Pleurotus ostreatus*: Effects of Growth Conditions. Environ. Sci. Technol. 49 (20), 12351-12362.

Helbling, D.E., Johnson, D.R., Honti, M. Fenner, K., 2012. Micropollutant biotransformation kinetics associate with WWTP process parameters and microbial community characteristics. Environ. Sci. Technol. 46 (19), 10579-10588.

Helbling, D.E., Hollender, J., Kohler, H.P.E., Singer, H. Fenner, K., 2010. High-throughput identification of microbial transformation products of organic micropollutants. Environ. Sci. Technol. 44 (17), 6621-6627.

Joss, A., Zabczynski, S., Göbel, A., Hoffmann, B., Löffler, D., McArdell, C.S., Ternes, T.A., Thomsen, A. Siegrist, H., 2006. Biological degradation of pharmaceuticals in municipal wastewater treatment: Proposing a classification scheme. Water Res. 40 (8), 1686-1696.

Kassotaki, E., Buttiglieri, G., Ferrando-Climent, L., Rodriguez-Roda, I. Pijuan, M., 2016. Enhanced sulfamethoxazole degradation through ammonia oxidizing bacteria co-metabolism and fate of transformation products. Water Res. 94, 111-119.

Keener, W.K. Arp, D.J., 1993. Kinetic studies of ammonia monooxygenase inhibition in *Nitrosomonas europaea* by hydrocarbons and halogenated hydrocarbons in an optimized whole-cell assay. Appl. Environ. Microbiol. 59 (8), 2501-2510.

Khunjar, W.O., Mackintosh, S.A., Skotnicka-Pitak, J., Baik, S., Aga, D.S. Love, N.G., 2011. Elucidating the relative roles of ammonia oxidizing and heterotrophic bacteria during the biotransformation of 17α-ethinylestradiol and trimethoprim. Environ. Sci. Technol. 45 (8), 3605-3612.

Kuai, L. Verstraete, W., 1998. Ammonium removal by the oxygen-limited autotrophic nitrification-denitrification system. Appl. Environ. Microbiol. 64 (11), 4500-4506.

Lauchnor, E.G. Semprini, L., 2013. Inhibition of phenol on the rates of ammonia oxidation by *Nitrosomonas europaea* grown under batch, continuous fed, and biofilm conditions. Water Res. 47 (13), 4692-4700.

Law, Y., Lant, P. Yuan, Z., 2011. The effect of pH on N2O production under aerobic conditions in a partial nitritation system. Water Res. 45 (18), 5934-5944.

Luo, Y., Guo, W., Ngo, H.H., Nghiem, L.D., Hai, F.I., Zhang, J., Liang, S. Wang, X.C., 2014. A review on the occurrence of micropollutants in the aquatic environment and their fate and removal during wastewater treatment. Sci. Total Environ. 473-474, 619-641.

Margot, J., Lochmatter, S., Barry, D.A. Holliger, C., 2016. Role of ammonia-oxidizing bacteria in micropollutant removal from wastewater with aerobic granular sludge. Water Sci. Technol. 73 (3), 564-575.

Men, Y., Han, P., Helbling, D.E., Jehmlich, N., Herbold, C., Gulde, R., Onnis-Hayden, A., Gu, A.Z., Johnson, D.R., Wagner, M. Fenner, K., 2016. Biotransformation of Two Pharmaceuticals by the Ammonia-Oxidizing Archaeon *Nitrososphaera gargensis*. Environ. Sci. Technol. 50 (9), 4682-4692.

Petrie, B., Barden, R. Kasprzyk-Hordern, B., 2015. A review on emerging contaminants in wastewaters and the environment: Current knowledge, understudied areas and recommendations for future monitoring. Water Res. 72, 3-27.

Pomiès, M., Choubert, J.M., Wisniewski, C. Coquery, M., 2013. Modelling of micropollutant removal in biological wastewater treatments: A review. Sci. Total Environ. 443, 733-748.

Radjenović, J., Pérez, S., Petrović, M. Barceló, D., 2008. Identification and structural characterization of biodegradation products of atenolol and glibenclamide by liquid chromatography coupled to hybrid quadrupole time-of-flight and quadrupole ion trap mass spectrometry. J. Chromatogr. A 1210 (2), 142-153.

Roh, H., Subramanya, N., Zhao, F., Yu, C.-P., Sandt, J. Chu, K.-H., 2009. Biodegradation potential of wastewater micropollutants by ammonia-oxidizing bacteria. Chemosphere 77 (8), 1084-1089.

Sathyamoorthy, S., Chandran, K. Ramsburg, C.A., 2013. Biodegradation and cometabolic modeling of selected beta blockers during ammonia oxidation. Environ. Sci. Technol. 47 (22), 12835-12843.

Schäfer, A. Bouwer, E.J., 2000. Toluene induced cometabolism of cis-1,2-dichloroethylene and vinyl chloride under conditions expected downgradient of a permeable Fe(0) barrier. Water Res. 34 (13), 3391-3399.

Sengupta, A., Lyons, J.M., Smith, D.J., Drewes, J.E., Snyder, S.A., Heil, A. Maruya, K.A., 2014. The occurrence and fate of chemicals of emerging concern in coastal urban rivers receiving discharge of treated municipal wastewater effluent. Environ. Toxicol. Chem. 33 (2), 350-358.

Silverman, R.B. (2002) Organic Chemistry of Enzyme-Catalyzed Reactions, pp. xiii-xv, Academic Press, San Diego.

Ternes, T.A., Bonerz, M., Herrmann, N., Teiser, B. Andersen, H.R., 2007. Irrigation of treated wastewater in Braunschweig, Germany: An option to remove pharmaceuticals and musk fragrances. Chemosphere 66 (5), 894-904.

Ternes, T., Joss, A. Oehlmann, J., 2015. Occurrence, fate, removal and assessment of emerging contaminants in water in the water cycle (from wastewater to drinking water). Water Res. 72, 1-2.

Tran, N.H., Urase, T. Kusakabe, O., 2009. The characteristics of enriched nitrifier culture in the degradation of selected pharmaceutically active compounds. J. Hazard. Mater. 171 (1–3), 1051-1057.

Tran, N.H., Urase, T., Ngo, H.H., Hu, J. Ong, S.L., 2013. Insight into metabolic and cometabolic activities of autotrophic and heterotrophic microorganisms in the biodegradation of emerging trace organic contaminants. Bioresour. Technol. 146, 721-731.

Tsien, H.C., Brusseau, G.A., Hanson, R.S. Wackett, L.P., 1989. Biodegradation of trichloroethylene by *Methylosinus trichosporium* OB3b. Appl. Environ. Microbiol. 55 (12), 3155-3161.

Verlicchi, P., Al Aukidy, M. Zambello, E., 2012. Occurrence of pharmaceutical compounds in urban wastewater: Removal, mass load and environmental risk after a secondary treatment—A review. Sci. Total Environ. 429, 123-155.

Yi, T. Harper Jr, W.F., 2007. The link between nitrification and biotransformation of 17α-ethinylestradiol. Environ. Sci. Technol. 41 (12), 4311-4316.

Table and figure legends

Table 1. Mass parameters for LC-MS/MS analysis.

Figure 1. Nitrification performance of the enriched nitrifying sludge based on the initial NH_4^+-N concentration of 20 mg L^{-1} and initial MLVSS concentration of 95 mg L^{-1} and (B) The calculated ammonia oxidation rate during the experimental period under different ammonium concentrations.

Figure 2. The effect of ammonium (NH_4^+-N) concentration on the degradation of atenolol (A) and on the formation of its biotransformation product atenolol acid (B).

Figure 3. The concentration profiles of atenolol and atenolol acid normalized to the initial concentration of atenolol during the time course in the experiments (A) with ammonia oxidation and (B) without ammonia oxidation.

Figure 4. The relationships between ammonia oxidation rate and atenolol degradation rate (A); between ammonia oxidation rate and atenolol acid formation rate (B).

Table 1. Mass parameters for LC-MS/MS analysis

Compounds	Precursor ion (*m/z*)	DP (V)	Q1 (quantification)	CE (eV) /CXP (V)	Q2 (confirmation)	CE (eV) /CXP (V)
Atenolol	267.2	71	145.3	37/12	190.2	29/16
Atenolol acid	268.2	71	145.3	37/12	191.2	29/16
Atenolol-d7	274.2	71	145.1	37/12	79.1	33/6

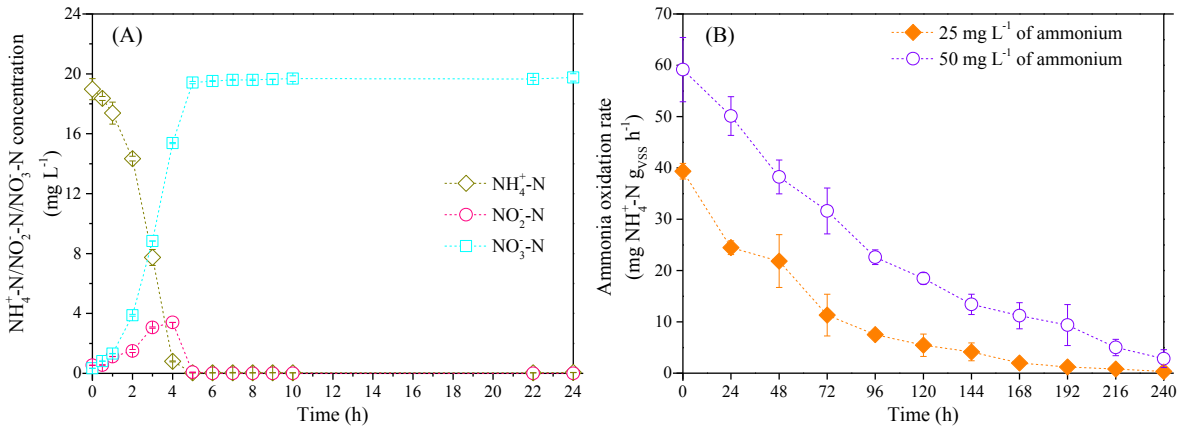

Figure 1. Nitrification performance of the enriched nitrifying sludge based on the initial NH_4^+-N concentration of 20 mg L^{-1} and initial MLVSS concentration of 95 mg L^{-1} and (B) The calculated ammonia oxidation rate during the experimental period under different ammonium concentrations.

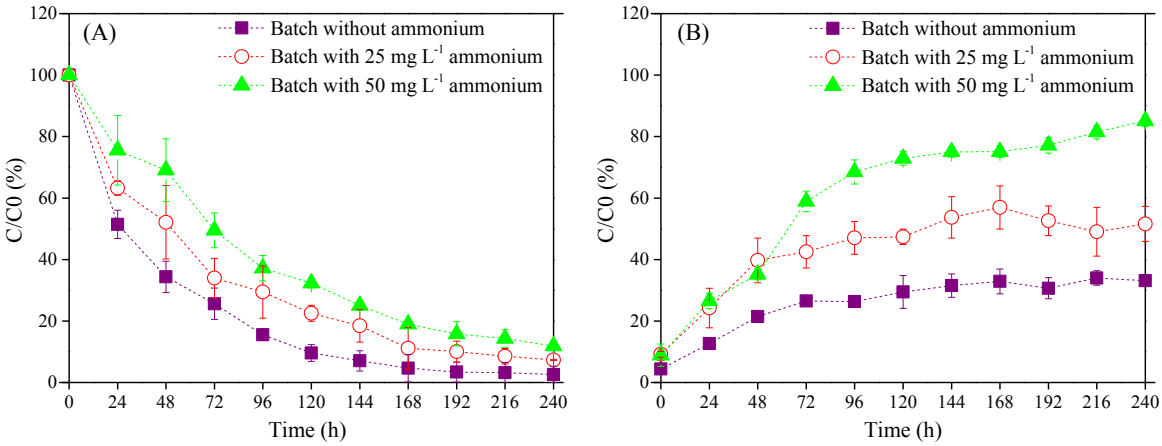

Figure 2. The effect of ammonium (NH_4^+-N) concentration on the degradation of atenolol (A) and on the formation of its biotransformation product atenolol acid (B).

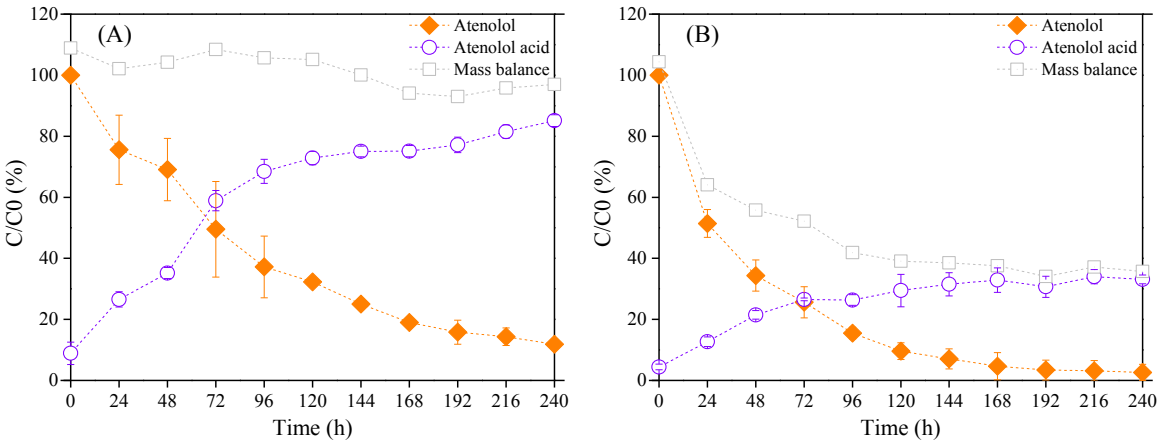

Figure 3. The concentration profiles of atenolol and atenolol acid normalized to the initial concentration of atenolol during the time course in the experiments (A) with ammonia oxidation and (B) without ammonia oxidation.

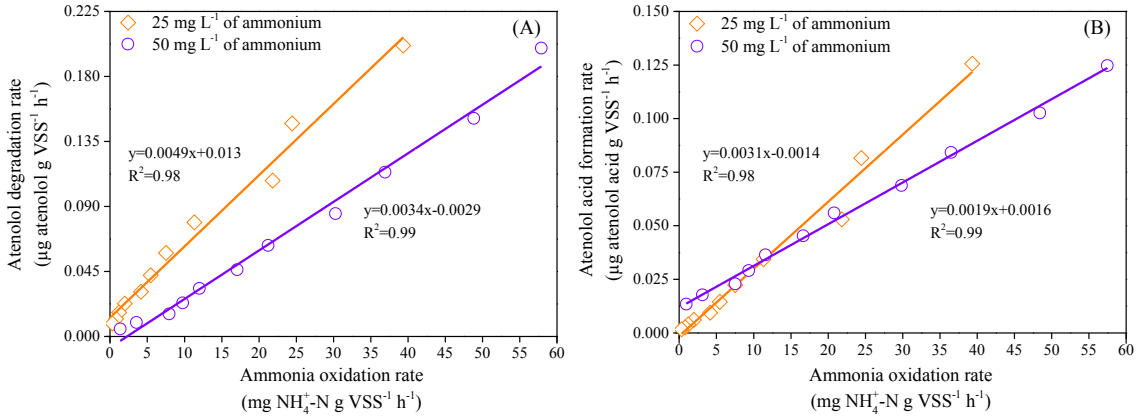

Figure 4. The relationships between ammonia oxidation rate and atenolol degradation rate (A); between ammonia oxidation rate and atenolol acid formation rate (B).

Supporting Information

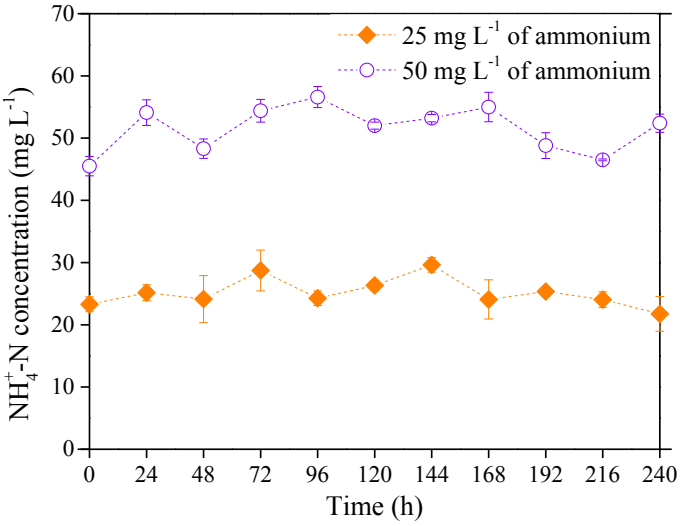

Figure S1. Controlled ammonium concentrations during the entire experimental period in the presence of ammonium.

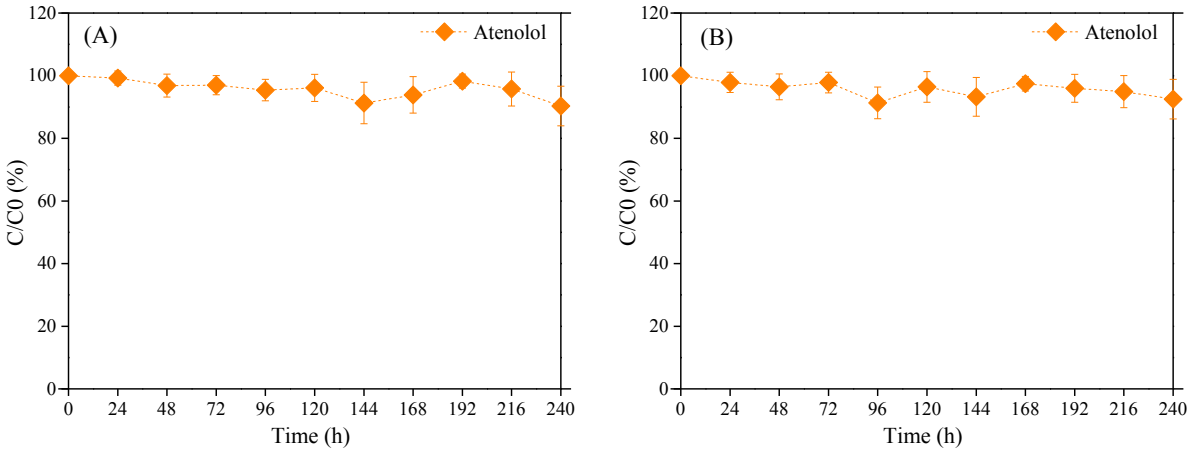

Figure S2. Concentration profiles of atenolol in the control experiments (A) with autoclaved biomass and (B) without biomass.

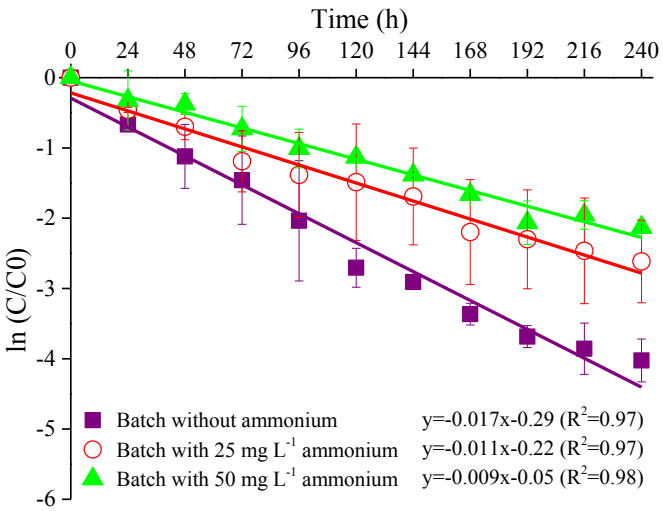

Figure S3. Degradation of atenolol in enriched nitrifying sludge at different concentrations of ammonium (0, 25 and 50 mg L^{-1}). Linear regressions are given assuming a pseudo first order kinetic.

Appendix C

Biotransformation of Acyclovir by an Enriched Nitrifying Culture

Yifeng Xu, Zhiguo Yuan, Bing-Jie Ni*

This paper is published in *Chemosphere*.

Advanced Water Management Centre, The University of Queensland, St. Lucia, Brisbane, QLD 4072, Australia

***Corresponding author:**

Dr. Bing-Jie Ni

Advanced Water Management Centre

The University of Queensland

Australia

Phone: + 61 7 3346 3230

Fax: +61 7 3365 4726

E-mail: b.ni@uq.edu.au

Abstract

This work evaluates the biodegradation of the antiviral drug acyclovir by an enriched nitrifying culture during ammonia oxidation and without the addition of ammonium. The study on kinetics was accompanied with the structural elucidation of biotransformation products through batch biodegradation experiments at two different initial levels of acyclovir (15 mg L^{-1} and 15 μg L^{-1}). The pseudo first order kinetic studies of acyclovir in the presence of ammonium indicated the higher degradation rates under higher ammonia oxidation rates than those constant degradation rates in the absence of ammonium. The positive correlation was found between acyclovir degradation rate and ammonia oxidation rate, confirming the cometabolism of acyclovir by the enriched nitrifying culture in the presence of ammonium. Formation of the product carboxy-acyclovir (P239) indicated the main biotransformation pathway was aerobic oxidation of the terminal hydroxyl group, which was independent on the metabolic type (i.e. cometabolism or metabolism). This enzyme-linked reaction might be catalyzed by monooxygenase from ammonia oxidizing bacteria or heterotrophs. The formation of carboxy-acyclovir was demonstrated to be irrelevant to the acyclovir concentrations

applied, indicating the revealed biotransformation pathway might be the dominant removal pathway of acyclovir in wastewater treatment.

Keywords: Biotransformation; nitrification; cometabolism; ammonia oxidizing bacteria; acyclovir; wastewater treatment.

1. Introduction

In recent years, the increasing concerns have been focused on the emerging pharmaceuticals in aquatic environment due to their potential hazardous effects on living organisms (Daughton and Ternes, 1999; Kümmerer, 2009; Sirés and Brillas, 2012). Large amounts of pharmaceuticals were used by human beings or manufactured for veterinary drugs, leading to their widespread occurrence in the wastewater, surface water and ground water (Luo et al., 2014). Wastewater treatment plant (WWTP) was an important pathway for pharmaceuticals entering into the environment (Kosma et al., 2010; Tijani et al., 2013). Inefficient removal efficiencies of these compounds were observed during treatment processes because WWTPs were mainly designed for bulk nutrient removal (Joss et al., 2006; Kosma et al., 2014; Ternes, 1998).

Nitrification process was observed to be able to enhance the removal of pharmaceuticals (Batt et al., 2006; Fernandez-Fontaina et al., 2012). The involved ammonia oxidizing bacteria (AOB) were probably responsible for cometabolic biodegradation of pharmaceuticals due to its non-specific enzyme ammonia monooxygenase (AMO), which was confirmed to degrade a broad range of organic substrates including aliphatic and aromatic compounds (Keener and Arp, 1994; Lauchnor and Semprini, 2013; Rasche et al., 1990; Skotnicka-Pitak et al., 2009). Furthermore, biotransformation products formed during treatment processes may be more persistent and could probably contribute to the overall toxicity (Miao and Metcalfe, 2003; Pérez et al., 2006; Quintana et al., 2005; Ternes et al., 2007). Therefore, the biotransformation products should also be considered in order to get a comprehensive understanding of the behavior and fate of pharmaceuticals in the environment and engineered systems.

As an important antiviral drug, acyclovir has been consumed largely especially for influenza epidemics. Due to their potential ecosystem alterations and the development of viral resistances, antiviral drugs have recently attracted the interest of research. For example, a substantial removal (98%) of acyclovir was found in the wastewater treatment with the concentration decreasing from 1780 ng L^{-1} to 27 ng L^{-1} (Prasse et al., 2010). Although lab-scale biodegradation of acyclovir was previously studied by the activated sludge from the nitrification zone of a real wastewater treatment

plant (Prasse et al., 2011), the effect of metabolic conditions on the formation of biotransformation products and the specific contributions of AOB and heterotrophs to acyclovir removal has not been clearly defined so far.

This study aims to investigate the biodegradation kinetics, products and pathways of acyclovir by an enriched nitrifying culture through batch biodegradation experiments under different metabolic conditions, i.e., with and without the addition of growth substrate, ammonium. The kinetic analysis was accompanied with the structural elucidation of biotransformation products. The initial acyclovir concentration at 15 mg L^{-1} and 15 μg L^{-1} were applied to verify if the biotransformation products and pathways formed under high concentration would occur at relatively realistic levels.

2. Materials and Methods

2.1 Chemicals

Acyclovir (>98%) was purchased from Thermo Fisher, Australia. Carboxy-acyclovir was provided by Toronto Research Chemicals. Isotope labeled compound acyclovir-d4 was obtained from Santa Cruz Biotechnology. HPLC grade organic solvents (methanol, acetonitrile, hexane and acetone) were supplied by Sigma-Aldrich, Australia. The individual standard stock solution of acyclovir was prepared on a weight basis in methanol at 1 mg mL^{-1} and stored at -20 °C. The calibration curve was obtained by diluting the stock solution appropriately in methanol/water (25:75, v/v). Acyclovir feed solution used in the batch experiments was prepared in Milli-Q water (Millipore, Inc.) at initial concentration of 1 g L^{-1}.

2.2 Enriched nitrifying culture

An 8-L lab-scale sequencing batch reactor (SBR) was inoculated with the activated sludge from a domestic wastewater treatment plant in Brisbane, Australia. It was operated with the aim for the enrichment of nitrifying culture (containing AOB and nitrite oxidizing bacteria (NOB) to perform full nitrification) in cycles of 6 h. For each cycle, it consisted of aerobic feeding (260 min), aeration (30 min), waste (1 min), settling (60 min) and decanting (9 min). 2 L synthetic wastewater consisting of 1 g L^{-1} NH_4^+-N was fed into the reactor during each feeding period, resulting in a hydraulic retention time (HRT) of 24 h. The solid retention time (SRT) was controlled at around 15 d. Dissolved oxygen (DO) was controlled between 2.5-3.0 mg L^{-1} using programmed logic controllers (PLC) and pH was maintained at the range of 7.5-8.0.

The synthetic wastewater for the enriching the nitrifying culture contained per liter (Kuai and Verstraete, 1998): 5.63 g of NH_4HCO_3 (1 g NH_4^+-N), 5.99 g of $NaHCO_3$, 0.064 g of each of KH_2PO_4

and K_2HPO_4 and 2 mL of a trace element solution. The trace element stock solution contained: 1.25 g L^{-1} EDTA, 0.55 g L^{-1} $ZnSO_4 \cdot 7H_2O$, 0.40 g L^{-1} $CoCl_2 \cdot 6H_2O$, 1.275 g L^{-1} $MnCl_2 \cdot 4H_2O$, 0.40 g L^{-1} $CuSO_4 \cdot 5H_2O$, 0.05 g L^{-1} $Na_2MoO_4 \cdot 2H_2O$, 1.375 g L^{-1} $CaCl_2 \cdot 2H_2O$, 1.25 g L^{-1} $FeCl_3 \cdot 6H_2O$ and 44.4 g L^{-1} $MgSO_4 \cdot 7H_2O$.

The biodegradation experiments in this study were conducted after more than 1 year of stable reactor operation with the AOB and NOB population accounting for over 80% of the microbial community with almost 100% conversion of NH_4^+ to NO_3^-. The mixed liquor volatile suspended solids (MLVSS) concentration was stable at 1437.6 ± 112.9 mg L^{-1} (mean and standard errors, respectively, n=10). According to the microbial community analysis with fluorescence *in-situ* hybridization (FISH) (Law et al., 2011), ammonia-oxidizing *beta-proteobacteria* accounted for 46 ± 6% (n=20) of the bacterial populations and the *Nitrospira* genera (nitrite oxidizers) constituted 38 ± 5% (n=20) of the bacterial populations.

2.3 Batch experiments

All batch experiments were conducted in 4 L beakers coupled with PLC controllers. Enriched nitrifying biomass was withdrawn from the SBR during aeration phase when ammonium was almost depleted. The biomass was added into the beaker to obtain the MLVSS concentration of approximately 1000 mg L^{-1} at the beginning of the batch tests. All the batch experiments were divided into two series according to the initial acyclovir concentration. High concentration (15 mg L^{-1}) was selected to identify any possible biotransformation products and elucidate the biotransformation pathways while low concentration (15 μg L^{-1}) was used to study its degradation profile and verify the biotransformation products under relatively realistic concentration. For each concentration level, different sets of experiments were performed (in duplicates for each experiment) (Table 1). EXP1 was conducted to assess biodegradation of acyclovir in the presence of ammonium. The constant ammonium concentration (50 mg L^{-1}) was provided by automatically adding a mixture of ammonium bicarbonate and sodium bicarbonate, which was controlled by PLC as a pH adjustment process. The adding volume was controlled to be minor, which would not change the total volume significantly. EXP2 was performed in the absence of ammonium during the overall time course. EXP3 was carried out with the initial addition of allylthiourea (ATU), which could inhibit ammonia oxidation probably by chelating the copper of AMO active site (Ginestet et al., 1998). The control experiments, EXP4 and EXP5, were used to assess the contribution of abiotic degradation and hydrolytic degradation to acyclovir losses using NaN_3 and pure water (without biomass), respectively. NaN_3 was a chemical inhibitor used for the inactivation of microbial activities (Rattier et al., 2014). Aerobic conditions were achieved with controlled air supply to obtain DO concentration of 2.5-3.0 mg L^{-1}. The pH was

maintained in the range of 7.5-8.0 during the time course in all tests. Mixed liquor samples were taken periodically and immediately frozen until analysis.

2.4 Sample preparation and chemical analysis

For experiments at initial acyclovir concentration of 15 mg L^{-1}, samples were centrifuged at 12000 g for 5 min without filtration to obtain 1 mL supernatant for further direct structural elucidation of the biotransformation products and quantification. For experiments at initial acyclovir concentration of 15 μg L^{-1}, the samples were concentrated through solid phase extraction (SPE) with vacuum manifold (J. T. Baker, The Netherlands) with the recovery for acyclovir of 87.2 ± 6.4% (n=3, 10 μg L^{-1} added). 50 mL samples were first centrifuged at 14000 rpm for 5 min. The supernatant was flowing through Oasis HLB cartridges (6 mL, 200 mg, Waters, USA) at a rate of 5 mL min^{-1} after conditioned with 10 mL methanol and 10 mL Milli-Q water. Then cartridges were dried under vacuum for 30 min before they were eluted with 10 mL methanol and 10 mL of hexane/acetone (50:50, v/v). The extracted elutes were evaporated to dryness under gentle nitrogen stream. The residue was reconstituted in 250 μL methanol and 750 μL Mmilli-Q water with 20 μL acyclovir-d4 (internal standard) added before further analysis.

The samples were analyzed by the ultra-fast liquid chromatography (UFLC) (Shimadzu, Japan) coupled with a 4000 QTRAP hybrid triple quadruple-linear ion trap mass spectrometer (QqLIT-MS) equipped with a Turbo Ion Spray source (Applied Biosystems-Sciex, USA). Chromatographic separation was carried out with the injection volume of 20 μL using an Alltima C18 column (Alltech Associates Inc., USA) at 40 °C. The mobile phase contained (A) H_2O and (B) CH_3CN at a flow rate of 1 mL min^{-1}. The gradient of (B) was conducted as follows: it was linearly increased to 5% B after 0.5 min, further increased to 20% B for 12.5 min, increased to 50% B within 5 min, increased to 100% B for 2 min, kept constant for 4 min and finally was decreased to 5% B for 1 min. The total running time including the conditioning of the column to the initial conditions was 27 min. Positive electrospray ionization (ESI+) mode was applied with the corresponding parameters: drying gas temperature of 500 °C, drying gas 50 psi, curtain gas 30 psi, spraying gas 50 psi. Tentative structures of biotransformation products were identified using the full scan mode at a declustering potential of 80 V and mass range of 50-300 amu followed by the product ion scan mode (MS^2) and sequential fragmentation using the ion trap. Concentrations of acyclovir and its biotransformation product were analyzed in the multiple reaction monitoring (MRM) mode with two transition ions for confirmation and quantification, respectively. The samples from the experiments at initial 15 mg L^{-1} acyclovir need to be diluted 100 times in methanol/Milli-Q water (25:75, v/v) prior to quantification. More detailed information could be obtained in Table S1 in the supporting information (SI).

Ammonium (NH_4^+-N) concentrations controlled in the batch biodegradation experiments were measured with a Lachat QuikChem8000 Flow Injection Analyzer (Lachat Instrument, Milwaukee) and were shown in Figure S1 in SI. Nitrite was not accumulated significantly with the concentration lower than 1 mg L^{-1} for the experimental period and same nitrate concentration was observed as the SBR effluent (up to 1000 mg L^{-1}).

3. Results

3.1 Control experiments

The sorption ability of acyclovir onto the biomass was considered negligible due to the low value of octanol-water partition coefficient (Log K_{ow}, -1.59) (Kasim et al., 2004), which could also be observed from the control experimental results in this study. Regardless of the initial concentration of acyclovir, both abiotic control (EXP4) and hydrolytic control (EXP5) experiments demonstrated the stability of acyclovir over the time course without any transformation products (Figure S2). Sorption and hydrolysis would not contribute to acyclovir removal. Given that the reactors were covered with aluminum foil from photodegradation, biodegradation by nitrifying biomass was the major pathway for acyclovir removal in all the experiments.

3.2 Acyclovir biodegradation in the presence of ammonium

The removal efficiency, transformation efficiency and degradation constant of acyclovir in all the biodegradation experiments were summarized in Table 2. Figure 1 shows the results from the biodegradation experiments in the presence of ammonium. The decrease of acyclovir and formation of the product were plotted using their respective concentrations normalized to the initial acyclovir concentration. At initial concentration of 15 mg L^{-1}, acyclovir underwent a gradual decrease with approximately 65.1% removal at the end of experiments (Figure 1A). After careful screening in the full scan chromatogram followed by spectrum analysis based on nitrogen rule and the existence of the peak [m+Na], etc, one major biotransformation product P239 was found at retention time of 4.88 min (data not shown) with nominal mass of 239. Its structural elucidation was carried out in the following section 3.5. With the available reference standard (carboxy-acyclovir), it was increased gradually from the beginning of the experiments to 6.95 mg L^{-1} (58.6% of conversion rate) at 240 h.

At initial 15 μg L^{-1} concentration, the removal efficiency for acyclovir (88.2%) was higher than that obtained at higher initial level (65.1%) (Figure 1B). The same major product P239 was continuously increased to 5.74 μg L^{-1}. Only 33.0% of the removed parent compound was transformed to P239 while the remaining might be transformed to other minor products or mineralized.

For both initial concentration levels, acyclovir biodegradation followed the pseudo first order degradation kinetics (Figure S3). Same as their concentration profiles, acyclovir also showed the higher degradation constant (0.0071 L g VSS^{-1} h^{-1}) at initial 15 μg L^{-1} concentration than 0.0034 L g VSS^{-1} h^{-1} at 15 mg L^{-1} concentration. These degradation constants were lower than the reported value (4.9 L g_{SS}^{-1} d^{-1}) (Prasse et al., 2011), probably due to unaccustomed sludge to acyclovir. Long-term adaption to pharmaceuticals would enhance the degradation ability of the activated sludge (Pomiès et al., 2015). The decreasing ammonia oxidation rate observed during the experimental period (Figure 2A) might be due to the inhibition of acyclovir or its transformation product (Radniechi et al., 2008; Sathyamoorthy et al., 2013), which could lead to decreasing rates of both substrates. NOB has been proved to be not associated with pharmaceutical (e.g., atenolol) degradation in previous work, with AMO as the main responsible of the cometabolism (Fernandez-Fontaina et al., 2012; Sathyamoorthy et al., 2013; Xu et al., 2016). Regardless of initial acyclovir concentration, the positive relationship between acyclovir degradation rate and ammonia oxidation rate suggested the cometabolic biodegradation of acyclovir by AOB in the presence of ammonium (Figure 2B). The cometabolism also applies to higher concentration of non-growth substrate although it was in the range of the growth substrate concentration (Quintana et al., 2005).

3.3 Acyclovir biodegradation in the absence of ammonium

Without the presence of growth substrate, acyclovir was removed by enriched nitrifying biomass up to 40.9% with the final concentration being 8.5 mg L^{-1} for the higher initial acyclovir concentration experiments (Figure 3A). Simultaneously, the product P239 showed a rapid growing profile compared with the results from experiments with ammonia oxidation. Its concentration was quantified as 8.7 mg L^{-1} at 240 h. Nearly closed mass balance during the time course indicated that almost all the acyclovir removed in the absence of ammonium was transformed to P239. Furthermore, the mass balance did not show a decreasing trend even after 15 d. Thus, P239 might be the only biotransformation product.

For the low initial acyclovir experiments, the removal rate of acyclovir only reached up to 47.8% without ammonia oxidation, which was significantly lower than that observed in the presence of ammonium (88.2%) (Figure 3B). Regardless of the initial acyclovir concentration, the cometabolism in the presence of growth substrate played a positive role in degrading acyclovir than the metabolic degradation without ammonia oxidation. The formation of P239 showed a slower increasing trend compared to that observed in the high initial acyclovir concentration experiments.

The linear regression on the concentration profiles of acyclovir in Figures S4A and B demonstrated the constant degradation rate of acyclovir in the biodegradation experiments without ammonia oxidation. Acyclovir degradation rates during the higher initial concentration and lower initial concentration experiments were 0.027 mg g VSS^{-1} h^{-1} and 0.043 μg g VSS^{-1} h^{-1}, respectively, which were lower than their corresponding degradation rates (0.051, 0.046, 0.042, 0.038, 0.034, 0.031, 0.028 mg g VSS^{-1} h^{-1} and 0.18, 0.15, 0.12, 0.090, 0.071, 0.056, 0.044 μg g VSS^{-1} h^{-1} at time 0, 24, 48, 72, 96, 120, 144 h) under higher ammonia oxidation rates in the experiments in the presence of ammonium, further confirmed the important role of cometabolic biodegradation by AOB for acyclovir removal.

3.4 Acyclovir biodegradation with ATU inhibition

ATU was added at the beginning of the experiments in order to inhibit the nitrifying activities of AOB, thus likely leading to the exclusive degradation of acyclovir by heterotrophs. As no external organic source was provided in the experiments, acyclovir degradation might attribute to heterotrophic metabolic activity. Figure 4A illustrates that acyclovir experienced a slow gradual decrease with a removal rate of 36.2% over the experimental period at the higher initial concentration, which was slightly lower than 40.9% obtained in the absence of ammonium. P239 was still the only product formed with the concentration increasing to 6.4 mg L^{-1} when nitrifying activities were inhibited. Practically 94.1% of the consumed acyclovir was transformed to P239 and the mass balance leveled off for the overall time course. Therefore, no other major products might be formed by heterotrophs.

As shown in Figure 4B, acyclovir at initial 15 μg L^{-1} also declined gradually with a removal efficiency of 50.3% accompanied by the continuous increase of its product P239 (4.9 μg L^{-1} at 240 h). The mass balance analysis also indicated the constant mass during the experimental period with only one product P239 formed.

The linear regression in Figures S4C and D showed acyclovir degradation constants for experiments at the higher initial concentration and the lower initial concentration were calculated as 0.02 mg g VSS^{-1} h^{-1} and 0.018 μg g VSS^{-1} h^{-1}, respectively. Compared to the values obtained in the absence of ammonium, heterotrophs played a major contribution to acyclovir degradation under the condition without ammonia oxidation by AOB. The role of AOB and heterotrophs has been investigated in previous studies on pharmaceutical biodegradation (Khunjar et al., 2011; Tran et al., 2013). The fact that the same biotransformation products for 17β-ethinylestradiol were formed by AOB or heterotrophs (Khunjar et al., 2011) was consistent to the observations in this study. The results

confirmed that P239 was the major biotransformation product of acyclovir by the enriched culture independent on its initial concentration.

3.5 Structural elucidation of biotransformation product

The full scan chromatogram of the samples indicated the formation of the product P239 during all biodegradation experiments. Its structure was then identified through the analysis and comparison of the product ion (MS^2) spectrum of the biodegradation samples with that of the available standard carboxy-acyclovir. Figure 5 showed the MS^2 spectrum of the molecular ion *m*/*z* 240, which was the protonated P239. The most abundant fragment ions were *m*/*z* 152 and 135. The molecular ion *m*/*z* 240 underwent the loss of 88 Da to produce the fragment ion *m*/*z* 152. Further fragmentation of *m*/*z* 152 led to a loss of NH_3 molecule to form *m*/*z* 135. The similar fragmentation pattern was previously reported in the literature (Prasse et al., 2011). Another minor fragmentation pathway was to form *m*/*z* 122 with a loss of 44 Da from *m*/*z* 164, following the loss of 76 Da from molecular ion *m*/*z* 240. Collision induced dissociation of the molecular ion *m*/*z* 240 could lead to the third route to obtain the fragment ion *m*/*z* 61, via the formation of the fragment ion 89. There were no further fragmentation pathways from the lowest *m*/*z* 61. The same fragment ions and fragment pattern observed in the standard solution further confirmed that P239 could be assigned to 9-carboxymethoxymethylguaine (carboxy-acyclovir) (Figure S5).

The same fragment ions *m*/*z* 152 and 135 were also formed in the MS^2 spectrums of the parent compound acyclovir, except *m*/*z* 164 and 122, which were also reported in previous literature (Prasse et al., 2011). The only difference between acyclovir and P239 was the third pathway forming *m*/*z* 75 and *m*/*z* 89, respectively (Figure S6), which was attributed to the oxidation of the hydroxyl group to the carboxy group. This also supported the structural identification of P239 in this work.

4. Discussion

In this work, the biodegradation of the antiviral drug acyclovir by an enriched nitrifying culture was investigated during ammonia oxidation and without the addition of ammonium. Acyclovir degradation rates based on pseudo first order kinetics under higher ammonia oxidation rate in the presence of ammonium were higher than those constant values in the absence of ammonium. The positive correlation observed between acyclovir degradation rate and ammonia oxidation rate further confirmed the cometabolism of acyclovir by the enriched nitrifying culture in the presence of ammonium, which was also supported from the similar relationship for 17α-ethinylestradiol (Yi and Harper, 2007).

Based on the identified product, the main biotransformation pathway was proposed for acyclovir degradation: from acyclovir to carboxy-acyclovir (P239). This reaction was attributed to the oxidation of the terminal hydroxyl group to the carboxy group, which was typically catalyzed by AMO from AOB or ammonia oxidizing archaea (AOA) for most pharmaceuticals including other antiviral drugs (abacavir, emtricitabine, ganciclovir, lamivudine and zidovudine), amide-containing compounds (e.g. propachlor) and tertiary amines such as mianserin (Funke et al., 2016; Helbling et al., 2010; Men et al., 2016). Although it was also observed in mammalian metabolism of acyclovir (Prasse et al., 2011), the enzyme-induced alcohol oxidation has not been investigated solely for heterotrophs previously. However, the formation of carboxy-acyclovir in experiments with ATU addition in this work indicated that the monooxygenase from heterotrophs could also catalyze the alcohol oxidation of such compound. Although other possibly formed products were not identified in the presence of ammonium, the same biotransformation product carboxy-acyclovir found with ammonia oxidation and with nitrification inhibited in this study was different from previous report on iopromide, where dehydroxylated and carboxylated products were formed, respectively (Batt et al., 2006). It was proposed that oxidation of acyclovir to carboxy-acyclovir might be catalyzed by monooxygenase from either AOB or heterotrophs (Men et al., 2016).

It was also noted that the formation of carboxy-acyclovir was independent on the metabolic type, i.e. regardless of the presence of ammonia oxidation by AOB. This was contradictory to the observation that the generation of 4-chlorobenzoic acid was related to the metabolic type and only produced by microbial hydrolysis of the amide bond of bezafibrate under cometabolism (Quintana et al., 2005). Comparing with acyclovir, the human metabolite carboxy-ibuprofen was not found in biodegradation of ibuprofen following alcohol oxidation (Quintana et al., 2005). The possible reason could be related to the specific structures of the studied pharmaceuticals. The guanine group of acyclovir showed no significant changes during biodegradation with the primary hydroxyl being the only vulnerable group. However, whether acyclovir could be biotransformed to other products is not confirmed in the product identification in this study although the mass balance analysis in the presence of ammonium demonstrated the possible formation of other products. Further work would be required to confirm the thorough biotransformation pathway of acyclovir.

The biotransformation pathway to carboxy-acyclovir by the enriched nitrifying culture was independent of the initial concentration of acyclovir, i.e. 15 μg L^{-1} or 15 mg L^{-1}. This was in consistency with the previous study on trimethoprim by nitrifying activated sludge (Eichhorn et al., 2005). Two metabolites were formed and the degradation route was independent on the initial concentration of trimethoprim (20 mg L^{-1} or 20 μg L^{-1}). However, biodegradation of trimethoprim

was also investigated by nitrifying activated sludge in another recent study (Jewell et al., 2016), resulting in different biotransformation products under different spiked concentration of trimethoprim (500 μg L^{-1} or 5 μg L^{-1}). From the mass balance analysis, carboxy-acyclovir seems to be the only product by heterotrophs either in higher initial concentration or lower initial concentration of acyclovir. There might be other minor biotransformation products formed through cometabolism by the enriched nitrifying culture as carboxy-acyclovir had a low final percentage and the total mass showed a decreasing trend, which was vastly different from those under other conditions (in the absence of ammonium and with addition of ATU), which could not be confirmed yet currently and required future efforts.

5. Conclusion

Biodegradation of acyclovir by an enriched nitrifying culture was investigated during ammonia oxidation and without the presence of ammonium at different initial concentrations of acyclovir in this study. The key conclusions are:

- Biodegradation of acyclovir was positively related to the ammonia oxidation rate, confirmed the key role of cometabolism by AOB in acyclovir removal.
- Carboxy-acyclovir was produced from acyclovir regardless of the presence of ammonium and thus unaffected by metabolic type.
- The same biotransformation pathway from acyclovir to carboxy-acyclovir was observed at different initial concentrations of acyclovir.
- Alcohol oxidation was the biotransformation reaction catalyzed by non-specific enzyme monooxygenase, probably either from AOB or heterotrophs.

Acknowledgement

This study was supported by the Australian Research Council (ARC) through Discovery Early Career Researcher Award DE130100451. Bing-Jie Ni acknowledges the support of ARC Discovery Project DP130103147 and The University of Queensland Foundation Research Excellence Award.

Reference

Batt, A.L., Kim, S., Aga, D.S., 2006. Enhanced biodegradation of iopromide and trimethoprim in nitrifying activated sludge. Environ. Sci. Technol. 40, 7367-7373.

Daughton, C.G., Ternes, T.A., 1999. Pharmaceuticals and personal care products in the environment: Agents of subtle change? Environ. Health Perspect. 107, 907-938.

Eichhorn, P., Ferguson, P.L., Pérez, S., Aga, D.S., 2005. Application of ion trap-MS with H/D exchange and QqTOF-MS in the identification of microbial degradates of trimethoprim in nitrifying activated sludge. Anal. Chem. 77, 4176-4184.

Fernandez-Fontaina, E., Omil, F., Lema, J.M., Carballa, M., 2012. Influence of nitrifying conditions on the biodegradation and sorption of emerging micropollutants. Water Res. 46, 5434-5444.

Funke, J., Prasse, C., Ternes, T.A., 2016. Identification of transformation products of antiviral drugs formed during biological wastewater treatment and their occurrence in the urban water cycle. Water Res. 98, 75-83.

Ginestet, P., Audic, J.M., Urbain, V., Block, J.C., 1998. Estimation of nitrifying bacterial activities by measuring oxygen uptake in the presence of the metabolic inhibitors allylthiourea and azide. Appl. Environ. Microbiol. 64, 2266-2268.

Helbling, D.E., Hollender, J., Kohler, H.-P.E., Fenner, K., 2010. Structure-based interpretation of biotransformation pathways of amide-containing compounds in sludge-seeded bioreactors. Environ. Sci. Technol. 44, 6628-6635.

Jewell, K.S., Castronovo, S., Wick, A., Falås, P., Joss, A., Ternes, T.A., 2016. New insights into the transformation of trimethoprim during biological wastewater treatment. Water Res. 88, 550-557.

Joss, A., Zabczynski, S., Göbel, A., Hoffmann, B., Löffler, D., McArdell, C.S., Ternes, T.A., Thomsen, A., Siegrist, H., 2006. Biological degradation of pharmaceuticals in municipal wastewater treatment: Proposing a classification scheme. Water Res. 40, 1686-1696.

Kasim, N.A., Whitehouse, M., Ramachandran, C., Bermejo, M., Lennernäs, H., Hussain, A.S., Junginger, H.E., Stavchansky, S.A., Midha, K.K., Shah, V.P., Amidon, G.L., 2004. Molecular properties of WHO essential drugs and provisional biopharmaceutical classification. Mol. Pharmaceutics 1, 85-96.

Keener, W.K., Arp, D.J., 1994. Transformations of aromatic compounds by *Nitrosomonas europaea*. Appl. Environ. Microbiol. 60, 1914-1920.

Khunjar, W.O., Mackintosh, S.A., Skotnicka-Pitak, J., Baik, S., Aga, D.S., Love, N.G., 2011. Elucidating the relative roles of ammonia oxidizing and heterotrophic bacteria during the biotransformation of 17α-ethinylestradiol and trimethoprim. Environ. Sci. Technol. 45, 3605-3612.

Kosma, C.I., Lambropoulou, D.A., Albanis, T.A., 2010. Occurrence and removal of PPCPs in municipal and hospital wastewaters in Greece. J. Hazard. Mater. 179, 804-817.

Kosma, C.I., Lambropoulou, D.A., Albanis, T.A., 2014. Investigation of PPCPs in wastewater treatment plants in Greece: Occurrence, removal and environmental risk assessment. Sci. Total Environ. 466–467, 421-438.

Kuai, L., Verstraete, W., 1998. Ammonium removal by the oxygen-limited autotrophic nitrification-denitrification system. Appl. Environ. Microbiol. 64, 4500-4506.

Kümmerer, K., 2009. The presence of pharmaceuticals in the environment due to human use – present knowledge and future challenges. J. Environ. Manage. 90, 2354-2366.

Lauchnor, E.G., Semprini, L., 2013. Inhibition of phenol on the rates of ammonia oxidation by *Nitrosomonas europaea* grown under batch, continuous fed, and biofilm conditions. Water Res. 47, 4692-4700.

Law, Y., Lant, P. Yuan, Z., 2011. The effect of pH on N2O production under aerobic conditions in a partial nitritation system. Water Res. 45, 5934-5944.

Luo, Y., Guo, W., Ngo, H.H., Nghiem, L.D., Hai, F.I., Zhang, J., Liang, S., Wang, X.C., 2014. A review on the occurrence of micropollutants in the aquatic environment and their fate and removal during wastewater treatment. Sci. Total Environ. 473-474, 619-641.

Men, Y., Han, P., Helbling, D.E., Jehmlich, N., Herbold, C., Gulde, R., Onnis-Hayden, A., Gu, A.Z., Johnson, D.R., Wagner, M., Fenner, K., 2016. Biotransformation of Two Pharmaceuticals by the Ammonia-Oxidizing Archaeon *Nitrososphaera gargensis*. Environ. Sci. Technol. 50, 4682-4692.

Miao, X.-S., Metcalfe, C.D., 2003. Determination of carbamazepine and Its metabolites in aqueous samples using liquid chromatography−electrospray tandem mass spectrometry. Anal. Chem. 75, 3731-3738.

Pérez, S., Eichhorn, P., Celiz, M.D., Aga, D.S., 2006. Structural characterization of metabolites of the X-ray contrast agent iopromide in activated sludge using ion trap mass spectrometry. Anal. Chem. 78, 1866-1874.

Pomiès, M., Choubert, J.M., Wisniewski, C., Miège, C., Budzinski, H. Coquery, M., 2015. Lab-scale experimental strategy for determining micropollutant partition coefficient and biodegradation constants in activated sludge. Environ. Sci. Pollut. Res. 22, 4383-4395.

Prasse, C., Schlüsener, M.P., Schulz, R., Ternes, T.A., 2010. Antiviral drugs in wastewater and surface waters: a new pharmaceutical class of environmental relevance? Environ. Sci. Technol. 44, 1728-1735.

Prasse, C., Wagner, M., Schulz, R., Ternes, T.A., 2011. Biotransformation of the antiviral drugs acyclovir and penciclovir in activated sludge treatment. Environ. Sci. Technol. 45, 2761-2769.

Quintana, J.B., Weiss, S., Reemtsma, T., 2005. Pathways and metabolites of microbial degradation of selected acidic pharmaceutical and their occurrence in municipal wastewater treated by a membrane bioreactor. Water Res. 39, 2654-2664.

Radniecki, T.S., Dolan, M.E. Semprini, L., 2008. Physiological and transcriptional responses of *Nitrosomonas europaea* to toluene and benzene inhibition. Environ. Sci. Technol. 42, 4093-

4098.

Rasche, M.E., Hicks, R.E., Hyman, M.R., Arp, D.J., 1990. Oxidation of monohalogenated ethanes and n-chlorinated alkanes by whole cells of *Nitrosomonas europaea*. J. Bacteriol. 172, 5368-5373.

Rattier, M., Reungoat, J., Keller, J. Gernjak, W., 2014. Removal of micropollutants during tertiary wastewater treatment by biofiltration: Role of nitrifiers and removal mechanisms. Water Res. 54, 89-99.

Sathyamoorthy, S., Chandran, K. Ramsburg, C.A., 2013. Biodegradation and cometabolic modeling of selected beta blockers during ammonia oxidation. Environ. Sci. Technol. 47, 12835-12843.

Sirés, I., Brillas, E., 2012. Remediation of water pollution caused by pharmaceutical residues based on electrochemical separation and degradation technologies: A review. Environ. Int. 40, 212-229.

Skotnicka-Pitak, J., Khunjar, W.O., Love, N.G., Aga, D.S., 2009. Characterization of metabolites formed during the biotransformation of 17α-ethinylestradiol by *Nitrosomonas europaea* in batch and continuous flow bioreactors. Environ. Sci. Technol. 43, 3549-3555.

Ternes, T.A., 1998. Occurrence of drugs in German sewage treatment plants and rivers. Water Res. 32, 3245-3260.

Ternes, T.A., Bonerz, M., Herrmann, N., Teiser, B., Andersen, H.R., 2007. Irrigation of treated wastewater in Braunschweig, Germany: An option to remove pharmaceuticals and musk fragrances. Chemosphere 66, 894-904.

Tijani, J.O., Fatoba, O.O., Petrik, L.F., 2013. A review of pharmaceuticals and endocrine-disrupting compounds: Sources, effects, removal, and detections. Water, Air, Soil Pollut. 224, 1770-1798.

Tran, N.H., Urase, T., Ngo, H.H., Hu, J., Ong, S.L., 2013. Insight into metabolic and cometabolic activities of autotrophic and heterotrophic microorganisms in the biodegradation of emerging trace organic contaminants. Bioresour. Technol. 146, 721-731.

Xu, Y., Yuan, Z. Ni, B.-J., 2016. Biotransformation of pharmaceuticals by ammonia oxidizing bacteria in wastewater treatment processes. Sci. Total Environ. 566–567, 796-805.

Yi, T. Harper Jr, W.F., 2007. The link between nitrification and biotransformation of 17α-ethinylestradiol. Environ. Sci. Technol. 41, 4311-4316.

Table and figure legends

Table 1. Conditions of conducted batch experiments with acyclovir (same design of key experimental conditions for experiments at initial acyclovir of 15 mg L^{-1} and 15 μg L^{-1})

Table 2. The acyclovir removal efficiency, biotransformation efficiency and degradation constant in the conducted biodegradation experiments (high, initial acyclovir concentration of 15 mg L^{-1}; low, initial acyclovir concentration of 15 μg L^{-1}) with possible mechanisms involved

Figure 1. Concentration profiles of acyclovir and its product normalized to the initial acyclovir of (A) 15 mg L^{-1} and (B) 15 μg L^{-1} in the experiments with ammonia oxidation.

Figure 2. (A) Ammonia oxidation rate during the time course in the acyclovir biodegradation experiments with ammonia oxidation; (B) the relationship between acyclovir degradation rate and ammonia oxidation rate in the presence of ammonium.

Figure 3. Concentration profiles of acyclovir and its product normalized to the initial (A) 15 mg L^{-1} and (B) 15 μg L^{-1} in the experiments without ammonia addition.

Figure 4. Concentration profiles of acyclovir and its product normalized to the initial (A) 15 mg L^{-1} and (B) 15 μg L^{-1} in the experiments with inhibition of ammonia oxidation of AOB by allythiourea (ATU) addition.

Figure 5. The fragmentation pathways of P239 under ESI+ conditions derived from MS^2 experiments in the QqLIT mass spectrometer.

Table 1. Conditions of conducted batch experiments with acyclovir (same design of key experimental conditions for experiments at initial acyclovir of 15 mg L^{-1} and 15 μg L^{-1})

Experiments	EXP1	EXP2	EXP3	EXP4	EXP5
Initial ammonium (mg L^{-1})	50	0	50	50	50
Ammonium control	Constant	0	Constant	Constant	Constant
Approximate VSS (mg L^{-1})	1000	1000	1000	1000	0
Volume (L)	4	4	4	4	4
ATU (mg L^{-1})	0	0	30	0	0
NaN_3 (mg L^{-1})	0	0	0	500	0

Table 2. The acyclovir removal efficiency, biotransformation efficiency and degradation constant in the conducted biodegradation experiments (high, initial acyclovir concentration of 15 mg L^{-1}; low, initial acyclovir concentration of 15 μg L^{-1}) with possible mechanisms involved

Experiments	EXP1-high	EXP1-low	EXP2-high	EXP2-low	EXP3-high	EXP3-low
Removal efficiency (%)	65.1	88.2	40.9	47.8	36.2	50.3
Biotransformation efficiency (%)	58.6	33.0	~100	72.6	94.1	83.8
Biodegradation constant	0.0034 L g VSS^{-1} h^{-1}	0.0071 L g VSS^{-1} h^{-1}	0.027 mg g VSS^{-1} h^{-1}	0.043 μg g VSS^{-1} h^{-1}	0.02 mg g VSS^{-1} h^{-1}	0.018 μg g VSS^{-1} h^{-1}
Main mechanisms	Cometabolism by AOB		Metabolism by AOB and heterotrophs		Metabolism by heterotrophs	

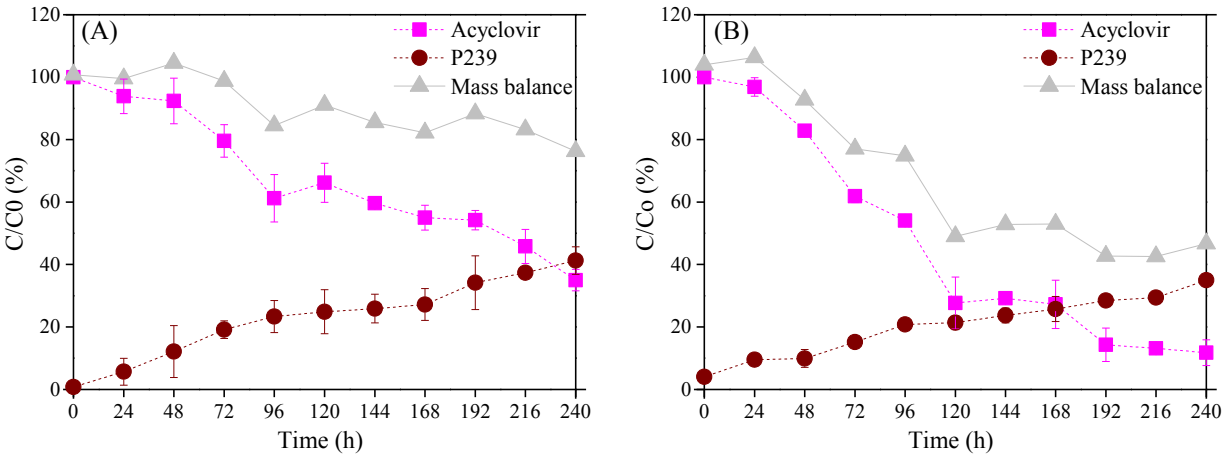

Figure 1. Concentration profiles of acyclovir and its product normalized to the initial acyclovir of (A) 15 mg L^{-1} and (B) 15 µg L^{-1} in the experiments with ammonia oxidation.

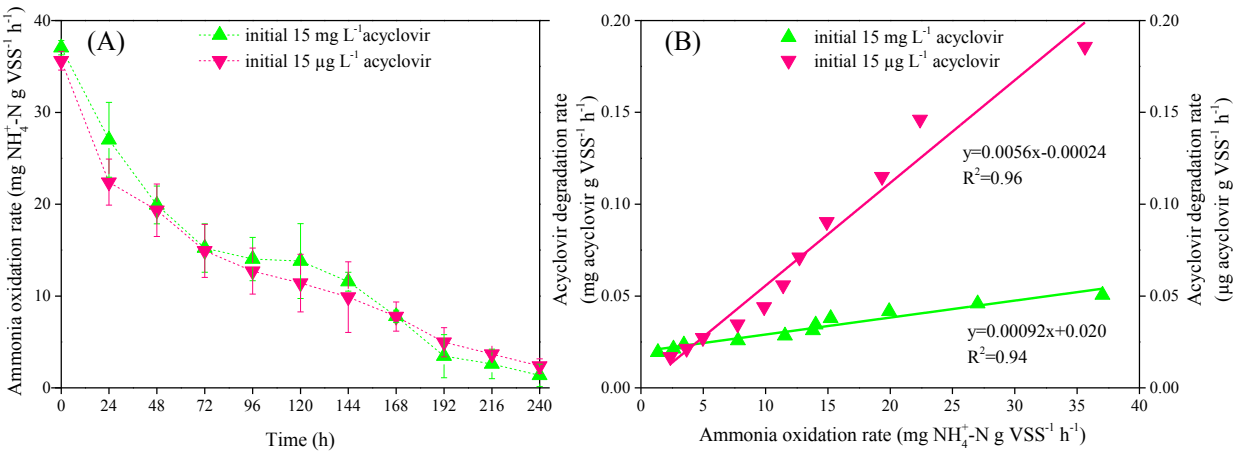

Figure 2. (A) Ammonia oxidation rate during the time course in the acyclovir biodegradation experiments with ammonia oxidation; (B) the relationship between acyclovir degradation rate and ammonia oxidation rate in the presence of ammonium.

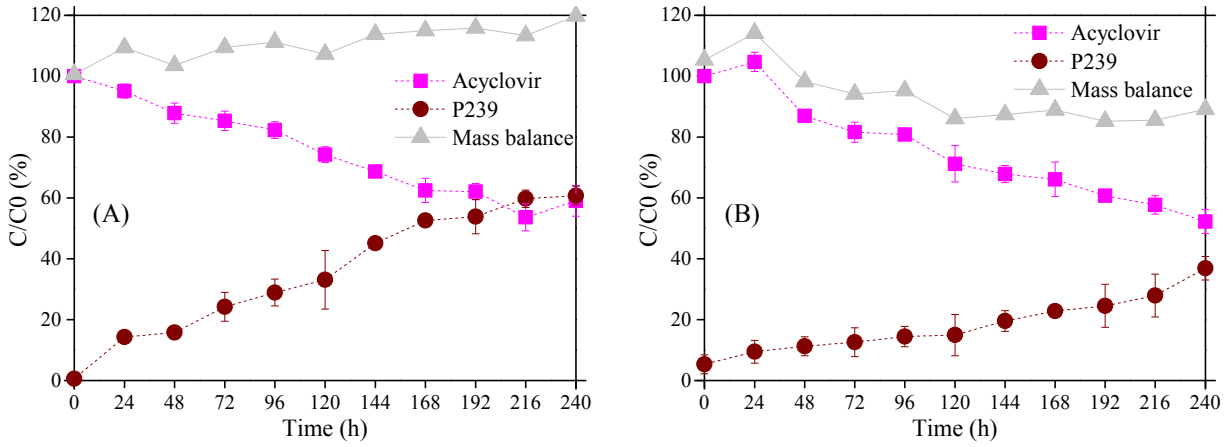

Figure 3. Concentration profiles of acyclovir and its product normalized to the initial (A) 15 mg L^{-1} and (B) 15 µg L^{-1} in the experiments without ammonia addition.

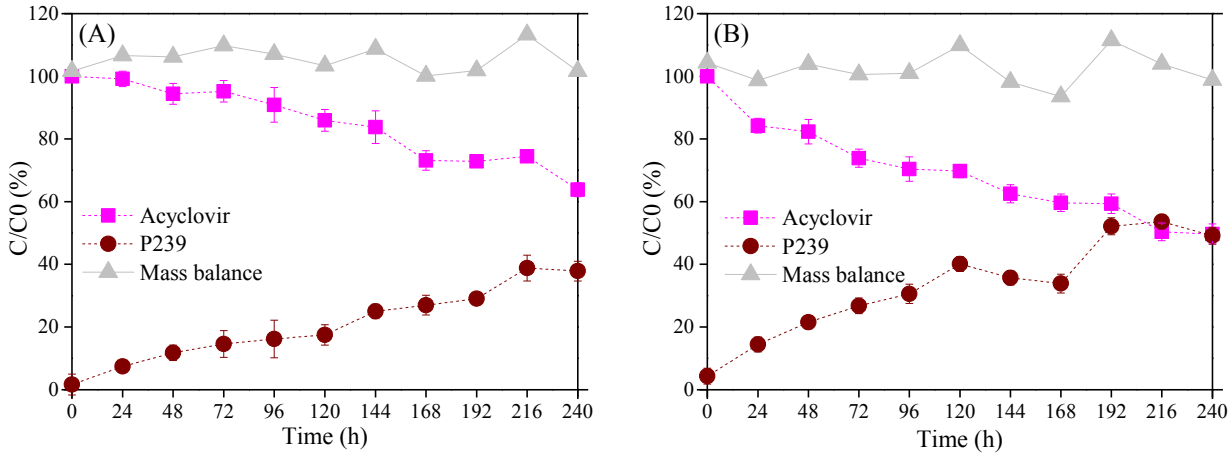

Figure 4. Concentration profiles of acyclovir and its product normalized to the initial (A) 15 mg L^{-1} and (B) 15 μg L^{-1} in the experiments with inhibition of ammonia oxidation of AOB by allythiourea (ATU) addition.

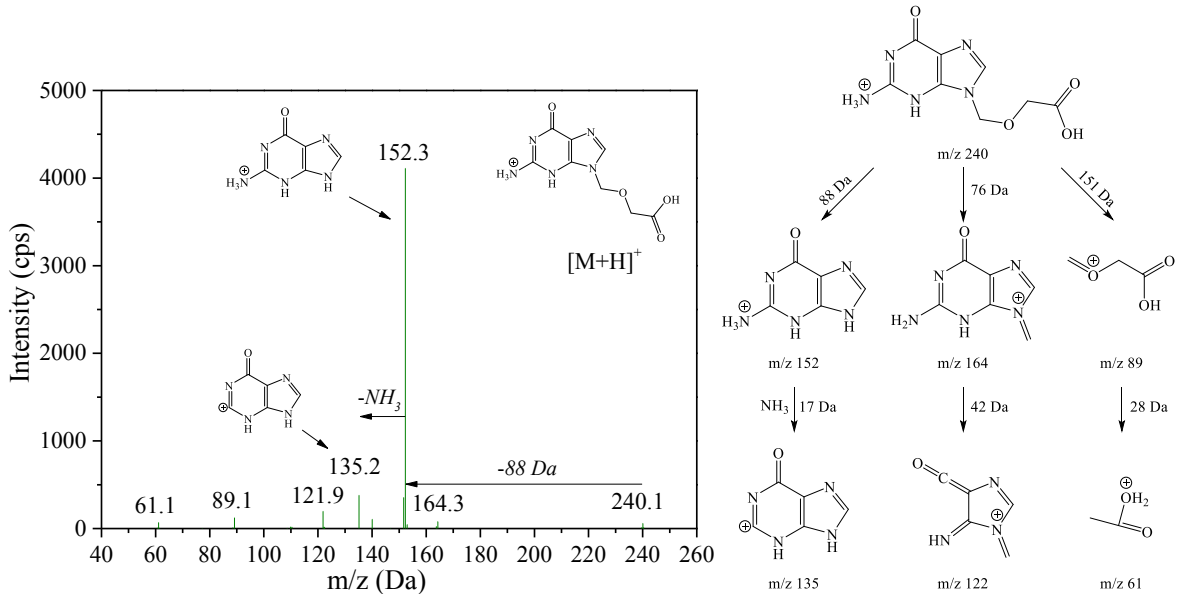

Figure 5. The fragmentation pathways of P239 under ESI+ conditions derived from MS^2 experiments in the QqLIT mass spectrometer.

Supporting Information

Table S1. Mass parameters applied for LC-MS/MS analysis

Compounds	Precursor ion (*m*/*z*)	DP (V)	Q1, *m*/*z* (quantification)	CE (eV) /CXP (V)	Q2, *m*/*z* (confirmation)	CE (eV) /CXP (V)
Acyclovir	226	71	152	17/12	135	43/14
Carboxy-acyclovir	240	46	152	19/12	135	43/12
Acyclovir-d4	230	46	152	19/12	135	41/10

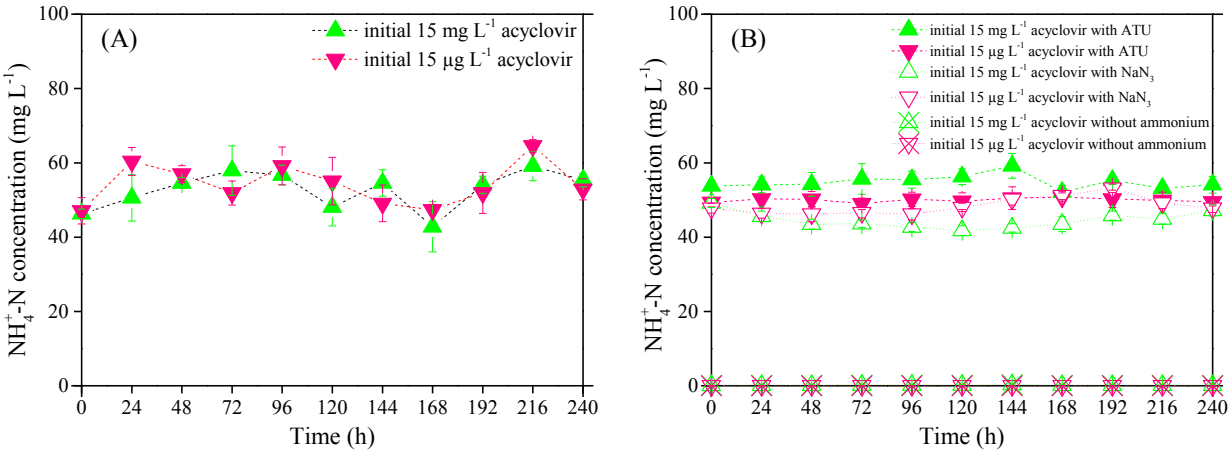

Figure S1. Ammonium concentrations in the biodegradation experiments (A) with the presence of ammonium and (B) other batch experiments (without the presence of ammonium, with addition of allylthiourea (ATU) and with addition of NaN_3).

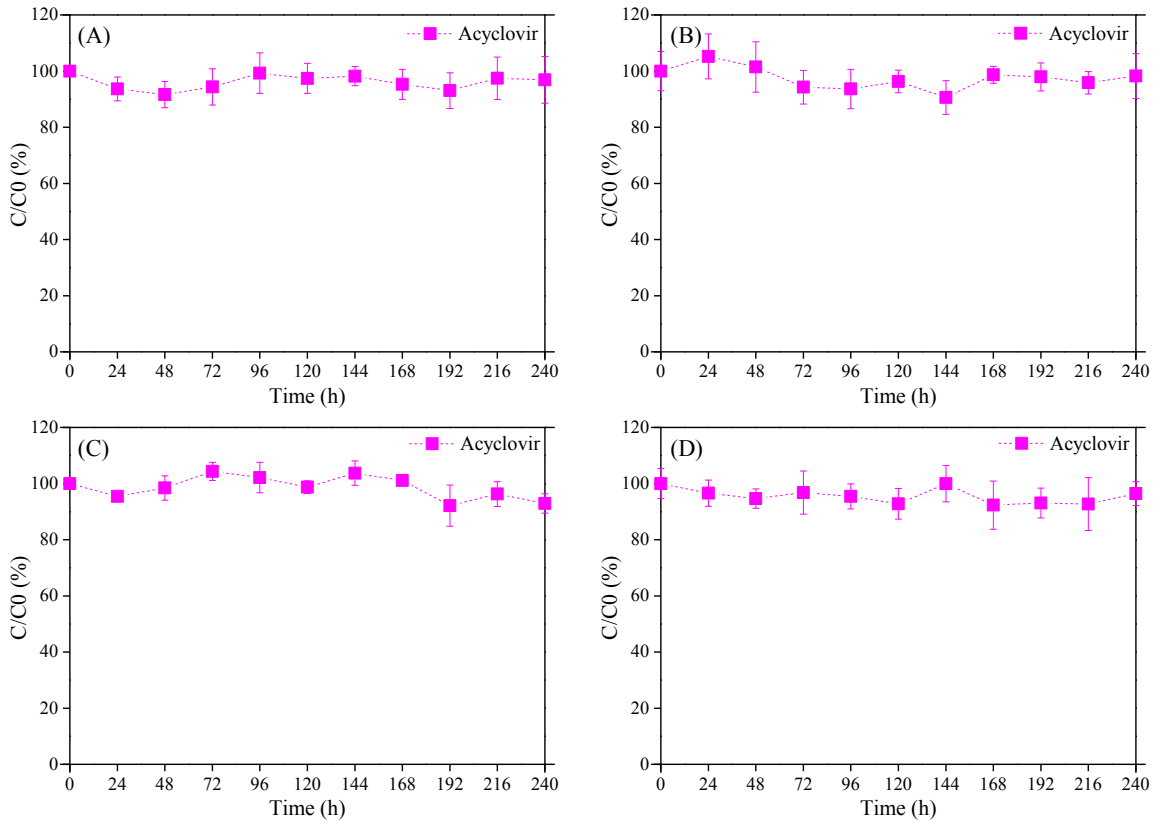

Figure S2. Concentration profiles of acyclovir with addition of NaN_3 (above panel) and without biomass (below panel): (A) and (C), at initial acyclovir of 15 mg L^{-1}; (B) and (D), at initial acyclovir of 15 μg L^{-1}.

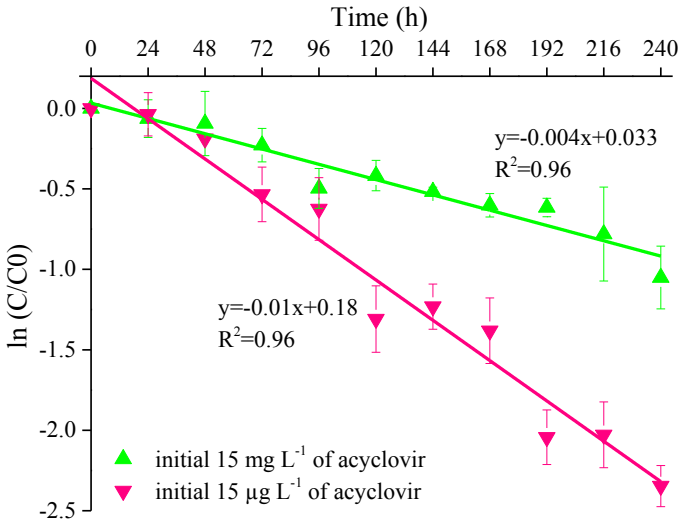

Figure S3. Degradation of acyclovir by the enriched nitrifying culture at initial concentrations of 15 mg L^{-1} and 15 µg L^{-1}, respectively in the experiments with the presence of ammonium. Linear regressions are given assuming a pseudo first order kinetic.

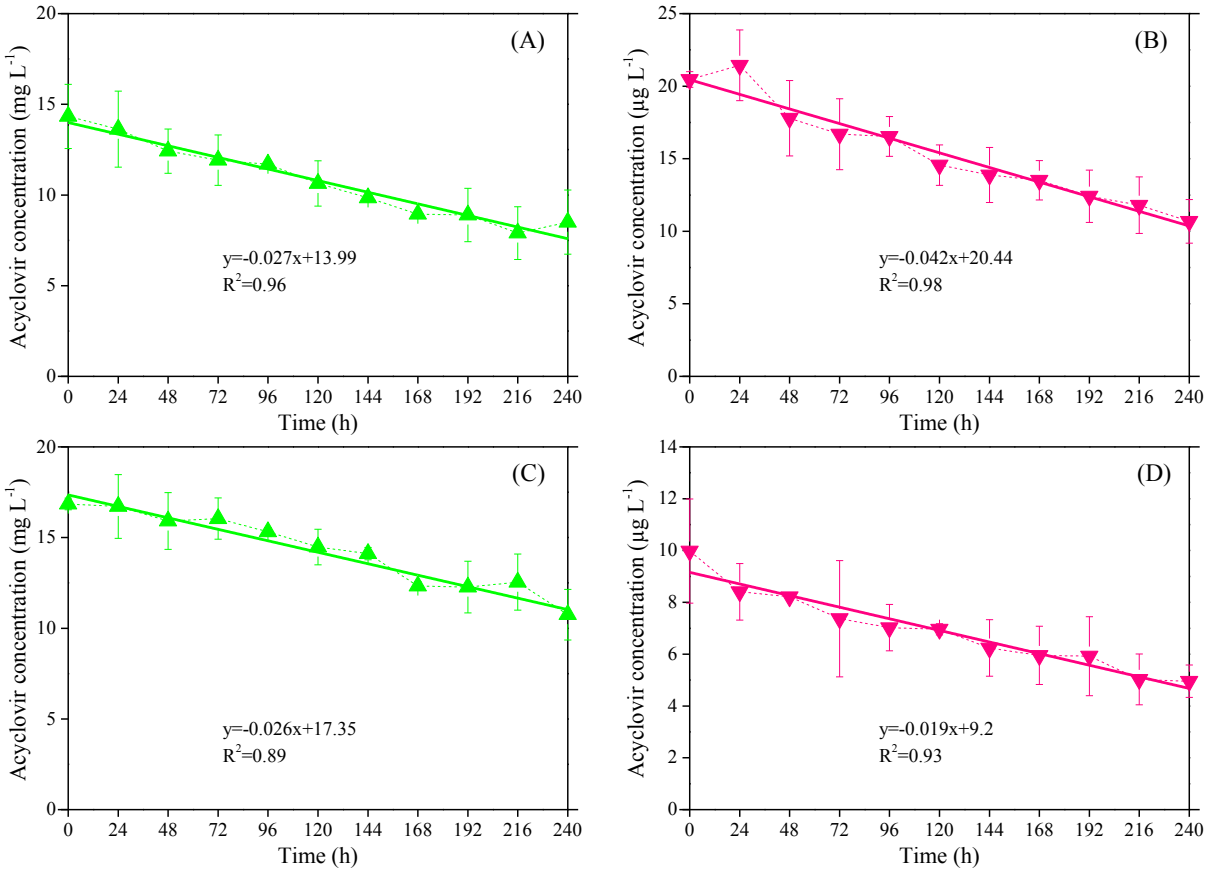

Figure S4. Degradation of acyclovir by the enriched nitrifying culture at initial concentrations of (A) 15 mg L^{-1} and (B) 15 µg L^{-1} in the experiments without the presence of ammonium (top panel) and (C) 15 mg L^{-1} and (D) 15 µg L^{-1} in the experiments with addition of allylthiourea (ATU, below panel).

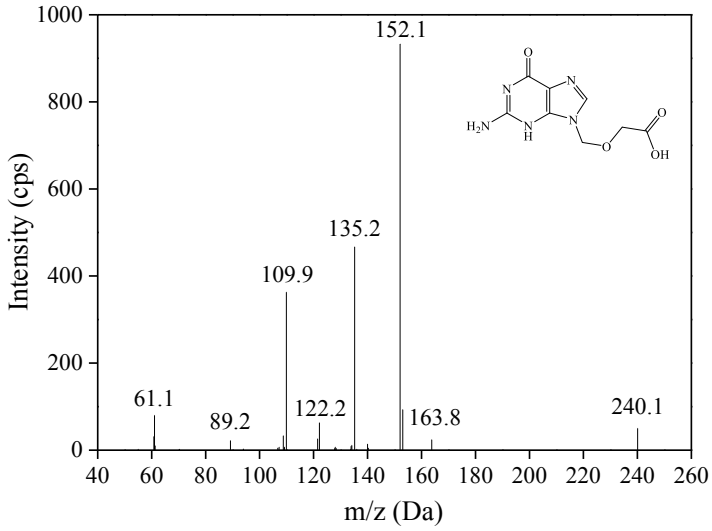

Figure S5. MS^2 spectrum of the standard solution of 9-carboxymethoxymethylguaine (carboxy-acyclovir).

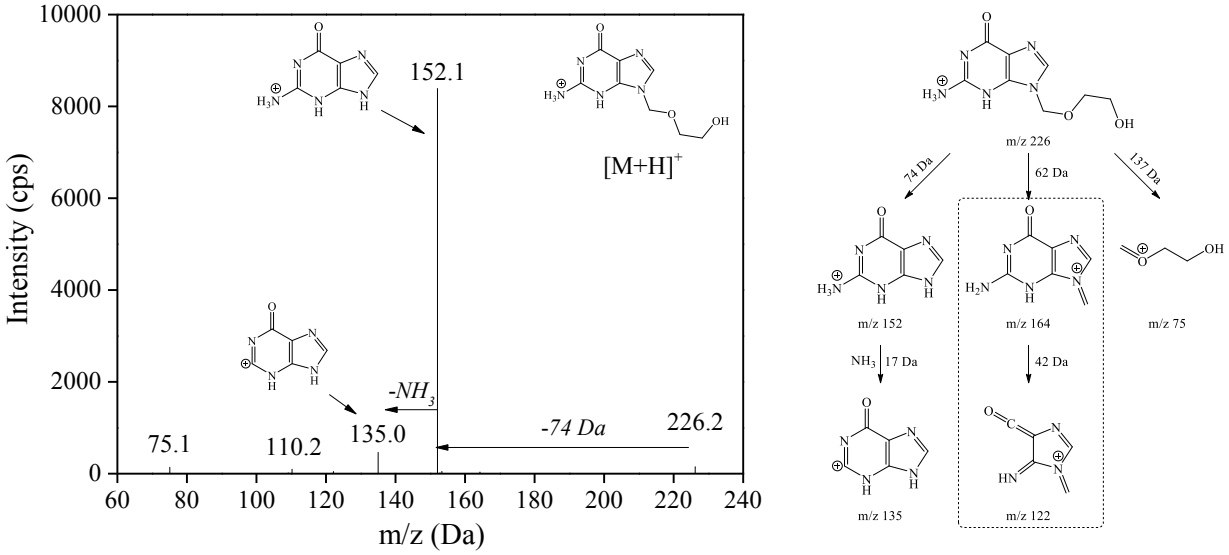

Figure S6. The fragmentation pathways of acyclovir under ESI+ conditions derived from MS^2 experiments in the QqLIT mass spectrometer (the pathways in the dash square were not identified in this study).

Appendix D

Modeling of Pharmaceutical Biotransformation by Enriched Nitrifying Culture under Different Metabolic Conditions

Yifeng Xu, Xueming Chen, Zhiguo Yuan, Bing-Jie Ni*

This manuscript is submitted for review.

Advanced Water Management Centre, The University of Queensland, St. Lucia, Brisbane, QLD 4072, Australia

***Corresponding author:**

Dr. Bing-Jie Ni

Advanced Water Management Centre

The University of Queensland

Australia

Phone: + 61 7 3346 3222

Fax: +61 7 3365 4726

E-mail: b.ni@uq.edu.au

Abstract

Pharmaceutical removal has been demonstrated to be significantly enhanced through cometabolism during nitrification processes. Mathematical model could be useful for understanding the fate and transformation of pharmaceuticals and optimizing the removal process. However, so far pharmaceutical biotransformation models have not considered the formation of transformation products associated with the metabolic type of microorganisms. Here we reported a comprehensive model to describe and evaluate the biodegradation of pharmaceuticals and the formation of their biotransformation products by the enriched nitrifying culture. The biotransformation of parent compounds was linked to the microbial processes via cometabolism induced by ammonium oxidizing bacteria (AOB) growth, metabolism by AOB, cometabolism by heterotrophs (HET) growth and metabolism by HET in the model framework. The model was calibrated and validated using experimental data from pharmaceuticals biodegradation experiments at environmentally-relevant levels, taking two different pharmaceuticals as examples, i.e., atenolol and acyclovir. The results demonstrated the good prediction performance of the established biotransformation model under

different metabolic conditions, as well as the reliability of the established model in predicting different pharmaceuticals biotransformations. The linear positive correlation between ammonia oxidation rate and pharmaceutical degradation rate confirmed the major role of cometabolism induced by AOB in the pharmaceutical removal. Dissolved oxygen (DO) was also revealed to be capable of regulating the pharmaceutical biotransformation cometabolically and the substrate competition between ammonium and pharmaceuticals existed especially at high ammonium concentrations.

Keywords: Cometabolism, pharmaceutical, model, ammonia oxidizing bacteria, biotransformation product, substrate competition

1. Introduction

The ubiquitous occurrence and fate of pharmaceuticals in the environment and engineering systems have attracted the concerns of the scientists and the public for decades due to their potential ecotoxic impact on aquatic ecosystems (Benner et al., 2013; Ternes, 1998). These organic compounds were present in the wastewater at concentrations ranging from pg L^{-1} to μg L^{-1} (Evgenidou et al., 2015; Petrie et al., 2015). As the wastewater treatment plants (WWTPs) were originally designed for bulk nutrients, the incomplete removal was found for pharmaceuticals in the treatment processes, being a major pathway for pharmaceuticals to enter the environment (Carballa et al., 2004).

Autotrophic biomass (e.g., enriched nitrifying sludge) was capable of transforming the pharmaceuticals cometabolically during the wastewater treatment process and thus the pharmaceutical removal was reported to be positively correlated to nitrification rate (Batt et al., 2006; Yi and Harper Jr, 2007). Ammonia oxidizing bacteria (AOB) in the nitrifying biomass could degrade a broad range of substrates including aromatic and aliphatic compounds due to the non-specific enzyme ammonia monooxygenase (AMO) (Keener and Arp, 1993; Keener and Arp, 1994; Xu et al., 2016). The presence of the growth substrate (i.e. ammonium) was required for cometabolism which should be taken into account when predicting the fate of pharmaceuticals (Tran et al., 2013). In addition to cometabolism, pharmaceuticals could also be degraded as the energy and carbon source for microorganisms through metabolic biotransformation (Tran et al., 2013). Furthermore, the formed biotransformation products might be more toxic and persistent (Quintana et al., 2005). Hence the biotransformation products should be considered for a more comprehensive understanding of the fate of pharmaceuticals in the nitrifying activated sludge.

Mathematical modeling offers a useful tool and is adopted widely to analyze complicated metabolic pathways. Cometabolic biotransformations were previously modeled through first-order kinetics and

mixed order kinetics like Monod expression (Fernandez-Fontaina et al., 2014; Liu et al., 2015; Oldenhuis et al., 1989) and have evolved from only considering the cometabolic substrates to incorporating the relationships between cometabolic substrates and growth substrates, such as competitive interaction and toxicity inhibition (Liu et al., 2015). However, the previous literature has rarely considered the formation of biotransformation products in the cometabolic biotransformaiton models for pharmaceuticals.

In this work, a comprehensive modeling framework was developed to describe the fate of pharmaceuticals at environmentally-related levels accompanied with the formation of their biotransformation products during the treatment by the enriched nitrifying sludge. Microbial processes contributing to the pharmaceutical biotransformation were considered as follows: growth-linked cometabolism by AOB, metabolic transformation by AOB, growth-linked cometabolism by heterotrophs (HET) and metabolic transformation by HET. To this end, atenolol and acyclovir were selected as the model compounds in this study as they were frequently found in the wastewater with the highest concentrations of 25 and 1.8 μg L^{-1}, respectively (Prasse et al., 2010; Verlicchi et al., 2012). It has been reported that they can be biotransformed into atenolol acid and carboxy-acyclovir (Prasse et al., 2011; Radjenović et al., 2008). Model calibration and validation were carried out with experimental data using atenolol as parent compounds under different metabolic conditions. Model evaluation was also conducted using the experimental data from acyclovir biotransformation. The effects of dissolved oxygen (DO) and ammonium concentrations on pharmaceutical biotransformation were investigated using the validated model to provide insights into the process dynamics. The reported model in this work is expected to be used as a tool to fully understand the fate of pharmaceuticals associated with different metabolisms by responsible microorganisms in the complicated activated sludge system.

2. Materials and Methods

2.1 Model development

A multi-species and multi-substrate model was developed to describe the pharmaceutical biotransformation processes by the enriched nitrifying sludge. This biotransformation model comprehensively considered the consumption of the pharmaceuticals and the formation of transformation products accompanied with the simultaneous ammonia oxidation in the enriched nitrifying sludge. It describes the relationships among six soluble substrates as defined in Table S1 in Supporting Information (SI), i.e., ammonium (S_{NH_4}), readily biodegradable substrates (S_S), oxygen (S_{O_2}), pharmaceutical (parent compound, PC, S_{PC}), primary biotransformation product (BP, S_{BP}) and other biotransformation products (OP, S_{OP}), and four particulate species, i.e., AOB (X_{AOB}), HET

(X_{HET}), slowly biodegradable substrates (X_S) and inert biomass (X_I). Seven processes are considered: (1) metabolic transformation of PC by AOB; (2) growth of AOB coupled to cometabolic transformation of PC; (3) endogenous decay of AOB; (4) hydrolysis; (5) metabolic transformation of PC by HET; (6) growth of HET coupled to cometabolic transformation of PC; (7) endogenous decay of HET. The kinetic expressions and the stoichiometric matrix of the proposed biotransformation model are summarized in Tables S2 and S3 in SI, respectively. The definitions, values, units and sources of all parameters used in the biotransformation model are listed in Table S4 in SI.

In this model, the microbial growth-linked kinetic expressions (processes 2 and 6 in Table S2 in SI) are described using the Monod equations, which are associated with cometabolic biotransformation of pharmaceuticals (Sathyamoorthy et al., 2013). The concentration of growth substrates S_{NH_4} and S_S is also involved in the Monod equations. The basis of the cometabolic biotransformation expressions is the concept of transformation coefficient parameters such as AOB growth-linked $T^c_{PC\text{-}AOB}$ and HET growth-linked $T^c_{PC\text{-}HET}$. The pharmaceutical biotransformation reactions directly conducted via metabolism by AOB and HET are described by pseudo-first order kinetic expressions (processes 1 and 5 in Table S2 in SI). For each reaction, the rate is expressed by an explicit function of the concentrations of relevant pharmaceuticals in the process. For microbial metabolic biodegradation of PC, the key parameters are biomass normalized PC degradation rate coefficients in the absence of AOB and HET growth, i.e. $k_{PC\text{-}AOB}$ and $k_{PC\text{-}HET}$. Processes 1, 2, 5 and 6 together contribute to pharmaceutical biotransformation in the enriched nitrifying sludge.

The formation of biotransformation products is modeled using the specific stoichiometry coefficients in processes 1, 2, 5 and 6. The coefficients α^m_{BP} and α^c_{BP} indicate the transformation of PC to BP under metabolism and cometabolism conditions by AOB, respectively. Similarly, the coefficients β^m_{BP} and β^c_{BP} present the transformation of PC to BP under metabolism and cometabolism conditions by HET, respectively.

2.2 Atenolol and acyclovir biotransformation experiments

Experimental data from our previous biodegradation experiments of atenolol (Case *I*) and acyclovir (Case *II*) under different conditions by an enriched nitrifying sludge were used for model evaluation in this work (Xu et al., 2017a; Xu et al., 2017b). The chemicals used in the batch experiments and the enrichment of nitrifying culture in the sequencing batch reactor (SBR) are described in Text S1 and S2 in SI. Details of the experimental conditions applied in different scenarios are provided in Table S5 in SI. Briefly, 4-L beaker was used as the batch reactor with enriched nitrifying culture inoculated to degrade parent compounds at an initial 15 μg L^{-1}. The mixed liquid suspended solid (MLVSS)

concentration was kept at approximately 1 g L^{-1}. All the batch experiments were conducted in duplicates. The designs for Experiments 1-3 were same for atenolol (Case *I*) and acyclovir (Case *II*). In Experiment 1, 30 mg L^{-1} allylthiourea (ATU) was added to inhibit nitrifying activities (Ali et al., 2013; Ginestet et al., 1998; Sathyamoorthy et al., 2013), leading to the dominant contribution from HET to pharmaceutical biotransformation (Tran et al., 2013). Initial ammonium concentration was provided at 50 mg-N L^{-1}. No external ammonium was supplied during the entire experimental period (240 h). In Experiment 2, no initial and external ammonium was provided during 240 h. In Experiment 3, constant ammonium concentration was maintained at 50 mg-N L^{-1} by dosing a mixture of ammonium bicarbonate and potassium bicarbonate as ammonium feeding solution and pH buffer at the same time, which could ensure the cometabolic biotransformation by AOB. The Experiment 4 was exclusively designed for atenolol biotransformation, where constant ammonium concentrations of 25 mg-N L^{-1} were provided using the dosing method in Experiment 3 during the experimental period. Samples were collected periodically to analyse mixed liquid suspended solid (MLSS) concentration and its volatile fraction (i.e., MLVSS), NH_4^+, NO_2^-, NO_3^-, atenolol, acyclovir and their biotransformation products atenolol acid and carboxy-acyclovir. The detailed chemical analysis procedures could be found in the previous work (Xu et al., 2017a; Xu et al., 2017b; Xu et al., 2017c).

The contribution of sorption to removal of atenolol and acyclovir was insignificant based on our previous studies (Xu et al., 2017a; Xu et al., 2017c). This is in consistency with low sorption coefficient K_D (0.04) and low octanol-water partition coefficient Log K_{OW} (0.16) of atenolol and Log K_{OW} (-1.59) of acyclovir (Kasim et al., 2004; Maurer et al., 2007; Mohsen-Nia et al., 2012). Volatilization was considered negligible given the low values of Henry's law constants for atenolol (1.37×10^{-18} atm m^3 mol^{-1}) and acyclovir (3.2×10^{-22} atm m^3 mol^{-1}) (Küster et al., 2010). Photodegradation was also insignificant considering the turbidity of the sludge and the aluminum foil covering the reactor. Therefore, microbially induced biodegradation should be the main mechanism for pharmaceutical removal in both atenolol and acyclovir biotransformation experiments.

2.3 Model calibration and validation

The biotransformation model used in this work consists of 7 biochemical processes and 22 stoichiometric and kinetic parameters (as shown in Tables S2 and S4 in SI). Most of these parameters were well established in previous literature, therefore the reported values were directly used in this developed model. However, the information on biomass growth-linked PC transformation coefficients $T^c_{PC\text{-}AOB}$ and $T^c_{PC\text{-}HET}$ and microbial endogenous transformation coefficients $k_{PC\text{-}AOB}$ and $k_{PC\text{-}HET}$ was limited (Sathyamoorthy et al., 2013). Considering the key role of cometabolism induced by AOB growth in biotransformation, the maximum specific growth rate of AOB $\mu_{max,AOB}$ was of

significance to the developed model. Furthermore, the sensitivity analysis suggested the four key parameters $k_{PC\text{-}AOB}$, $k_{PC\text{-}HET}$, $T^c_{PC\text{-}AOB}$ and $\mu_{max,AOB}$ are highly sensitive to the biotransformation processes in terms of the experimental measurements (examples shown in Figure S1 in SI). Model calibration was therefore conducted to estimate the values of $k_{PC\text{-}AOB}$, $k_{PC\text{-}HET}$, $T^c_{PC\text{-}AOB}$ and $\mu_{max,AOB}$ based on experimental measurements through minimizing the sum of squares of the deviations between the measured and modeled values for the concentrations of parent compounds and biotransformation products under different conditions. In addition, the four stoichiometric coefficients, i.e., α^m_{BP}, α^c_{BP}, β^m_{BP} and β^c_{BP}, for the transformation of PC to BP under metabolism and cometabolism conditions could be determined based on the concentrations of BP and PC measured in the experiments.

Experimental data from atenolol biotransformation (Case *I*) of Experiments 1-3 were firstly used for model calibration. Concentrations of atenolol and atenolol acid from Experiment 1 and Experiment 2 were fitted by model simulations to estimate $k_{PC\text{-}HET}$ and $k_{PC\text{-}AOB}$, respectively, whereas concentrations of atenolol and atenolol acid from Experiment 3 were fitted to estimate $\mu_{max,AOB}$ and $T^c_{PC\text{-}AOB}$, using the $k_{PC\text{-}HET}$ and $k_{PC\text{-}AOB}$ values obtained in previous experiments (Experiment 1 and Experiment 2). Model validation was then carried out with the calibrated parameters using the independent experimental data sets from atenolol biotransformation of Experiment 4 (Xu et al., 2017b): Batch experiments with atenolol as the parent compound were conducted at an initial concentration of 15 μg L^{-1} in the constant presence of ammonium of 25 mg-N L^{-1}. The ammonium concentration applied was different from of Experiment 3 at 50 mg-N L^{-1} (Table S5 in SI). To further verify the validity and applicability of the model, the model was also applied to evaluating the acyclovir biotransformation data from Case *II* of Experiments 1-3. The key model parameters were recalibrated for Case *II* using the three sets of batch experimental data (Table S5 in SI).

3. Results

3.1 Model calibration with experimental data from atenolol biotransformation

The model was first calibrated to illustrate the biotransformation of atenolol catalysed solely by HET in Experiment 1 (i.e. with addition of ATU to inhibit the nitrifying activity). Given that no exogenous organic carbon was supplied during culture enrichment and the only organic carbon in the batch experiments was pharmaceuticals, the growth of HET was considered extremely low and the cometabolism related coefficient $T^c_{PC\text{-}HET}$ was set as zero (Sathyamoorthy et al., 2013). With AOB related parameters $k_{PC\text{-}AOB}$ and $T^c_{PC\text{-}AOB}$ set to zero, only the parameter $k_{PC\text{-}HET}$ was estimated with its best-fit value shown in Table 1 for Experiment 1. The predicted atenolol and atenolol acid

concentration profiles with the established model were demonstrated in Figure 1A, along with the measured experimental values. Atenolol experienced continuous decreasing by 94.3% from the beginning to the end of experiments accompanied with a gradual increase of atenolol acid until 168 h and a stable stage until 240 h at a conversion efficiency of 62.6% (Figure 1A), which was well captured by the model predictions.

The experimental data obtained from Experiment 2 (i.e., in the absence of ammonium) were used to further calibrate the developed model in terms of atenolol and atenolol acid dynamics. Without the presence of the growth substrate, AOB growth-linked cometabolism would be considered to have negligible contribution to atenolol biotransformation. Therefore, only the metabolic biotransformation by AOB and HET were involved in the biotransformation of atenolol for Experiment 2. The parameter value of $k_{PC\text{-}HET}$ obtained in Experiment 1 was used directly without any modification. Another key model parameter $k_{PC\text{-}AOB}$ related to AOB metabolism was thus reliably estimated during atenolol biotransformation (value as shown in Table 1). As shown in Figure 1B, although atenolol demonstrated a sharp decrease by 97.4% over the whole experimental period, the production of atenolol acid indicated a lower transformation efficiency in the absence of ammonium (29.1%) compared with the experiments with addition of ATU (see Figure 1A), again well matching the model predictions.

In Experiment 3, the presence of ammonium was provided constantly to ensure the cometabolic biodegradation of atenolol by AOB. Together with the rest of the parameters involved, the parameter values of $k_{PC\text{-}HET}$ and $k_{PC\text{-}AOB}$ estimated in the previous two experiments were applied in the biotransformation model. The key parameters related to AOB induced cometabolism, i.e., $T^{c}_{PC\text{-}AOB}$ and $\mu_{max,AOB}$, were then estimated with the optimum values listed in Table 1. As shown in Figure 1C, concomitant with the gradual decrease of atenolol at a removal efficiency of 88.0%, atenolol acid was formed at an increasing trend with 86.9% conversion efficiency. This was obviously higher than the experiments in the absence of ammonium and with the addition of ATU, indicating a positive role of AOB induced cometbaolism in atenolol transformation. The model described these observations reasonably well.

Overall, the developed model could satisfactorily capture all dynamics associated with atenolol and atenolol acid in all batch biodegradation experiments under different metabolic conditions. The good agreement between model simulations and measured data in Figure 1 supports the capability of the developed model in describing the microbial growth related biotransformation of atenolol in the enriched nitrifying culture. The obtained parameter linked to AOB growth during ammonia oxidation,

i.e., AOB-induced cometabolic atenolol transformation coefficient $T^c_{PC\text{-}AOB}$, was estimated at 0.026 ± 0.000036 m^3 g COD^{-1}. It was lower than the reported value of 0.0715 ± 0.0227 m^3 g COD^{-1} for atenolol biodegradation by an enriched nitrifying sludge (Sathyamoorthy et al., 2013). The non-growth metabolism by HET and the non-growth metabolism by AOB on atenolol biodegradation also described the experimental data with the addition of ATU and in the absence of ammonium well. The estimated parameters of $k_{PC\text{-}HET}$ and $k_{PC\text{-}AOB}$ were 0.000180 ± 0.000017 and 0.000140 ± 0.000012 m^3 g COD^{-1} h^{-1}, which were lower than but in the same order of magnitude as the literature reported values (0.00093 ± 0.00018 and 0.00067 ± 0.00023 m^3 g COD^{-1} h^{-1}, respectively) (Sathyamoorthy et al., 2013).The discrepancy in these parameters values could be probably ascribed to the difference in the community structure in the adopted nitrifying cultures or different operating conditions. The model could be potentially applied to a widespread extent despite that the parameter values would vary according to the experimental conditions. As suggested, it was difficult to compare these coefficients ($k_{PC\text{-}HET}$, $k_{PC\text{-}AOB}$ and $T^c_{PC\text{-}AOB}$) with other pharmaceuticals as most existing models did not consider the specific biochemical processes (Sathyamoorthy et al., 2013). However, the observed high value of T^c_{PC-AOB} compared to other two parameters $k_{PC\text{-}HET}$ and $k_{PC\text{-}AOB}$ supported the previous finding of the major role of cometabolism in atenolol biodegradation (Xu et al., 2017c).

3.2 Model validation with atenolol biotransformation under different conditions

In order to further confirm the validity and reliability of the developed model, model validation was carried out to compare the model simulations to the independent experimental data, which were not used for model calibration. Based on the measured concentrations of atenolol and atenolol acid, the stoichiometric coefficients α^c_{BP} and α^m_{BP} were calculated as 0.58 and 0.58, respectively. Applied with previously calibrated parameters in Table 1, the proposed biotransformation model was used to predict dynamics of atenolol and atenolol acid in the presence of ammonium at a constant concentration of 25 mg-N L^{-1} (significantly different from the 50 mg-N L^{-1} used for model calibration). The modeled and measured concentrations of atenolol and atenolol acid were plotted in Figure 2. Atenolol continuously dropped from initial 15 μg L^{-1} with a final degradation efficiency of 92.9%. The conversion rate of atenolol acid transformed from atenolol was calculated as 57.9%. The model predictions could capture these trends of atenolol degradation and atenolol acid formation very well, which again supports the validity of the developed model.

3.3 Model evaluation with experimental data from acyclovir biotransformation

The experimental results obtained with Case *II* for biotransformation of acyclovir were used to further evaluate the developed model. The developed biotransformation model was recalibrated for acyclovir biodegradation and carboxy-acyclovir formation dynamics under different conditions. Most of the

literature reported model parameters were employed at same values as the case of atenolol except the stoichiometry coefficients (α^{m}_{BP}, α^{c}_{BP}, β^{m}_{BP} and β^{c}_{BP}) for formation of carboxy-acyclovir associated with specific biochemical processes (as shown in Table S4 in SI), which were calculated based on the experimental data. The values for the three key parameters $k_{PC\text{-}HET}$, $k_{PC\text{-}AOB}$ and $T^{c}_{PC\text{-}AOB}$ were recalibrated, which were associated with the investigated parent compound. As the enriched nitrifying biomass utilized in the batch biodegradation experiments of acyclovir were same as those in case of atenolol, the maximum growth rate of AOB $\mu_{max,AOB}$ was set to be the same as in case of atenolol during model calibration for acyclovir biotransformation in the presence of ammonium. The obtained parameter values for acyclovir biotransformation were 0.00035 ± 0.00002 m^3 g COD^{-1} h^{-1} ($k_{PC\text{-}HET}$), 0.00005 ± 0.00003 m^3 g COD^{-1} h^{-1} ($k_{PC\text{-}AOB}$) and 0.00093 ± 0.00049 m^3 g COD^{-1} ($T^{c}_{PC\text{-}AOB}$).

The model predictions of acyclovir biotransformation matched the experimental results well under different conditions (Figure 3), further demonstrating the validity of the established model. Parameters values giving the optimum fits with the experimental data were difficult to compare reliably with literature values as this study firstly reported the AOB cometabolic acyclovir transform coefficient $T^{c}_{PC\text{-}AOB}$. However, compared to other reported compounds, e.g. atenolol (Sathyamoorthy et al., 2013), it was obvious that parameters $k_{PC\text{-}AOB}$ and $T^{c}_{PC\text{-}AOB}$ for acyclovir were lower than those values for atenolol (Table 1), indicating a stronger degradation ability of the AOB culture studied on atenolol than acyclovir. Considering the molecular differences between these two pharmaceuticals, this may imply an affinity property of AOB for different compounds probably due to a preferential substrate selection to AMO active sites (Fernandez-Fontaina et al., 2012). The parameter $k_{PC\text{-}HET}$ for acyclovir was 0.00035 ± 0.00002 m^3 g COD^{-1} h^{-1}, which was in the same order of magnitude of the value estimated in this study (0.000180 ± 0.000013 m^3 g COD^{-1} h^{-1}) for atenolol. The conversion efficiencies from acyclovir to carboxy-acyclovir were 83.9%, 43.0% and 29.9% in Experiments 1, 2 and 3, respectively (see Figure 3). These results indicated the importance of metabolism of acyclovir by HET. Oxidation of acyclovir to carboxy-acyclovir might be dominated by unspecific monoxygenase from HET (Men et al., 2016), which needs to be confirmed in the further work.

4. Discussion

In this work, a comprehensive mathematical model is developed to describe the biotransformation of pharmaceuticals and the formation of their products by the enriched nitrifying culture. In the proposed model, processes 1 and 2 (Table S2 in SI) depict the AOB-induced cometabolic and metabolic biotransformation of pharmaceuticals, while processes 5 and 6 (Table S2 in SI) describe the HET-induced cometabolic and metabolic biotransformation of pharmaceuticals, respectively. Sensitivity

analysis indicated that four key parameters $k_{PC\text{-}HET}$, $k_{PC\text{-}AOB}$, $T^{c}_{PC\text{-}AOB}$ and $\mu_{max,AOB}$ were critical to the model output and therefore estimated through model calibration. The validity of this biotransformation model is confirmed by independent atenolol biodegradation data and further evaluation by acyclovir biotransformation experiments. This microbial processes linked biotransformation model could enhance our ability to predict the fate of pharmaceuticals and their transformation products during wastewater treatment processes. Nevertheless, more model verification should be conducted in the future using other pharmaceuticals biotransformation data for this developed model to facilitate its application as a useful tool in prediction of pharmaceutical fate in different systems.

The modeling results in this work suggested the cometabolism induced by AOB could play an important role in the pharmaceutical removal in the studied ratio ranges of pharmaceuticals to ammonia for cometabolism. Indeed a positive linear relationship was observed between ammonia oxidation rate and pharmaceutical degradation rates in terms of atenolol and acyclovir based on the validated model (Figure 4A). The atenolol degradation rate increased from 0.012 to 0.16 μg g VSS^{-1} h^{-1} while the nitrification rate increased from 2.84 to 59.15 mg NH_4^+-N g VSS^{-1} h^{-1}. With respect to acyclovir, the degradation rate changed from 0.014 to 0.10 μg g VSS^{-1} h^{-1} whereas the ammonia oxidation rate showed an increase from 2.37 to 36.63 mg NH_4^+-N g VSS^{-1} h^{-1}. Such a positive correlation was also reported in previous literature under certain conditions (Xu et al., 2017a; Xu et al., 2017c; Yi and Harper Jr, 2007), supporting the notion that majority of atenolol and acyclovir could be cometabolically degraded in the enriched nitrifying cultures. A further assessment on the wide application of the relationship was carried out by simulating the concentration profiles of pharmaceuticals after 240 h. The molar ratio of atenolol to ammonia calculated based on their concentrations from 8.42×10^{-7} to 1.91×10^{-5} was observed to be a valid range for cometabolic biodegradation of atenolol by the enriched nitrifying culture used in this work, and the relationship maintained at a same slope (Black solid squares in Figure 4A demonstrated the predicted atenolol degradation rate after 240 h). However, a different slope was found for the relationship between ammonia oxidation rate and the acyclovir degradation rate after 240 h predicted using the developed model (Figure 4B). If the ammonia oxidation rate was higher than the critical value (2.3 mg NH_4^+-N g VSS^{-1} h^{-1} in this study), the lower slope might indicate a slower increasing trend in acyclovir degradation rate with an increasing ammonia oxidation rate (Figure 4A). Compared with the situation at the lower ammonia oxidation rate, a higher increasing trend in acyclovir degradation rate would arise at higher slope (Figure 4B). The observation that pharmaceutical would not be degraded until the ammonia was depleted (Dawas-Massalha et al., 2014) revealed a higher pharmaceutical degradation rate at lower ammonia oxidation rate, which supported the findings in this study.

Regardless of the different slopes for the relationship, the molar ratios of acyclovir to ammonia ranging from 1.62×10^{-11} to 2.26×10^{-5} was obtained to be a valid application range for the cometabolic biodegradation of acyclovir by the enriched nitrifying culture used in this work.

The proposed model framework was expected to be a useful tool to predict the biotransformation of pharmaceuticals and the formation of transformation products under varying conditions, therefore providing the guidance in designing, upgrading and optimizing of the biological reactor. The influence of DO on pharmaceutical biotransformation was investigated by performing model simulations in the enriched nitrifying systems. The pharmaceutical removal efficiencies at 240 h at different DO concentrations ranging from 0 to 4 mg L^{-1} with ammonium concentration of 50 mg-N L^{-1} are shown in Figure 5. Overall DO concentration had a positive effect on pharmaceutical removal efficiencies. The concentrations of atenolol and acyclovir decreased rapidly with a prompt increase of atenolol acid and carboxy-acyclovir as DO increased to 1 mg L^{-1}. With DO further increased to 4 mg L^{-1}, a gradual decrease of pharmaceutical concentrations was observed accompanied with a slight increase of their biotransformation products. The degradation efficiencies for atenolol at DO concentrations of 0, 1 and 4 mg L^{-1} were 44.3%, 83.2% and 94.0%, respectively. With regard to acyclovir, its degradation efficiencies were observed to be 36.2%, 81.2% and 87.3%, respectively at DO of 0, 1 and 4 mg L^{-1}. The simulation results revealed that the DO concentration would play an important role in pharmaceutical biotransformation. This was contrary to the previous report that DO in the WWTP had no influence on oxidative biotransformation of selected micropollutants (Helbling et al., 2012). The possible reason could be that the experiments conducted in this study were nitrifying culture based instead of the regular activated sludge in WWTP, suggesting that DO might regulate the pharmaceutical biotransformation cometabolically.

The growth substrate might also have an impact on the pharmaceutical biotransformation. Different ammonium concentrations ranging from 0 to 100 mg L^{-1} were applied in the model simulations at different DO concentrations as shown in Figure 6. It was obvious that the degradation efficiencies of studied pharmaceuticals and the formation rates of their transformation products would increase dramatically when ammonium concentrations increase from 0 to 20 mg-N L^{-1}, especially in case of atenolol suggesting the importance of cometabolism on its biotransformation. However, there was no significant enhancement with the increase of ammonium concentrations from 20 to 250 mg-N L^{-1} (data of 100-250 mg-N L^{-1} were not shown). This was contrary to the previous report where the removal efficiencies of the selected pharmaceuticals were enhanced at higher initial ammonium concentrations (Tran et al., 2009). This could be probably due to the substrate competition between growth substrate (ammonium) and cometabolic substrates (e.g. atenolol or acyclovir). Pharmaceutical

levels applied in this study were several orders of magnitude lower than the investigated ammonium concentrations, leading to a competition for AMO active sites and therefore potential decreasing degradation rates at higher ammonium concentrations (Dawas-Massalha et al., 2014; Fernandez-Fontaina et al., 2012).

In summary, a comprehensive model that considers all microbial processes contributing to pharmaceutical biotransformation as well as the formation of biotransformation products by the enriched nitrifying culture is developed in this work. The proposed model was successfully calibrated and validated using the biotransformation experiments of atenolol and acyclovir under different metabolic conditions. The linear positive correlation between ammonia oxidation rate and pharmaceutical degradation rate confirmed the major role of cometabolism induced by AOB in the pharmaceutical removal. DO was revealed to be capable of regulating the pharmaceutical biotransformation cometabolically and the substrate competition between ammonium and pharmaceuticals existed at high ammonium concentrations. More verification should be conducted using other pharmaceuticals biotransformation data for this developed model to facilitate its application as a useful tool in prediction of pharmaceutical fate.

Acknowledgement

This study was supported by the Australian Research Council (ARC) through Future Fellowship FT160100195. Dr. Bing-Jie Ni acknowledges the support of ARC Discovery Project DP130103147.

Reference

Ali, T.U., Kim, M. Kim, D.J., 2013. Selective inhibition of ammonia oxidation and nitrite oxidation linked to n2o emission with activated sludge and enriched nitrifiers. J. Microbio. Biotechnol. 23 (5), 719-723.

Batt, A.L., Kim, S. Aga, D.S., 2006. Enhanced biodegradation of iopromide and trimethoprim in nitrifying activated sludge. Environ. Sci. Technol. 40 (23), 7367-7373.

Benner, J., Helbling, D.E., Kohler, H.P.E., Wittebol, J., Kaiser, E., Prasse, C., Ternes, T.A., Albers, C.N., Aamand, J., Horemans, B., Springael, D., Walravens, E. Boon, N., 2013. Is biological treatment a viable alternative for micropollutant removal in drinking water treatment processes? Water Res. 47 (16), 5955-5976.

Carballa, M., Omil, F., Lema, J.M., Llompart, M.a., García-Jares, C., Rodríguez, I., Gómez, M. Ternes, T., 2004. Behavior of pharmaceuticals, cosmetics and hormones in a sewage treatment plant. Water Res. 38 (12), 2918-2926.

Dawas-Massalha, A., Gur-Reznik, S., Lerman, S., Sabbah, I. Dosoretz, C.G., 2014. Co-metabolic oxidation of pharmaceutical compounds by a nitrifying bacterial enrichment. Bioresou. Technol. 167, 336-342.

Evgenidou, E.N., Konstantinou, I.K. Lambropoulou, D.A., 2015. Occurrence and removal of transformation products of PPCPs and illicit drugs in wastewaters: A review. Sci. Total Environ. 505, 905-926.

Fernandez-Fontaina, E., Omil, F., Lema, J.M. Carballa, M., 2012. Influence of nitrifying conditions on the biodegradation and sorption of emerging micropollutants. Water Res. 46 (16), 5434-5444.

Fernandez-Fontaina, E., Carballa, M., Omil, F. Lema, J.M., 2014. Modelling cometabolic biotransformation of organic micropollutants in nitrifying reactors. Water Res. 65, 371-383.

Ginestet, P., Audic, J.M., Urbain, V. Block, J.C., 1998. Estimation of nitrifying bacterial activities by measuring oxygen uptake in the presence of the metabolic inhibitors allylthiourea and azide. Appl. Environ. Microbiol. 64 (6), 2266-2268.

Helbling, D.E., Johnson, D.R., Honti, M. Fenner, K., 2012. Micropollutant biotransformation kinetics associate with WWTP process parameters and microbial community characteristics. Environ. Sci. Technol. 46 (19), 10579-10588.

Kasim, N.A., Whitehouse, M., Ramachandran, C., Bermejo, M., Lennernäs, H., Hussain, A.S., Junginger, H.E., Stavchansky, S.A., Midha, K.K., Shah, V.P. Amidon, G.L., 2004. Molecular properties of WHO essential drugs and provisional biopharmaceutical classification. Mol Pharm 1 (1), 85-96.

Keener, W.K. Arp, D.J., 1993. Kinetic studies of ammonia monooxygenase inhibition in Nitrosomonas europaea by hydrocarbons and halogenated hydrocarbons in an optimized whole-cell assay. Appl. Environ. Microbiol. 59(8), 2501-2510.

Keener, W.K. Arp, D.J., 1994. Transformations of aromatic compounds by Nitrosomonas europaea. Appl. Environ. Microbiol. 60(6), 1914-1920.

Küster, A., Alder, A.C., Escher, B.I., Duis, K., Fenner, K., Garric, J., Hutchinson, T.H., Lapen, D.R., Péry, A., Römbke, J., Snape, J., Ternes, T., Topp, E., Wehrhan, A. Knackerk, T., 2010. Environmental risk assessment of human pharmaceuticals in the European union: A case study with the β-blocker atenolol. Integr. Environ. Assess. Manage. 6 (SUPPL. 1), 514-523.

Liu, L., Binning, P.J. Smets, B.F., 2015. Evaluating alternate biokinetic models for trace pollutant cometabolism. Environ. Sci. Technol. 49 (4), 2230-2236.

Maurer, M., Escher, B.I., Richle, P., Schaffner, C. Alder, A.C., 2007. Elimination of β-blockers in sewage treatment plants. Water Res. 41(7), 1614-1622.

Men, Y., Han, P., Helbling, D.E., Jehmlich, N., Herbold, C., Gulde, R., Onnis-Hayden, A., Gu, A.Z., Johnson, D.R., Wagner, M. Fenner, K., 2016. Biotransformation of Two Pharmaceuticals by the

Ammonia-Oxidizing Archaeon Nitrososphaera gargensis. Environ. Sci. Technol. 50 (9), 4682-4692.

Mohsen-Nia, M., Ebrahimabadi, A.H. Niknahad, B., 2012. Partition coefficient n-octanol/water of propranolol and atenolol at different temperatures: Experimental and theoretical studies. J. Chem. Thermodyn. 54, 393-397.

Oldenhuis, R., Vink, R.L.J.M., Janssen, D.B. Witholt, B., 1989. Degradation of chlorinated aliphatic hydrocarbons by Methylosinus trichosporium OB3b expressing soluble methane monooxygenase. Appl. Environ. Microbiol. 55 (11), 2819-2826.

Petrie, B., Barden, R. Kasprzyk-Hordern, B., 2015. A review on emerging contaminants in wastewaters and the environment: Current knowledge, understudied areas and recommendations for future monitoring. Water Res. 72, 3-27.

Prasse, C., Schlüsener, M.P., Schulz, R. Ternes, T.A., 2010. Antiviral drugs in wastewater and surface waters: a new pharmaceutical class of environmental relevance? Environ. Sci. Technol. 44 (5), 1728-1735.

Prasse, C., Wagner, M., Schulz, R. Ternes, T.A., 2011. Biotransformation of the antiviral drugs acyclovir and penciclovir in activated sludge treatment. Environ. Sci. Technol. 45 (7), 2761-2769.

Quintana, J.B., Weiss, S. Reemtsma, T., 2005. Pathways and metabolites of microbial degradation of selected acidic pharmaceutical and their occurrence in municipal wastewater treated by a membrane bioreactor. Water Res. 39 (12), 2654-2664.

Radjenović, J., Pérez, S., Petrović, M. Barceló, D., 2008. Identification and structural characterization of biodegradation products of atenolol and glibenclamide by liquid chromatography coupled to hybrid quadrupole time-of-flight and quadrupole ion trap mass spectrometry. J. Chromatogr. A 1210 (2), 142-153.

Sathyamoorthy, S., Chandran, K. Ramsburg, C.A., 2013. Biodegradation and cometabolic modeling of selected beta blockers during ammonia oxidation. Environ. Sci. Technol. 47(22), 12835-12843.

Ternes, T.A., 1998. Occurrence of drugs in German sewage treatment plants and rivers. Water Res. 32 (11), 3245-3260.

Tran, N.H., Urase, T. Kusakabe, O., 2009. The characteristics of enriched nitrifier culture in the degradation of selected pharmaceutically active compounds. J. Hazard. Mater. 171 (1–3), 1051-1057.

Tran, N.H., Urase, T., Ngo, H.H., Hu, J. Ong, S.L., 2013. Insight into metabolic and cometabolic activities of autotrophic and heterotrophic microorganisms in the biodegradation of emerging trace organic contaminants. Bioresour. Technol. 146, 721-731.

Verlicchi, P., Al Aukidy, M. Zambello, E., 2012. Occurrence of pharmaceutical compounds in urban wastewater: Removal, mass load and environmental risk after a secondary treatment—A review. Sci. Total Environ. 429, 123-155.

Xu, Y., Yuan, Z. Ni, B.-J., 2016. Biotransformation of pharmaceuticals by ammonia oxidizing bacteria in wastewater treatment processes. Sci. Total Environ. 566–567, 796-805.

Xu, Y., Yuan, Z. Ni, B.-J., 2017a. Biotransformation of acyclovir by an enriched nitrifying culture. Chemosphere 170, 25-32.

Xu, Y., Yuan, Z. Ni, B.-J., 2017b. Impact of ammonium availability on atenolol biotransformation during nitrification. ACS Sustainable Chem. Eng. 5 (8): 7137-7144.

Xu, Y., Radjenovic, J., Yuan, Z. Ni, B.J., 2017c. Biodegradation of atenolol by an enriched nitrifying sludge: Products and pathways. Chem. Eng. J. 312, 351-359.

Yi, T. Harper Jr, W.F., 2007. The link between nitrification and biotransformation of 17α-ethinylestradiol. Environ. Sci. Technol. 41(12), 4311-4316.

Table and Figure Legends

Table 1. Estimated parameter values for the biotransformation model in this study

Figure 1. Model calibration with experimental data from atenolol biodegradation: (A) Experiment 1, with addition of allylthiourea (ATU); (B) Experiment 2, in the absence of ammonium; and (C) Experiment 3, in the presence of ammonium (50 mg NH_4^+-N L^{-1}).

Figure 2. Model validation results of atenolol biotransformation by the enriched nitrifying culture in the presence of ammonium of 25 mg-N L^{-1} (Experiment 4).

Figure 3. Model evaluation with experimental data from acyclovir biodegradation: (A) Experiment 1, with addition of allylthiourea (ATU), (B) Experiment 2, in the absence of ammonium and (C) Experiment 3, in the presence of ammonium (50 mg NH_4^+-N L^{-1}).

Figure 4. (A) The relationship between ammonia oxidizing rate and the pharmaceutical degradation rates in terms of atenolol and acyclovir (black solid squares indicate the atenolol degradation rates after 240 h); and (B) The relationship between ammonia oxidizing rate and the acyclovir degradation rate after 240 h at a different linear fit slope.

Figure 5. Predicted final concentrations of (A) atenolol and atenolol acid and (B) acyclovir and carboxy-acyclovir at time of 240 h at different concentrations of dissolved oxygen (DO) in the enriched nitrifying culture system.

Figure 6. Predicted concentrations of pharmaceuticals and their transformation products at time of 240 h at initial concentrations of 15 μg L^{-1} with different ammonium concentrations ranging from 0 to 100 mg-N L^{-1} at different DO levels.

Table 1. Estimated parameter values for the biotransformation model in this study

Parameters	Definition	Unit	Estimated	
			atenolol	acyclovir
$k_{PC\text{-}HET}$	Heterotrophs (HET) transformation coefficient	m^3 g COD^{-1} h^{-1}	0.000180 ± 0.000017	0.00035 ± 0.00002
$k_{PC\text{-}AOB}$	Ammonia oxidizing bacteria (AOB) transformation coefficient	m^3 g COD^{-1} h^{-1}	0.000140 ± 0.000012	0.00005 ± 0.00003
$T^{c}_{PC\text{-}AOB}$	Parent compound biotransformation coefficient rate linked to AOB growth (cometabolism)	m^3 g COD^{-1}	0.012 ± 0.000036	0.00093 ± 0.00049
$\mu_{max,AOB}$	Maximum specific growth rate of AOB	h^{-1}	0.012 ± 0.0023	

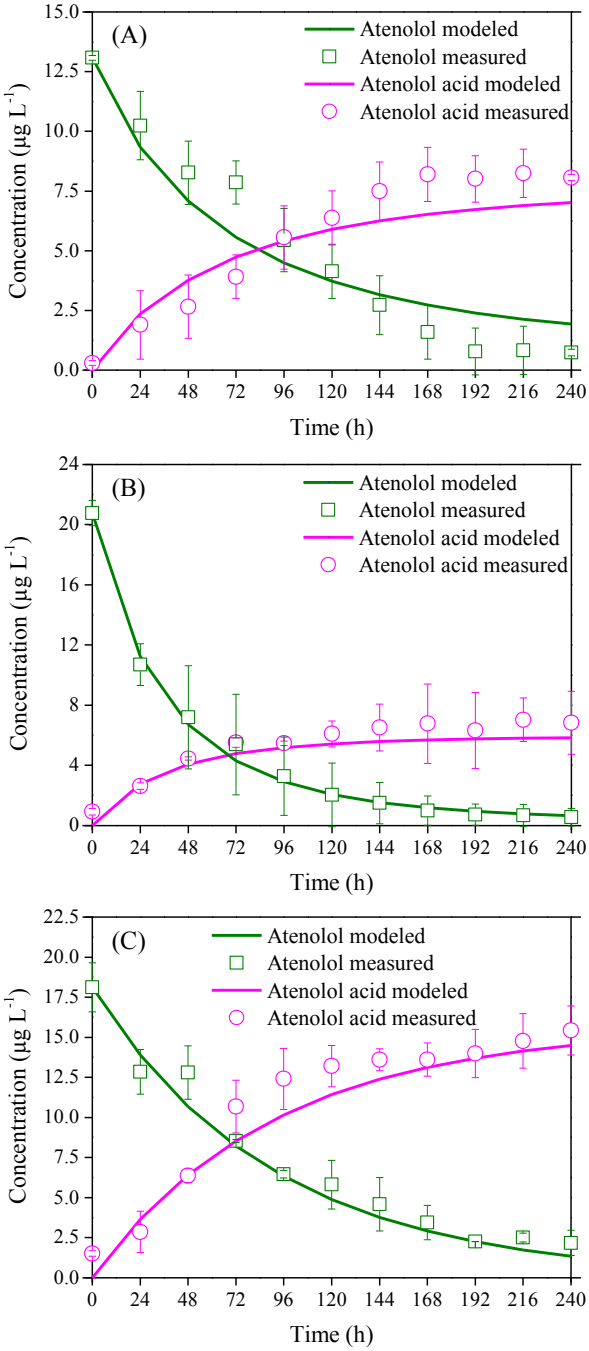

Figure 1. Model calibration with experimental data from atenolol biodegradation: (A) Experiment 1, with addition of allylthiourea (ATU); (B) Experiment 2, in the absence of ammonium; and (C) Experiment 3, in the presence of ammonium (50 mg NH_4^+-N L^{-1}).

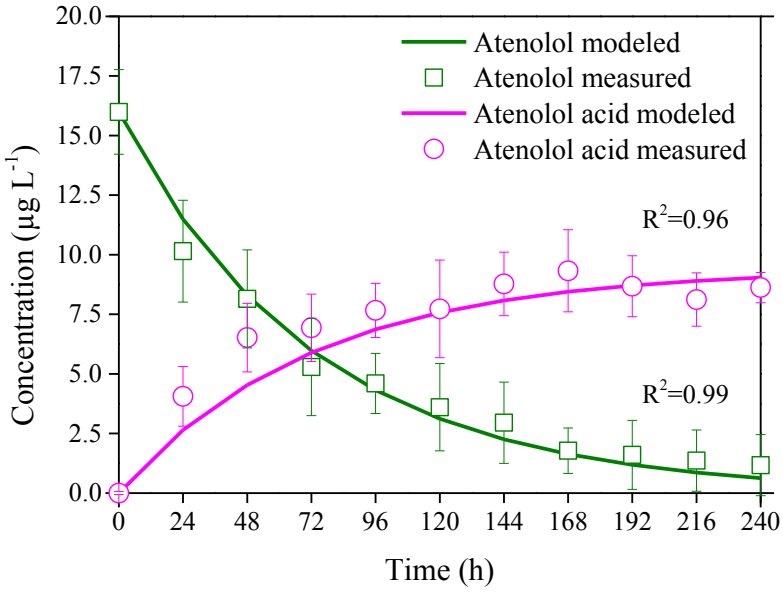

Figure 2. Model validation results of atenolol biotransformation by the enriched nitrifying culture in the presence of ammonium of 25 mg-N L^{-1} (Experiment 4).

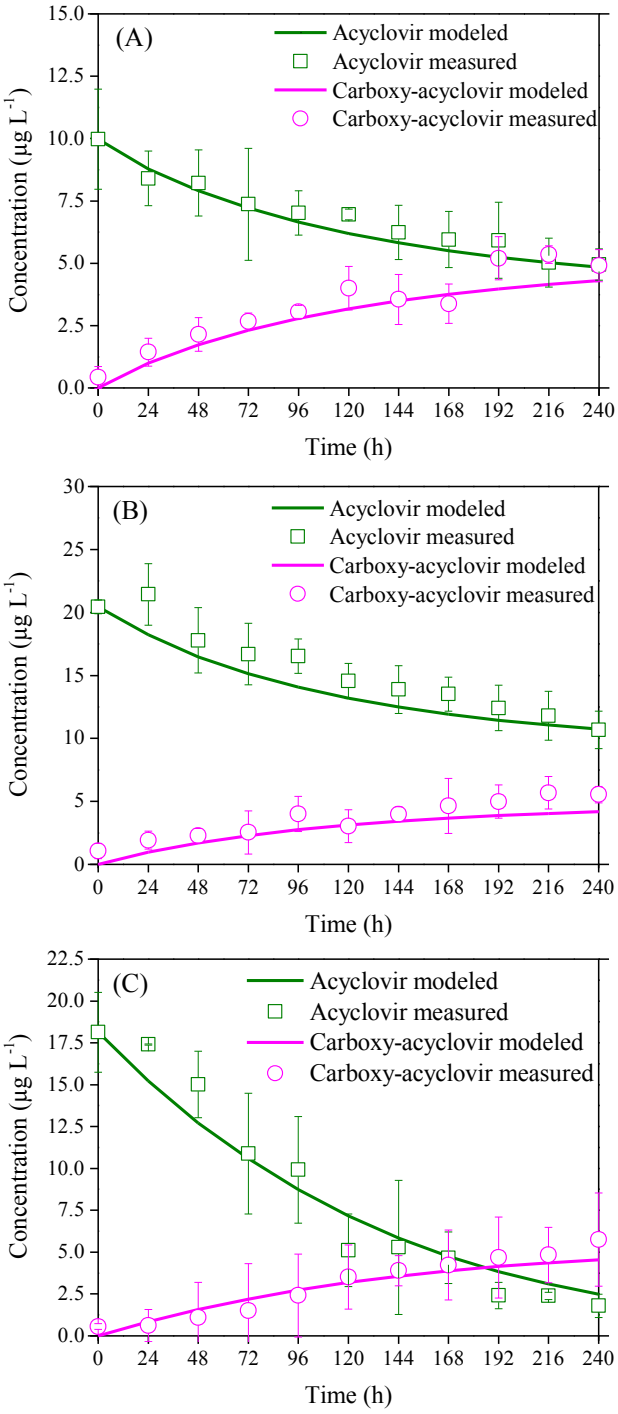

Figure 3. Model evaluation with experimental data from acyclovir biodegradation: (A) Experiment 1, with addition of allylthiourea (ATU), (B) Experiment 2, in the absence of ammonium and (C) Experiment 3, in the presence of ammonium (50 mg NH_4^+-N L^{-1}).

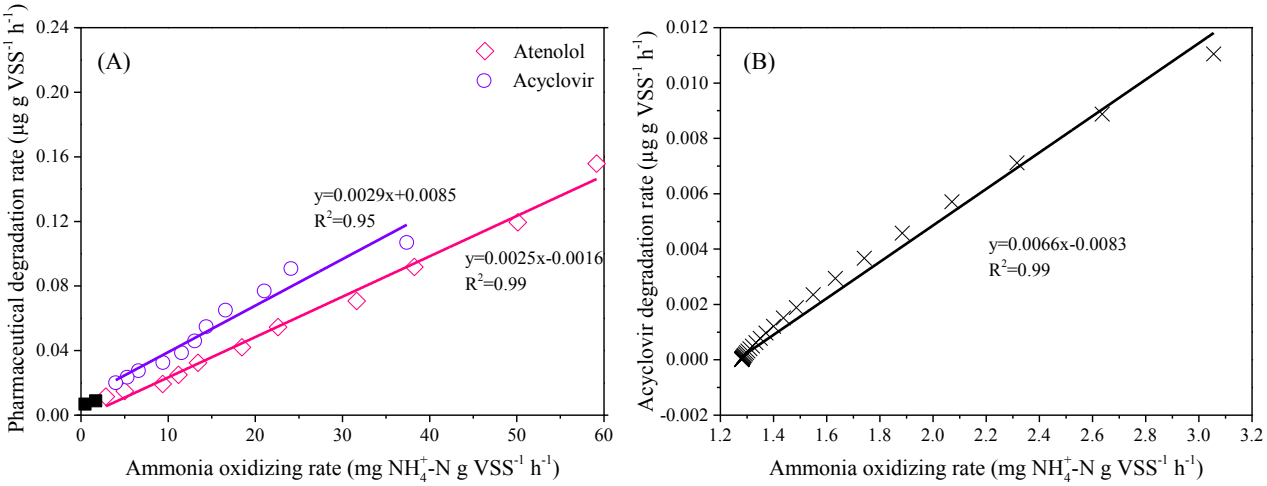

Figure 4. (A) The relationship between ammonia oxidizing rate and the pharmaceutical degradation rates in terms of atenolol and acyclovir (black solid squares indicate the atenolol degradation rates after 240 h); and (B) The relationship between ammonia oxidizing rate and the acyclovir degradation rate after 240 h at a different linear fit slope.

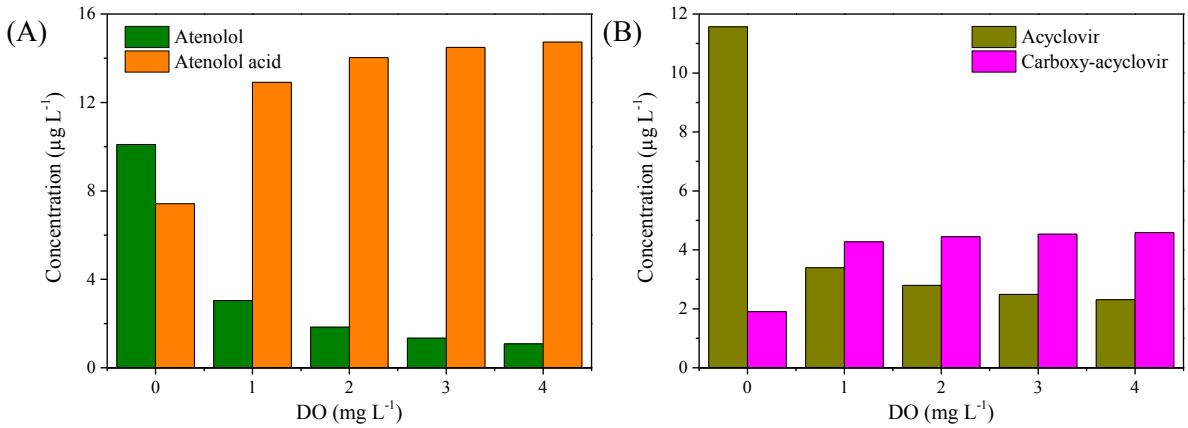

Figure 5. Predicted final concentrations of (A) atenolol and atenolol acid and (B) acyclovir and carboxy-acyclovir at time of 240 h at different concentrations of dissolved oxygen (DO) in the enriched nitrifying culture system.

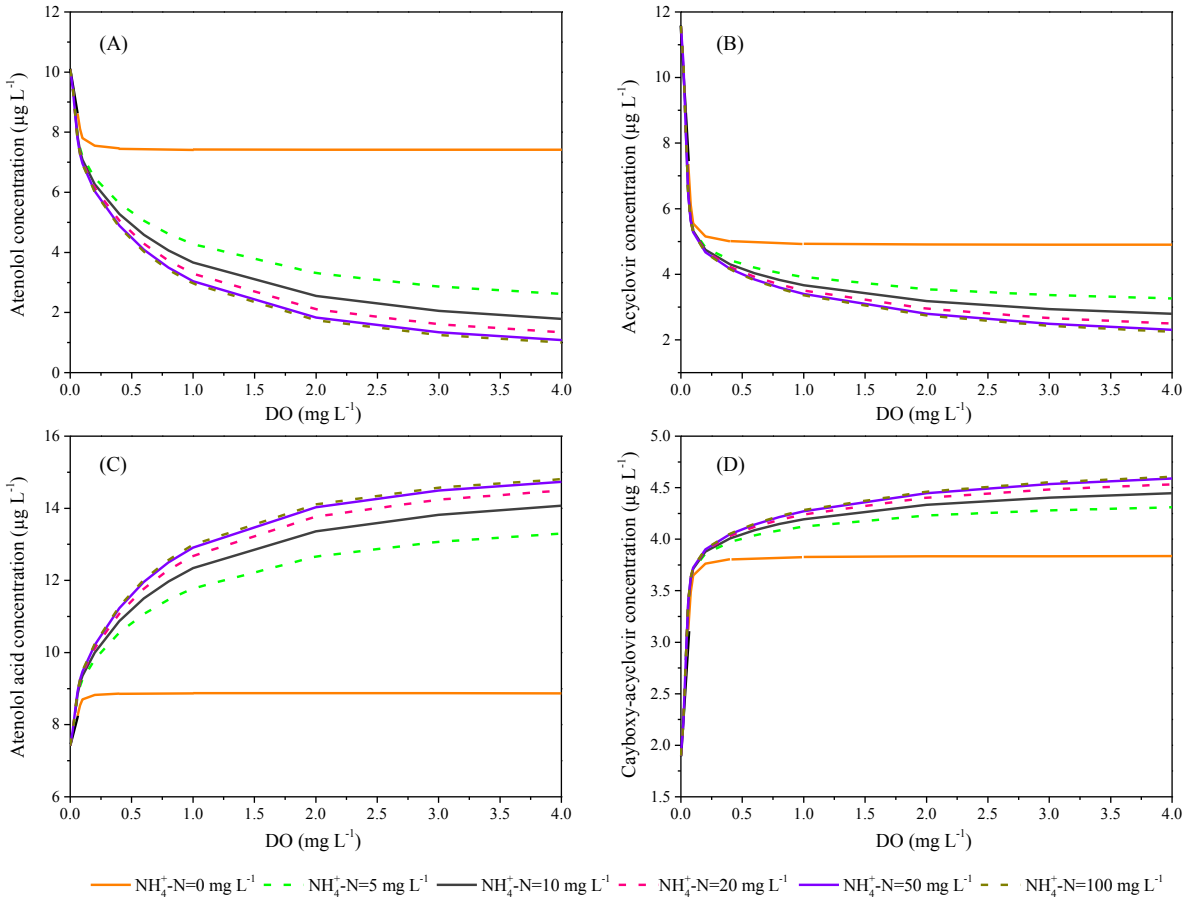

Figure 6. Predicted concentrations of pharmaceuticals and their transformation products at time of 240 h at initial concentrations of 15 μg L^{-1} with different ammonium concentrations ranging from 0 to 100 mg-N L^{-1} at different DO levels.

Supporting Information

Text S1 Chemicals

Atenolol (≥98%) and atenolol acid were purchased from Sigma-Aldrich, Australia. Acyclovir (>98%) was obtained from Thermo Fisher, Australia. Carboxy-acyclovir was provided by Toronto Research Chemicals. Isotope labeled internal standard atenolol-d7 was obtained from Sigma-Aldrich, Australia and acyclovir-d4 from Santa Cruz Biotechnology. Allylthiourea (ATU, 98%) and all the other HPLC grade organic solvents (methanol, acetonitrile, hexane and acetone) were supplied by Sigma-Aldrich, Australia.

The individual standard stock solution for each compound was prepared in methanol at 1 g L^{-1} and stored at -20 °C. The calibration curve including the internal standard was obtained using a series working standards (1-200 μg L^{-1}), diluted from the stock solution. With the aim of providing initial 15 μg L^{-1} of pharmaceuticals for the batch biodegradation experiments, the feed solution for each compound was prepared at concentration of 1 mg L^{-1} in Milli-Q water.

Text S2 Culture enrichment

An 8-L lab-scale sequencing batch reactor (SBR) seeded with activated sludge from a municipal wastewater treatment plant in Brisbane, Australia was used to enrich the nitrifying cultures consisting of ammonia oxidizing bacteria (AOB) and nitrite oxidizing bacteria (NOB). A 6-h cycle was performed to run the SBR: 260 min aerobic feeding, 30 min aerobic reacting, 1 min wasting, 60 min settling and 9 min decanting. During each cycle, 2 L synthetic wastewater was fed into the reactor resulting in a hydraulic retention time (HRT) of 24 h. The solid retention time (SRT) was maintained at 15 d. Dissolved oxygen (DO) was controlled between 2.5-3.0 mg L^{-1} using programmed logic controllers (PLC) and pH was maintained at the range of 7.5-8.0. The synthetic wastewater for the enriching the nitrifying culture contained per liter (Kuai and Verstraete, 1998): 5.63 g of NH_4HCO_3 (1 g NH_4^+-N), 5.99 g of $NaHCO_3$, 0.064 g of each of KH_2PO_4 and K_2HPO_4 and 2 mL of a trace element solution. The trace element stock solution contained: 1.25 g L^{-1} EDTA, 0.55 g L^{-1} $ZnSO_4 \cdot 7H_2O$, 0.40 g L^{-1} $CoCl_2 \cdot 6H_2O$, 1.275 g L^{-1} $MnCl_2 \cdot 4H_2O$, 0.40 g L^{-1} $CuSO_4 \cdot 5H_2O$, 0.05 g L^{-1} $Na_2MoO_4 \cdot 2H_2O$, 1.375 g L^{-1} $CaCl_2 \cdot 2H_2O$, 1.25 g L^{-1} $FeCl_3 \cdot 6H_2O$ and 44.4 g L^{-1} $MgSO_4 \cdot 7H_2O$.

The SBR was operated in a steady state for more than 1 year with almost 100% conversion of NH_4^+ to NO_3^-, prior to using the enriched nitrifying sludge for batch biodegradation experiments. The mixed liquor volatile suspended solids (MLVSS) concentration was stable at 1437.6 ± 112.9 mg L^{-1} (mean and standard errors, respectively, n=10). According to the microbial community analysis with

fluorescence *in-situ* hybridization (FISH) (Law et al., 2011), ammonia-oxidizing *beta-proteobacteria* accounted for 46 ± 6% (n=20) of the bacterial populations and the *Nitrospira* genera (nitrite oxidizers) constituted 38 ± 5% (n=20) of the bacterial populations.

Table S1. The definition of all model components

Variable	Description	Unit
S_{NH_4}	Ammonium concentration	g N m^{-3}
S_S	Readily biodegradable COD concentration	g COD m^{-3}
S_{O_2}	Dissolved oxygen concentration	g O_2 m^{-3}
X_{AOB}	Ammonia oxidizing bacteria (AOB) biomass concentration	g COD m^{-3}
X_{HET}	Heterotrophs (HET) biomass concentration	g COD m^{-3}
X_S	Slowly biodegradable COD concentration	g COD m^{-3}
X_I	Inert biomass concentration	g COD m^{-3}
S_{PC}	Parent compound (PC) concentration	mol m^{-3}
S_{BP}	Primary biotransformation product (BP) concentration	mol m^{-3}
S_{OP}	Other biotransformation product (OP) concentration	mol m^{-3}

Table S2. Process kinetic rate equations for the biotransformation model

	Process	Rate expression
1	Biotransformation of parent compound (PC) by ammonia oxidizing bacteria (AOB) under metabolism	$k_{PC\text{-}AOB} X_{AOB} S_{PC}$
2	Biotransformation of PC by AOB under cometabolism	$\mu_{max,AOB} \frac{S_{NH_4}}{S_{NH_4}+K_{NH_4}} \frac{S_{O_2}}{S_{O_2}+K_{O_2,AOB}} X_{AOB}$
3	Decay of AOB	$b_{AOB} X_{AOB}$
4	Hydrolysis	$k_{hyd} \frac{X_S/X_{HET}}{X_S/X_{HET}+K_X} X_{HET}$
5	Biotransformation of PC by heterotrophs (HET) under metabolism	$k_{PC\text{-}HET} X_{HET} S_{PC}$
6	Biotransformation of PC by HET under cometabolism	$\mu_{max,HET} \frac{S_S}{S_S+K_S} \frac{S_{O_2}}{S_{O_2}+K_{O_2,HET}} X_{HET}$
7	Decay of HET	$b_{HET} X_{HET}$

Table S3. The stoichiometric matrix for the biotransformation model (AOB, ammonia oxidizing bacteria; HET, heterotrophs)

Component (*i*)		Substance			Biomass				Substrate		
		1	2	3	4	5	6	7	8	9	10
Process (*j*)		S_{NH_4}	S_s	S_{O_2}	X_{AOB}	X_{HET}	X_S	X_I	S_{PC}	S_{BP}	S_{OP}
AOB	1								-1	α^m_{BP}	$1-\alpha^m_{BP}$
	2	$-i_{NBM}-\frac{1}{Y_{AOB}}$		$-\frac{3.43-Y_{AOB}}{Y_{AOB}}$	1				$-T^c_{PC-AOB}S_{PC}$	$\alpha^c_{BP}T^c_{PC-AOB}S_{PC}$	$(1-\alpha^c_{BP})T^c_{PC-AOB}S_{PC}$
	3				-1		$1-f_I$	f_I			
HET	4		1				-1				
	5								-1	β^m_{BP}	$1-\beta^m_{BP}$
	6	$-i_{NBM}$	$-\frac{1}{Y_{HET}}$	$-\frac{1-Y_{HET}}{Y_{HET}}$		1			$-T^c_{PC-HET}S_{PC}$	$\beta^c_{BP}T^c_{PC-HET}S_{PC}$	$(1-\beta^c_{BP})T^c_{PC-HET}S_{PC}$
	7					-1	$1-f_I$	$1-f_I$			

Table S4. Stoichiometric and kinetic parameters of the developed model

Parameter	Definition	Unit	Value	Source
Stoichiometric parameters				
Y_{AOB}	Yield coefficient for AOB	g COD g N^{-1}	0.15	(Sathyamoorthy et al., 2013)
Y_{HET}	Yield coefficient for HET	g COD g COD^{-1}	0.67	(Henze et al., 2000)
i_{NBM}	Nitrogen fraction of biomass	g N g COD^{-1}	0.086	(Henze et al., 2000)
f_I	Fraction of X_I in biomass decay	g COD g COD^{-1}	0.1	(Henze et al., 2000)
α_{BP}^{m}	Stoichiometry coefficient for primary biotransformation product (BP) by AOB under metabolism	-	0.29 (atenolol) 0.43 (acyclovir)	Calculated from experimental data
α_{BP}^{c}	Stoichiometry coefficient for BP by AOB under cometabolism	-	0.87 (atenolol) 0.29 (acyclovir)	Calculated from experimental data
β_{BP}^{m}	Stoichiometry coefficient for BP by HET under metabolism	-	0.63 (atenolol) 0.84 (acyclovir)	Calculated from experimental data
β_{BP}^{c}	Stoichiometry coefficient for BP by HET under cometabolism	-	0.63 (atenolol) 0.84 (acyclovir)	Calculated from experimental data
Ammonia oxidizing bacteria (AOB)				
$\mu_{max,AOB}$	Maximum specific growth rate of AOB	h^{-1}	Estimated in this study	-
b_{AOB}	AOB decay rate	h^{-1}	0.00625	(Sathyamoorthy et al., 2013)
$K_{O_2,AOB}$	Half saturation value for S_{O_2} of AOB	g O_2 m^{-3}	1.1	(Ghimire, 2012)
K_{NH_4}	Half saturation value for S_{NH_4}	g N m^{-3}	1.31 (25°C)	(Wiesmann, 1994)

$k_{PC\text{-}AOB}$	AOB transformation coefficient	m^3 g COD^{-1} h^{-1}	Estimated in this study	-
$T^c_{PC\text{-}AOB}$	Parent compound (PC) biotransformation coefficient rate linked to AOB growth (cometabolism)	m^3 g COD^{-1}	Estimated in this study	-
Heterotrophs (HET)				
k_{hyd}	Maximum hydrolysis rate of HET	h^{-1}	0.125	(Henze et al., 2000)
$\mu_{max,HET}$	Maximum specific growth rate of HET	h^{-1}	0.25	(Henze et al., 2000)
b_{HET}	HET decay rate	h^{-1}	0.026	(Henze et al., 2000)
$K_{O_2,HET}$	Half saturation value for S_{O_2} of HET	g O_2 m^{-3}	0.2	(Henze et al., 2000)
K_S	Half saturation value for S_{COD}	g COD m^{-3}	20	(Henze et al., 2000)
K_X	Half saturation value for hydrolysis	g COD g COD^{-1}	1.0	(Henze et al., 2000)
$k_{PC\text{-}HET}$	HET transformation coefficient	m^3 g COD^{-1} h^{-1}	Estimated in this study	-
$T^c_{PC\text{-}HET}$	PC biotransformation coefficient rate linked to HET growth (cometabolism)	m^3 g COD^{-1}	0	(Sathyamoorthy et al., 2013)

Table S5. Experimental conditions and designs for model calibration and validation

Purpose	Model calibration			Model validation	Model evaluation		
	Atenolol (Case *I*)				Acyclovir (Case *II*)		
	EXP 1	EXP 2	EXP 3	EXP 4	EXP 1	EXP 2	EXP 3
Parameters calibrated	$k_{PC\text{-}HET}$	$k_{PC\text{-}AOB}$	$T_{PC\text{-}AOB}$, $\mu_{max,\ AOB}$	N/A	$k_{PC\text{-}HET}$	$k_{PC\text{-}AOB}$	$T_{PC\text{-}AOB}$, $\mu_{max,\ AOB}$
Initial parent compound concentration	15 μg L^{-1}						
Experimental conditions	NH_4^+-N: 50 mg L^{-1} (initial) ATU: 30 mg L^{-1} MLVSS: 1 g VSS L^{-1} Volume: 4 L DO: 2.5-3.0 pH: 7.55-7.60	NH_4^+-N: 0 mg L^{-1} MLVSS: 1 g VSS L^{-1} Volume: 4 L DO: 2.5-3.0 pH: 7.55-7.60	NH_4^+-N: 50 mg L^{-1} (constant) MLVSS: 1 g VSS L^{-1} Volume: 4 L DO: 2.5-3.0 pH: 7.55-7.60	NH_4^+-N: 25 mg L^{-1} (constant) MLVSS: 1 g VSS L^{-1} Volume: 4 L DO: 2.5-3.0 pH: 7.55-7.60	NH_4^+-N: 50 mg L^{-1} (initial) ATU: 30 mg L^{-1} MLVSS: 1 g VSS L^{-1} Volume: 4 L DO: 2.5-3.0 pH: 7.55-7.60	NH_4^+-N: 0 mg L^{-1} MLVSS: 1 g VSS L^{-1} Volume: 4 L DO: 2.5-3.0 pH: 7.55-7.60	NH_4^+-N: 50 mg L^{-1} (constant) MLVSS: 1 g VSS L^{-1} Volume: 4 L DO: 2.5-3.0 pH: 7.55-7.60
Experimental period	240 h						
Chemical analysis	NH_4^+, NO_2^-, NO_3^-, atenolol, atenolol acid, MLVSS				NH_4^+, NO_2^-, NO_3^-, acyclovir, carboxy-acyclovir, MLVSS		

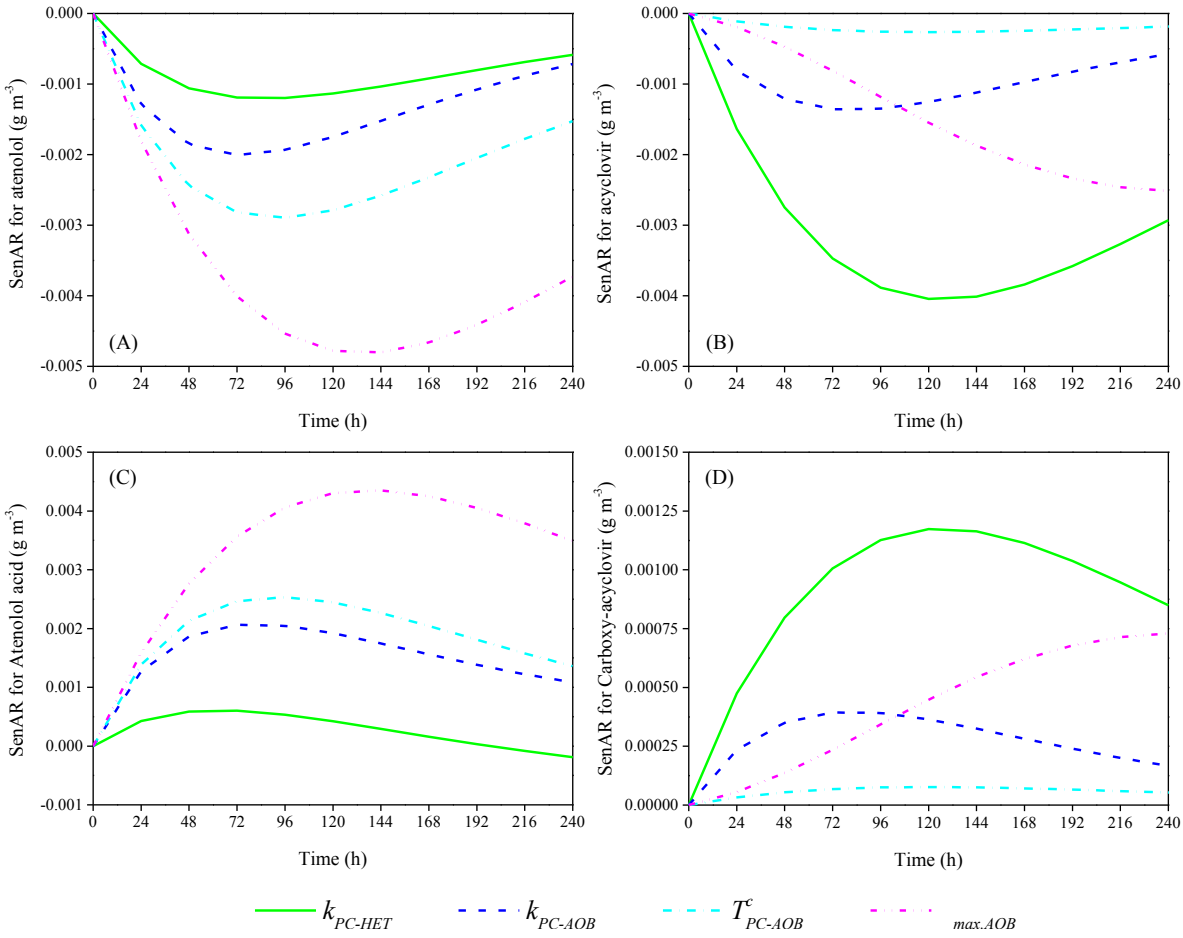

Figure S1. Time course of the sensitivity functions of atenolol (A), acyclovir (B), atenolol acid (C) and carboxy-acyclovir (D) with respect to four parameters $k_{PC\text{-}AOB}$, $k_{PC\text{-}AOB}$, $T^{c}_{PC\text{-}AOB}$ and $\mu_{max,\ AOB}$.

Additional References:

Ghimire, B.K. 2012. Investigation of Oxygen Half Saturation Coefficients for Nitrification. M.S., The George Washington University, Ann Arbor.

Henze, M., Gujer, W., Mino, T. van Loosdrecht, M.C.M., 2000. Activated sludge models ASM1, ASM2, ASM2d and ASM3, IWA Publishing, London.

Kuai, L. Verstraete, W., 1998. Ammonium removal by the oxygen-limited autotrophic nitrification-denitrification system. Appl. Environ. Microbiol. 64 (11), 4500-4506.

Law, Y., Lant, P. Yuan, Z., 2011. The effect of pH on N2O production under aerobic conditions in a partial nitritation system. Water Res. 45 (18), 5934-5944.

Sathyamoorthy, S., Chandran, K. Ramsburg, C.A., 2013. Biodegradation and cometabolic modeling of selected beta blockers during ammonia oxidation. Environ. Sci. Technol. 47 (22), 12835-12843.

Wiesmann, U. 1994. Biological nitrogen removal from wastewater. In: Ghosh, P., Hasegawa, S., and Kuhad, R. Ch. eds. Biotechnics/Wastewater. Springer Berlin Heidelberg, Berlin, Heidelberg, pp. 113-154.